Distribution Agreement

In presenting this thesis or dissertation as a partial fulfillment of the requirements for an advanced degree from Emory University, I hereby grant to Emory University and its agents the non-exclusive license to archive, make accessible, and display my thesis or dissertation in whole or in part in all forms of media, now or hereafter known, including display on the world wide web. I understand that I may select some access restrictions as part of the online submission of this thesis or dissertation. I retain all ownership rights to the copyright of the thesis or dissertation. I also retain the right to use in future works (such as articles or books) all or part of this thesis or dissertation.

Signature:

_____   _____

Pablo Elohim Guzmán   Date

ASYMMETRIC REACTIONS OF DONOR/ACCEPTOR RHODIUM CARBENOIDS: FROM FORMAL CYCLOADDITIONS TO C-H INSERTION

By

Pablo Elohim Guzmán
Doctor of Philosophy

Chemistry

_____
Dr. Huw M. L. Davies
Advisor

_____
Dr. Dennis C. Liotta
Committee Member

_____
Dr. Simon B. Blakey
Committee Member

Accepted:

_____
Lisa A. Tedesco, Ph.D.
Dean of the James T. Laney School of Graduate Studies

_____
Date

ASYMMETRIC REACTIONS OF DONOR/ACCEPTOR RHODIUM CARBENOIDS: FROM FORMAL CYCLOADDITIONS TO C-H INSERTION

By

Pablo Elohim Guzmán

M.A., University at Buffalo, State University of New York, 2009

Advisor: Huw M. L. Davies, Ph.D.

An abstract of

A dissertation submitted to the Faculty of the

James T. Laney School of Graduate Studies of Emory University

in partial fulfillment of the requirements for the degree of

Doctor of Philosophy

in Chemistry

2013

Abstract

ASYMMETRIC REACTIONS OF DONOR/ACCEPTOR METALLOCARBENOIDS:
FROM FORMAL CYCLOADDITIONS TO C-H INSERTION

By Pablo Elohim Guzmán

Rhodium(II)-stabilized donor/acceptor carbenoids, derived from donor/acceptor diazo compounds, have enriched modern organic synthesis and revolutionized our approach towards complex target synthesis. These transient species continue to permit entry to relevant structural motifs, provide the basis for new reaction development, and serve as surrogates to traditional functional group interconversion approaches. They have, and continue to be, the central focus in the Davies group research program. Donor/acceptor metallocarbenoids delicately balance the interplay of selectivity and reactivity. Such a balance allows these carbenoids to be more stable compared to conventional acceptor or acceptor/acceptor carbenoids, and thus capable of achieving remarkable levels of diastereoselectivity and asymmetric induction.

The first chapter of this dissertation describes the development of a new formal [4+3] cycloaddition reaction between siloxyvinyldiazoacetates and dienes. Vinylcarbenoids exhibit electrophilic character at both the carbenoid carbon and at the vinylogous position. Initiating reactivity at the electrophilic terminus in the presence of an electron-rich diene allowed us to formulate the concept of a rhodium-catalyzed inverted [4+3] cycloaddition. This reactivity leads to the enantio- and diastereoselective synthesis of a series of regiochemically inverted products thus broadening the synthetic potential of the [4+3] cycloaddition. The combination of siloxyvinyldiazoacetates with sterically demanding triarylcyclopropanecarboxylate catalyst, $Rh_2(S\text{-}BTPCP)_4$, is very effective in achieving high levels of asymmetric induction.

Chapter two discusses a ReactIR™ guided exploratory study in which investigations were conducted seeking optimum sets of reaction conditions and possible combinations of donor/acceptor, acceptor, and acceptor/acceptor diazo compounds in attempt to design, synthesize and modulate the reactivity of bis-diazo systems containing nonequivalent diazo groups. It was determined that multiple variables such as catalyst loading, chiral dirhodium catalyst, pyrazole additives as well as sterically demanding esters all directly impact the decomposition profile of diazo compounds. Conditions in which a donor/acceptor diazo is selectively decomposed in the presence of an acceptor/acceptor diazo compound were identified and directed towards the construction of the tetracyclic core of phorbol.

The final chapter of this dissertation focuses on the examination of stereoselective benzylic C-H insertion reactions. A non-diastereoselective benzylic C-H insertion reaction was rendered diastereoselective as a result of simple substrate modifications inferred by a recent predictive C-H insertion model developed in the Davies group. The insertion reactions were conducted in the presence of phenyldiazoacetate and chiral rhodium tetraprolinate catalysts $Rh_2(S\text{-}DOSP)_4$ and $Rh_2(R\text{-}DOSP)_4$. Insertion onto the activated benzylic position is substrate controlled while the stereochemistry of the carbenoid carbon is catalyst controlled.

ASYMMETRIC REACTIONS OF DONOR/ACCEPTOR RHODIUM

CARBENOIDS: FROM FORMAL CYCLOADDITIONS TO C-H

INSERTION

By

Pablo Elohim Guzmán

M.A., University at Buffalo, State University of New York, 2009

Advisor: Huw M. L. Davies, Ph.D.

A dissertation submitted to the Faculty of the

James T. Laney School of Graduate Studies of Emory University

in partial fulfillment of the requirements for the degree of

Doctor of Philosophy

in Chemistry

2013

Acknowledgements

I would like to begin by thanking Professor Huw M. L. Davies for accepting me into his group. I am very grateful for your guidance and support throughout the years. I would also like to thank Professors Dennis C. Liotta and Simon Blakey for serving as my committee members. I will never forget your work ethic, attention to detail, support and limitless knowledge of organic chemistry. Your constructive criticisms during my yearly exams and original proposal were extremely valuable as it helped me to think outside of the "rhodium carbenoid box". I would like to thank Professor Albert Padwa, your never-ending passion for synthesis and discovery is truly inspiring and your willingness to share your knowledge and experiences has given me the opportunity to appreciate the field of organic synthesis. Also, thank you for letting me use your lab space to write this dissertation. For the last few months, I felt like I was part of your group. I would like to also thank Josh and Whitney Alford for letting me stay in their home for the my last six weeks at Emory. I would also like to thank all the past and present members of the Davies group and wish them nothing but the best in their careers.

The Ph.D. is an accomplishment that could not have been realized by myself. During my undergraduate and graduate school years, I have been extremely blessed to meet and befriend some of the most talented, incredible and inspiring people for which I have tremendous love and admiration. At Emory, I would like to thank Dr. Daniel Morton, Dr. Étienne Nadeau, Ms. Felicia A. Fullilove, Dr. Vyacheslav V. Boyarskikh, Mr. Gertrudes Najera-Trejo, Mr. David G. Jones, Professor Cora E. MacBeth, Ms. Kathyrn M. Chepiga, Dr. Sara A. Bonderoff, Dr. Damien Valette, Dr. Yan Zhou, Dr. Sezgin Kiren, Dr. Donny Magaña, Dr. Yajing Lian, Mr. Steve Krebs, Dr. Hao Li, Mr. Clayton P. Owens, Ms.

Cynthia Gaillard, Mr. Eric Miller and Dr. José Soria. From the University at Buffalo I would like to thank Professors Jerome B. Keister, David F. Watson, Steven T. Diver, Sarbajit Banerjee, Luis A. Colón, Dr. Dominic L. Ventura and Dr. Maan T. Khayat. From Chicago State University, I would like to thank Mr. Ron Glowinski, Mr. Fernando Ortiz, Professors Quinetta D. Shelby, Michael Mimnaugh, Warren V. Sherman, Mel Sabella, David Kanis, Mr. Brian Wright, Mr. and Mrs. Ray Kujawa, Mrs. Janette Dryjanski, Dr. Tyvette Hilliard, Mr. Byeong-gyu Park and Dr. Mark-Eugene Duban. From Olive-Harvey College, I would like to thank Professor Gide Colinet. I would like to make a special acknowledgement to Professors LeRoy Jones II and Félix M. Rivas. From the beginning, you have always believed in me even when I struggled to believe in myself. You have always supported my decisions even if it meant pursuing areas outside of chemistry. You both are the truest definition of what it means to be a mentor and are the best role models a student could ever ask for.

I would also like to send the most heartfelt thank you to the Arce and Covarrubias families and Guadalupe Serna. You have helped my family and I so much through the years. I will always be there for you.

Lastly and most importantly, I would like to thank my wife, children and parents. If I did not have you in my life, I guarantee you that I would have never made it this far. Your love and support gave me the energy and will to not quit and overcome the numerous difficult moments I went through as a graduate student. I love you all more than anything in the whole world and I thank God everyday for blessing me with such a beautiful family. This thesis is a gift from me to you.

Table of contents

Chapter I

Chapter II

Chapter III

List of figures

Chapter I

Chapter II

List of schemes

Chapter II

Chapter III

List of tables

Chapter II

Chapter III

List of abbreviations

Ac	Acetyl
p-ABSA	4-Acetamidobenzenesulfonyl azide
Ar	Aryl
Boc	*tert*-Butyloxycarbonyl
coe	cyclooctene
t-Bu	*tert*-Butyl
DBU	1,8-Diazabicyclo[5,4,0]undec-7-ene
DCM (CH_2Cl_2)	Dichloromethane
2,2-DMB	2,2-Dimethylbutane
DMAD	Dimethyl acetylenedicarboxylate
DOSP	*N*-(4-dodecylbenzenesulfonyl)prolinate
dr	Diastereomeric ratio
ee	Enantiomeric excess
EDG	Electron-donating group
ESI	Electrospray ionization
Et	Ethyl
EWG	Electron-withdrawing group
Equiv.	Equivalent
FAB-MS	Fast atom bombardment mass spectroscopy
HCl	Hydrochloric acid
c-Hex	Cyclohexyl
OHex	Hexanoate

Hz	Hertz
HPLC	High-performance liquid chromatography
IR	Infrared spectroscopy
L	Ligand
M	Metal
Me	Methyl
MeO	Methoxy
nOe	Nuclear Overhauser effect
OAc	Acetate
OEt	Ethoxy
OOct	Octanoate
Ph	Phenyl
(*R*)-(*S*)-PPFOMe	(*R*)-1-[(*S*)-2-(diphenylphosphino)ferrocenyl]ethyl methyl ether
Ph	Phenyl
POCl$_3$	Phosphorous oxychloride
*i*Pr	Isopropyl
Rh	Rhodium
rt	Room temperature
TBS	*tert*-Butyldimethylsilyl
TBSP	(4-*tert*-butylphenyl)sulfonyl-prolinate
TFA	Trifluoroacetic acid (trifluoroacetyl)
THF	Tetrahydrofuran
TIPS	Triisopropylsilyl

TISP	2,4,6-tri-iso-propyl-benzenesulfonyl
TMEDA	*N,N,N',N'*,-Tetramethylethylenediamine
TMS	Trimethylsilyl

CHAPTER I

Development of the Rhodium-Catalyzed Asymmetric Vinylogous [4+3] Cycloaddition Between Vinyldiazoacetates and Dienes

1.1 Introduction

Seven-membered carbocyclic systems are intriguing structures that have captured the attention of synthetic organic chemists due their prevalence in natural products and pharmaceutical compounds (Figure 1.1).[1-5] In contrast to their five and six-membered ring congeners, the introduction of stereogenicity onto the cycloheptane ring has also proven to be generally more challenging as a result of conformational mobility and elevated entropic barriers associated with these systems.[6,7]

Phorbol   Frondosin A   Sundiversifolide   Clarinex
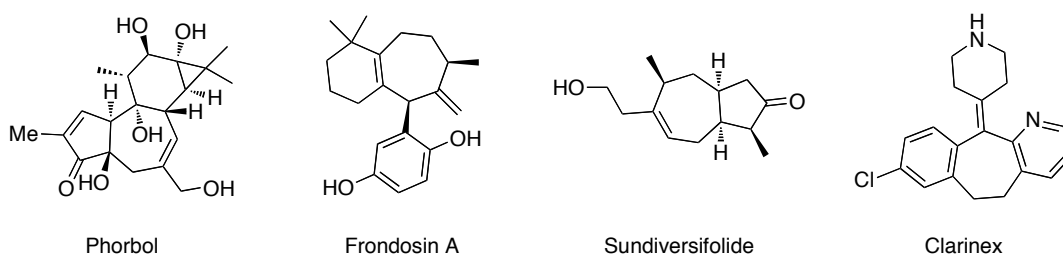
Figure 1.1 Representative examples of natural products and drug molecules that contain seven-membered rings.

Generally, entry to the cycloheptyl motif requires the use of ring-closing or ring expansion strategies.[6,8-18] Consequently, these transformations typically necessitate multistep synthesis of reaction precursors and are often plagued by low levels of atom and step economy. Unfortunately, this disadvantage ultimately impacts the overall practicality of such processes, especially in the synthesis of fused ring structures.

1

Moreover, compared to smaller ring systems, the synthesis of seven-membered rings is not as well developed, especially in catalytic and intermolecular processes. However, in the intramolecular mode, extraordinary advances have been made.[7] For example, the Wender laboratory has made spectacular advances in the area of cycloheptane formation. Wender and his co-workers were first to report the Wilkinson catalyst-catalyzed intramolecular [5+2] cycloaddition of vinylcyclopropanes (VCPs) and alkynes as homologues of the Diels-Alder cycloaddition for the synthesis of seven-membered rings (Scheme 1.1).[19]
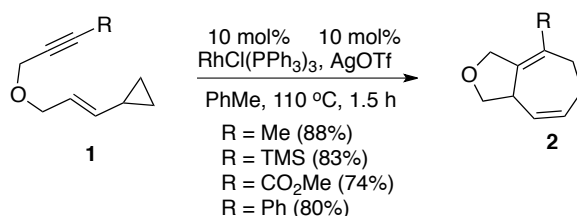
Scheme 1.1 Wender's Rh(I)-catalyzed intramolecular [5+2] cycloaddition of

vinylcyclopropanes and alkynes.

Enyne ether **1**, in the presence of catalytic amounts of Wilkinson's catalyst and silver(I) triflate in refluxing toluene, participates in a thermal cycloaddition to give functionalized fused cycloheptadienes **2** in excellent yields (74-88 %). As illustrated, the reaction is quite tolerable to a number of functional groups. Mechanistically, two general pathways have been proposed for the transition-metal-catalyzed [5+2] cycloaddition (Scheme 1.2). One involves the formation of metallacyclohexene intermediate **4a** followed by 2π insertion to produce metallacyclooctadiene **5** (path a). The second occurs *via* an oxidative cyclization process to generate metallacyclopentene **4b** followed by rupture of the

cyclopropane, generating common metallacyclooctadiene intermediate **5**, which then undergoes a subsequent reductive elimination (path b).
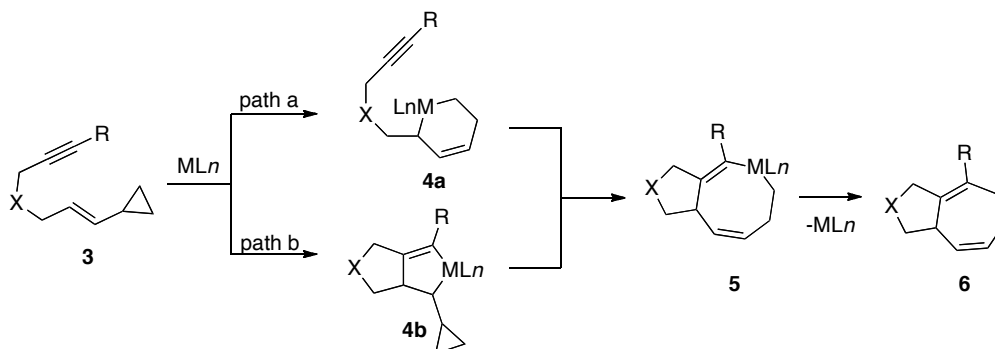
Scheme 1.2 Proposed mechanism for the metal-catalyzed intramolecular [5+2]
cycloaddition of vinylcyclopropanes and alkynes.

Recent theoretical studies conducted by the Houk laboratory indicated that in the presence of rhodium catalysts, the metallacyclohexene pathway is preferred and the rate-determining step for the process is the 2π insertion to form the metallacyclooctadiene intermediate.[20-22] The Wender type [5+2] cycloaddition has made an enormous impact in organic synthesis and has provided a conceptual foundation leading to applications in total synthesis and the discovery of many new cycloaddition methodologies, such as the [5+2+1],[23] [5+1+2+1],[24] [3+2],[25] and [5+1][26] reactions all of which occur through vinylcyclopropanes (Scheme 1.3).
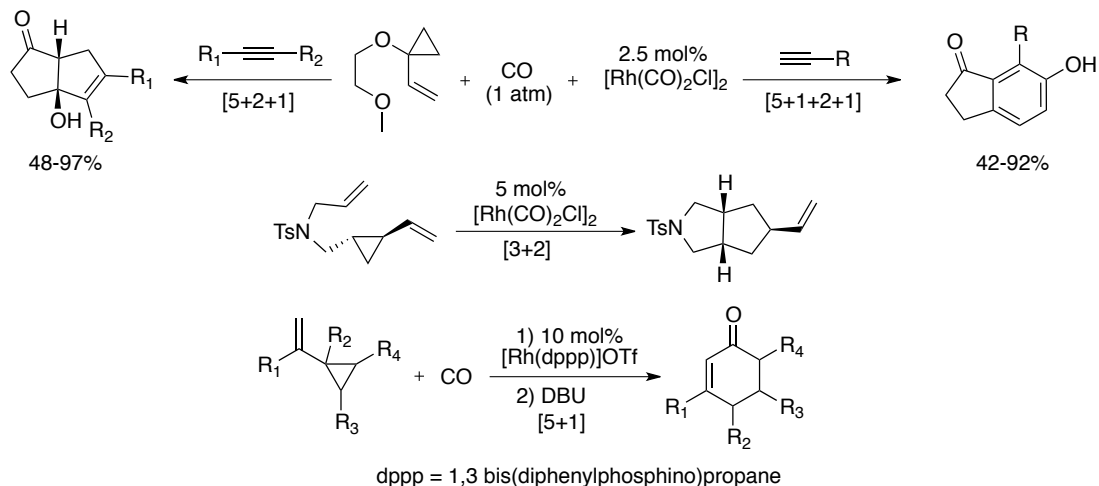
Scheme 1.3 Representative cycloaddition reactions inspired by Wender's [5+2]

methodology.

In addition to the intramolecular [5+2] methodology, Wender and co-workers have also demonstrated that VCPs are indeed capable of reacting with π-systems in an intermolecular fashion. For example, in the presence of $[Rh(CO)_2Cl]_2$, vinylcyclopropanes and alkynes undergo a formal [5+2] cycloaddition to yield cycloheptadienes (Scheme 1.4).
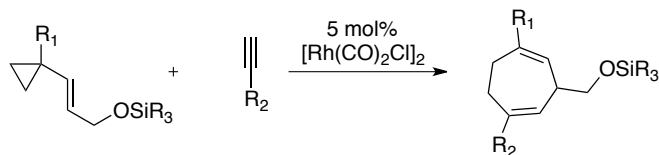
Scheme 1.4 Wender's intermolecular [5+2] cycloaddition.

During the course of their investigations, the Wender group indicated that in striking contrast to the facile reactions of siloxyVCPs, intermolecular cycloadditions of VCP itself (R = H) failed to react with various alkynes and catalysts and requires the presence of a heteroatom substituent (R = OR, equation 1.1).[27]

$$(1.1)$$
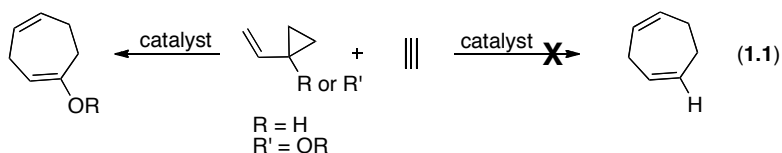
This large difference in reactivity could have been attributed solely to electronic effects of the heteroatom substituent. Wender, however, rationalized that conformational effects were also present and responsible for the distinct reactivity profiles.[28] Alkyl substitution of VCPs, specifically at the 1-position, have been shown to reduce the energetic difference between the *s*-trans (**7b**) and *s*-cis conformations, allowing for the increased population of **7a** (Scheme 1.5).[29] Moreover, this conformational effect could favor the formation of the *Z*-allyl[30] intermediate **8** over *E*-allyl[31] intermediate **3**. Notably, only **8** has the desired dihedral angle ($\phi = 0°$) for formation of the *cis*-alkene of cycloadduct **11**.
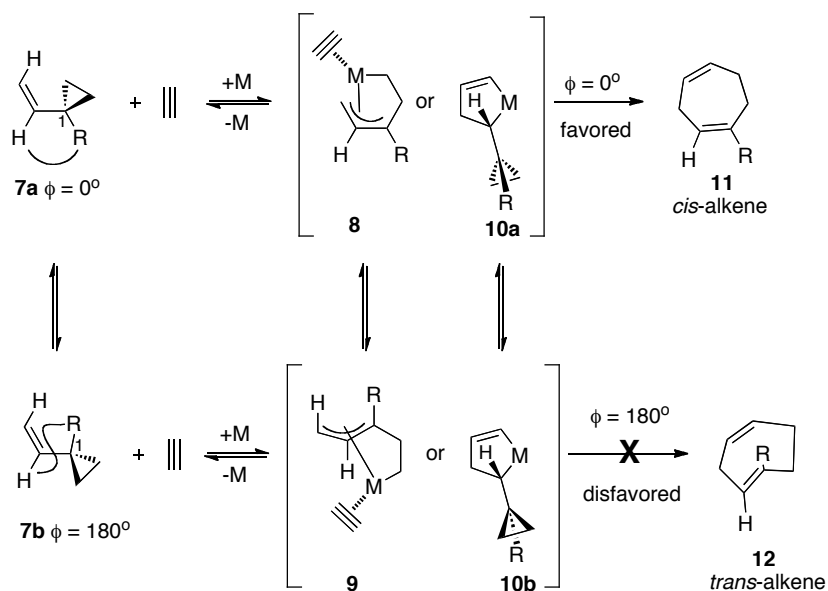
Scheme 1.5 Proposed confirmations for Wender [5+2] cycloaddition.

In an alternative mechanism, occurring *via* an initial cyclometalation reaction, similar steric effects accounts for the formation and further reaction of metallacycles **10a** and

10b.[32,33] To examine the conformational hypothesis, isopropyl-substituted VCP **13** was synthesized and reacted with numerous alkynes (Table 1.1).

Table 1.1 Cycloadditions of VCP **13** with representative alkynes.
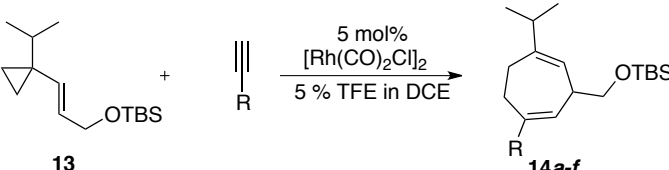
entry	R	time (h)	yield (%)	product
1	CO$_2$Me	1	95	**14a**
2	Ph	2	81	**14b**
3	CH$_2$OMe	5	90	**14c**
4	CH$_2$OH	5	90	**14d**
5	C$_3$H$_7$	23	81	**14e**
6	TMS	23	90	**14f**

TFE = 2,2,2-trifluoroethanol, DCE = 1,2-dichloroethane

In the presence of [Rh(CO)$_2$Cl]$_2$, the substituted alkynes readily react with VCP **13** to yield a number of cycloheptadiene products (**14a-f**) in excellent yields. The cycloadditions proceeds effortlessly with alkynes containing ester, aryl, ether, hydroxyl, alkyl and silicon functional groups. Notably, an important aspect of this methodology is

the excellent level of regiocontrol. In each case, the authors report that a single regioisomer is obtained.

Accordingly, a systematic study of cyclopropane substituent effects and functional group tolerance was conducted through reaction of a range of VCPs with methyl propiolate (Table 1.2).

Table 1.2. Substituent effects on the [5+2] cycloaddition with methyl propiolate.

entry	VCP	cond.[a]/yield	product	entry	VCP	cond.[a]/yield	product	entry	VCP	cond.[a]/yield	product
1	15	A 2h/82%	16	5	23	A 72h/38% B 6h/dec.	24	9	31	A 20h/75% B 3h/76%.	32
2	17	A 1.5h/76%	18	6	25	A 72h/64% B 45min/69%	26	10	33	A 15h/63% d.r. = 2:1	34
3	19	A 8h/81%	20	7	27	A 3h/53%	28	11	35	A >24h/no rxn B 21h/62% d.r. 1:1	36
4	21	A 30h/23% B 2h/dec.	22	8	29	A 2h/82%	30				

conditions = A= 5 mol % [Rh(CO)$_2$Cl]$_2$, DCE, 80 ºC; B = A= 5 mol % [Rh(CO)$_2$Cl]$_2$, 5 % TFE in DCE, 80 ºC

Free hydroxyl and unsubstituted VCPs (entries 1 and 2), react similarly in terms of rate and efficiency compared to siloxy VCP **13**. However, replacement of the isopropyl functionality with a methyl group decreased the reaction rate considerably (entry 3). Nonetheless, full conversion was achieved within 8 hours and an excellent isolated yield

was obtained (81%). Replacement of the methyl group with hydrogen, entry 4, led to synthetically impractical levels of the desired cycloadduct **22** (23%) after a significantly extended reaction time (30h). In the late 1980's, the De Mare laboratory conducted studies on VCPs indicating that substitution on the internal position of the vinyl moiety affects the conformation equilibrium of VCPs.[34] Accordingly, VCPs **23** and **25** were synthesized and subjected to optimized [5+2] cycloaddition conditions (entry 5 and 6). VCP **23** provided a 15% increase in isolated yield, however the reaction time increased by 42 hours (entry 4 vs 5). Siloxy-protected VCP **25** reacted more efficiently in DCE and significantly more rapidly in the presence of 5% TFE (entry 6). Interestingly, VCPs **21** and **23** decomposed in the presence of TFE. Due to the slow reaction of the H-substituted VCPs **21** and **23**, introduction of a TMS surrogate system proved advantageous as VCP **27** reacted in only 3 hours (entry 7). Primary as well as secondary siloxy functionalities were also tolerated (entries 8-10) which gave access to cycloadducts possessing three distinct groups strategically positioned on a cycloheptadiene scaffold. The free alcohol **35** was unreactive in DCE due to unfavorable coordination to the metal to the hydroxyl group. However, this lack of reactivity was circumvented by introduction of co-solvent TFE (5%) which provided adduct **36** in 62% yield as a 1:1 mixture of diastereomers (entry 11). In general, the [5+2] cycloaddition has a broad substrate scope. Notably, high regioselectivities (>10:1) were observed with all of the di- and trisubstituted VCPs. With monosubstituted alkynes, the substitution on the olefin terminus directs formation of a single regioisomer. The observed regioselectivity is consistent with minimization of steric effects during C-C bond formation involving either of the two generally accepted mechanistic paths (Figure 1.2).
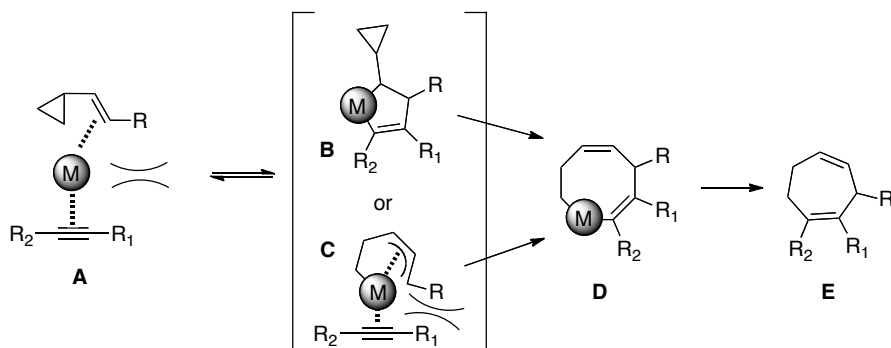
Figure 1.2 Wender's [5+2] regiochemical rational.

The broad substrate variation and excellent regiochemical control has made Wender type [5+2] cycloadditions an attractive method for the formation of cycloheptane scaffolds. However, a significant limitation to the methodology resides in the lack of an asymmetric variant. Moreover, another constraint is the low diastereoselectivity of the cycloaddition which renders the methodology rather limited.

1.2 Chiral auxiliary-mediated tandem cyclopropanation/Cope rearrangement

A longstanding approach to the cycloheptyl motif has been through formal [4+3] cycloaddition reaction through the capture of allyl cations with dienes (equation 1.2).[35,36] Perhaps the most practical and resourceful method for the generation of allyl cations has been achieved by the heterolysis of allyl halides promoted by Ag(I) Lewis acids.[35] However, the yields from these cycloadditions tend to be relatively modest as a result of competing electrophilic additions and carbocation rearrangements, thus presenting a conspicuous limitation to the methodology. Moreover, the reactions are susceptible to

reacting through stepwise pathways which often result in variable levels of stereoselection.[35]

R = O⁻, OR, OM, NR₂, CH₂SiR₃, alkyl, etc

(if R is a nucleophile)

(1.2)
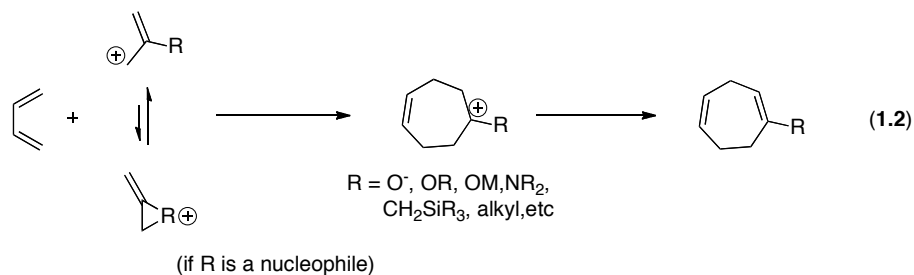
The aforementioned shortcomings were efficiently addressed in 1985, when the Davies laboratory introduced seminal work describing the rhodium(II)-catalyzed tandem cyclopropanation/Cope rearrangement (CPCR) as a reliable method for the formation of the 1,5 cycloheptadiene ring system.[37] The combination of $Rh_2(OAc)_4$, furan and vinyldiazoacetate **37** produced bicyclo[3.2.1]octane adduct **38** in 45% yield (Scheme 1.6).
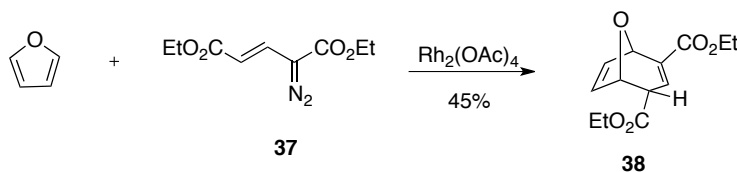
Scheme 1.6 Davies' cyclopropanation/Cope rearrangement with furan.

The intermolecular CPCR reaction has shown to be compatible with a broad range of substrates such as cyclopentadiene,[38] acyclic alkylated dienes,[39] acyclic oxygenated dienes,[40] and pyrroles.[41] This methodology initiated the development of a new area of chemistry with regard to cycloheptane formation derived from dienes and vinylcarbenoids. The proposed mechanistic rational for the CPCR reaction commences with an initial cyclopropanation reaction leading to a *cis*-divinylcyclopropane which is

10

appropriately organized to undergo a Cope rearrangement *via* a stereodefined boat transition state (Scheme 1.7).
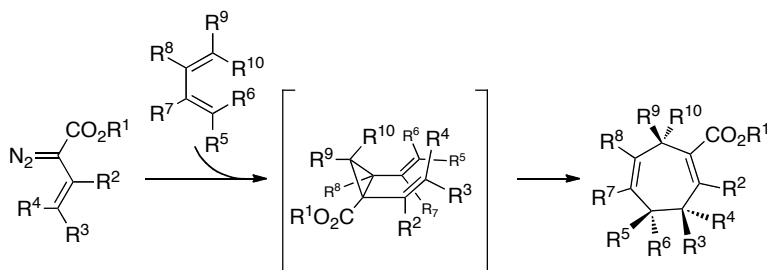
Scheme 1.7 Tandem cyclopropanation/Cope rearrangement.

The cyclopropanation/Cope rearrangement reaction between vinylcarbenoids and dienes has been shown to be a highly diastereoselective process.[4,42,43] The remarkable stereospecificity of this formal [4+3] cycloaddition originates from a highly regio- and stereoselective cyclopropanation event which is then conserved through the Cope rearrangement..[44] Consequently, several studies have been conducted with particular attention to the development of an asymmetric CPCR variant. Since the CPCR reaction is a stereospecific tandem process, an asymmetric synthesis would indeed be possible if the original cyclopropanation step was achieved with asymmetric induction. As such, initial studies initiated by the Davies group focused on the use of α-hydroxy esters as stoichiometric chiral auxiliaries.[45] A broad range of auxiliaries were studied and (*R*)-pantolactone afforded the highest levels of asymmetric induction. For example as illustrated in equation 1.3, the cyclopropanation of styrene with vinyldiazoacetate **39** using $Rh_2(OOct)_4$ at 0 °C afforded **40** in 97 % de.

$$(1.3)$$
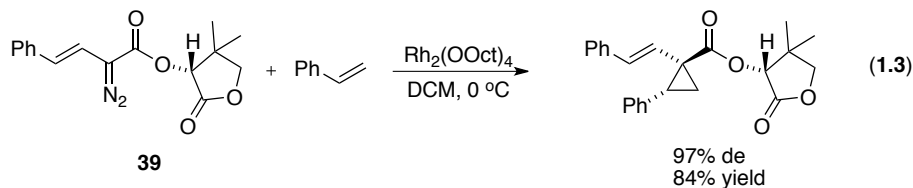
Extensive studies were subsequently undertaken to explain the observed stereochemistry of the cyclopropanation products. Experimental results suggested that a substantially rigid transition state must be present to account for the elevated degree of diastereocontrol. Such rigidity was thought to be built-up by the interaction of the carbonyl of the auxiliary with the vinylcarbenoid carbon (Figure 1.3).[46]
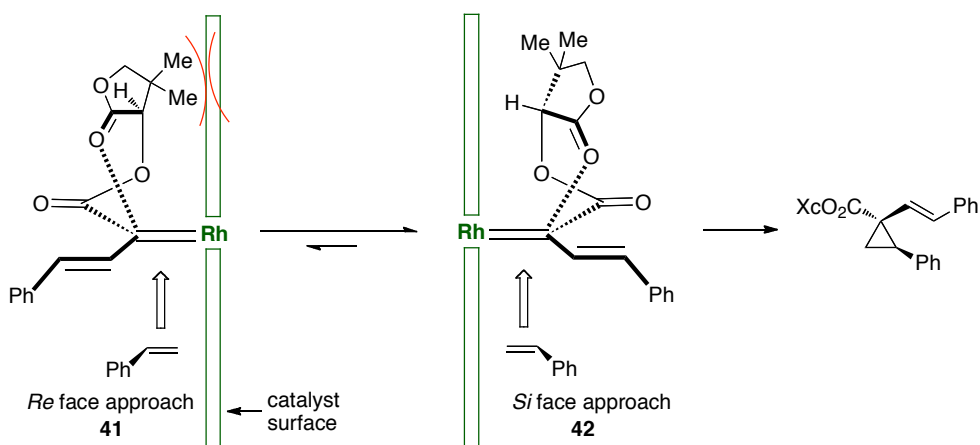
Figure 1.3 Proposed model for cyclopropanation with (*R*)-pantolactone auxiliary.

Moreover, an additional critical control element is the negative steric interaction between the chiral auxiliary and the catalyst surface. Specifically, conformer **42** is favored over conformer **41** due to the pantolactone ring pointing directly into the catalyst thereby generating an unfavorable transition state assembly. As such, the olefin is then restricted to approach the carbenoid from the *si*-face thus minimizing steric interactions between the auxiliary and the catalyst. This thorough study, provided a consistent working model

for the asymmetric cyclopropanation with α-hydroxy esters and rationalization of the observed absolute stereochemistry.

Having established an effective auxiliary-mediated asymmetric cyclopropanation approach, the methodology was extended to the CPCR reaction. Remarkably, the $Rh_2(OAc)_4$-catalyzed decomposition of vinyldiazoacetate **43** in the presence of cyclopentadiene resulted in the formation of the [4+3] cycloadduct **44** in 87% yield and 76% de (equation 1.4).

(1.4)

The successful combination of vinyldiazoacetates modified bearing a chiral auxiliary and cyclic dienes prompted the Davies group to investigate the use of acyclic dienes. In the presence of vinyldiazoacetate **45** and $Rh_2(OHex)_4$, an efficient formal [4+3] cycloaddition occurred to give hydroazulene **46** in 80% yield and >90% de (equation 1.5).[46] Such a reaction proved to be extremely valuable for facile entry to the hydroazulene core which is found in numerous natural product subfamilies.[47,48]

(1.5)
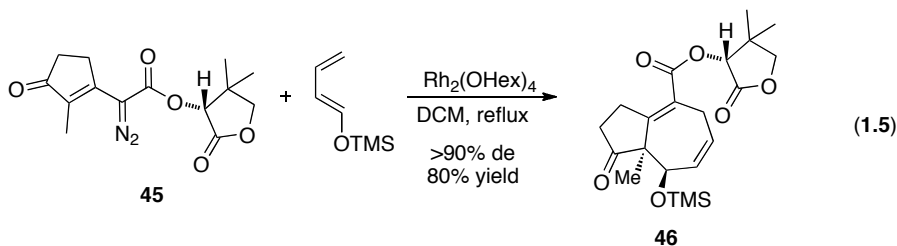
The incorporation of chiral auxiliaries as a means to invoke asymmetry provided the foundation for the asymmetric synthesis of cycloheptadiene ring systems. Following the

aforementioned studies, tremendous efforts were made to showcase the broad utility of the [4+3] cycloaddition. For example, furans served as excellent substrates leading to the formation of 8-oxabicyclo[3.2.1]octane derivatives.[43] In addition, the total synthesis of natural products such as norhalichondrin B[49] and englerin A[50] were feasible due to this extremely favorable reaction.
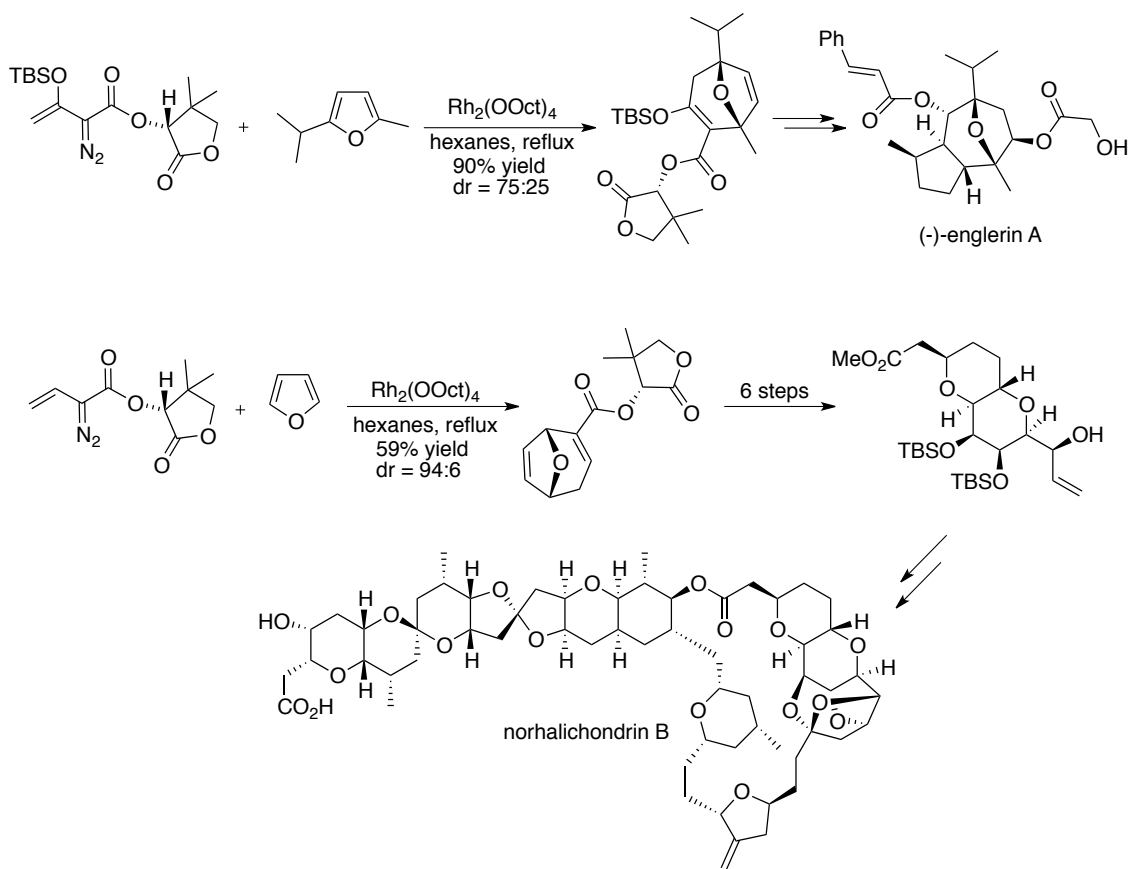
Scheme 1.8 Total synthesis of (-)-englerin A and norhalichondron B.

The [4+3] annulation approach has also proven to work well with *N*-Boc-protected pyrroles.[51] This reactivity provided entry to the extremely sought after tropane skeleton which is present in numerous alkaloids, many of which possess potent biological

activity.[52,53] As shown in Table 1.3, A wide range of tropanes were prepared in 30-85%

yield and 25-79% de.

Table 1.3 Asymmetric synthesis of tropanes using (*R*)-pantolactone as a chiral auxiliary.

entry	R$_1$	R$_2$	R$_3$	X	Yield (%)	de (%)
1	H	H	H	H	64	69
2	H	H	H	OTBS	66	68
3	Ph	H	H	OTBS	56	52
4	Ac	H	H	OTBS	69	78
5	-(CH2)$_4$		H	OTBS	31	37

The synthetic utility of this chemistry has been highlighted by the succinct synthesis of

several biologically relevant tropanes (Figure 1.4). Natural products ferruginine (**49**) and

anhydroecgonine methyl ester (**50**) were prepared by selectively hydrogenating the

appropriate [4+3] cycloaddition adduct followed by removal of the Boc protecting group

and subsequent *N*-methylation.[51,54] Moreover, several 4β-aryl-3β-propanoyl tropanes

such as **51**, a selective dopamine re-uptake inhibitor, and **52**, a selective serotonin re-uptake inhibitor, have been prepared using the chiral auxiliary approach.[55,56]
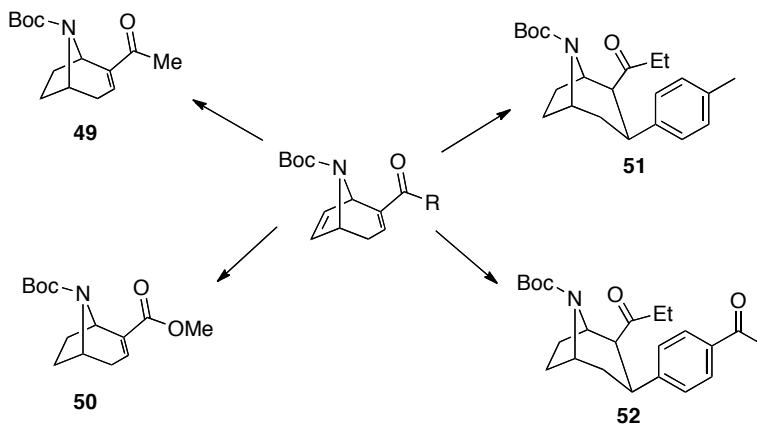
Figure 1.4 Biologically relevant tropanes accessed by CPCR reaction of *N*-Boc pyrrole.

The efficiency of the chiral auxiliary approach deserves merit as it is a reliable method leading to cycloheptadienes with high levels of asymmetric control. However, a major disadvantage to the methodology is the requirement of stoichiometric amounts of chiral auxiliary. Furthermore, the removal of the auxiliary by chemical modification introduces additional synthetic steps thus reducing time and conservation of atom economy for the entire process. These drawbacks have encouraged the development of chiral dirhodium catalysts for the decomposition of vinyldiazoacetates.

1.3 Rhodium-catalyzed enantioselective tandem cyclopropanation/Cope rearrangement

The first examples of intermolecular chiral dirhodium-catalyzed [4+3] cycloaddition reactions were conducted by Davies and co-workers.[57] The reaction of cyclopentadiene with vinyldiazoacetates using Rh$_2$(*S*-TBSP)$_4$ resulted in the asymmetric

construction of cycloheptadienes **53a-d** which were formed in 64-92% yield and 63-91% ee (Table 1.4).

Table 1.4 Rh$_2$(S-TBSP)$_4$ catalyzed decomposition of vinyldiazoacetates trapped by cyclopentadiene.
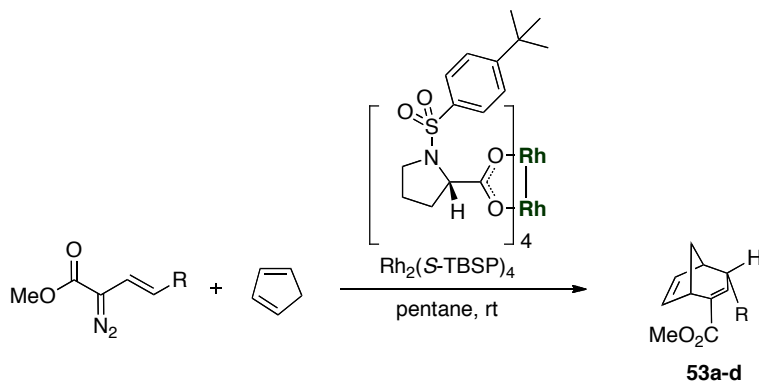
entry	R	ee (%)	yield (%)	product
1	H	63	76	**a**
2	CH=CH$_2$	91	64	**b**
3	Me	83	75	**c**
4	Ph	75	92	**d**

A broader substrate scope was efficiently established through the reaction of stryryldiazoacetate and various dienes (Scheme 1.9). In general, the Rh$_2$(S-TBSP)$_4$-catalyzed [4+3] cycloaddition produces synthetically useful levels of asymmetric induction (85-90% ee) and moderate to excellent isolated yields (41-95% yield).
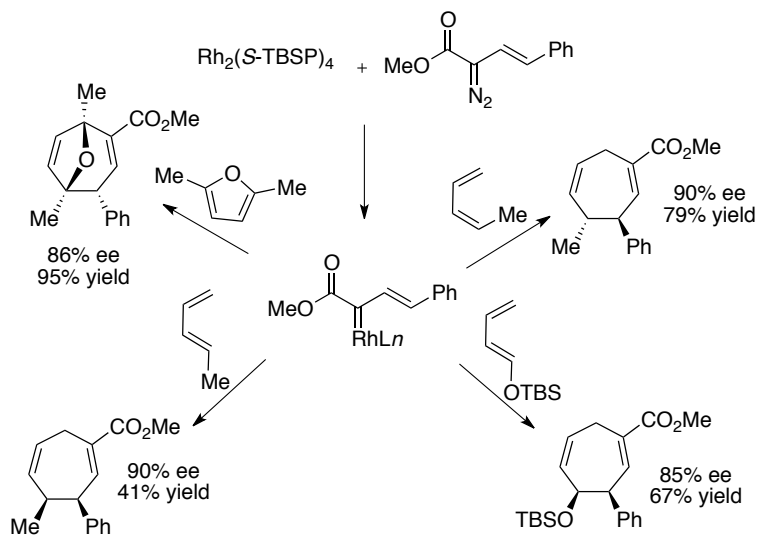
Scheme 1.9 Rh$_2$(S-TBSP)$_4$-catalyzed decomposition of vinyldiazoacetates in the presence

of various dienes.

Although the majority of the aforementioned reactions proceed in good yield and excellent levels of enantioinduction, identifying enantioselectivity optimization conditions especially for challenging [4+3] cycloadditions (Table 1.4, entries 1 and 3) proved to be difficult with Rh$_2$(S-TBSP)$_4$ due to inherent solubility issues. To address this problem, Davies disclosed Rh$_2$(S-DOSP)$_4$ as an extremely active and efficient catalyst for the asymmetric [4+3] cycloaddition reaction.[58] The major advantage to this catalyst is its superb solubility in hydrocarbon solvents and reactivity at temperatures as low as -78 °C, which significantly enhances the enantioinduction.

$$(1.6)$$
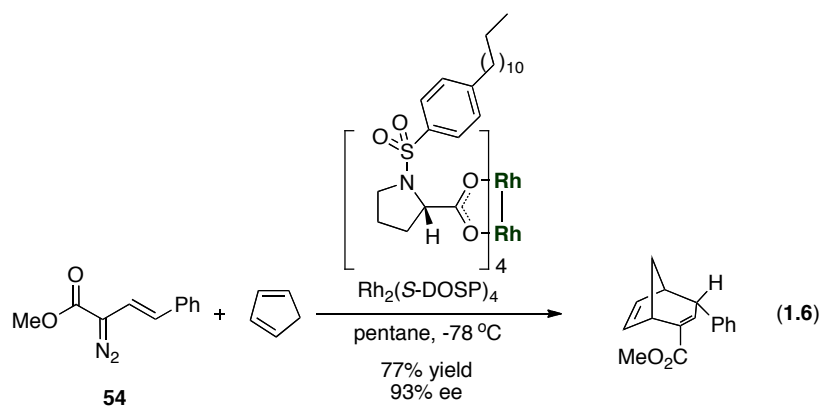
As illustrated in Equation 1.6, decomposition of **54** with Rh$_2$(*S*-DOSP)$_4$ in pentane at -78 °C allowed the formal [4+3] cycloaddition with cyclopentadiene to occur in 77% yield and 93% ee. Optimized conditions with Rh$_2$(*S*-DOSP)$_4$ provided entry to various cycloheptadiene systems with excellent levels of regio- and enantioselectivity. A comparison of selected CPCR reactions with Rh$_2$(*S*-DOSP)$_4$ and Rh$_2$(*S*-TBSP)$_4$ is shown in Scheme 1.10.
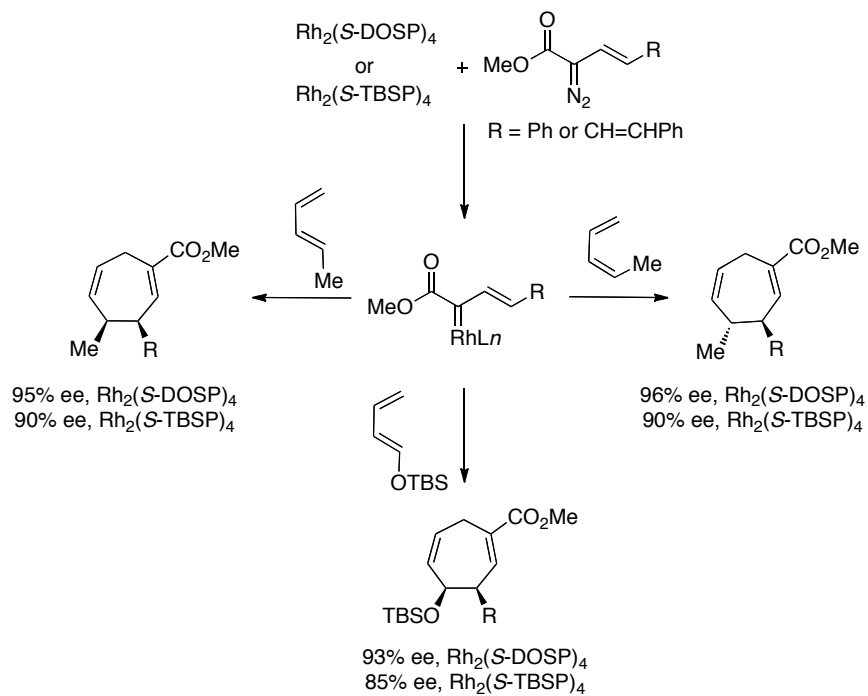
Scheme 1.10 Selected examples for the comparison of Rh$_2$(S-DOSP)$_4$ and Rh$_2$(S-TBSP)$_4$.

In general, the decomposition of vinyl terminus-substituted vinydiazoacetates by chiral rhodium prolinate catalysts provides a powerful means of generating the cycloheptyl motif with high levels of asymmetric induction and excellent regiochemical control. However, in the presence of Rh$_2$(S-DOSP)$_4$, the efficiency of enantioinduction for the CPCR reaction diminishes significantly when unsubstituted vinydiazoacetates are used as carbenoid precursors.[58] For example, unsubstituted vinydiazoacetate **3e** generated bicyclo[3.2.1]octadiene adduct **56e** in 70% yield and 63% ee (Table 1.5). Reactions with Me and OTBS substituents at the 3-position of the vinyldiazo, **55f** and **55g,** formed adducts **56f** and **56g** in 62% and 74% ee.

Table 1.5. CPCR reactions of Rh$_2$(S-DOSP)$_4$ with cyclopentadiene.
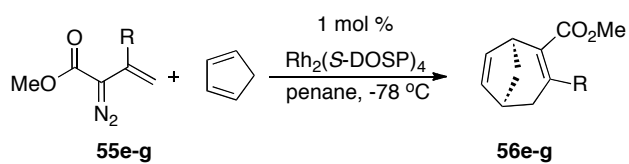
entry	R	ee (%)	yield (%)	product
1	H	63	70	**e**
2	Me	62	74	**f**
3	OTBS	74	97	**g**

Similar levels of asymmetric induction have been observed in the reaction with acyclic dienes.[59] As shown in Table 1.6, 3-siloxy-2-diazobutenoate **57** with *trans*-piperylene and

Rh$_2$(S-DOSP)$_4$ provided cycloheptadiene **58** in 43% ee when conducted at room temperature followed by heating at refluxing temperatures.

Table 1.6 Reaction of *trans*-piperylene with diazo **57** and Rh$_2$(S-DOSP)$_4$.

entry	conditions	ee (%)	yield (%)	product
1	hexanes, rt then reflux	43	85	**a**
2	hexanes, -26 then reflux	53	35	**b**
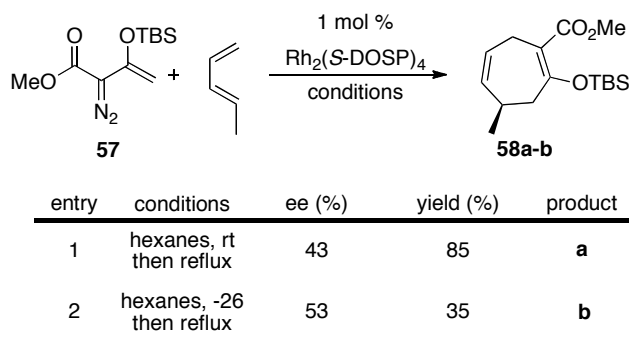
Initiating the reaction at -26 °C followed by reflux minimally improved the enantioselectivity to 53% ee. Moreover, this temperature modification was ultimately deleterious to the reaction yield as adduct **58b** was isolated in 35% yield. Recently, adamantylglycine derived dirhodium tetracarboxylate, Rh$_2$(S-PTAD)$_4$, has been shown to be a very effective chiral catalyst for carbenoid reactions when Rh$_2$(S-DOSP)$_4$ is not capable of providing efficient selectivity.[60,61] For example, in the CPCR reaction of **57** and *N*-Boc-pyrroles, Rh$_2$(S-PTAD)$_4$ gave excellent yields and enantioinduction compared to Rh$_2$(S-DOSP)$_4$ (Table 1.7, entries 2, 3 vs 1).[62]

Table 1.7 Comparison of Rh$_2$(S-PTAD)$_4$ and Rh$_2$(S-DOSP)$_4$ in the CPCR reaction of *N*-Boc pyrrole.

entry	catalyst	temperature (°C)	yield (%)	ee (%)
1	Rh$_2$(S-DOSP)$_4$	23	31	-29
2	Rh$_2$(S-PTAD)$_4$	23	38	91
3	Rh$_2$(S-PTAD)$_4$	50	86	92
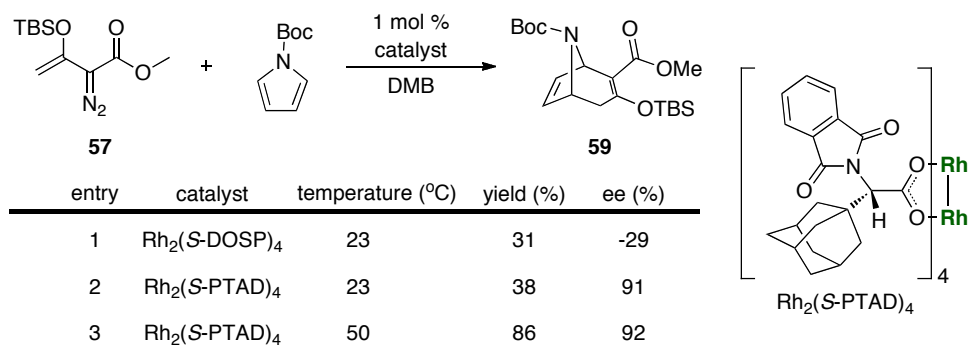
As expected, Rh$_2$(S-DOSP)$_4$ reacted poorly with the trapping agent to give tropane **59** in 31% yield and -29% ee (entry 1). At room temperature and in the presence of Rh$_2$(S-PTAD)$_4$ the desired tropane was formed albeit in a modest 38% yield due to poor conversion. However, adduct **59** was formed with excellent asymmetric induction (91% ee, entry 2). Increasing the temperature to 50 °C, solved the conversion issue and formed **59** in 86% yield without any erosion of asymmetric induction (92% ee, entry 3).

Given the successful combination of 3-siloxy-2-diazobutenoates and Rh$_2$(S-PTAD)$_4$, the chemistry was extended to address the difficulties associated the Rh$_2$(S-DOSP)$_4$/unsubstituted vinyldiazoacetate systems (Table 1.8).

Table 1.8. Rh$_2$(S-PTAD)$_4$-catalyzed CPCR reaction between siloxyvinyldiazoacetate **57** and various dienes.
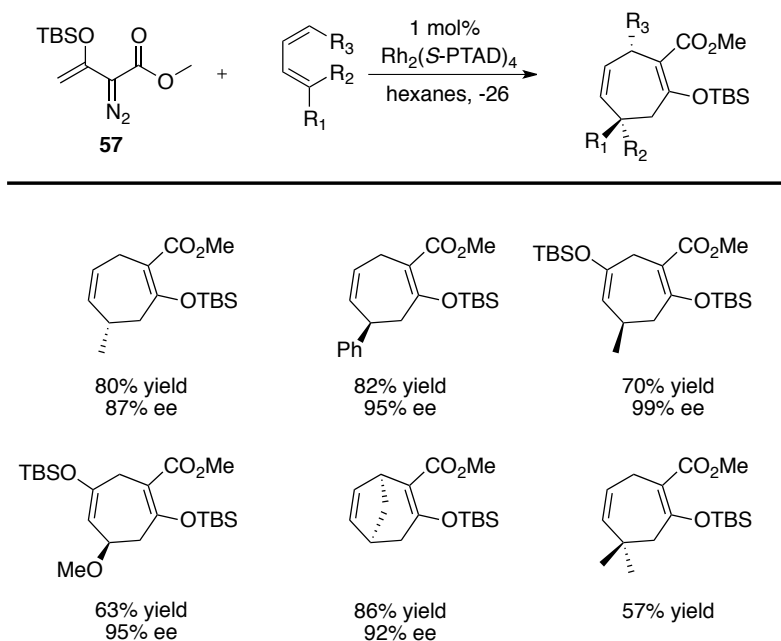
In all examples, the cycloheptadiene adducts were generated in good yields (57-86%).

Most importantly, all of the cycloadducts were synthesized with excellent levels of

enantioinduction (92-99% ee). The synthetic practicality of this new diazo/catalyst

combination has been elegantly showcased by Davies and co-workers in natural product

synthesis. Notably, the total synthesis of 5-*epi*-vibsanin E, (+)-barekoxide, (-)-barekol

were achieved using the Rh_2(*S*-PTAD)$_4$-catalyzed CPCR reaction between diazo **57** and

dienes as the key core-generating step. (Scheme 1.11).[63,64]
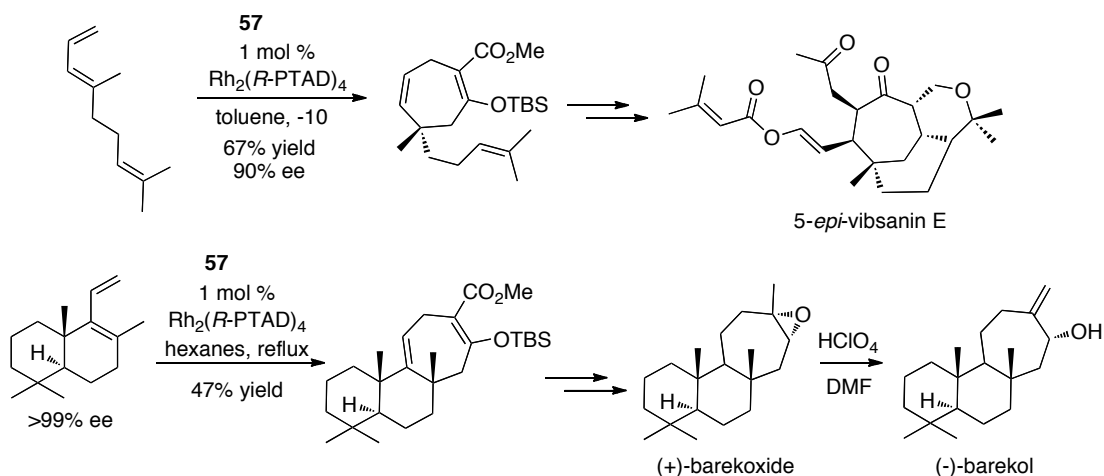
Scheme 1.11 Total synthesis of 5-*epi*-vibsanin E, barekoxide and barekol using the

Rh$_2$(*S*-PTAD)$_4$-catalyzed CPCR reaction between diazo **57** and dienes.

1.4 Vinylogous reactivity of vinylcarbenoids

In the early 1990's, Davies' longstanding interest in vinylcarbenoids led to the discovery that terminally unsubstituted vinyldiazoacetates were prone to nucleophilic attack at the terminus position as a result of solvent and catalyst effects.[65] For example, in the presence of vinyldiazoacetate **60**, cyclopentadiene, Rh$_2$(OAc)$_4$, and pentane as solvent the expected CPCR adduct was isolated as the major product (Table 1.9, entry 1, isomer B). However, a small amount of bicyclo[2.2.1]heptene **62** (5%) was formed along with the major product. Solvent as well as catalyst variation studies were explored to explain the unexpected appearance of **62**.

Table 1.9. Effect of catalyst and solvent on the Rh(II)-catalyzed decomposition of **60** in

the presence of cyclopentadiene.
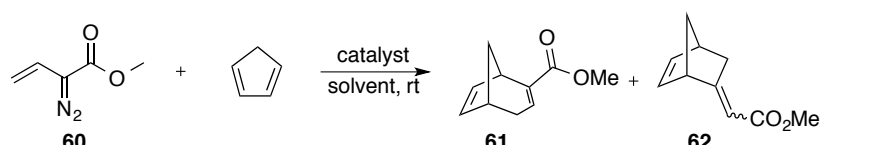
entry	catalyst	solvent	ratio (**61:62**)	yield (**61+62**), %
1	Rh$_2$(OAc)$_4$	pentane	95:5	85
2	Rh$_2$(OAc)$_4$	DCM	67:33	81
3	Rh$_2$(TFA)$_4$	DCM	32:68	60[a]

[a] reaction achieved 88 % conversion
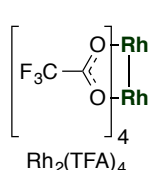
Conducting the reaction in a polar solvent such as DCM in the presence of Rh$_2$(OAc)$_4$ (entry 2) increased the formation of adduct **62** to a ratio of 67:33 indicating preference over the "cabenoid-reactivity" derived adduct **61**. Interestingly, the formation of **62** was significantly enhanced (32:68) by using an electron deficient catalyst, Rh$_2$(TFA)$_4$ in DCM. The possibility of an intermolecular Diels-Alder cycloaddition between **60** and cycloheptadiene was omitted as removal or late introduction of the catalyst showed no enhancement of **62**. Therefore, the formation of **62** was attributed to competition of the vinyl terminus as an electrophilic center.
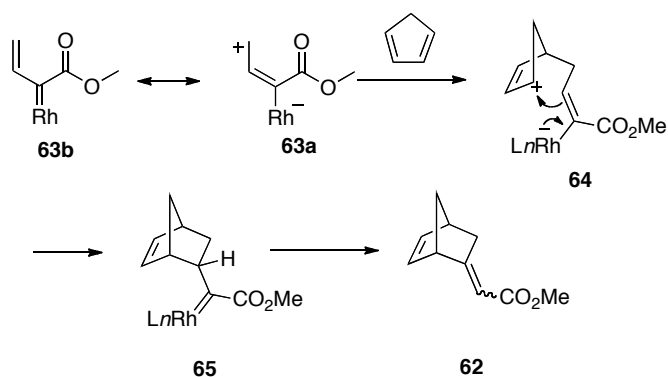
Scheme 1.12 Proposed mechanism for the formation of **62**.

A proposed mechanism is outlined in Scheme 1.12. Interaction at the terminus position of dipolar resonance structure **63a** with cyclopentadiene generates dipolar structure **64** which then undergoes efficient ring closure to afford metallocarbenoid **65**. Lastly, rearrangement of **65** *via* a 1,2-hydride shift[66] provides bicycloadduct **62**. Four years later, additional studies were disclosed by Davies describing the guiding principles to carbenoid versus vinylogous reactivity of rhodium(II)-stabilized vinylcarbenoids.[67]

Table 1.20 Steric effects of ester on vinylogous reactivity.

entry	66		67	68
1	**60** (R = Me)		**67a** (24%)	**68a** (37%)
2	**66b** (R = ^{t}Bu)		**67b** (22%)	**68b** (33%)
3	**66c** (R = BHT)		**67c** (90%)	**68c** (0%)
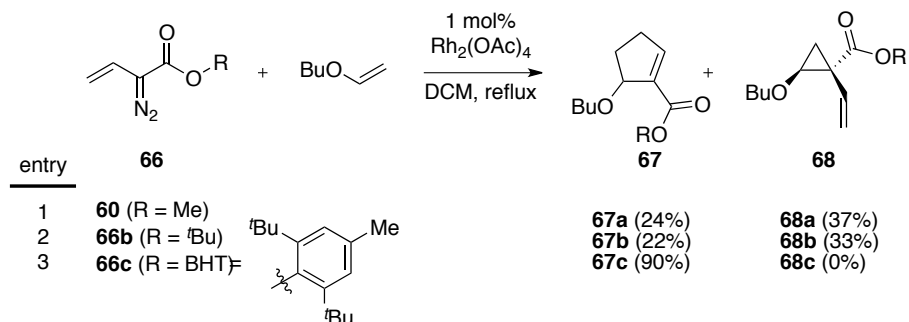
Under refluxing conditions using DCM as solvent, the $Rh_2(OAc)_4$-catalyzed decomposition of vinyldiazoacetate **60** in the presence of butyl vinyl ether led to the formation of cyclopentene **67a** (24% yield) and vinylcyclopropane **68a** (37% yield, Table 1.20, entry 1). The formation of vinylcyclopropane **68a** is a product of reactivity occurring at the carbenoid center. In stark contrast, the formation of adduct **67a** is attributed to the initial interaction between the vinyl ether and the terminus position of the vinylcarbenoid. Changing the ester substituent from methyl to *tert*-butyl resulted in only minor changes on product ratio (entry 2). However, increasing the steric demand of the ester to the 2,6-di-(*tert*-butyl)-4-dihydroxytolyl (BHT) derivative resulted in complete selectivity in favor of cyclopentene **67c** (entry 3). This result further supports the hypothesis that cyclopentene formation occurs through initial attack at the vinylogous position of **66c** as sterically demanding ester groups would be expected to obstruct the trajectory of nucleophiles to the carbenoid center. Further studies conducted by Davies indicated that cyclopentene formation did not occur via a concerted process. Instead, likely involvement of zwitterionic intermediates was proposed due to the nature of the reactant and reaction conditions.[67] Compiling the studies conducted by Davies and co-

workers, a group of guiding principles was established which suggest conditions which promote vinylogous reactivity of vinyldiazoacetates.
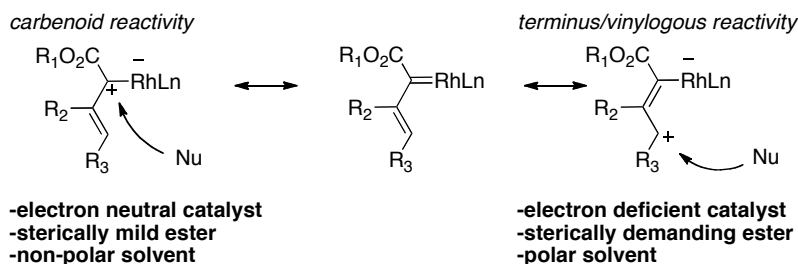
Figure 1.5 Electrophilic sites of vinylcarbenoids.

As illustrated in Figure 1.5, carbenoid reactivity is generally favored when electron neutral catalysts, sterically mild esters and non-polar hydrocarbon solvents are combined with vinyldiazoacetates. If the primary interest is to exploit terminus reactivity, highly electron-deficient catalysts, sterically demanding esters and polar halogenated solvents prove to be the most favorable set of reaction conditions.

As previously described in the rhodium-catalyzed asymmetric tandem cyclopropanation/Cope rearrangement reaction, 3-siloxy-2-diazobutenoates are excellent vinylcarbenoid precursors. Unsubstituted vinyldiazoacetates are known to readily undergo electrocyclization to the corresponding pyrazole derivatives.[68-70] However, an added benefit to siloxyvinyldiazoacetates is their resistance to the formation of pyrazoles making them excellent candidates for various rhodium-catalyzed decomposition reactions. Moreover, these vinylcarbenoids are also capable of undergoing attack at the vinylogous position under optimized reaction conditions. As such, several recent studies cogenerated independently by the Doyle and Davies laboratories have taken advantage of this unique vinylcarbenoid reactivity in various vinylogous-initiated reactions.
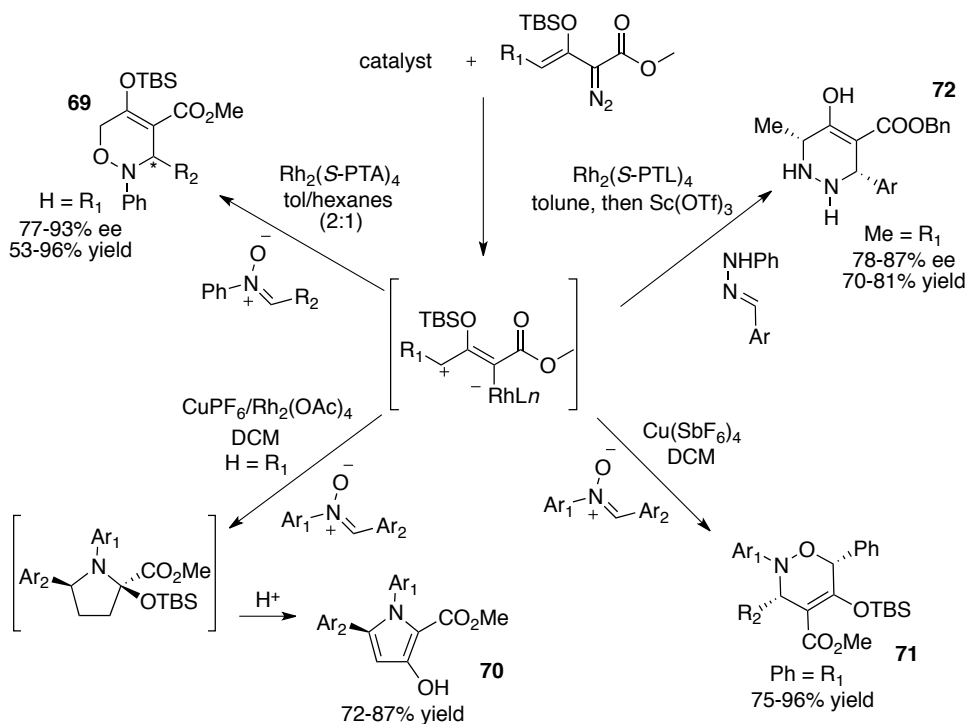
Scheme 1.13 Synthesis of various heterocycles *via* Dolye's vinylogous methodology.

As shown in Scheme 1.13, the Doyle laboratory has elegantly used siloxyvinyldiazo carbenoids with nitrones to access several interesting heterocycles **69**,[71] **70**,[72] and **71**[73]. Judicious choice of transition-metal catalyst affords access to distinct products. In the presence of $Rh_2(S\text{-PTL})_4$ and $Sc(OTf)_3$, hydrazones undergo a vinylogous N-H insertion followed by a Lewis acid catalyzed Mannich addition reaction to efficiently construct various tetrahydropyridazines (**72**) in good yields (70-81%) and excellent levels of asymmetric induction (78-87% ee).[74]

In the Davies group, the combination of unsubstituted siloxyvinyldiazoacetates and cyclic silyl enol ethers catalyzed by $Rh_2(esp)_2$ led to the development of a new method to access alkynoates of type **75** *via* vinylogous reactivity in moderate to excellent yield (33-98%) and excellent diastereoselectivity (Scheme 1.14).[75]
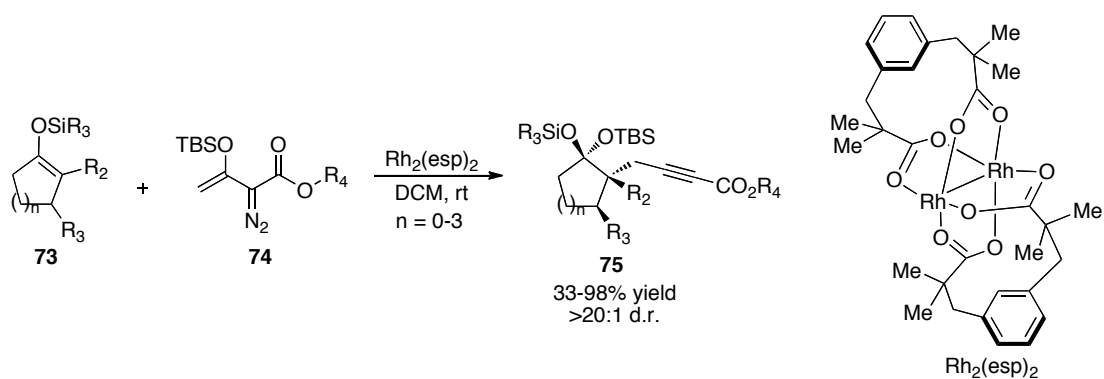
Scheme 1.14 Alkynoate synthesis *via* vinylogous reactivity of siloxyvinylcarbenoids.

This new reaction encompassed three mechanistically distinct transformations which were particularly interesting because i) the formation of alkynoate **75** was formed as the result of a rhodium(II)-catalyzed vinylogous addition reaction ii) the disiloxy ketal functional group was constructed *via* an unprecedented siloxy group migration event from siloxyvinylcarbenoid **76/77** which was previously unknown in the carbenoid literature, and iii) the reaction occurs though an extremely diastereoselective manifold. A proposed mechanism for alkynoate formation is outlined in Scheme 1.15.
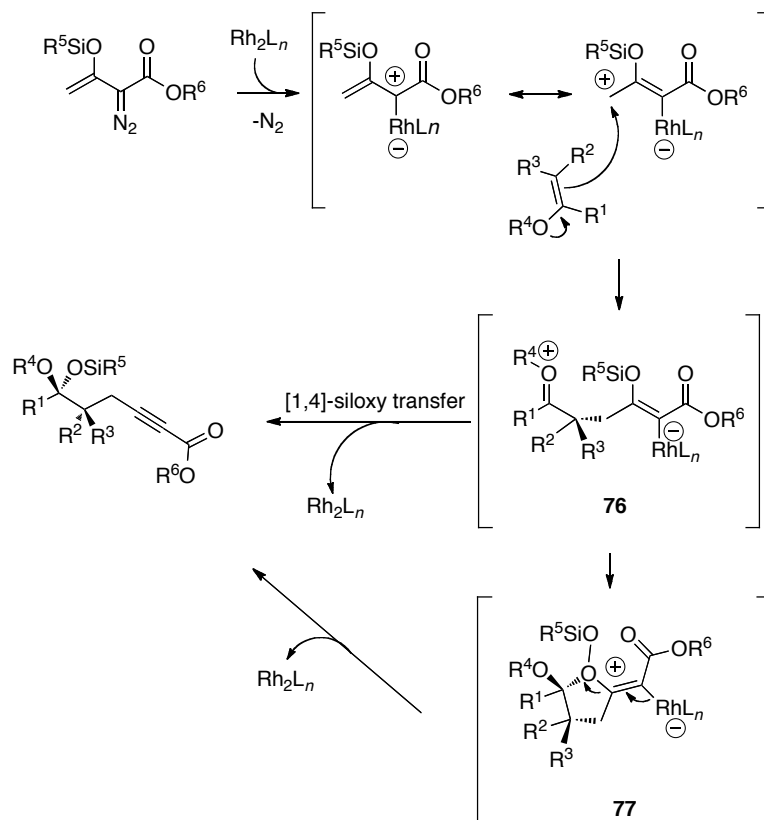
Scheme 1.15 Mechanistic rational for alkynoate formation.

Nucleophilic attack of the enol ether's electron rich terminus onto the electrophilic vinylogous position of the siloxyvinylcarbenoid gives rise to zwitterionic intermediate **76**. Subsequent [1,4]-siloxy group transfer or stepwise addition to the oxocarbenium ion *via* intermediate **77** followed by β-elimination leads to the observed alkynoate. Notably, previous studies have shown that Rh(II)-stabilized β-siloxy vinylcarbenoids adopt an *s-cis* conformation, in which the siloxy group is directed away from the catalyst surface.[76,77] This orientation was found to be consistent with the rhodium carboxylate and the siloxy group adopting and anti-periplanar arrangement, thus facilitating the β-elimination process.

30

Subsequent studies showed that highly asymmetric vinylogous additions were indeed possible in the presence of acyclic silyl enol ethers catalyzed by Rh$_2$(S-PTAD)$_4$ (Scheme 1.16).[78] Interestingly, excellent product selectivity is obtained depending on the nature of the silyl enol ether substrate (path a). For example, it was determined that small silyl enol ethers prefer the formation of acyclic alkynoates. A broad range of alkynoates can be accessed in good yields (48-84% yield) with excellent enantioselectivites (80-97% ee). In contrast, when sterically demanding silyl enol ethers are employed, an enantioselective formal [3+2] cycloaddition pathway is preferred (path b).
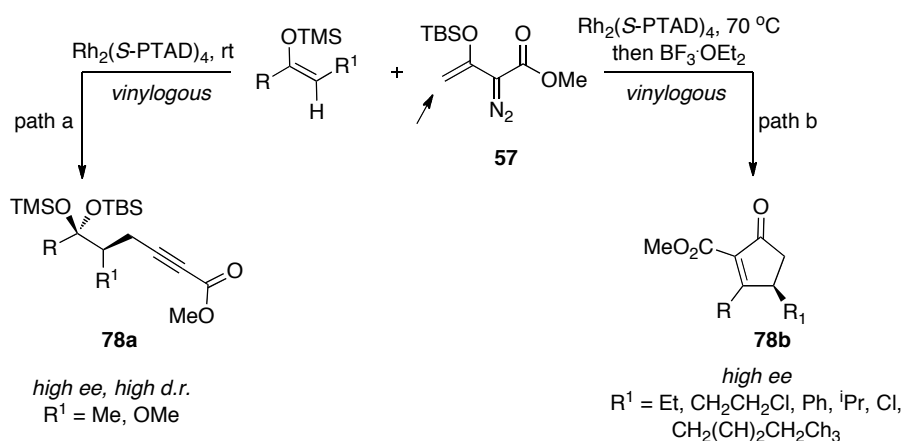
Scheme 1.16 Enantioselective synthesis of acylic alkynoates and cyclopentenones *via* vinylogous addition of acyclic silyl enol ethers.

The [3+2] adducts can be efficiently converted into cyclopentenones by treatment with BF$_3$·OEt$_2$ in DCM at 0 °C. As such, a series of cyclopentenones were synthesized in moderate to good yields (29-70%) and in excellent levels of enantioselectivity (90-94% ee). A tentative mechanism was formulated to explain the formation of compounds **81** and **84** (Scheme 1.17). Based on experimental results, it is proposed that the silyl enol ether approaches the chiral rhodium carbenoid from the *re*-face as drawn (**79**). The (Z)-

geometry of the enol ether strongly commands the attack *via* an end-on mode, in which both the OTMS and R[1] groups are pointed away from the phthalimido blocking groups.[79-82] Vinylogous addition followed by subsequent OTBS group transfer/β-elimination from momentary intermediate **80** in which the oxocarbenium ion is appropriately aligned with a participating lone pair on the OTBS group. In contrast, when the R1 group is sterically demanding, the side-on approach of the silyl enol ether provides **83** which is correctly aligned to undergo a diastereoselective ring closing reaction to access compound **84**. Notably, the similar but not identical levels of asymmetric induction for the two products are consistent with two distinct mechanisms that are distinguished by minute alteration in the approach of the nucleophile to the vinylcarbenoid.
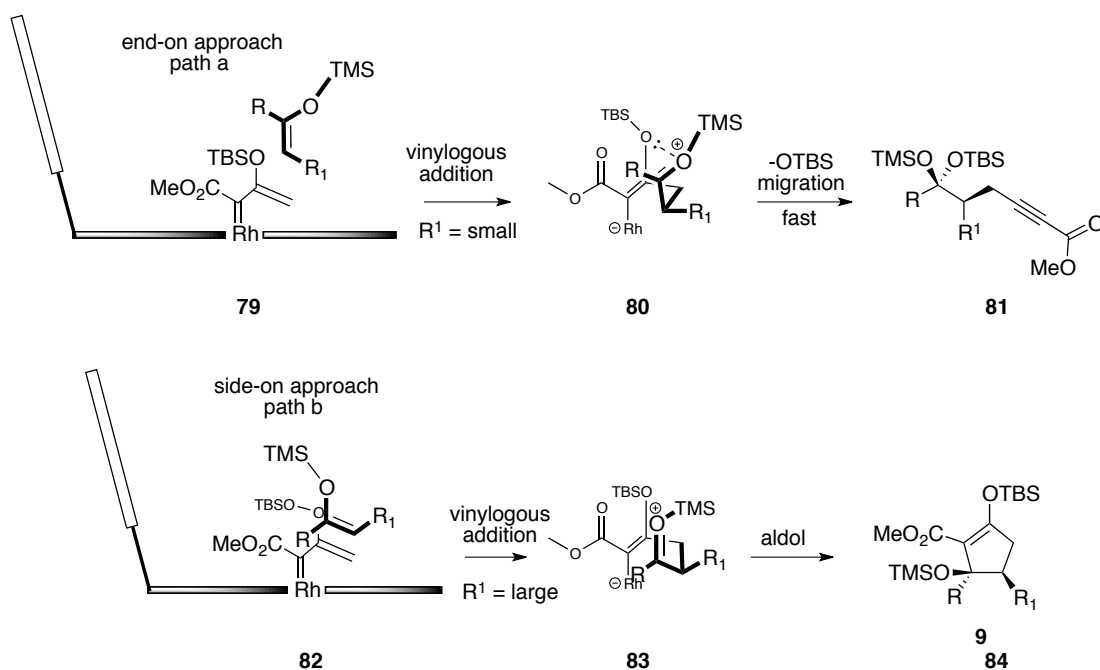
Scheme 1.17 Tentative mechanism for the formation of **81** and **84**.

1.5 Results and discussion

The Diels-Alder cycloaddition reaction is revered as one of the most effective methods for the stereoselective formation of six-membered rings and has shown its synthetic capability through the synthesis of numerous natural products.[83-87] Excellent regioselectivity is consistently achieved as a result of efficient overlap between the HOMO of the diene and the LUMO of the dieneophile.[88,89] As a consequence, the incapacity to access the opposite Diels-Alder regioisomer exposes an inherent limitation to the methodology (Scheme 1.18).
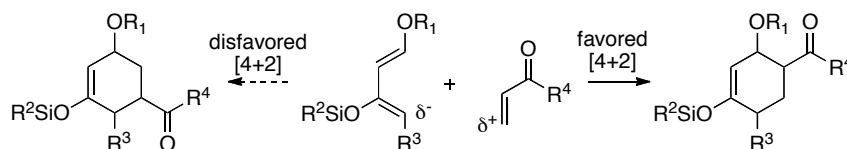
Scheme 1.18 Intermolecular regioselective Diels-Alder cycloaddition.

As a homolog of the [4+2] cycloaddition, the formal [4+3] cycloaddition of vinylcarbenoids and dienes provides an attractive method to access 7-membered rings. Despite the presence of seven-membered rings in many naturally occurring structures, the [4+3]-cycloaddition has received a fraction of the attention given to the [4+2] transformation. During the investigation of the $Rh_2(S\text{-PTAD})_4$-catalyzed tandem cyclopropanation/Cope rearrangement (CPCR) reaction, Dr. Yajing Lian discovered the possibility of reversing the regiochemistry of the cycloaddition adduct, a feature that has not been possible for the [4+2] transformations. To validate this hypothesis, Dr. Lian

conducted a proof-of-concept reaction under conditions that would favor vinylogous reactivity (equation 1.7).
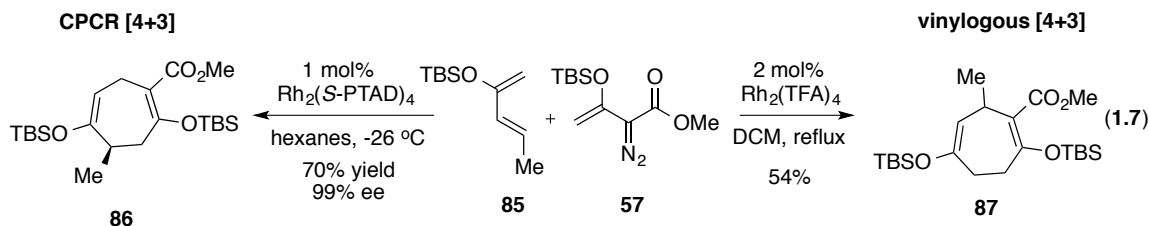
Indeed, in the presence of $Rh_2(TFA)_4$ and DCM, siloxy diene **85** initiated attack at the vinylogous position of siloxyvinyldiazo **57** to yield vinylogous [4+3] adduct **87** in 54 % yield with no trace of the CPCR [4+3] adduct. The purpose of this project was to develop an asymmetric variant of the vinylogous [4+3] cycloaddition and to determine its synthetic scope.

Reaction development was initiated with (E)-pent-3-en-2-one-derived diene **85** and efforts were focused on evaluating the significance of polar and non-polar solvent effects in the presence of chiral Rh^{II} catalysts. Specifically, dichloromethane and pentane were evaluated as they are well documented to enhance vinylogous reactivity of vinylcarbenoids[67] and increase the degree of asymmetric induction.[78]

Table 1.21 Catalyst and solvent optimization.
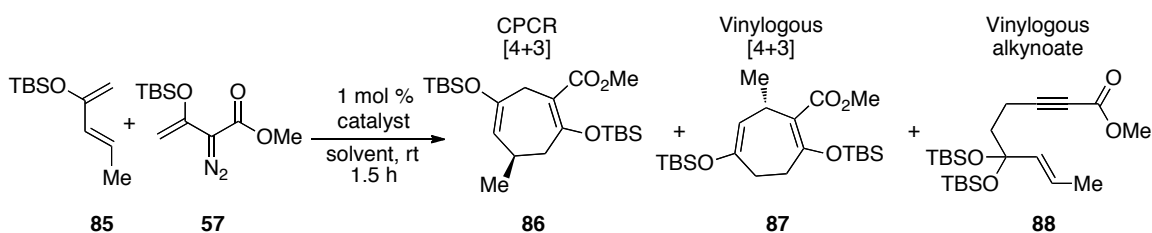
entry	solvent	catalyst	ratio[a] **86** : **87** : **88**	yield (%)	% ee[c]
1	DCM	Rh$_2$(S-DOSP)$_4$	30 : 70 : 0	61[b]	5
2	DCM	Rh$_2$(S-PTAD)$_4$	87 : 13 : 0	43[b]	-71
3	DCM	Rh$_2$(S-BTPCP)$_4$	4 : 70 : 26	37, 16[d]	54
4	pentane	Rh$_2$(S-DOSP)$_4$	79 : 21 : 0	62[b]	33
5	pentane	Rh$_2$(S-PTAD)$_4$	94 : 6 : 0	55	-73
6	pentane	Rh$_2$(S-BTPCP)$_4$	9 : 29 : 62	23[b], 42[d]	87

[a] Determined by ^{1}H NMR of crude reaction mixture, [b] regioisomer **86** and **87** combined, [c] %ee for **87**, [d] isolated yield for **88**.

As summarized in Table 1.21, after an extensive screening of chiral dirhodium catalysts, it was discovered that Rh$_2$(S-BTPCP)$_4$ is an excellent catalyst to achieve promising levels of regiochemical control and thus was optimal for this reaction. Two products were isolated both of which arose from terminus reactivity. The desired vinylogous adduct **87** was isolated in 37% yield and 54% ee along with alkynoate **88** which was isolated in 16 % yield (entry 3). Rh$_2$(S-DOSP)$_4$ produced a 30:70 mixture of cycloadducts **86:87** with poor enantioselectivity and Rh$_2$(S-PTAD)$_4$, entry 5, strongly favored the CPCR derived cycloadduct **86**. Interestingly, the formation of alkynoate **88** was not observed with Rh$_2$(S-PTAD)$_4$ or Rh$_2$(S-DOSP)$_4$. The use of nonpolar solvents proved to be critical as a significant increase in enantioselectivity for adduct **87** was observed; 87% ee (entry 6). However, the chemoselectivity of the reaction also shifted towards substantial formation of alkynoate **88** which was isolated in 42% yield. Rh$_2$(S-PTAD)$_4$ and Rh$_2$(S-DOSP)$_4$ (entries 4 and 5) gave similar regioselectivities to entries 1 and 2 and exhibited a low to

moderate increases in enantioinduction. Having established parameters for the formation of **87**, studies proceeded to investigate conditions directed towards inhibiting the formation of alkynoate **88**. As previously mentioned, the Davies group has reported a method for the synthesis of alkynoates derived from cyclic and acyclic silyl enol ethers *via* vinylogous reactivity of vinyldiazoacetates.[75,78] Similarly, the formation of alkynoate **88** is proposed to occur by nucleophilic attack of the diene **85** onto the electrophilic terminus of siloxy-vinylcarbenoid **89b** which leads to zwitterionic intermediate **90a** (Scheme 1.19). A 1,4-siloxy group migratory event (**90a** to **88**) or ring closure to generate dihydrofuran intermediate **90b**, *via* addition of an oxygen lone pair from vinyldiazoacetate's (**89b**) OTBS group, to the nascent oxocarbenium ion and subsequent β-elimination generates compound **88**.

36
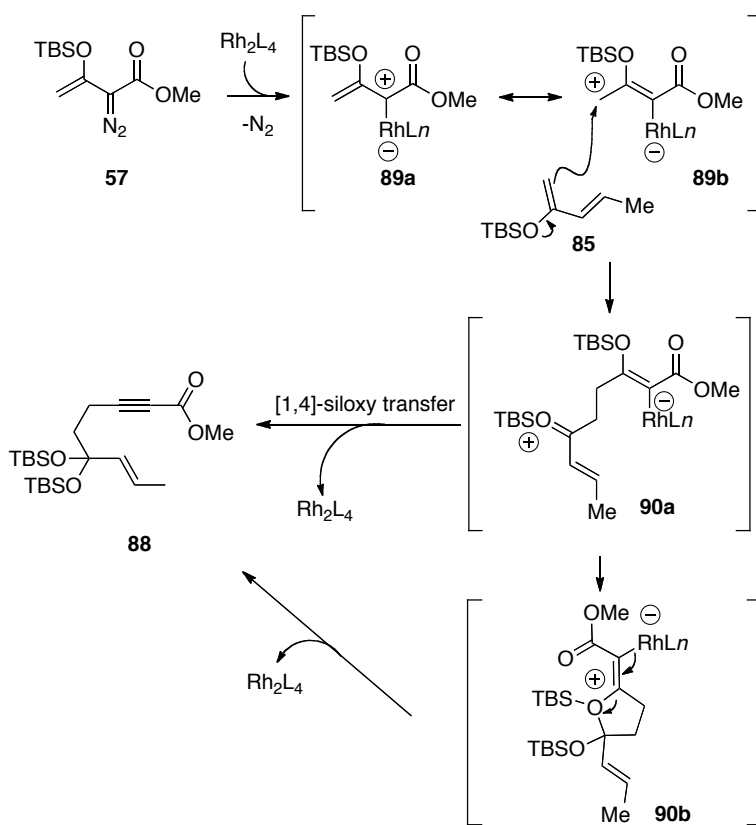
Scheme 1.19 Proposed mechanism for the formation of **88**.

With an understanding of the mechanistic pathway leading towards alkynoate formation, the incorporation of a butadiene trapping agent bearing a sterically demanding silyl enol ether was proposed to drastically increase the steric environment about the transient oxocarbenium ion thereby reducing the propensity for siloxy group transfer or siloxy lone pair participation. The modifications are summarized in Table 1.22.

Table 1.22. Reduction of alkynoate formation.
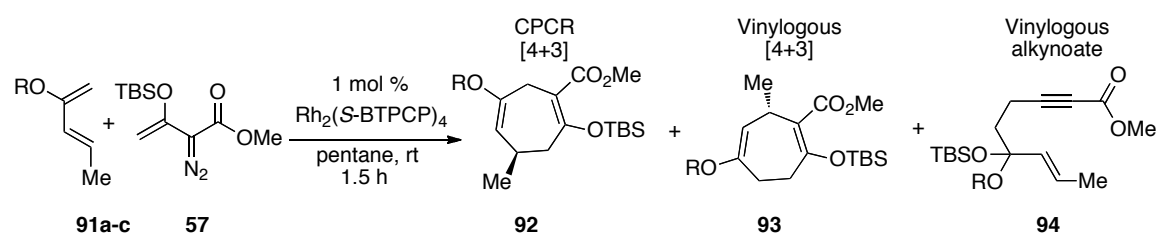
entry	diene	R	ratio[a] 11a : 11b : 11c	yield (%)	% ee[c]
1	**91a**	TMS	14 : 18 : 68	16[b], 45[d]	70
2	**91b**	TBS	9 : 29 : 62	23[b], 42[d]	87
3	**91c**	**TIPS**	**5 : 95 : trace**	**59**	**96**

[a] Determined by ^{1}H NMR of crude reaction mixture, [b] yield for **92** and **93** combined, [c] adduct **94**.

Indeed, variation of the diene's siloxy group steric demand induced a profound effect on the chemo-, regio- and enantioselectivity of the reaction (entries 1-3). Trimethylsilyl functionalized butadiene favored the formation of alkynoate **94**, which was isolated in 45 % yield and produced a 43:56 mixture of cycloadducts **92:93**. It was hypothesized that the low levels of regioselectivity with OTMS functionalized dienes is due to the lack of discrimination between cyclopropanation and vinylogous reactivity. To test this hypothesis, exposure of siloxybutadiene **81c** to optimized CPCR reaction conditions

produced the CPCR adduct in 33% yield and 67% ee (equation 1.8) which strongly correlates with previous examples that describe the difficulty of cyclopropanation of sterically demanding 1,1-di-substituted electron rich alkenes.[90]
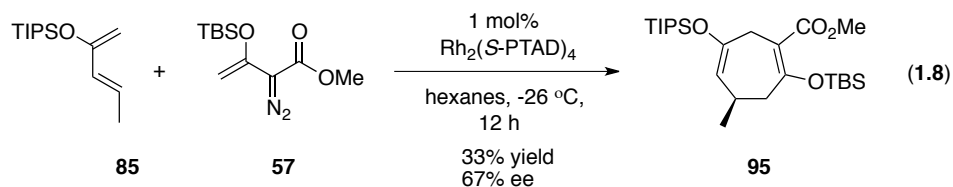
Most notably, the triisopropylsiloxy functionalized butadiene simultaneously decreased the formation of alkynoate **94** to trace levels, inverted the regioselectivity to 5:95 in favor of the vinylogous adduct **93** and elevated the degree of asymmetric induction to 96% ee. These reactions provided crucial insight for the subtle governing factors associated with the observed regioselectivities. Having established optimized conditions for the formation of adducts of type **93**, the study continued and explored the scope of silyl enol ether and vinyldiazoacetate substrates. As described in Table 1.23, a variety of cycloadducts are readily accessed in high yield with excellent levels of stereocontrol (59-80% yield, >30:1 dr, 90-99% ee, **98a-i**).

Table 1.23 Vinylogous [4+3] substrate scope.

57 : R$_3$ = H
97 : R$_3$ = Me (E:Z = 91:9)

91a-i

98a-i, >20:1 d.r.

98a

40 % yield[a], 94% ee
77 % yield[b], 95% ee

98b

complex mixture

98c

no reaction[b]

98d

38% yield[a], 90% ee
78% yield[b], 87% ee

98e

50% yield[a], 92% ee
65% yield[b], 82% ee

98f

38% yield[a], 99% ee
59% yield[b], 99% ee

98g

45% yield[a], 99% ee
57% yield[b], 99% ee

98h

52% yield[b], 99% ee

98i

80% yield[b], 92% ee[c]

[a] 5 equivalents of diene, pentane, rt, [b] 2 equivalents of vinyldiazo, hexanes, reflux. [c] % ee of corresponding allylic alcohol. Enantiomeric excess was determined by chiral HPLC. Yield refers to isolated yield after silica gel chromatography.

Elevated temperatures and a two-fold excess of vinylsiloxydiazoacetate afforded increased reaction yields with slight erosion of enantioselectivity in certain cases (**98d**, **98e**). Ambient temperatures gave moderate to good yields with excellent levels of asymmetric induction (**98a, 98d-f**). 1-(cyclohex-1-en-1-yl)ethanone and 1-(cyclopent-1-

en-1-yl)ethanone derived dienes afforded structurally interesting bicyclic motifs (**98d** and **98e**).

Methyl-substituted (*Z*)-vinylsiloxydiazoacetate **97** proved to also be susceptible to nucleophilic attack and provided mono- and bicyclic adducts featuring two remote *cis*-stereocenters (**98f-i** 38-80% yield, 92-99% ee). The relative stereochemistry for these compounds was established by extensive nOe correlation experiments of adducts **98g** and **100b** (Figure 1.6).

98g
R^1 = CO_2Me
R^2 = OTBS
R^3 = *p*ClPh

100b
R^1 = OTIPS
R^2 = *p*ClPh
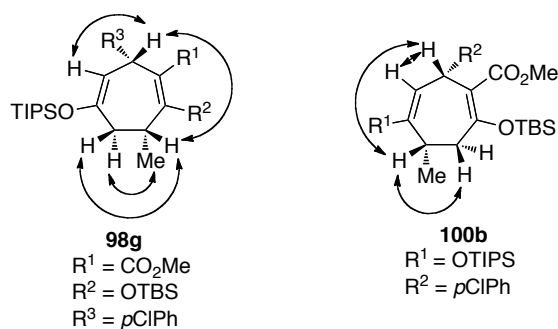
Figure 1.6 Key nOe correlations for compounds **18h** and **20b**.

Notably, an apparent limitation to the vinylogous [4+3] is its restriction to moderately electron rich diene substrates. For example, highly electron-rich dienes such as the triisopropyl variant of Danishefky's diene results in the formation of a complex mixture of products (**98b**) while dienes substituted with electron withdrawing aryl functional groups (**98c**) resisted reaction with vinylcarbenoids even under forcing conditions. In an effort to extend the synthetic utility for this new formal cycloaddition process, an extended diastereoselective vinylogous [4+3] reaction was investigated by introducing geometrically enriched isomer mixtures of the diene.

Table 1.24 Diasterereoselective vinylogous [4+3] cycloaddition.

Entry	diene	catalyst	Product	Yield (%)[a]	ee(%)[b]	d.r.
1	**99a** (Z,E) : (E,E) = 91 : 9	Rh$_2$(S-BTPCP)$_4$	**100a**	68	96	>20:1
2	**99b** (Z,E) : (E,E) = 88 : 12	Rh$_2$(S-BTPCP)$_4$	**100b**	71	96	>20:1
3[c]	**99b**	Rh$_2$(pfb)$_4$	**100c**	39	-	46:54

[a] Yield refers to isolated yield after silica gel chromatography, [b] Enantiomeric excess was determined by chiral HPLC. [c] 2 equivalents of siloxyvinyldiazo, 2 mol% catalyst, DCM, reflux, combined yield.

A shown in Table 1.24, a 91:9 mixture of (Z,E):(E,E)-**99a** was subjected to optimized reaction conditions. Vinylogous adduct **100a** was isolated in 68% yield and 96% ee as a single diastereoisomer. An 88:12 mixture of (Z,E):(E,E)-**99b** (entry 2) gave similar results (71% yield, 96% ee). Exposure of **99b** to electron-deficient achiral dirhodium catalyst Rh$_2$(pfb)$_4$, in dichloromethane, resulted in the formation of a 46:54 mixture of diastereomeric vinylogous adducts (entry 3). The emergence of this mixture establishes the critical combination of pentane as solvent and chiral dirhodium triaryalcylcopropanecarboxylate Rh$_2$(S-BTPCP)$_4$ as catalyst.

41

Furthermore, as a result of the absence of steric bias delivered by the catalyst, this finding suggests a reaction pathway involving both s-*cis* and s-*trans* isomers of **99b** reacting with the vinylcarbenoid thus resulting in diminished facial selectivity upon ring closure.

As a highlight to this method, the formation of three contiguous stereocenters was investigated by reacting diene **99a** with vinyldiazoacetate **97** (equation 1.9). Vinylogous cycloadduct **101** was isolated in 72% yield using elevated temperatures to increase conversion. The relative configuration of **101** was determined, by means on nOe analysis, to have the three methyl groups in a *cis* orientation. Chiral HPLC analysis of **101** was not effective for the determination of the level of enantioselectivity in the [4+3] cycloaddition. Therefore, **101**, was treated with DIBAL in DCM at 0 °C. These conditions generated the allylic alcohol **102**, consistent with a related transformation used in the synthesis of barekoxide.[64] The relative configuration of **102** is tentatively assigned, assuming hydride attack occurs from the more accessible convex face, but more importantly, **102** was used to determine that the cycloaddition had proceeded in 85% ee.
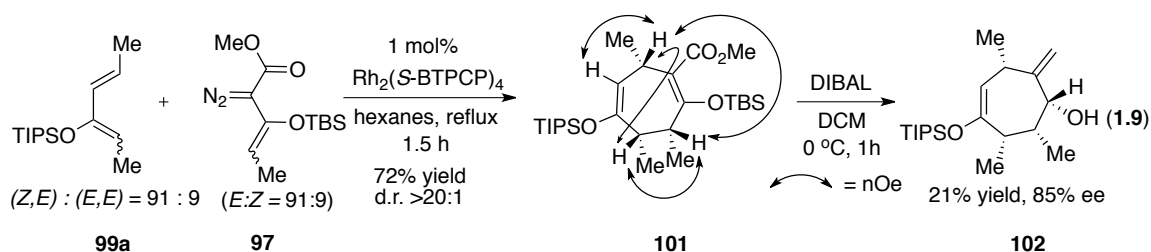
Attempts to obtain crystalline samples of the cycloadducts for X-ray crystallographic analysis were unsuccessful. Therefore efforts were made to generate crystalline derivatives.

Cycloadduct **98a** was exposed to DIBAL reduction conditions followed by treatment
with aqueous 2N HCl to provide **103** as a 64:36 mixture of diastereomers (Scheme 1.20).
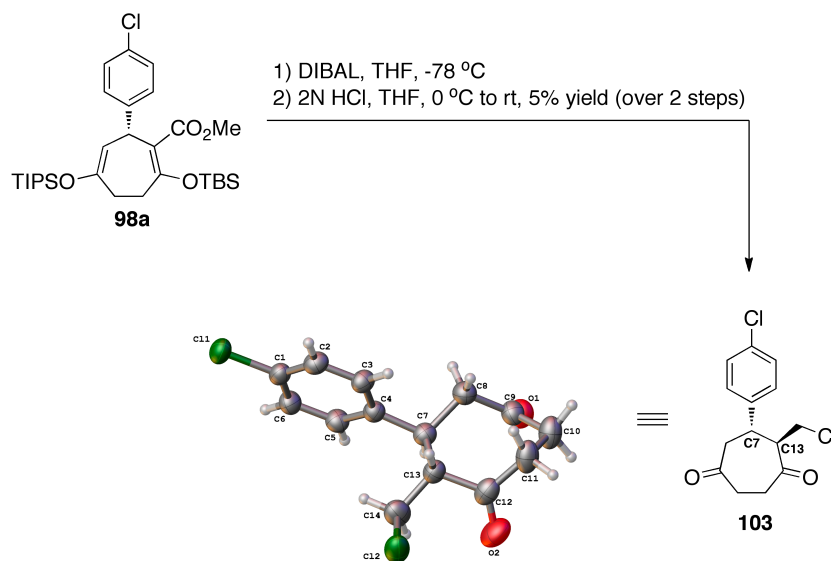
Scheme 1.20 X-ray crysallographic structure of **103**.

From this mixture a single isomer suitable for X-ray diffraction was obtained. The
absolute stereochemistry at C7 was determined to be of (*S*)-configuration. The tentative
assignment of the absolute configuration of the other cycloheptadienes was made by
analogy.

The combination of experimental, X-ray crystallographic, and NMR correlation
experiments enabled the development of a tentative proposed reaction mechanism, which
explains the observed enantio- and diastereoselectivity (Scheme 1.21).
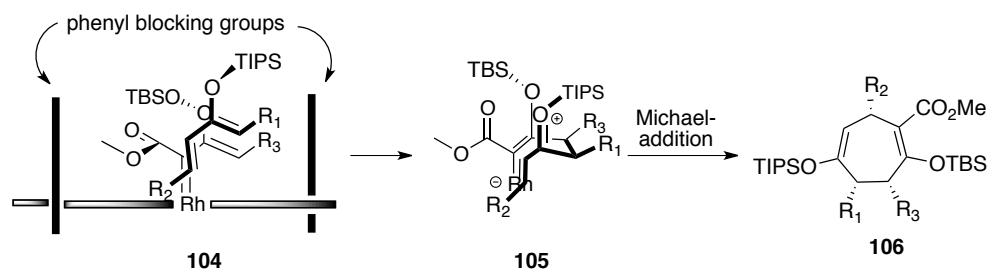
Scheme 1.21 Proposed mechanism for the vinylogous [4+3] cycloaddition.

Previous vinylogous addition studies conducted in our group suggest that highly diastereoselective ring closure occurs when the incoming nucleophile (acyclic silyl enol ethers) approaches the carbenoid via a "side-on" mode resulting in an asymmetric formal [3+2] cycloaddition reaction.[78] As such, a similar rationale was proposed due to the substantial similarities between the two nucleophiles (pathway b, Scheme 1.17). The *s*-cis conformer of the siloxybutadiene predominates and approaches the *re*-face of the *s-cis*-metallocarbenoid by a "side-on" fashion (**18**) which orients the OTIPS and R^1 groups away from the catalyst surface thus suppressing any steric interactions. Reaction through this manifold provides the zwitterionic intermediate **105**, which is aligned to undergo a highly facially selective 7-exo-trig ring closing event to access **106**.

One of the most intriguing aspects of the abnormal [4+3] cycloaddition is that highly diastereoselective reactions are obtained even when the vinyldiazoacetates and the dienes are *E/Z* mixtures. These can be rationalized as illustrated in Scheme 1.22. The *E*-isomers of both the vinyldiazoacetate and the diene will have the substituent pointing into to the catalyst surface, and thus would be highly unfavorable. Therefore, only the *Z*-

vinyldiazoacetate and the *Z,E* diene are suitably arranged for a productive [4+3] cycloaddition.
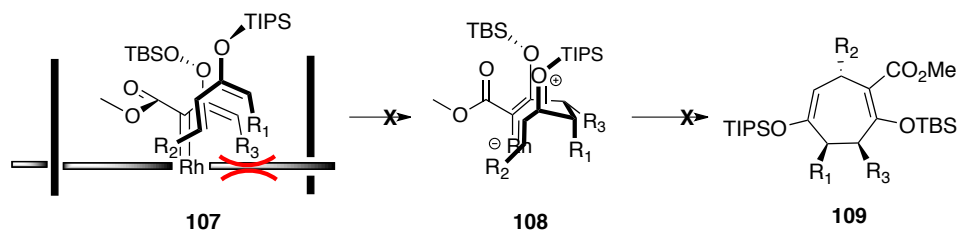
Scheme 1.22 Proposed rational for the disfavored vinylogous [4+3].

1.6 Conclusion

In summary, a systematic study was conducted that led to the development of an asymmetric vinylogous [4+3] cycloaddition. During the course of the investigation, it was discovered that $Rh_2(S\text{-BTPCP})_4$ is a superior catalyst for this new enantioselective vinylogous-initiated transformation. Moreover, the combination of sterically demanding TIPS functionalized butadienes and non-polar hydrocarbon solvent yielded an efficient formal cycloaddition reaction with high enantioselectivites. In addition, substitution on the dienes termini or the terminal position of the siloxyvinyldiazoacetate, enabled the elegant introduction of multiple stereocenters *via* a highly facially selective ring closing event. Moreover, the 7-membered rings are regiochemically complementary to cycloadducts derived from the tandem cyclopropanation/Cope rearrangement, a process that remains a great challenge to the corresponding [4+2] homolog and significantly increases the utility of this methodology for the synthesis of seven-membered rings.

1.7 References

(1) Maimone, T. J.; Baran, P. S. *Nat. Chem. Biol.* **2007**, *3*, 396-407.

(2) Salem, M. M.; Werbovetz, K. A. *Curr. Med. Chem.* **2006**, *13*, 2571-2598.

(3) Fukuyama, Y.; Minami, H.; Matsuo, A.; Kitamura, K.; Akizuki, M.; Kubo, M.; Kodama, M. *Chem. Pharm. Bull.* **2002**, *50*, 368-371.

(4) Davies, H. M. L.; Clark, T. J. *Tetrahedron* **1994**, *50*, 9883-9892.

(5) Sosa, M. E.; Tonn, C. E. *Phytochem. Rev.* **2008**, *7*, 3-24.

(6) Kantorowski, E. J.; Kurth, M. J. *Tetrahedron* **2000**, *56*, 4317-4353.

(7) Yet, L. *Chem. Rev.* **2000**, *100*, 2963-3007.

(8) Byrne, L. A.; Furlong, P. J.; Gilheany, D. G. *Synth. Commun.* **2004**, *34*, 1631-1643.

(9) Byrne, L. A.; Gilheany, D. G. *Synlett.* **2004**, 933-943.

(10) Matsuda, T.; Makino, M.; Murakami, M. *Angew. Chem., Int. Ed.* **2005**, *44*, 4608-4611.

(11) Tite, T.; Tsimilaza, A.; Lallemand, M. C.; Tillequin, F.; Leproux, P.; Libot, F.; Husson, H. P. *Eur. J. Org. Chem.* **2006**, 863-868.

(12) Hashimoto, T.; Naganawa, Y.; Maruoka, K. *J. Am. Chem. Soc.* **2009**, *131*, 6614-6617.

(13) Laventine, D. L.; Cullis, P. M.; Garcia, M. D.; Jenkins, P. R. *Tetrahedron Lett.* **2009**, *50*, 3657-3660.

(14) Yadav, D. B.; Morgans, G. L.; Aderibigbe, B. A.; Madeley, L. G.; Fernandes, M. A.; Michael, J. P.; de Koning, C. B.; van Otterlo, W. A. L. *Tetrahedron* **2011**, *67*, 2991-2997.

(15) Pulido, F. J.; Barbero, A.; Castreno, P. *J. Org. Chem.* **2011**, *76*, 5850-5855.

(16) Cao, H.; Vieira, T. O.; Alper, H. *Org. Lett.* **2011**, *13*, 11-13.

(17) Li, X. X.; Zhang, M.; Shu, D. X.; Robichaux, P. J.; Huang, S. Y.; Tang, W. P. *Angew. Chem., Int. Ed.* **2011**, *50*, 10421-10424.

(18) Usanov, D. L.; Yamamoto, H. *Org. Lett.* **2012**, *14*, 414-417.

(19) Wender, P. A.; Takahashi, H.; Witulski, B. *J. Am. Chem. Soc.* **1995**, *117*, 4720-4721.

(20) Yu, Z. X.; Wender, P. A.; Houk, K. N. *J. Am. Chem. Soc.* **2004**, *126*, 9154-9155.

(21) Liu, P.; Cheong, P. H. Y.; Yu, Z. X.; Wender, P. A.; Houk, K. N. *Angew. Chem., Int. Ed.* **2008**, *47*, 3939-3941.

(22) Yu, Z. X.; Cheong, P. H. Y.; Liu, P.; Legault, C. Y.; Wender, P. A.; Houk, K. N. *J. Am. Chem. Soc.* **2008**, *130*, 2378-2379.

(23) Wender, P. A.; Gamber, G. G.; Hubbard, R. D.; Zhang, L. *J. Am. Chem. Soc.* **2002**, *124*, 2876-2877.

(24) Wender, P. A.; Gamber, G. G.; Hubbard, R. D.; Pham, S. M.; Zhang, L. *J. Am. Chem. Soc.* **2005**, *127*, 2836-2837.

(25) Jiao, L.; Ye, S. Y.; Yu, Z. X. *J. Am. Chem. Soc.* **2008**, *130*, 11240-11240.

(26) Jiang, G. J.; Fu, X. F.; Li, Q.; Yu, Z. X. *Org. Lett.* **2012**, *14*, 692-695.

(27)   Wender, P. A.; Miranda, E. *Unpublished results. Over 75 reactions, combining monoalkenylcyclopopanes with a variety of dienophles and catalysts, were investigated using previouly reported conditions.*

(28)   Binger, P.; Wedemann, P.; Kozhushkov, S. I.; de Meijere, A. *Eur. J. Org. Chem.* **1998**, 113-119.

(29)   Plemenkov, V. V.; Butenko, O. J.; Zverev, V. V.; Ermolaeva, L. V.; Vakar, V. M.; Ignatchenko, A. V.; Bolesov, I. G. *J. Mol. Struct.* **1990**, *218*, 195-200.

(30)   Ryu, I.; Ikura, K.; Tamura, Y.; Maenaka, J.; Ogawa, A.; Sonoda, N. *Synlett.* **1994**, 941-942.

(31)   Hanzawa, Y.; Harada, S.; Nishio, R.; Taguchi, T. *Tetrahedron Lett.* **1994**, *35*, 9421-9424.

(32)   Wender, P. A.; Rieck, H.; Fuji, M. *J. Am. Chem. Soc.* **1998**, *120*, 10976-10977.

(33)   Wender, P. A.; Dyckman, A. J.; Husfeld, C. O.; Scanio, M. J. C. *Org. Lett.* **2000**, *2*, 1609-1611.

(34)   Demare, G. R. *Theochem-J. Mol. Struc.* **1987**, *38*, 341-356.

(35)   Hoffmann, H. M. R. *Angew. Chem., Int. Ed.* **1984**, *23*, 1-19.

(36)   Noyori, R. *Acc. Chem. Res.* **1979**, *12*, 61-66.

(37)   Davies, H. M. L.; Clark, D. M.; Smith, T. K. *Tetrahedron Lett.* **1985**, *26*, 5659-5662.

(38)   Davies, H. M. L.; Smith, H. D.; Korkor, O. *Tetrahedron Lett.* **1987**, *28*, 1853-1856.

(39)   Davies, H. M. L.; Clark, T. J.; Smith, H. D. *J. Org. Chem.* **1991**, *56*, 3817-3824.

(40)   Davies, H. M. L.; Clark, T. J.; Kimmer, G. F. *J. Org. Chem.* **1991**, *56*, 6440-6447.

(41)   Davies, H. M. L.; Young, W. B.; Smith, H. D. *Tetrahedron Lett.* **1989**, *30*, 4653-4656.

(42)   Davies, H. M. L.; Huby, N. J. S. *Tetrahedron Lett.* **1992**, *33*, 6935-6938.

(43)   Davies, H. M. L.; Ahmed, G.; Churchill, M. R. *J. Am. Chem. Soc.* **1996**, *118*, 10774-10782.

(44)   Wong, H. N. C.; Hon, M. Y.; Tse, C. W.; Yip, Y. C.; Tanko, J.; Hudlicky, T. *Chem. Rev.* **1989**, *89*, 165-198.

(45)   Davies, H. M. L.; Cantrell, W. R. *Tetrahedron Lett.* **1991**, *32*, 6509-6512.

(46)   Davies, H. M. L.; Huby, N. J. S.; Cantrell, W. R.; Olive, J. L. *J. Am. Chem. Soc.* **1993**, *115*, 9468-9479.

(47)   Dudley, G. B.; Tan, D. S.; Kim, G.; Tanski, J. M.; Danishefsky, S. J. *Tetrahedron Lett.* **2001**, *42*, 6789-6791.

(48)   Dudley, G. B.; Danishefsky, S. J. *Org. Lett.* **2001**, *3*, 2399-2402.

(49)   Jackson, K. L.; Henderson, J. A.; Motoyoshi, H.; Phillips, A. J. *Angew. Chem., Int. Ed.* **2009**, *48*, 2346-2350.

(50)   Xu, J.; Caro-Diaz, E. J. E.; Theodorakis, E. A. *Org. Lett.* **2010**, *12*, 3708-3711.

(51)   Davies, H. M. L.; Matasi, J. J.; Hodges, L. M.; Huby, N. J. S.; Thornley, C.; Kong, N.; Houser, J. H. *J. Org. Chem.* **1997**, *62*, 1095-1105.

(52)	Murthy, V.; Davies, H. M. L.; Hedley, S. J.; Childers, S. R. *Biochem. Pharmacol.* **2007**, *74*, 336-344.

(53)	Murthy, V.; Martin, T. J.; Kim, S.; Davies, H. M. L.; Childers, S. R. *J Pharmacol. Exp. Ther.* **2008**, *326*, 587-595.

(54)	Davies, H. M. L.; Matasi, J. J.; Thornley, C. *Tetrahedron Lett.* **1995**, *36*, 7205-7208.

(55)	Davies, H. M. L.; Saikali, E.; Huby, N. J. S.; Gilliatt, V. J.; Matasi, J. J.; Sexton, T.; Childers, S. R. *J. Med. Chem.* **1994**, *37*, 1262-1268.

(56)	Davies, H. M. L.; Kuhn, L. A.; Thornley, C.; Matasi, J. J.; Sexton, T.; Childers, S. R. *J. Med. Chem.* **1996**, *39*, 2554-2558.

(57)	Davies, H. M. L.; Peng, Z. Q.; Houser, J. H. *Tetrahedron Lett.* **1994**, *35*, 8939-8942.

(58)	Davies, H. M. L.; Stafford, D. G.; Doan, B. D.; Houser, J. H. *J. Am. Chem. Soc.* **1998**, *120*, 3326-3331.

(59)	Lian, Y., Ph.D. Thesis, Emory University, 2011.

(60)	Reddy, R. P.; Lee, G. H.; Davies, H. M. L. *Org. Lett.* **2006**, *8*, 3437-3440.

(61)	Denton, J. R.; Sukumaran, D.; Davies, H. M. L. *Org. Lett.* **2007**, *9*, 2625-2628.

(62)	Reddy, R. P.; Davies, H. M. L. *J. Am. Chem. Soc.* **2007**, *129*, 10312-+.

(63)	Schwartz, B. D.; Denton, J. R.; Lian, Y. J.; Davies, H. M. L.; Williams, C. M. *J. Am. Chem. Soc.* **2009**, *131*, 8329-8332.

(64)	Lian, Y. J.; Miller, L. C.; Born, S.; Sarpong, R.; Davies, H. M. L. *J. Am. Chem. Soc.* **2010**, *132*, 12422-12425.

(65)	Davies, H. M. L.; Saikali, E.; Clark, T. J.; Chee, E. H. *Tetrahedron Lett.* **1990**, *31*, 6299-6302.

(66)	Doyle, M. P. *Chem. Re.v* **1986**, *86*, 919-939.

(67)	Davies, H. M. L.; Hu, B. H.; Saikali, E.; Bruzinski, P. R. *J. Org. Chem.* **1994**, *59*, 4535-4541.

(68)	Pincock, J. A.; Murray, K. P. *Can. J. Chem.* **1979**, *57*, 1403-1410.

(69)	Pincock, J. A.; Mathur, N. C. *J. Org. Chem.* **1982**, *47*, 3699-3706.

(70)	Brewbaker, J. L.; Hart, H. *J. Am. Chem. Soc.* **1969**, *91*, 711-715.

(71)	Wang, X. C.; Xu, X. F.; Zavalij, P. Y.; Doyle, M. P. *J. Am. Chem. Soc.* **2011**, *133*, 16402-16405.

(72)	Xu, X. F.; Ratnikov, M. O.; Zavalij, P. Y.; Doyle, M. P. *Org. Lett.* **2011**, *13*, 6122-6125.

(73)	Qian, Y.; Xu, X. F.; Wang, X. C.; Zavalij, P. J.; Hu, W. H.; Doyle, M. P. *Angew. Chem., Int. Ed.* **2012**, *51*, 5900-5903.

(74)	Xu, X. F.; Zavalij, P. Y.; Doyle, M. P. *Angew. Chem., Int. Ed.* **2012**, *51*, 9829-9833.

(75)	Valette, D.; Lian, Y. J.; Haydek, J. P.; Hardcastle, K. I.; Davies, H. M. L. *Angew. Chem., Int. Ed.* **2012**, *51*, 8636-8639.

(76)	Lian, Y. J.; Hardcastle, K. I.; Davies, H. M. L. *Angew. Chem., Int. Ed.* **2011**, *50*, 9370-9373.

(77)	Hansen, J. H.; Gregg, T. M.; Ovalles, S. R.; Lian, Y. J.; Autschbach, J.; Davies, H. M. L. *J. Am. Chem. Soc.* **2011**, *133*, 5076-5085.

(78)	Smith, A. G.; Davies, H. M. L. *J. Am. Chem. Soc.* **2012**, *134*, 18241-18244.

(79)   Takahashi, T.; Tsutsui, H.; Tamura, M.; Kitagaki, S.; Nakajima, M.; Hashimoto, S. *Chem. Commun.* **2001**, 1604-1605.

(80)   Minami, K.; Saito, H.; Tsutsui, H.; Nambu, H.; Anada, M.; Hashimoto, S. *Adv. Synth. Cata.l* **2005**, *347*, 1483-1487.

(81)   Lindsay, V. N. G.; Lin, W.; Charette, A. B. *J. Am. Chem. Soc.* **2009**, *131*, 16383-16385.

(82)   DeAngelis, A.; Dmitrenko, O.; Yap, G. P. A.; Fox, J. M. *J. Am. Chem. Soc.* **2009**, *131*, 7230-7231.

(83)   Diels, O.; Alder, K. *Liebig.s Ann. Chem.* **1928**, *460*, 98-122.

(84)   Oppolzer, W. *Comprehensive Organic Synthesis*; Pergamon: New York, 1991; Vol. 5.

(85)   Corey, E. J. *Angew. Chem., Int. Ed.* **2002**, *41*, 1650-1667.

(86)   Nicolaou, K. C.; Snyder, S. A.; Montagnon, T.; Vassilikogiannakis, G. *Angew. Chem., Int. Ed.* **2002**, *41*, 1668-1698.

(87)   Roush, W. R. *Comperhensive Organic Synthesis*; Pergamon Press: New York, 1991; Vol. 5.

(88)   Zhao, F.; Zhang, S. G.; Xi, Z. F. *Chem. Commun.* **2011**, *47*, 4348-4357.

(89)   Girling, P. R.; Kiyoi, T.; Whiting, A. *Org. Biomo.l Chem.* **2011**, *9*, 3105-3121.

(90)   Ventura, D. L.; Li, Z. J.; Coleman, M. G.; Davies, H. M. L. *Tetrahedron* **2009**, *65*, 3052-3061.

(91)   Nadeau, E.; Ventura, D. L.; Brekan, J. A.; Davies, H. M. L. *J. Org. Chem.* **2010**, *75*, 1927-1939.

1.8 Experimental Section

1.81 General Considerations

All experiments were performed in anhydrous conditions under an atmosphere of dry argon using flame-dried glassware. Solvents were dried by a Grubbs-type solvent purification system. Hexanes and pentanes were degassed with argon for 10 minutes prior to use. Unless otherwise noted, all other reagents were obtained from commercial sources and used as received. [1]H Nuclear Magnetic Resonance (NMR) spectra were recorded at 400, 500 or 600 MHz. Data is presented as follows: chemical shift (in ppm on the δ scale relative to δH 7.26 for the residual protons in $CDCl_3$ or δH 7.16 for the residual protons in C_6D_6), multiplicity (s = singlet, d = doublet, t = triplet, q = quartet, m = multiplet, br = broad), coupling constant (J/Hz), integration. Coupling constants were taken directly from the spectra and are uncorrected. ^{13}C NMR spectra were recorded at 75, 100, 125 or 150 MHz, and all chemical shift values are reported in ppm on the δ scale, with an internal reference of δC 77.0 for $CDCl_3$ or δC 128.39 for C_6D_6. Mass spectral determinations were carried out using APCI, ESI, or NSI as ionization source. Melting points are uncorrected. Infrared spectral data are reported in units of cm^{-1}. Analytical TLC was performed on glass-backed silica gel F254 plates (EMD Chemicals). Visualization of developed plates was performed by fluorescence quenching or by staining with aqueous potassium permanganate ($KMnO_4$) or phosphomolybdic acid (PMA) in ethanol stain followed by heating. Flash column chromatography was performed on silica gel 60Å (230-400 mesh) according to the literature procedure described by Still. Optical rotations were measured on a Jasco P-2000 polarimeter.

Analytical chromatographies, using isopropanol/hexane as gradient, were measured on a Varian Prostar instrument. $Rh_2(S\text{-BTPCP})_4$, $Rh_2(S\text{-PTAD})_4$, and $Rh_2(S\text{-DOSP})_4$ were lyophilized prior to use using an SP VirTis BenchTop K freeze-dryer and were stored in a desiccator over Drierite™. Methyl 3-((tert-butyldimethylsilyl)oxy)-2-diazobut-3-enoate[63] and (Z)-methyl 3-((tert-butyldimethylsilyl)oxy)-2-diazopent-3-enoate[91] were prepared according to published literature procedures.

1.82 General procedures

Procedure A

Enantioselective vinylogous [4 + 3] cycloaddition (Condition A: Room temperature)

To a 25 mL round-bottom flask was added the corresponding diene (1.51 mmol, 5.00 equiv), pentane (3.5 mL), and $Rh_2(S\text{-BTPCP})_4$ (5.3 mg, 0.0030 mmol 0.010 equiv). A solution of methyl 3-((tert-butyldimethylsilyl)oxy)-2-diazobut-3-enoate (77.0 mg, 0.30, mmol, 1.00 equiv) in pentane (3.5 mL) was added by syringe pump over 1 h. Once the addition was complete, the reaction was allowed to stir at 23 °C for 0.5 h. The reaction was stopped by concentration under reduced pressure and purified by flash chromatography on silica gel to provide pure products.

Procedure B

Enantioselective vinylogous [4 + 3] cycloaddition (Condition B: Reflux)

To a 10 mL round-bottom flask was added the corresponding diene (0.15 mmol, 1.00 equiv), hexanes (2.0 mL), and $Rh_2(S\text{-BTPCP})_4$ (2.7 mg, 0.0015 mmol 0.010 equiv). The reaction vessel was equipped with a water-cooled reflux condenser and heated to 73 °C. A solution of methyl 3-((tert-butyldimethylsilyl)oxy)-2-diazobut-3-enoate (77.0 mg, 0.30, mmol, 2.00 equiv) in hexanes (2.0 mL) was added by syringe pump over 1 h. Once the addition was complete, the reaction was allowed to stir at 76 °C for 0.5 h. The reaction was stopped by concentration under reduced pressure and purified by flash chromatography on silica gel to provide pure products.

Procedure C

Enantioselective vinylogous [4 + 3] cycloaddition (Condition A: Room temperature)

To a 10 mL round-bottom flask was added the corresponding diene (0.151 mmol, 1.00 equiv), pentanes (2.0 mL), and Rh$_2$(*S*-BTPCP)$_4$ (2.7 mg, 0.00151 mmol 0.010 equiv). A solution of (*Z*)-methyl 3-((tert-butyldimethylsilyl)oxy)-2-diazopent-3-enoate (82.0 mg, 0.30, mmol, 2.00 equiv) in pentanes (2.0 mL) was added by syringe pump over 1 h. Once the addition was complete, the reaction was allowed to stir at 23 °C for 0.5 h. The reaction was stopped by concentration under reduced pressure and purified by flash chromatography on silica gel to provide pure products.

Procedure D

Enantioselective vinylogous [4 + 3] cycloaddition (Condition A: Reflux)

To a 10 mL round-bottom flask was added the corresponding diene (0.187 mmol, 1.00 equiv), pentanes (2.0 mL), and Rh$_2$(*S*-BTPCP)$_4$ (3.3 mg, 0.00187 mmol 0.010 equiv). The reaction vessel was equipped with a water-cooled reflux condenser and heated to 73 °C. A solution of (*Z*)-methyl 3-((tert-butyldimethylsilyl)oxy)-2-diazopent-3-enoate (101 mg, 0.374, mmol, 2.00 equiv) in pentanes (2.0 mL) was added by syringe pump over 1 h. Once the addition was complete, the reaction was allowed to stir at 73 °C for 0.5 h. The reaction was stopped by concentration under reduced pressure and purified by flash chromatography on silica gel to provide pure products.
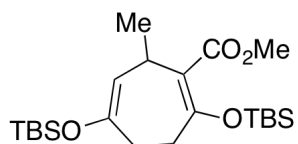
Methyl 2,5-bis((tert-butyldimethylsilyl)oxy)-7-methylcyclohepta-1,dienecarboxylate (87):

Prepared *via* Procedure A. Derived from (E)-tert-butyldimethyl(penta-1,3-dien-2-yloxy)silane (300 mg, 1.51 mmol, 5.0 equiv) and purified by flash chromatography (98:2 pentane/Et_2O) on silica gel to provide the vinylogous [4+3] product as colorless oil (30 mg, 23% yield). Rf = 0.10 (98:2 Pentane/Et_2O); ^{1}H NMR (600 MHz; C_6D_6) δ 5.07 (dd, 1H, *J* = 6.0, 12.0 Hz), 3.64 (p, *J* = 6 Hz, 1H), 3.46 (s, 3H), 2.69-2.64 (m, *J* = 1 Hz, 1H), 2.37-2.32 (m, 1H), 2.11-2.05 (m, 2H), 1.31 (d, *J* = 6 Hz, 3H), 0.98 (s, 9H), 0.97 (s, 9H), 0.17 (s, 3H), 0.14 (s, 3H), 0.11 (s, 3H), 0.09 (s, 3H); ^{13}C NMR (100 MHz, $CDCl_3$) δ 169.3, 159.3, 150.7, 116.8, 111.9, 51.2, 32.5, 30, 25.7, 21.1, 18.2, 17.9, -3.9, -4.0, -4.3, -4.6; IR (neat): 2954, 2929, 2857, 1716, 1694, 836, 778; HRMS-(APCI) m/z 427.2694 [$(M+H)^+$ requires 427.2689]. HPLC analysis: (S,S-Whelk-O 1, 100 % hexanes, 0.5 ml/min), UV: 254 nm, retention time of 12.82 min (minor) and 16.35 min (major), 87 % ee.
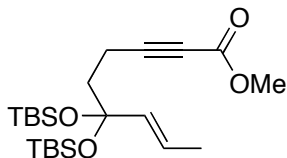
(E)-methyl 6,6-bis((tert-butyldimethylsilyl)oxy)non-7-en-2-ynoate (88):

Prepared *via* procedure A.   Derived from (E)-tert-butyldimethyl(penta-1,3-dien-2-yloxy)silane (300 mg, 1.51 mmol, 5.0 equiv) and purified by flash chromatography (98:2 pentane/Et$_2$O) on silica gel to provide the alkynoate product as colorless oil (54 mg, 42% yield). Rf = 0.14 (98:2 Pentane:Et$_2$O); ^{1}H NMR (600 MHz; C$_6$D$_6$) δ 5.67 (dq, 1H, J = 6.6, 13.2, 15.0 Hz), 5.40 (dd, J = 1.8.15.6 Hz, 1H), 3.27 (s, 3H), 2.38 (app dd, J = 8.4, 10.2 Hz, 2H), 1.93 (app dd, J = 6.6, 8.4 Hz, 2H), 1.47 (dd, J = 1.8, 6.6 Hz, 3H), 0.94 (s, 18H), 0.13 (s, 6H), 0.10 (s, 6H); ^{13}C NMR (150 MHz, C$_6$D$_6$) δ 154.5, 135.4, 126.3, 98.6, 89.7, 74.2, 52.2, 42, 26.6, 18.8, 17.6, 14.6, 1.82, 2.04; IR (neat): 2954, 2929, 2857, 2240, 1718, 1247; HRMS-(APCI) m/z 427.2697 [(M+H)$^+$ requires 427.2694].
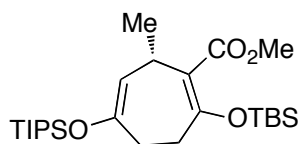
Methyl2-((tert-butyldimethylsilyl)oxy)-7-methyl-5-

((triisopropylsilyl)oxy)cyclohepta-1,5-dienecarboxylate (87):

Prepared *via* procedure A. Derived from (E)-triisopropyl(penta-1,3-dien-2-yloxy)silane (363 mg, 1.51 mmol, 5.0 equiv) and purified by flash chromatography (98:2 pentane/Et$_2$O) on silica gel to provide the vinylogous [4+3] product as colorless oil (84 mg, 59% yield). R$_f$ = 0.10 (98:2 Pentane:Et$_2$O); $[\alpha]_D^{20}$: 26.3 (*c*. 1.0, CHCl$_3$); ^{1}H NMR (600 MHz; C$_6$D$_6$) δ 5.10 (d, 1H, *J* = 7.8 Hz), 3.65 (p, *J* = 7.2 Hz, 1H), 3.46 (s, 3H), 2.68 (ddd, *J* = 15.0, 12.0, 3.0 Hz, 1H), 2.41 (ddd, *J* = 14.4, 14.4 Hz, 1H), 2.17 (m, 1H), 2.09 (ddd, *J* = 14.4, 6.6, 3.0 Hz, 1H), 1.32 (d, *J* = 7.2 Hz, 3H), 1.11 (bs, 21H), 0.98 (s, 9H), 0.17 (s, 3H), 0.14 (s, 3H); ^{13}C NMR (100 MHz, C$_6$D$_6$) δ 168.7, 159.6, 152, 117.7, 111.3, 51.1, 33.1, 30.8, 30.7, 26.3, 21.7, 18.9, 18.6, 13.4, -3.44; IR (neat): 2944, 2865, 1719, 1626, 1178; HRMS-(ESI) m/z 491.2986 [(M+Na)$^+$ requires 491.2983]. HPLC: (S,S-Whelk-O 1, 100 % hexane, 0.5 ml/min), UV: 254 nm, retention time of 12.24 min (minor) and 14.36 min (major), 96 % ee.
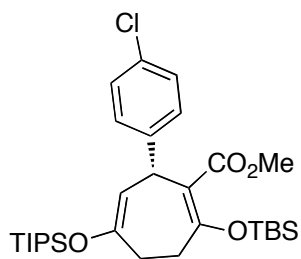
Methyl 2-((tert-butyldimethylsilyl)oxy)-7-(4-chlorophenyl)-5-((triisopropylsilyl)oxy)cyclohepta-1,5-dienecarboxylate (98a):

Prepared *via* procedure B. Derived from (E)-((4-(4-chlorophenyl)buta-1,3-dien-2-yl)oxy)triisopropylsilane (51.0 mg, 0.151 mmol, 1.00 equiv) and purified by flash chromatography (98:2 pentane/Et$_2$O) on silica gel to provide the vinylogous [4+3] product as colorless oil (66 mg, 77 % yield). R$_f$ = 0.10 (98:2 pentane/Et$_2$O); [α]$_D^{20}$: 42.1 (*c*. 0.49, CHCl$_3$); ^{1}H NMR (600 MHz; C$_6$D$_6$) δ 7.78 (dd, 2H, *J* = 8.8, 2.4 Hz), 7.15 (m, 2H), 5.32 (d, *J* = 9.6 Hz, 1H), 5.05 (dd, *J* = 9.6, 6.6 Hz, 1H), 3.50 (s, 3H), 2.50 (app t, *J* = 28, 13.8 Hz, 1H), 2.38 (app t, *J* = 16.8, 31.2 Hz, 1H), 2.12 (d, *J* = 17.4 Hz, 1H), 1.76 (app dt, *J* = 2.4, 2.4, 13.8 Hz, 1H), 1.09 (d, *J* = 8.4 Hz, 21H), 0.93 (s, 9H), 0.10 (d, *J* = 3.6 Hz, 6H); ^{13}C NMR (100 MHz, C^{6}D^6) δ 168.7, 163.6, 154, 144.5, 132.3, 129.7, 128.7, 117.4, 107, 51.5, 38.7, 32.3, 30.6, 26.2, 18.9, 18.6, 13.33, 3.4, 3.3; IR (neat): 2945, 2864, 1687, 1185; HRMS-(APCI) m/z 565.2949 [(M+H)$^+$ requires 565.2930]. HPLC: (S,S-Whelk-O 1, 100 % hexane, 0.5 ml/min), UV: 254 nm, retention time of 28.14 min (minor) and 32.29 min (major), 95 % ee.
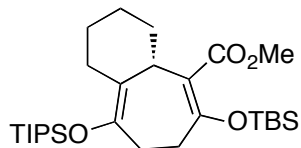
methyl 6-((*tert*-butyldimethylsilyl)oxy)-9-((triisopropylsilyl)oxy)-2,3,4,4a,7,8-hexahydro-1*H*-benzo[7]annulene-5-carboxylate (98d):

Prepared *via* procedure A. Derived from ((1-(cyclohex-1-en-1-yl)vinyl)oxy)triisopropylsilane (423 mg, 1.51 mmol, 5.0 equiv) and purified by flash chromatography (98:2 pentane/Et$_2$O) on silica gel to provide the vinylogous [4+3] product as colorless oil (58 mg, 38 % yield). R_f = 0.13 (98:2 Pentane/Et$_2$O); $[\alpha]_D^{20}$: 72.8 (*c*. 0.60, CHCl$_3$); ^{1}H NMR (600 MHz; C$_6$D$_6$) δ 3.5 (d, 1H, *J* = 10.2 Hz), 3.45 (s, 3H), 3.29-3.25 (m, 1H), 2.84 (ddd, *J* = 1.8, 12.6, 12.6 Hz, 1H), 2.71 (ddd, *J* = 2.4, 13.8, 13.8 Hz, 1H), 2.25 (dd, *J* = 6.0, 16.2 Hz, 1H), 2.11-2.05 (m, 2H), 1.77 (t, *J* = 9.6 Hz, 2H), 1.67-1.57 (m, 3H), 1.45-1.38 (m, 1H), 1.10-1.09 (m, 21H), 0.99 (s, 9H), 0.17 (d, *J* = 5.4 Hz, 6H); ^{13}C NMR (100 MHz, C$_6$D$_6$) δ 168.9, 161.5, 143.2, 120.6, 115.9, 51.2, 42.7, 35.7, 34.9, 33.5, 31.9, 28.9, 28.7, 26.3, 18.9, 18.7, 13.9, -3.51; IR (neat): 2927, 2864, 1715, 1194; HRMS-(ESI) m/z 509.3476 [(M+H)$^+$ requires 509.3476]. HPLC: (S,S-Whelk-O 1, 100 % hexane, 0.25 ml/min), UV: 254 nm, retention time of 26.55 min (minor) and 29.51 min (major), 90 % ee.

methyl 5-((tert-butyldimethylsilyl)oxy)-8-((triisopropylsilyl)oxy)-1,2,3,3a,6,7-hexahydroazulene-4-carboxylate (98e):

Prepared *via* procedure A. Derived from ((1-(cyclopent-1-en-1-yl)vinyl)oxy)triisopropylsilane (402 mg, 1.51 mmol, 5.0 equiv) and purified by flash chromatography (98:2 pentane/Et$_2$O) on silica gel to provide the vinylogous [4+3] product as colorless oil (74 mg, 50 % yield). R_f = 0.10 (98:2 Pentane:Et$_2$O); $[\alpha]_D^{20}$: 23.0 (*c*. 1.08, CHCl$_3$); ^{1}H NMR (600 MHz; C$_6$D$_6$) δ 3.49 (s, 3H), 2.61 (dd, *J* = 7.8, 16.8 Hz, 1H), 2.49-2.44 (m, 1H), 2.43-3.36 (m, 1H), 2.34-2.30 (m, 2H,), 2.18-2.13 (m, 1H), 2.10 (ddd, *J* = 5.4, 7.2, 24.6 Hz, 1H), 1.68-1.63 (m, 1H), 1.61-1.56 (m, 1H), 1.95 (dd, *J* = 4.2, 7.2 Hz, 2H), 1.35-1.08 (m, 21H), 0.97 (s, 9H), 0.18 (s, 3H), 0.15 (s, 3H); ^{13}C NMR (100 MHz, C$_6$D$_6$) δ 169.2, 151.7, 143.6, 123.4, 119.4, 51, 39.4, 34.4, 31.9, 31.5, 31.2, 26.2, 25.4, 18.7, 14.1, -3.3, -3.5; IR (neat): 2945, 2864, 1723, 155; HRMS-(APCI) m/z 495.3321 [(M+H)$^+$ requires 495.3320. HPLC: (S,S-Whelk-O 1, 100 % hexane, 0.25 ml/min), UV:210 nm retention time of 20.68 min (minor) and 18.24 min (major), 92 % ee.

Methyl 2-((tert-butyldimethylsilyl)oxy)-4,7-dimethyl-5-

((triisopropylsilyl)oxy)cyclohepta-1,5-dienecarboxylate(100a):

Prepared *via* procedure A. Derived from ((2Z,4E)-hexa-2,4-dien-3-yloxy)triisopropylsilane (384 mg, 1.51 mmol, 5.0 equiv) and purified by flash chromatography (98:2 pentane/Et$_2$O) on silica gel to provide the vinylogous [4+3] product as colorless oil (100 mg, 68 % yield). R$_f$ = 0.18 (98:2 Pentane:Et$_2$O); [α]$_D^{20}$: 36.8 (*c*. 0.50, CHCl$_3$); ^{1}H NMR (600 MHz; C$_6$D$_6$) δ 5.04 (dd, 1H, *J* = 7.8, 1.8 Hz), 3.69 (p, *J* = 1.2 Hz, 1H), 3.45 (s, 3H), 2.67 (dd, *J* = 11.4, 14.4 Hz, 1H), 2.60-2.54 (m, 1H), 2.15 (dd, *J* = 3.0, 14.4 Hz, 1H), 1.33 (d, *J* = 7.2 Hz, 3H), 1.21 (d, *J* = 7.2 Hz, 3H), 1.11-1.09 (m, 21H), 1.00 (s, 9H), 0.23 (s, 3H), 0.18 (s, 3H); ^{13}C NMR (100 MHz, C$_6$D$_6$) δ 168.3, 158.7, 155.2, 117.7, 110.9, 51.1, 41.1, 34.9, 30.6, 26.4, 21.1, 20.5, 18.9, 18.7, 13.5, -3.4, -3.3; IR (neat): 2945, 2865, 1719, 1179; HRMS-(APCI) m/z 483.3334 [(M+H)$^+$ requires 483.3320]. HPLC: AD-H, 100 % hexane, 1.0 ml/min), UV: 254nm, retention time of 6.08 min (minor) and 5.26 min (major), 96 % ee.

(4S,7R)-methyl 2-((tert-butyldimethylsilyl)oxy)-7-(4-chlorophenyl)-4-methyl-5-((triisopropylsilyl)oxy)cyclohepta-1,5-dienecarboxylate(100b):

Prepared *via* procedure A. Derived from ((1*E*)-1-(4-chlorophenyl)penta-1,3-dien-3-yl)oxy)triisopropylsilane (529 mg, 1.51 mmol, 5.0 equiv) and purified by flash chromatography (98:2 pentane/Et$_2$O) on silica gel to provide the vinylogous [4+3] product as colorless oil (124 mg, 71 % yield). Rf = 0.16 (98:2 Pentane/Et$_2$O); $[\alpha]_D^{20}$: 43.4 (*c*. 0.58, CHCl$_3$); ^{1}H NMR (600 MHz; C$_6$C$_6$) δ 7.39 (d, 2H, *J* = 7.8 Hz), 7.14 (d, *J* = 8.4 Hz, 2H), 5.30 (dd, *J* = 1.2, 10.2 Hz, 1H), 5.06 (d, *J* = 10.2 Hz, 1H), 3.52 (s, 3H), 2.57-2.52 (m, 1H), 2.48 (app t, *J* = 13.2 Hz, 1H), 1.79 (dd, *J* = 3.0, 13.2 Hz, 1H), 1.17 (d, *J* = 6.6 Hz, 3H), 1.12-1.09 (m, 21H), 0.95 (s, 9H), 0.15 (s, 3H), 0.13 (s, 3H); ^{13}C NMR (100 MHz, C$_6$C$_6$) δ 167.9, 162.6, 156.7, 144, 131.8, 129.1, 128.2, 117.5, 105.8, 50.9, 40, 38.2, 34.9, 25.7, 20.1, 18.1, 12.9, 12.2, -3.8; IR (neat): 2945, 2865, 1687, 1184; HRMS-(APCI) m/z 579.3102 [(M+H)$^+$ requires 579.3087]. HPLC: (S,S-Whelk-O 1, 100 % hexane, 0.5 ml/min), UV: 254 nm, retention time of 20.70 min (minor) and 25.10 min (major), 96 % ee.

(3*R*,7*S*)-methyl 2-((*tert*-butyldimethylsilyl)oxy)-3,7-dimethyl-5-

((triisopropylsilyl)oxy)cyclohepta-1,5-dienecarboxylate (98f):

Prepared *via* procedure C. Derived from ((1*E*)-1-(4-chlorophenyl)penta-1,3-dien-3-yl)oxy)triisopropylsilane (43 mg, 0.151 mmol, 1.0 equiv) and(Z)-methyl 3-((tert-butyldimethylsilyl)oxy)-2-diazopent-3-enoate. Purified by flash chromatography (98:2 pentane/Et$_2$O) on silica gel to provide the vinylogous [4+3] product as colorless oil (28 mg, 38 % yield). Rf = 0.15 (98:2 Pentane/Et$_2$O); [α]$_D^{20}$: 21.9 (*c*. 0.7, CHCl$_3$); ^{1}H NMR (600 MHz; C$_6$D$_6$) δ 4.98 (dd, 1H, *J* = 5.4 Hz), 3.53-3.49 (m, 1H), 3.48 (s, 3H), 2.55 (d, *J* = 14.4 Hz, 1H), 2.51-2.48 (m, 1H), 2.19 (dd, *J* = 7.2, 15.6 Hz. 1H), 1.26 (d, *J* = 7.2 Hz, 3H), 1.22 (d, *J* = 6.6 Hz, 3H), 1.12 (s, 21H), 0.98 (s, 9H), 0.16 (d, *J* = 16.8 Hz, 6H); ^{13}C NMR (100 MHz, C$_6$D$_6$) δ 170.5, 156.2, 150.9, 119.8, 111, 51.2, 38.2, 37, 30.7, 26.3, 21.5, 19.5, 18.8, 18.6, 13.3, -3.3, -3.5; IR (neat): 2945, 2865, 1720, 1251; HRMS-(APCI) m/z 483.3324 [(M+H)$^+$ requires 483.3320]. HPLC: (OD-H, 100 % hexane, 0.25 ml/min), UV: 254 nm, retention time of 17.66 min (minor) and 16.81 min (major), 99 % ee.
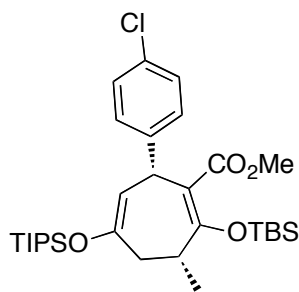
(3*R*,7*R*)-methyl 2-((*tert*-butyldimethylsilyl)oxy)-7-(4-chlorophenyl)-3-methyl-5-((triisopropylsilyl)oxy)cyclohepta-1,5-dienecarboxylate (98g):

Prepared *via* procedure C. Derived from (E)-((4-(4-chlorophenyl)buta-1,3-dien-2-yl)oxy)triisopropylsilane (51 mg, 0.151 mmol, 1.0 equiv) and (Z)-methyl 3-((tert-butyldimethylsilyl)oxy)-2-diazopent-3-enoate. Purified by flash chromatography (98:2 pentane/Et$_2$O) on silica gel to provide the vinylogous [4+3] product as colorless oil (39 mg, 45 % yield). Rf = 0.11 (98:2 Pentane/Et$_2$O); [α]$_D^{20}$: -18.5 (*c*. 0.9, CHCl$_3$); ^{1}H NMR (600 MHz; C$_6$D$_6$) δ 7.24 (d, 2H, *J* = 8.4 Hz), 7.12 (d, *J* = 8.4 Hz, 2H), 5.44 (d, *J* = 9 Hz, 1H), 4.79 (d, *J* = 8.4 Hz, 1H), 3.36 (s, 3H), 2.55-2.49 (m, 1H), 2.21 (dd, *J* = 11.4, 15.0 Hz, 1H), 1.99 (dd, *J* = 3.6, 15.0 Hz, 1H), 1.16 (d, *J* = 6.6 Hz, 3H), 1.09-1.07 (m, 21H), 0.99 (s, 9H), 0.165 (d, *J* = 31.2 Hz, 6H); ^{13}C NMR (100 MHz, C$_6$D$_6$) δ 170.7, 160.8, 154.5, 143.8, 132.3, 130, 128.7, 117.3, 109.4, 51.6, 40.7, 38.1, 37.9, 26.3, 20.7, 18.8, 18.6, 13.2, -3.4, -3.8; IR (neat): 2945, 2864, 1716, 1175; HRMS-(ESI) m/z 579.3089 [(M+H)$^+$ requires 579.3087]. HPLC: (ADH, 100 % hexane, 0.25 ml/min), UV: 254 nm, retention time of 31.14 min (minor) and 24.86 min (major), 99 % ee.
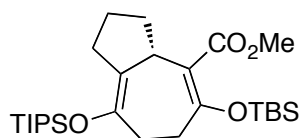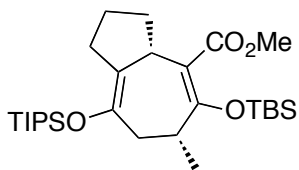
(3aS,6R)-methyl 5-((tert-butyldimethylsilyl)oxy)-6-methyl-8-((triisopropylsilyl)oxy)-1,2,3,3a,6,7-hexahydroazulene-4-carboxylate (98h):

Prepared *via* procedure D. Derived from ((1-(cyclopent-1-en-1-yl)vinyl)oxy)triisopropylsilane (51 mg, 0.151 mmol, 1.0 equiv) and (Z)-methyl 3-((tert-butyldimethylsilyl)oxy)-2-diazopent-3-enoate. Purified by flash chromatography (98:2 pentane/Et$_2$O) on silica gel to provide the vinylogous [4+3] product as colorless oil (49 mg, 52 % yield). Rf = 0.11 (98:2 Pentane/Et$_2$O); Rf = 0.16 (98:2 Pentane/Et$_2$O); [α]$_D^{20}$: 68.9 (*c*. 1.4, CHCl$_3$); ^{1}H NMR (600 MHz; C$_6$D$_6$) δ 3.47 (s, 3H), 3.39-3.36 (m, 1H), 3.30-3.27 (m, 1H), 3.03-3.00 (m, 1H), 2.55-2.51 (m, 1H), 2.17 (dd, *J* = 4.8, 15.6 Hz, 1H), 2.13 (d, *J* = 13.2 Hz, 1H), 1.71-1.68 (m, 3H), 1.63-1.57 (m, 1H), 1.39 (d, *J* = 7.2 Hz, 3H), 1.13-1.11 (m, 21H), 1.00 (s, 9H), 0.20 (d, *J* = 13.2 Hz, 6H); ^{13}C NMR (100 MHz, C$_6$D$_6$) δ 170.5, 158.8, 139.3, 118.1, 117.9, 51.4, 42.1, 39.6, 39.4, 35.4, 30, 28, 27.6, 26.3, 18.7, 18.6, 14, -3.4; IR (neat): 2924, 2864, 1720, 1462, 1192; HRMS-(APCI) m/z 509.3479 [(M+H)$^+$ requires 509.3476]; HPLC: (DACHDNB, 100 % hexane, 0.25 ml/min), UV: 254 nm, retention time of 61.38 min (minor) and 50.81 min (major), 99 % ee.
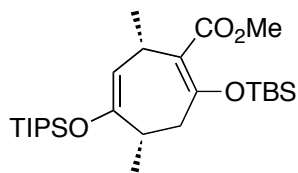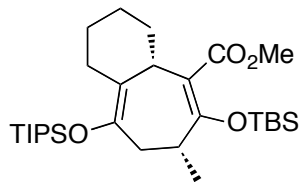
(4aS,7R)-methyl 6-((tert-butyldimethylsilyl)oxy)-7-methyl-9-((triisopropylsilyl)oxy)-2,3,4,4a,7,8-hexahydro-1H-benzo[7]annulene-5-carboxylate (98i):

Prepared *via* procedure D. Derived from ((1-(cyclohex-1-en-1-yl)vinyl)oxy)triisopropylsilane (51 mg, 0.178 mmol, 1.0 equiv) and (Z)-methyl 3-((tert-butyldimethylsilyl)oxy)-2-diazopent-3-enoate. Purified by flash chromatography (98:2 pentane/Et$_2$O) on silica gel to provide the vinylogous [4+3] product as colorless oil (74 mg, 80 % yield). Rf = 0.10 (98:2 Pentane/Et$_2$O); ^{1}H NMR (600 MHz; C$_6$D$_6$) δ 3.54-3.53 (m, 1H), 3.51 (s, 3H), 2.73 (d, *J* = 14.4 Hz, 1H), 2.54 (dd, *J* = 7.2, 16.2 Hz, 1H), 2.46-2.44 (m, 1H), 2.40-2.37 (m, 1H), 2.02-1.94 (m, 2H), 1.64-1.59 (m, 2H), 1.32-1.30 (m, 5H), 1.12-1.11 (m, 22H), 1.00 (s, 9H), 0.19 (d, *J* = 10.2 Hz, 6H); ^{13}C NMR (100 MHz, C$_6$D$_6$) δ 170.5, 158.8, 139.3, 118.1, 117.9, 51.4, 42.1, 39.6, 39.4, 35.4, 30, 28, 27.6, 26.3, 18.7, 18.6, 14, -3.4; IR (neat): 2928, 2864, 1719, 1189; HRMS-(APCI) m/z 523.3636 [(M+H)$^+$ requires 523.3633].
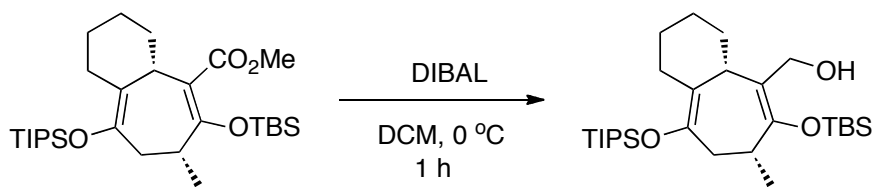
((4aS,7R)-6-((tert-butyldimethylsilyl)oxy)-7-methyl-9-((triisopropylsilyl)oxy)-2,3,4,4a,7,8-hexahydro-1H-benzo[7]annulen-5-yl)methanol:

To a 25 mL round-bottom flask was added (4aS,7R)-methyl 6-((tert-butyldimethylsilyl)oxy)-7-methyl-9-((triisopropylsilyl)oxy)-2,3,4,4a,7,8-hexahydro-1H-benzo[7]annulene-5-carboxylate (*98i*) (125 mg, 0.239 mmol, 1.0 eq) and DCM (14 mL). The solution was cooled to 0 °C. Once cool, DIBAL 1M in DCM (1.1 mL, 1.07 mmol, 4.5 eq) was slowly added to the reaction over 5 minutes. The reaction was allowed to stir, at 0 °C, for 1 hour. The reaction was then stopped by diluting with Et_2O followed by addition of saturated aqueous solution of Rochelle's salt. The mixture was aggressively stirred for 1 h. The mixtures was then transferred to a separation funnel and diluted with H_2O (100 mL). The two layers were separated and the aqueous layer was washed with Et_2O (3 x 50 mL). The organic layers were combined, dried over $MgSO_4$, filtered through a glass frit and concentrated under reduced pressure. Purified by flash chromatography (95:5 hexanes/EtOAc) on silica gel to provide the reduced product as colorless oil (99 mg, 84 % yield). Rf = 0.43 (90:10 Hexanes/EtOAc); $[\alpha]_D^{20}$: 88.7 (*c.* 0.81, $CHCl_3$); ^{1}H NMR (600 MHz; C_6D_6) δ 4.31 (dd, 1H, *J* = 4.8, 11.4 Hz), 3.99 (dd, *J* = 5.4, 11.4 Hz, 1H), 3.40 (d, *J* = 13.2 Hz, 1H), 3.06 (dd, *J* = 3.0, 15.6 Hz, 1H), 2.84 (d, J = 12 Hz, 1H), 2.53-2.48 (m, 1H), 2.22 (dd, *J* = 4.8, 16.2 Hz, 1H), 1.99 (d, *J* = 11.4 Hz, 1H), 1.79-1.73 (m, 2H), 1.64-1.59 (m, 1H), 1.48-1.42 (m, 2H), 1.38-1.37 (m, 5H), 1.16-1.13 (m, 21H), 0.98 (s, 9H), 0.13 (d, *J* = 29.4 Hz, 6H); ^{13}C NMR (100 MHz, C_6D_6) δ 153.4,

138.9, 122.5, 118.4, 63.3, 44.2, 40.3, 38.7, 35.3, 30.7, 28.7, 28.3, 26.3, 18.8, 18.7, 14.1, -3.3, -3.6; IR (neat): 3440, 2927, 2864, 1169; HRMS-(NSI) m/z 495.3687 [(M+H)$^+$ requires 495.3684]; HPLC: (S,S-Whelk, 100 % hexane, 0.5 ml/min), UV: 230 nm, retention time of 36.24 min (minor) and 43.36 min (major), 92 % ee.
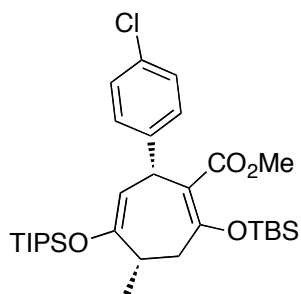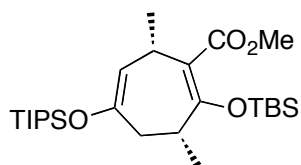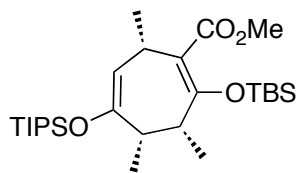
(3R,4S,7S)-methyl 2-((tert-butyldimethylsilyl)oxy)-3,4,7-trimethyl-5-((triisopropylsilyl)oxy)cyclohepta-1,5-dienecarboxylate (101):

Prepared *via* procedure D. Derived from ((2Z,4E)-hexa-2,4-dien-3-yloxy)triisopropylsilane (100 mg, 0.393 mmol, 1.0 equiv) and (Z)-methyl 3-((tert-butyldimethylsilyl)oxy)-2-diazopent-3-enoate (212 mg, 0.786, mmol, 2.00 equiv). Purified by flash chromatography (98:2 pentane/Et$_2$O) on silica gel to provide the vinylogous [4+3] product as colorless oil (141 mg, 72% yield). Rf = 0.14 (98:2 pentane:diethyl ether); [α]$_D^{20}$: 26.1 (*c*. 0.2, CHCl$_3$); 1H NMR (600 MHz; C$_6$D$_6$) δ 4.73 (d, 1H, *J* = 3.6 Hz), 3.52-3.50 (m, 1H), 3.49 (s, 3H), 2.96 (app q, *J* = 7.2 Hz, 1H), 2.27-2.22 (m, 1H), 1.22 (t, *J* = 7.2 Hz, 6H), 1.12-1.10 (m, 21H), 1.05 (t, *J* = 9.6 Hz, 3H), 0.99 (s, 9H), 0.23 (s, 3H), 0.20 (s, 3H); 13C NMR (100 MHz, C$_6$D$_6$) δ 169.3, 153.5, 152.8, 118.3, 108.5, 50, 41.9, 36.9, 28.1, 25.3, 20.5, 17.7, 14.8, 13.2, 12.5, -4.07, -4.6; IR (neat): 2944, 2865, 1721, 1158; HRMS- m/z 439.34328 (M+H)$^+$ requires 439.34221);
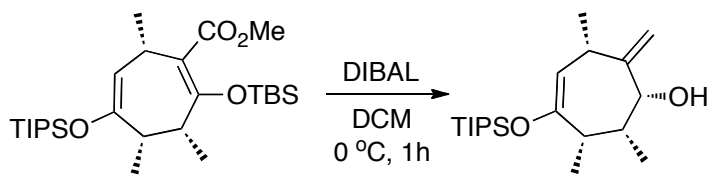
(1R,2R,3S,6S)-2,3,6-trimethyl-7-methylene-4-((triisopropylsilyl)oxy)cyclohept-4-enol:

To a 25 mL round-bottom flask was added (3R,4S,7S)-methyl 2-((tert-butyldimethylsilyl)oxy)-3,4,7-trimethyl-5-((triisopropylsilyl)oxy)cyclohepta-1,5-dienecarboxylate (**101**) (132 mg, 0.266 mmol, 1.0 eq) and DCM (14 mL). The solution was cooled to 0 $^\circ$C. Once cool, DIBAL 1M in DCM (1.1 mL, 1.07 mmol, 4.5 eq) was slowly added to the reaction over 5 minutes. The reaction was allowed to stir, at 0 $^\circ$C, for 1 hour. The reaction was then stopped by diluting with Et$_2$O followed by addition of saturated aqueous solution of Rochelle's salt and was aggressively stirred for 1 h. The mixtures was then transferred to a separation funnel and diluted with H$_2$O (100 mL). The two layers were separated and the aqueous layer was washed with Et$_2$O (3 x 50 mL). The organic layers were combined, dried over MgSO$_4$, filtered through a glass frit and concentrated under reduced pressure. Purified by flash chromatography (90:10 hexanes/EtOAc) on silica gel to provide the reduced product as colorless oil (19 mg, 21 % yield). Rf = 0.31 (90:10 hexanes:EtOAc); 1H NMR (400 MHz; C$_6$D$_6$) δ 5.11 (s, 1H), 4.91 (s, 1H), 4.53 (d, J = 4.8 Hz, 1H), 3.86 (s, 1H), 2.63 (q, J = 7.2 Hz, 1H), 2.55 (q, J = 6.6 Hz, 1H), 1.85 (q, J = 6 Hz, 1H), 1.19 (d, J = 7.2 Hz, 3H), 1.13 (s, J = 7.2 Hz, 3H), 1.12-1.11 (m, 21H), 0.92 (d, J = 7.2 Hz, 3H), 0.42 (bs, 1H); 13C NMR (100 MHz, C$_6$D$_6$) δ 153.4, 151.4, 108.3, 103.7, 79.8, 42.5, 38.7, 33, 19.5, 18.4, 16.3, 13.1, 7.5; IR (neat): 3384, 2964, 2943, 2866, 1645; HRMS- m/z 339.2716 (M+H)$^+$ requires 339.2713);

HPLC: (S,S-Whelk, 100 % hexane, 0.25 ml/min), UV: 230 nm, retention time of 53.24 min (minor) and 56.11 min (major), 85 % ee.
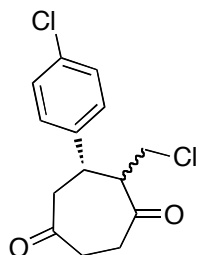
**(6S)-5-(chloromethyl)-6-(4-chlorophenyl)cycloheptane-1,4-dione (103):**

To a 250 mL round-bottom flask was added (R)-methyl 2-((tert-butyldimethylsilyl)oxy)-7-(4-chlorophenyl)-5-((triisopropylsilyl)oxy)cyclohepta-1,5-dienecarboxylate (**98a**) (1.00 g, 1.77 mmol, 1.0 eq) and DCM (70 mL). The solution was cooled to 0 °C. Once cool, DIBAL 1M in DCM (5.31 mL, 5.31 mmol, 3.0 eq) was slowly added to the reaction over 5 minutes. The reaction was allowed to stir, at 0 °C, for 1 hour. The reaction was then stopped by diluting with Et$_2$O followed by addition of saturated aqueous solution of Rochelle's salt. The mixture was aggressively stirred for 1 h. The mixture was then transferred to a separation funnel and diluted with H$_2$O (100 mL). The two layers were separated and the aqueous layer was washed with Et$_2$O (3 x 50 mL). The organic layers were combined, dried over MgSO$_4$, filtered through a glass frit and concentrated under reduced pressure. To a round bottomed flask was added anhydrous THF (12 mL) and cooled to 10 °C. Once cool, 2 M HCl (4 mL) was added. The reaction was allowed to stir and gradually warm to room temperature overnight. The reaction was then cooled to 0 °C and quenched with saturated aqueous NaHCO$_3$ solution.

70

The mixture was then transferred to a separation funnel and diluted with Et$_2$O. The two layers were separated and the aqueous layer was washed with Et$_2$O (3 x 25 mL). The organic layers were combined, dried over MgSO$_4$, filtered through a glass frit and concentrated under reduced pressure to give a 64:36 mixture of diastereomers. Purified by flash chromatography (75:25 hexanes/EtOAc) on silica gel to provide the reduced product as white solid (22 mg, 5 % yield). Rf = 0.17 (75:25 hexanes:EtOAc); 1H NMR (600 MHz; C$_6$D$_6$) Selected chemical shifts for major diastereomer: δ 6.995 (dd, 2H, J = 1.8, 8.4 Hz), 6.35 (dd, J = 1.8, 8.4 Hz, 2H), 3.25 (app t, J = 11.4 Hz, 1H), 2.95 (dd, J = 2.4, 10.8 Hz, 1H), 2.74-2.70 (m, 1H), 2.42 (m, 1H); 13C NMR (100 MHz, C$_6$D$_6$) chemical shifts for major diastereomer: δ 208.7, 207.6, 129.8, 129.6, 129.3, 128.5, 59.7, 49.7, 42.6, 41.8, 38.9, 38.5; IR (neat): 2959, 2920, 2852, 1700; HRMS- m/z 285.0437 (M+H)$^+$ requires 285.0443).

1.8.3 X-Ray crystallographic data
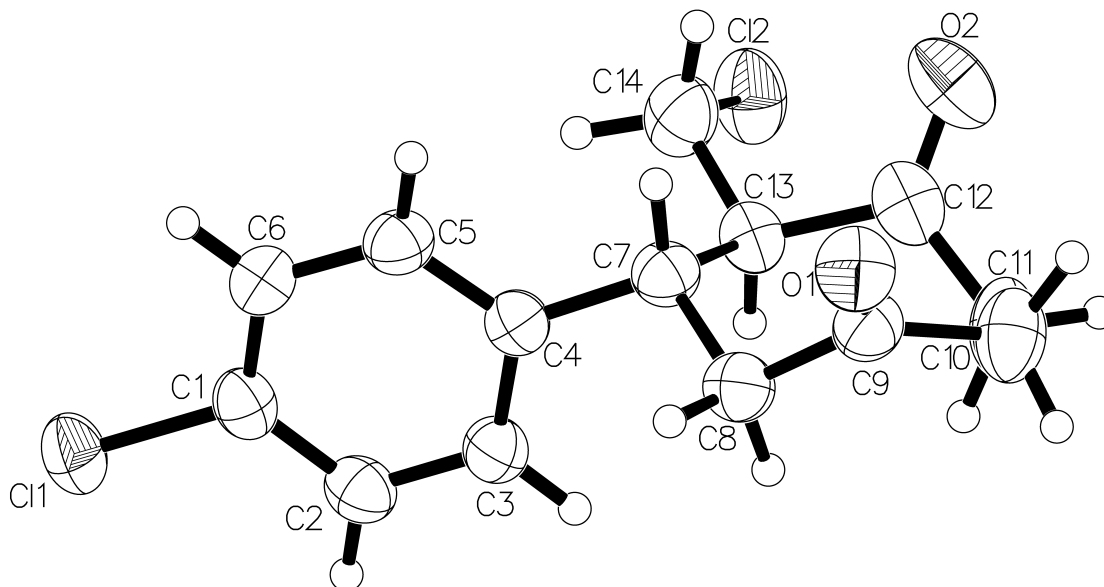
Table 1. Crystal data and structure refinement for peg1121.

Identification code	peg1121
Empirical formula	C14 H14 Cl2 O2
Formula weight	285.15
Temperature	173.0 K
Wavelength	1.54178 ≈
Crystal system	Orthorhombic
Space group	P 21 21 21
Unit cell dimensions	a = 5.8584(3) ≈ α= 90∞.
	b = 7.5562(4) ≈ β= 90∞.
	c = 30.2791(16) ≈ γ = 90∞.
Volume	1340.37(12) ≈^{3}

Z	4
Density (calculated)	1.413 Mg/m^3
Absorption coefficient	4.284 mm^{-1}
F(000)	592
Crystal size	$0.142 \text{ x } 0.14 \text{ x } 0.069 \text{ mm}^3$
Theta range for data collection	2.92 to 68.93∞.
Index ranges	-6<=h<=7, -8<=k<=9, -36<=l<=36
Reflections collected	7125
Independent reflections	2387 [R(int) = 0.0433]
Completeness to theta = 68.93∞	98.8 %
Absorption correction	Semi-empirical from equivalents
Max. and min. transmission	0.7531 and 0.5776
Refinement method	Full-matrix least-squares on F^2
Data / restraints / parameters	2387 / 0 / 163
Goodness-of-fit on F^2	1.028
Final R indices [I>2sigma(I)]	R1 = 0.0471, wR2 = 0.1245
R indices (all data)	R1 = 0.0532, wR2 = 0.1295
Absolute structure parameter	0.00(3)
Largest diff. peak and hole	0.330 and -0.363 e.≈$^{-3}$

Table 2. Atomic coordinates (x 10^4) and equivalent isotropic displacement parameters ($\approx^2$x 10^3) for peg1121. U(eq) is defined as one third of the trace of the orthogonalized U^{ij} tensor.

	x	y	z	U(eq)
C(1)	7283(5)	-25(5)	2437(1)	42(1)
C(2)	6232(6)	714(4)	2803(1)	45(1)
C(3)	7289(6)	617(4)	3210(1)	43(1)
C(4)	9409(5)	-244(4)	3256(1)	39(1)
C(5)	10418(6)	-930(5)	2880(1)	44(1)
C(6)	9386(6)	-840(5)	2471(1)	46(1)
C(7)	10524(5)	-450(4)	3705(1)	42(1)
C(8)	11007(6)	1405(5)	3911(1)	48(1)
C(9)	12672(6)	1282(5)	4292(1)	46(1)
C(10)	11784(7)	988(7)	4750(1)	60(1)
C(11)	9617(6)	-147(7)	4761(1)	60(1)
C(12)	9933(6)	-1768(5)	4476(1)	51(1)
C(13)	9033(6)	-1674(4)	4002(1)	44(1)
C(14)	8904(8)	-3490(5)	3798(1)	56(1)
Cl(1)	5931(1)	89(1)	1923(1)	52(1)
Cl(2)	6698(2)	-4800(1)	4052(1)	63(1)
O(1)	14701(5)	1390(4)	4225(1)	58(1)
O(2)	10897(6)	-3067(5)	4610(1)	74(1)

74

Table 3.   Bond lengths [Å] and angles [°] for peg1121.

_____

Cl(1)-C(1)	1.748(3)
Cl(2)-C(14)	1.800(4)
O(1)-C(9)	1.209(5)
O(2)-C(12)	1.202(5)
C(1)-C(2)	1.386(5)
C(1)-C(6)	1.381(5)
C(2)-C(3)	1.381(5)
C(3)-C(4)	1.409(5)
C(4)-C(5)	1.384(5)
C(4)-C(7)	1.516(4)
C(5)-C(6)	1.381(5)
C(7)-C(8)	1.560(5)
C(7)-C(13)	1.558(5)
C(8)-C(9)	1.512(5)
C(9)-C(10)	1.498(5)
C(10)-C(11)	1.532(6)
C(11)-C(12)	1.509(6)
C(12)-C(13)	1.531(5)
C(13)-C(14)	1.507(5)
C(2)-H(2)	0.9500
C(3)-H(3)	0.9500

C(5)-H(5)	0.9500
C(6)-H(6)	0.9500
C(7)-H(7)	1.0000
C(8)-H(8A)	0.9900
C(8)-H(8B)	0.9900
C(10)-H(10A)	0.9900
C(10)-H(10B)	0.9900
C(11)-H(11A)	0.9900
C(11)-H(11B)	0.9900
C(13)-H(13)	1.0000
C(14)-H(14A)	0.9900
C(14)-H(14B)	0.9900
Cl(1)-C(1)-C(2)	119.4(2)
Cl(1)-C(1)-C(6)	119.5(2)
C(2)-C(1)-C(6)	121.1(3)
C(1)-C(2)-C(3)	119.6(3)
C(2)-C(3)-C(4)	120.5(3)
C(3)-C(4)-C(5)	117.9(3)
C(3)-C(4)-C(7)	121.1(3)
C(5)-C(4)-C(7)	121.0(3)
C(4)-C(5)-C(6)	122.2(3)
C(1)-C(6)-C(5)	118.6(3)

C(4)-C(7)-C(8)	110.2(3)
C(4)-C(7)-C(13)	109.7(2)
C(8)-C(7)-C(13)	113.8(3)
C(7)-C(8)-C(9)	111.5(3)
O(1)-C(9)-C(8)	120.2(3)
O(1)-C(9)-C(10)	120.5(3)
C(8)-C(9)-C(10)	119.4(3)
C(9)-C(10)-C(11)	113.0(3)
C(10)-C(11)-C(12)	109.9(3)
O(2)-C(12)-C(11)	121.9(4)
O(2)-C(12)-C(13)	121.0(3)
C(11)-C(12)-C(13)	117.1(3)
C(7)-C(13)-C(12)	112.1(3)
C(7)-C(13)-C(14)	109.3(3)
C(12)-C(13)-C(14)	111.1(3)
Cl(2)-C(14)-C(13)	111.2(3)
C(1)-C(2)-H(2)	120.00
C(3)-C(2)-H(2)	120.00
C(2)-C(3)-H(3)	120.00
C(4)-C(3)-H(3)	120.00
C(4)-C(5)-H(5)	119.00
C(6)-C(5)-H(5)	119.00
C(1)-C(6)-H(6)	121.00

C(5)-C(6)-H(6)	121.00
C(4)-C(7)-H(7)	108.00
C(8)-C(7)-H(7)	108.00
C(13)-C(7)-H(7)	108.00
C(7)-C(8)-H(8A)	109.00
C(7)-C(8)-H(8B)	109.00
C(9)-C(8)-H(8A)	109.00
C(9)-C(8)-H(8B)	109.00
H(8A)-C(8)-H(8B)	108.00
C(9)-C(10)-H(10A)	109.00
C(9)-C(10)-H(10B)	109.00
C(11)-C(10)-H(10A)	109.00
C(11)-C(10)-H(10B)	109.00
H(10A)-C(10)-H(10B)	108.00
C(10)-C(11)-H(11A)	110.00
C(10)-C(11)-H(11B)	110.00
C(12)-C(11)-H(11A)	110.00
C(12)-C(11)-H(11B)	110.00
H(11A)-C(11)-H(11B)	108.00
C(7)-C(13)-H(13)	108.00
C(12)-C(13)-H(13)	108.00
C(14)-C(13)-H(13)	108.00
Cl(2)-C(14)-H(14A)	109.00

Cl(2)-C(14)-H(14B)   109.00

C(13)-C(14)-H(14A)   109.00

C(13)-C(14)-H(14B)   109.00

H(14A)-C(14)-H(14B)   108.00

_____

Symmetry transformations used to generate equivalent atoms:

Table 4.   Anisotropic displacement parameters ($\approx^2$x 10^3) for peg1121. The anisotropic

displacement factor exponent takes the form: $-2\pi^2[\ h^2\ a^{*2}U^{11} + ... + 2\ h\ k\ a^*\ b^*\ U^{12}\ ]$

	U^{11}	U^{22}	U^{33}	U^{23}	U^{13}	U^{12}
C(1)	46(1)	41(1)	39(1)	4(1)	-4(1)	-6(1)
C(2)	38(1)	47(2)	48(2)	6(1)	0(1)	3(1)
C(3)	42(2)	48(2)	39(2)	3(1)	3(1)	5(1)
C(4)	38(1)	38(1)	39(1)	2(1)	0(1)	-2(1)
C(5)	39(1)	45(2)	47(2)	-2(1)	2(1)	4(1)
C(6)	50(2)	46(2)	41(2)	-4(1)	1(1)	3(1)
C(7)	38(1)	44(2)	43(2)	1(1)	2(1)	2(1)
C(8)	50(2)	46(2)	49(2)	0(1)	-2(2)	2(2)
C(9)	43(2)	48(2)	47(2)	-5(1)	-1(1)	1(1)
C(10)	48(2)	86(3)	46(2)	-6(2)	-1(2)	-10(2)
C(11)	51(2)	87(3)	41(2)	-5(2)	4(1)	-14(2)
C(12)	41(2)	64(2)	48(2)	10(2)	-3(1)	-9(2)
C(13)	44(2)	48(2)	40(2)	4(1)	-1(1)	-1(1)
C(14)	65(2)	54(2)	49(2)	3(2)	11(2)	-8(2)
Cl(1)	57(1)	57(1)	42(1)	4(1)	-12(1)	-6(1)
Cl(2)	77(1)	63(1)	49(1)	6(1)	-3(1)	-23(1)
O(1)	45(1)	68(2)	60(2)	-1(1)	-1(1)	-7(1)
O(2)	68(2)	83(2)	73(2)	20(2)	-21(2)	3(2)

Table 5.   Hydrogen coordinates (x 10^4) and isotropic displacement parameters ($\approx^2$x 10 ^{3})

for peg1121.

	x	y	z	U(eq)
H(2)	4794	1284	2774	54
H(3)	6581	1134	3461	51
H(5)	11870	-1482	2905	52
H(6)	10108	-1329	2218	55
H(7)	12026	-1051	3660	50
H(8A)	11639	2199	3682	58
H(8B)	9556	1925	4017	58
H(10A)	11454	2149	4887	72
H(10B)	12982	402	4928	72
H(11A)	9287	-509	5069	71
H(11B)	8306	552	4651	71
H(13)	7454	-1173	4012	53
H(14A)	10392	-4095	3833	67
H(14B)	8591	-3376	3478	67

Table 6. Torsion angles [∞] for peg1121.

Cl(1)-C(1)-C(2)-C(3)	179.6(3)
C(6)-C(1)-C(2)-C(3)	-0.8(5)
Cl(1)-C(1)-C(6)-C(5)	-179.5(3)
C(2)-C(1)-C(6)-C(5)	0.9(5)
C(1)-C(2)-C(3)-C(4)	-0.8(5)
C(2)-C(3)-C(4)-C(5)	2.1(5)
C(2)-C(3)-C(4)-C(7)	-176.5(3)
C(3)-C(4)-C(5)-C(6)	-1.9(5)
C(7)-C(4)-C(5)-C(6)	176.7(3)
C(3)-C(4)-C(7)-C(8)	-60.7(4)
C(3)-C(4)-C(7)-C(13)	65.3(4)
C(5)-C(4)-C(7)-C(8)	120.7(3)
C(5)-C(4)-C(7)-C(13)	-113.3(3)
C(4)-C(5)-C(6)-C(1)	0.5(6)
C(4)-C(7)-C(8)-C(9)	-164.3(3)
C(13)-C(7)-C(8)-C(9)	72.0(4)
C(4)-C(7)-C(13)-C(12)	-173.7(3)
C(4)-C(7)-C(13)-C(14)	62.7(3)
C(8)-C(7)-C(13)-C(12)	-49.7(4)
C(8)-C(7)-C(13)-C(14)	-173.4(3)
C(7)-C(8)-C(9)-O(1)	89.1(4)

C(7)-C(8)-C(9)-C(10)	-89.6(4)
O(1)-C(9)-C(10)-C(11)	-146.0(4)
C(8)-C(9)-C(10)-C(11)	32.7(5)
C(9)-C(10)-C(11)-C(12)	47.6(5)
C(10)-C(11)-C(12)-O(2)	82.5(5)
C(10)-C(11)-C(12)-C(13)	-95.8(4)
O(2)-C(12)-C(13)-C(7)	-106.2(4)
O(2)-C(12)-C(13)-C(14)	16.5(5)
C(11)-C(12)-C(13)-C(7)	72.0(4)
C(11)-C(12)-C(13)-C(14)	-165.3(3)
C(7)-C(13)-C(14)-Cl(2)	-166.5(2)
C(12)-C(13)-C(14)-Cl(2)	69.2(4)

_____

Symmetry transformations used to generate equivalent atoms:

Table 7. Hydrogen bonds for peg1121 [≈ and ∞].

_____

D-H...A	d(D-H)	d(H...A)	d(D...A)	<(DHA)
C(3)-H(3)...O(1)#1	0.9500	2.5700	3.475(5)	160.00
C(11)-H(11A)...O(2)#2	0.9900	2.4600	3.194(5)	131.00
C(11)-H(11B)...O(1)#1	0.9900	2.5500	3.504(5)	161.00

_____

Symmetry transformations used to generate equivalent atoms:

#1+0   #2+1

CHAPTER II

An Exploratory Study to the Bis-Diazo Approach Towards Phorbol

2.1 Introduction

Diazo compounds have proven to be extremely useful building blocks in organic synthesis. They are now widely recognized as versatile and useful reagents for a myriad of chemical transformations and are far from losing any of their long-standing fascination. Commonly used methods for the synthesis of diazo compounds are summarized below in Scheme 2.1.
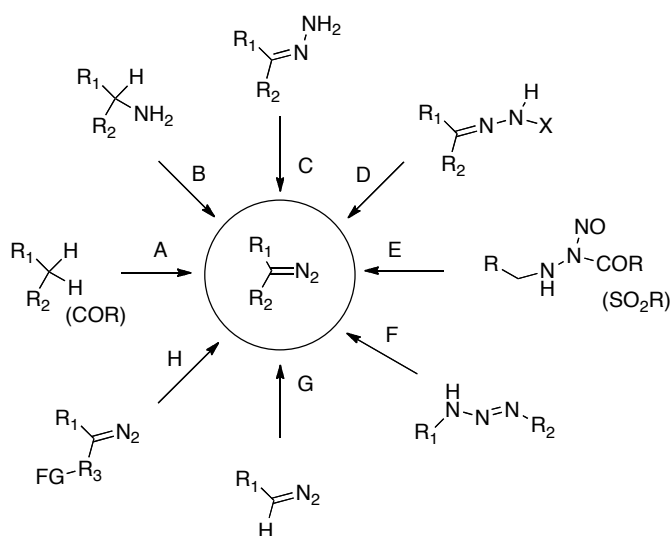
Scheme 2.1 Major synthetic routes to diazo compounds.

The methods include A) diazo-group transfer onto activated methylene or methine compounds, B) diazotization of α-acceptor-substituted primary aliphatic amines, C) dehydrogenation of hydrazones, D) base treatment of sulfonylhyrazones, E) alkaline cleavage of *N*-alkyl-*N*-nitroso sulfonamides, carboxamides, ureas and urethanes, F)

triazene fragmentation (rare), G) electrophilic substitution at diazomethyl compounds and H) substituent modification of and existing diazo compound.[1-5] Photochemical or thermally induced extrusion of dinitrogen provides facile entry to free carbenes. As a result of their high reactivity, these carbenes tend to be unselective.[6,7] Fortunately, great advances have been made with transition metal-catalyzed diazo decomposition which give rise to highly reactive, yet stabilized, transient metallo-carbenoid complexes. These species continue to be used to develop a broad range of new transformations that often feature an extraordinary degree of chemo-, regio-, and stereoselectivity. For example, cyclopropanation of alkenes and alkynes,[8] C-H, O-H, Si-H and N-H insertions,[9,10] ylide formation,[2,9,11-16] formal cycloadditions[17-19] and diazo cross coupling have been intensively studied (Figure 2.1).[20]
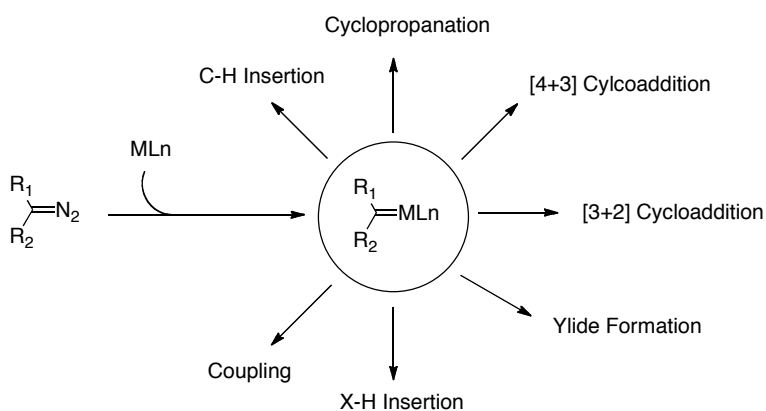
Figure 2.1 Reaction scope of metallocarbenoids.

88

2.11 Transition-metal catalyzed complexity generating reactions involving mono-diazo compounds

Cascade reactions represent an intriguing area of organic chemistry. The rapid and controlled increase in molecular complexity constitutes an enormous challenge for the construction of polycyclic natural products and biologically active molecules. Interestingly, complexity can be obtained through intramolecular manifolds. Diazo compounds are known to take part in 1,3-dipolar cycloaddition reactions with a wide range of dipolarophiles and are extremely efficient in complexity generating cascades.[21,22] Several laboratories have elegantly displayed the practicality of this reaction through the synthesis of various natural products.[23] A clever extension of this chemistry is the cyclization-cycloaddition cascade of rhodium carbenoids. The Padwa laboratory was first to report the formation of a cyclic six-membered ring carbonyl ylide, derived from a Rh(II)-catalyzed reaction between α-diazoacetophenone **1a** (or **1b**), reacting in an intramolecular fashion with an olefin tethered to the substrate (Scheme 2.2).[24] The reaction involves the formation of a rhodium carbenoid intermediate and subsequent transannular cyclization of the ester group to generate cyclic carbonyl ylide **2a** or **2b**, followed by a 1,3-dipolar cycloaddition to provide **3a** or **3b**.

1a; R = H
1b; R = Me

2a; R = H
2b; R = Me

3a; R = H : 85%
3b; R = Me : 87%
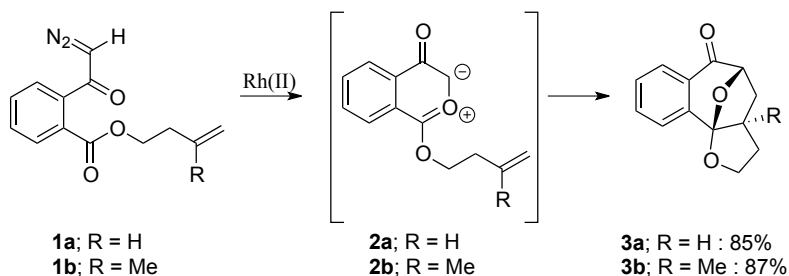
Scheme 2.2 First example of intramolecular cyclization-cycloaddition strategy.

The intramolecular trapping of a five-membered ring carbonyl ylide dipole with an appended alkene was subsequently reported (Scheme 2.3).[25]
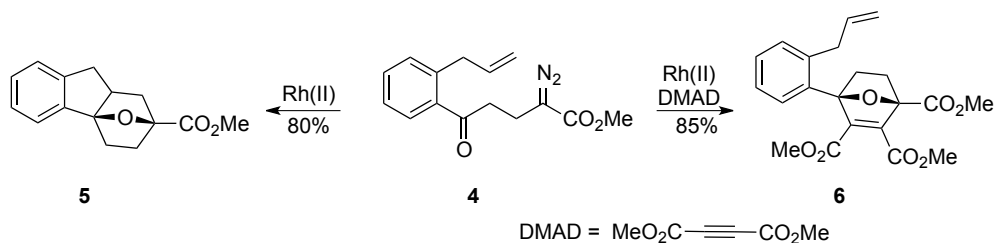
Scheme 2.3 Inter- and intramolecular cyclization-cycloaddition methodology.

The treatment of **6** with Rh$_2$(OAc)$_4$ provided cycloadduct **5** in 80 % yield. Interestingly, in the presence of dimethyl acetylenedicarboxylate, intermolecular adduct **6** was isolated in 85 % yield. This intramolecular cycloaddition is the result of the significant difference in reactivity of the two dipolarophiles where the carbonyl ylide reacts exclusively with the more reactive acetylenic π-bond thus broadening the synthetic utility of the domino dipole cascade sequence. This powerful complexity generating methodology has been used by several synthetic laboratories[23] and showcased by the Padwa group for the construction of the *Aspidosperma* alkaloid aspidophytine.[26] The alkaloid skeleton is rapidly accessed in a single chemical step (Scheme 2.4).

(±)-aspidophytine

90
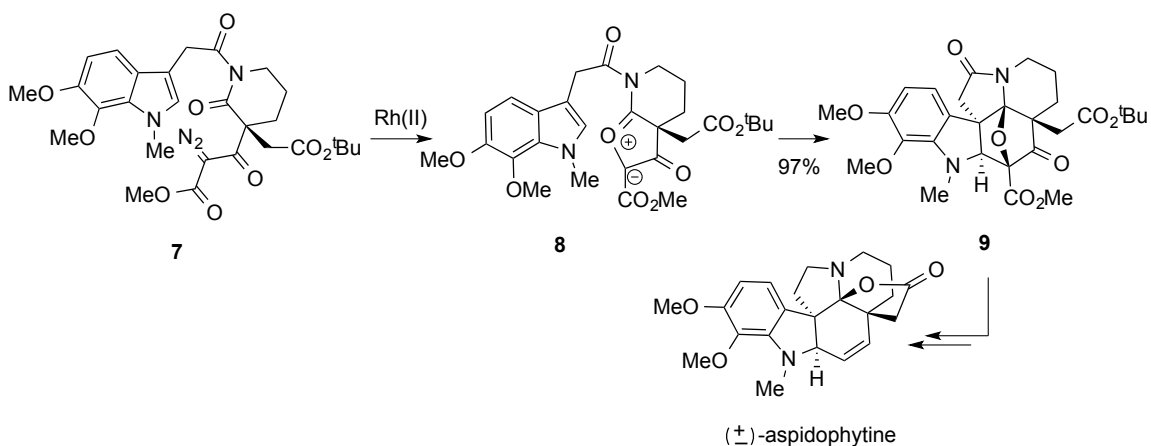
Scheme 2.4 Padwa's approach towards (±)-aspidophytine.

The key sequence of reactions involves a 1,3 dipolar cycloaddition of dipole **8** across the indole π-system. In contrast to previous cycloadditions,[27-29] the *exo*-cycloadduct **9** was the exclusive product isolated from the Rh(II)-catalyzed reaction. It is hypothesized that in this reaction, the bulky *tert*-butyl-ester functionality obstructs the *endo* approach thereby resulting in cycloaddition taking place from the less-congested *exo*-face.

In the early 1990's, the Dauben laboratory provided one of the first examples of the intramolecular trapping of a carbonyl ylide dipole with an alkene for natural product synthesis. Dauben elegantly showcased this methodology in the formation the of the complete tigliane core (Scheme 2.5).[30]
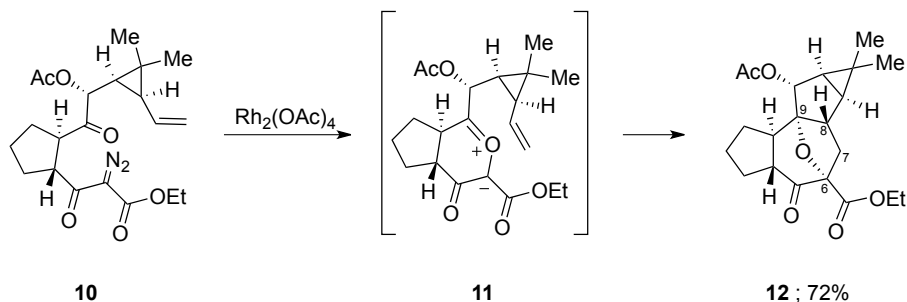
Scheme 2.5 Dauben's approach to the tigliane skeleton.

In this transformation, carbonyl ylide **11**, generated from the diazocarbonyl **10** in the presence of $Rh_2(OAc)_4$ underwent an intramolecular addition with the olefin to form the C_6,C_9-oxido-bridged tigliane ring system **12**. The two new stereocenters at C_8 and C_9 were formed with the correct configurations relative to C_{14} and C_{15} presented in natural tigliane compounds. The high stereospecificity in the ring closure reaction was

rationalized on the basis of steric interactions or the introduction of conformational strain in the tether, which disfavors the transition state when the cyclopropane ring and the oxo bridge are on the same face of the molecule.

Recently, the Boger laboratory enlisted a diastereoselective intramolecular [4+2]/[3+2]-cycloaddition reaction of 1,3,4-oxadiazoles, which occurs through the formation of a 1,3 dipole. This chemistry was used for the total synthesis of (-)-vindoline (Scheme 2.6).[31]
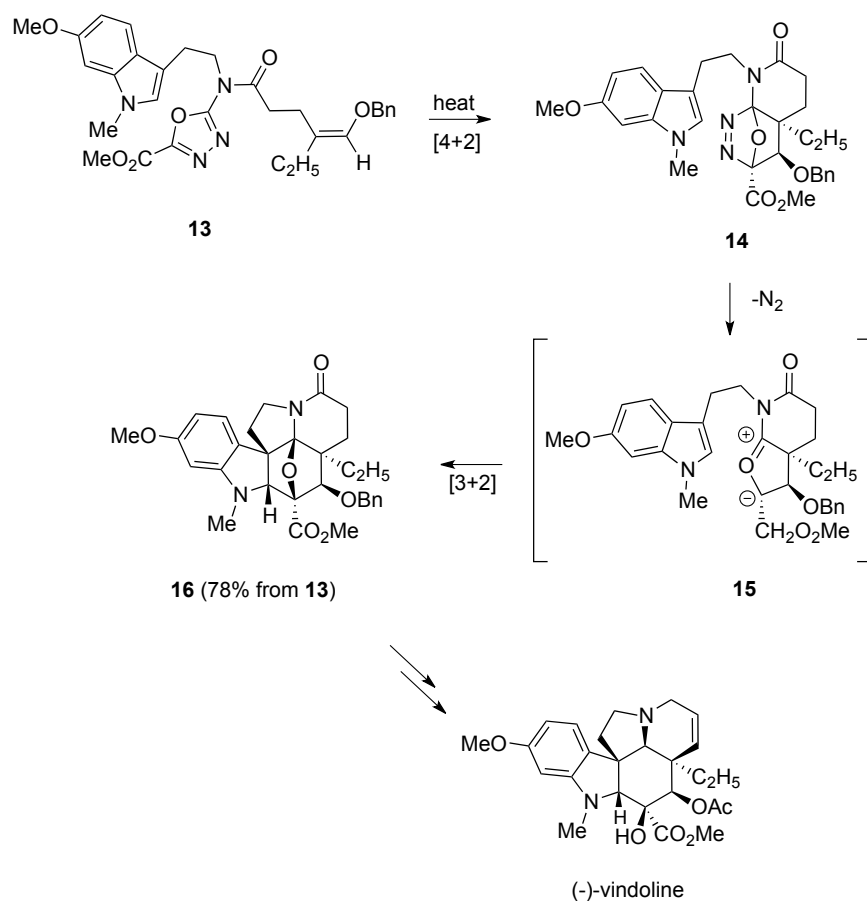
Scheme 2.6 Boger's [4+2]/[3+2] cycloaddition approach to (-)-vindoline.

This unique cascade sequence constructs the fully functionalized pentacyclic ring system of vindoline in a single step that forms four C-C bonds and three rings while introducing all the relevant functionality and setting all six stereocenters within the central ring including three contiguous and four total quaternary centers. The reactions leading to **16** is initiated by an intramolecular inverse electron demand Diels-Alder cycloaddition of the 1,3,4-oxadiazole **14** with the tethered enol ether. Extrusion of dinitrogen from the initial Diels-Alder adduct yields the desired carbonyl ylide **15**, ensuing to a precedented 1,3 dipolar cycloaddition with the tethered indole. The Boger laboratory conducted additional studies, which elucidated the controlling elements for this new cascade (Figure 2.2).
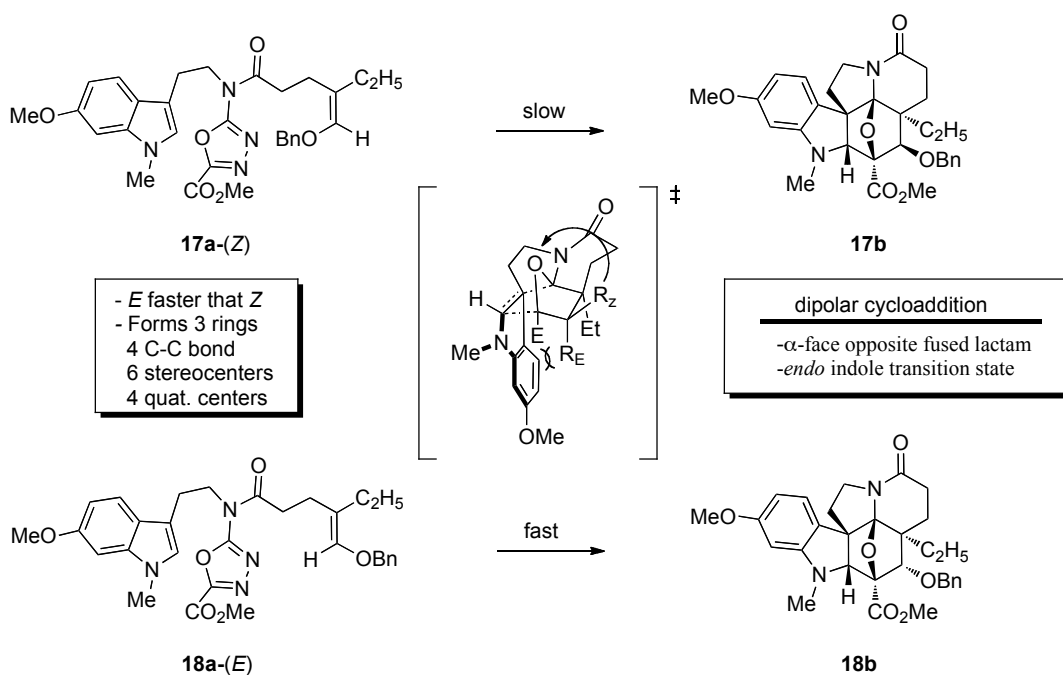
Figure 2.2 Boger's [4+2]/[3+2] cycloaddition rationale.

Notably, the diene and dienophile substituents complement and fortify the [4+2]-cycloaddition regioselectivity dictated by the linking tether. The relative stereochemistry

in the cycloadduct is controlled by a combination of i) the dienophile geometry and ii) an exclusive *endo*-indole [3+2]-cycloaddition sterically directed to the α-face opposite the newly formed fused lactam. This *endo* diastereoselectivity for the 1,3-dipolar cycloaddition has been attributed to a conformational (strain) preference dictated by the dipolarophile tether.[32-34] Extension of these cascade studies by the Boger group has lead to the total synthesis of the bisindole alkaloids vinblastine and vincristine.[35] The spectacular transformations described above provided the inspiration to develop our own cascade approach through the use of bis-diazo compounds.

2.12 Overview of complexity generating reactions with bis-diazo compounds: photo- and thermal decomposition studies

Bis-diazo compounds have been the source of ample synthetic utility and mechanistic inquiry for over 50 years. Initial studies of these "exotic" compounds began with photochemical and thermal mediated studies. α-Bis-diazo compounds, formed by dehydrogenation of the bis-hydrazones of 1,2-diketones, are relatively unstable and readily extrude nitrogen to give alkynes.[6,36] The complex nature of α-bis-diazo decomposition, to give bis-carbenes, and their Wolff rearrangements have initiated numerous studies.[37-47] For example, in the early 1970's Trost and coworkers critically re-examined initial reports, described by Kirmse,[48] for the ring contraction of 2,6-bis-(diazo)cyclohexanone which was rationalized to occur through a Wolff rearrangement pathway and give rise to methyl ester **23** (Scheme 2.7).
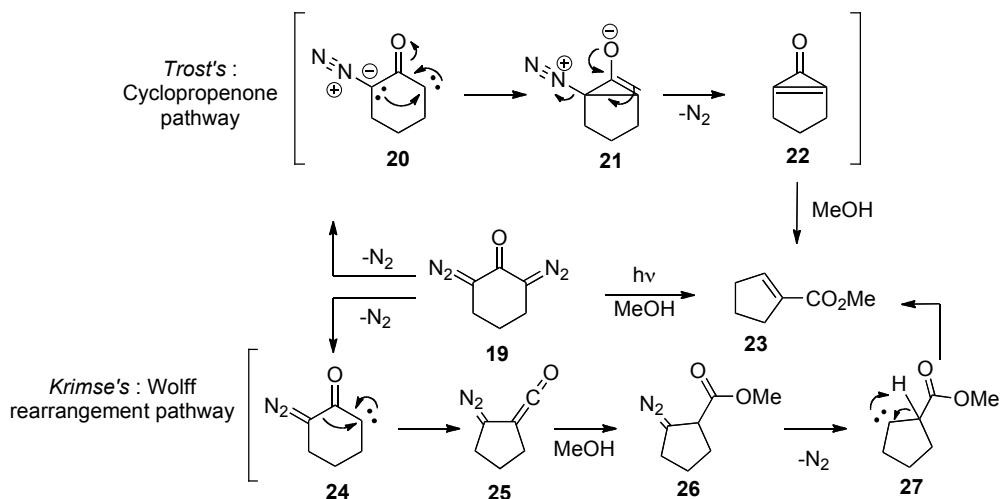
Scheme 2.7 Comparison of Krimse and Trost's rationale for the formation of **23**.

Based on detailed mechanistic studies, the Trost laboratory excluded the possibility of a simple Wolff rearrangement and proposed the intermediacy of a cyclopropenone which is capable of forming alkynes.[49] In support of this mechanistic study, Chapman and co-workers synthesized the highly strained acetylene derivative acenaphthyne (Scheme 2.8).
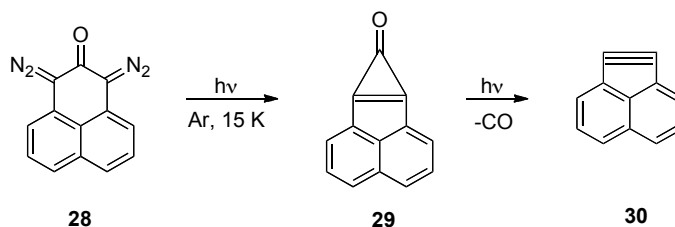
Scheme 2.8. Chapman's synthesis of acenapthyne.

Tris-diazo compounds have also been used as substrates designed for the synthesis of new materials (Scheme 2.9). Drawing inspiration from interstellar molecules, the Maier laboratory used the photochemical decomposition of bis- and tris-diazo compounds to synthesize unusual oxides of carbon, C_xO_y, and other reactive species.[50,51]
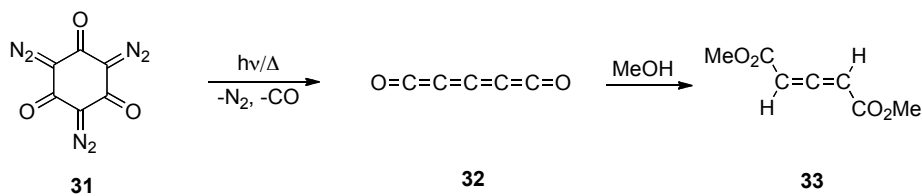
Scheme 2.9. Maier's approach to unusual oxides of carbon.

Oxide **32** was obtained as the sole product upon irradiation of tris-diazo **31** at 254 nm in an argon matrix at 12 °K. Compound **32** could also be obtained by subjecting **31** to pyrolysis in the gas phase (700 °C). The Maier group was able unequivocally prove that **32** is a stable yellow solid to temperatures reaching approximately -90 °C. Moreover, proof of structure **32** was based on the observation that a yellow solution of **31** lost its color immediately upon addition of methanol to give the known dimethyl allenedicarboxylate **33**.

Bis-diazo compounds bearing nonequivalent diazo groups have been reported by Cava and Fields.[37,38] Though the photochemistry of the bis-diazo ketones studied were of special interest, the authors primarily reported that the photolysis of these compounds in solution afforded a complex mixture of products from which nothing could be characterized. A significant advancement regarding the photodecomposition of nonequivalent bis-diazo ketones was introduced by Tomioka in the late 1990's.[52] As a result of their studies, it was concluded that bis-diazo **34** can undergo remarkable wavelength-dependant photochemical reactions in argon matrices (Scheme 2.10) and in solution (Scheme 2.11). Specifically, the selective photodecomposition of one of the two nonequivalent diazo groups was practically achieved. In an argon matrix, >350 nm light induces the release of nitrogen from the 2-position of acceptor/acceptor portion of **34** and

undergoes a Wolff rearrangement to generate ketene **35a**. Similarly, >420nm light causes the donor/acceptor diazo to extrude nitrogen from the 4-position and undergo the same rearrangement/ketene formation event and generate compound **35b**.
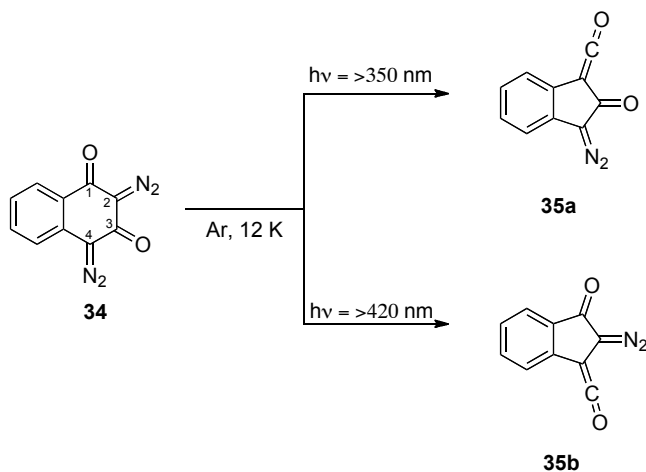
Scheme 2.10 Tomioka's selective photodecomposition of **34** in an argon matrix.

Irradiation of **34** in benzene containing 1% (v/v) MeOH with a high pressure Hg lamp (>300 nm) yielded a mixture of spironorcaradiene **36a** (21%) and methyl 3-oxo-2-diazoindan-1-carboxylate **36b** (9%) as the only isolable photoproducts. Interestingly, when light with a wavelength of >420 nm was used the product distribution shifted dramatically. An increase of diazo ketone **36b** and a decrease of spironorcaradiene was observed (**36a** : **36b** = 6 : 94). The authors proposed that **36a** was derived from diazo ketene **35a**, which is formed by the initial decomposition of the diazo group at the 2-position of **34**. The formation of **36b** was rationalized to occur by capture of the diazo ketene **35b**, generated by disengaging N_2 from the 4-position of bis-diazo **34**, with methanol. The wavelength effect observed in the photolysis of **34** in benzene containing MeOH strongly suggested that the photolysis with the long-wavelength light (>420 nm) can initiate the decomposition of the diazo group at the 4-position but fails to cause

97

extrusion of N_2 from the 2-position of the bis-diazo ketone. This report was the first example of the reactivity control of a poly(diazo) compound by the excitation wavelength.
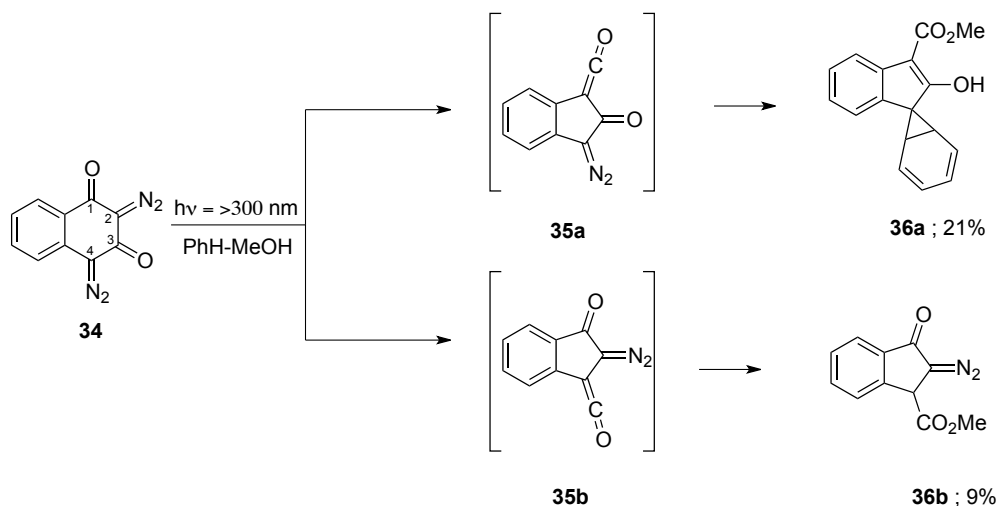
Scheme 2.11 Photodecomposition of **34** in solution.

2.13 Overview of transition-metal-mediated decomposition of bis-diazo compounds

The transition-metal-catalyzed decomposition of bis-diazo compounds has been an area of interest for organic and materials chemists alike for nearly four decades. Early studies, conducted by Serratosa and his co-workers, focused on the Cu(II)-catalyzed intramolecular cyclization of bis-α-diazoketones.[53] With this methodology, a new expedited synthesis of γ-tropolone (**41**) was accomplished (Scheme 2.12).
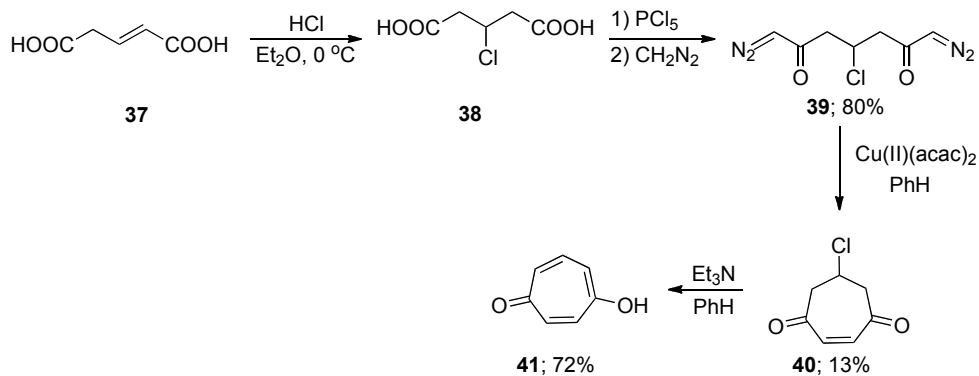
Scheme 2.12 Serratosa's synthesis of γ-tropolone.

β-chloroglutaric acid **38** was prepared by the addition of anhydrous hydrogen chloride to glutoconic acid **37** in ethereal solution. Treatment of **38** with PCl$_5$ followed by excess diazomethane provided 1,7-bis-diazo-4-chloro-heptane-2,6-dione (**39**) in 80% yield. Decomposition of this bis-α-diazoketone with Cu(II)-acetylacetonate in benzene solution at 65 °C led to 6-chlorocyclohept-2-ene-1,4-dione (**40**) in 13% yield. Elimination of HCl by slow drop-wise addition of Et$_3$N afforded γ-tropolone **41** in 72% yield.

Four years later, the McKervey laboratory used a similar methodology for the preparation of medium- and large-ring cycloalk-2-ene-1,4 diones with yields ranging from 30-80 %*via* a Cu(acac)$_2$-catalyzed intramolecular coupling of α,ω-bis-diazoketones (Scheme 2.13).[54] This methodology has proven to be a general process for the synthesis of enedione derivatives which are themselves versatile synthetic intermediates.
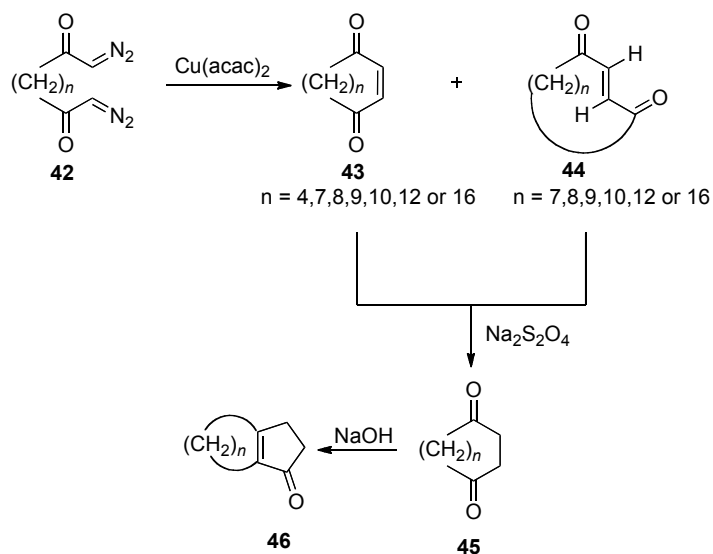
Scheme 2.13 McKervey's synthesis of cycloalk-2-ene-1,4-diones.

As such, McKervey was able to increase the synthetic utility of the enedione products by treatment with sodium dithionite and sodium hydroxide. This reaction efficiently converted the enediones to their corresponding fused ring cyclopentenones.

Twenty-two years later, Doyle and co-workers introduced a new approach towards the construction of diverse macrocyclic compounds. Their efforts led them to accomplish the total synthesis of patulolides A and B *via* a Rh(II)-catalyzed intramolecular coupling of bis-diazocarbonyl compounds (Scheme 2.14).[55] Patulolides A and B are biologically active macrocyclic lactones isolated from *Penicillium urticae* mutant S11R59.[56,57] These lactones are generally synthesized through ring-closing esterification[58] or alkene metathesis.[59]
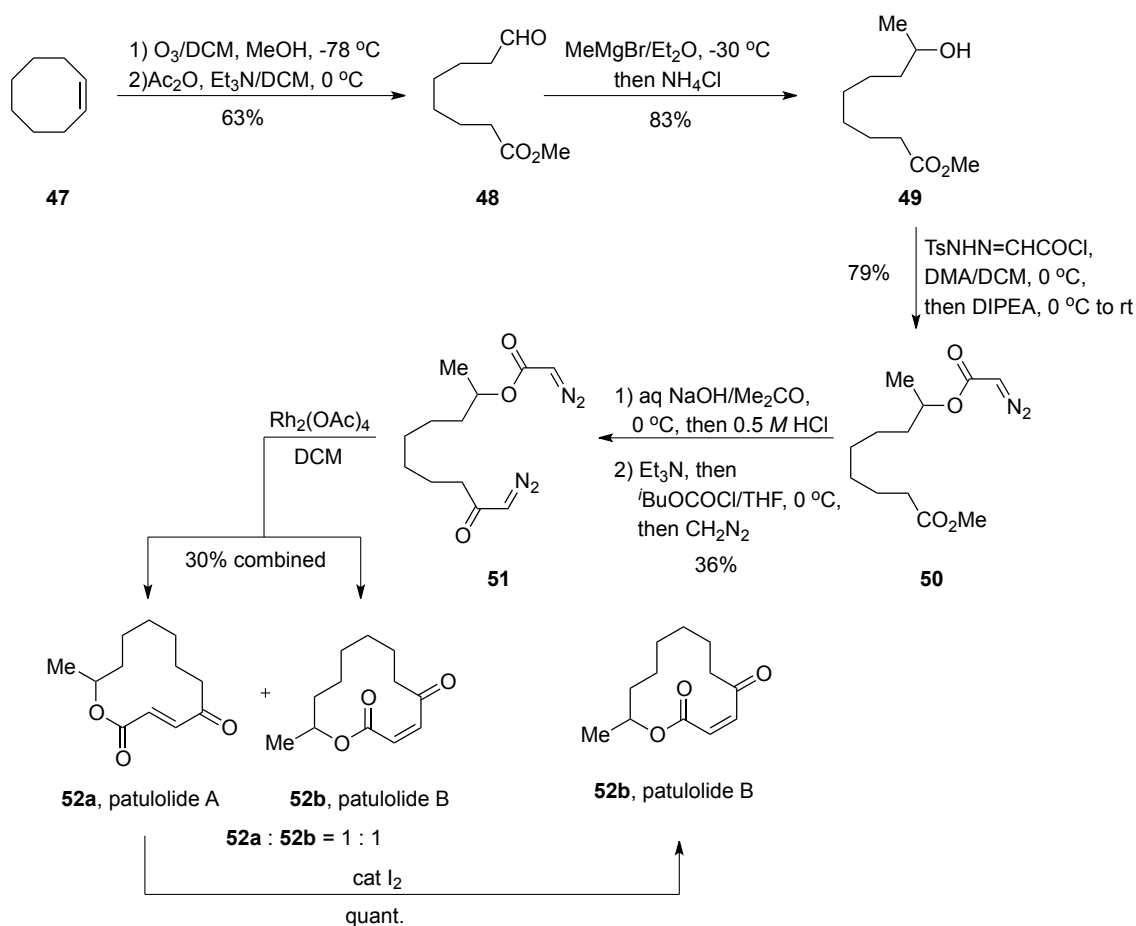
Scheme 2.14 Doyle's total synthesis of patulolide A and B.

Following conditions previously described by Corey,[60] diazo ester **50** was accessed in four high-yielding synthetic manipulations. Saponification of **50** with NaOH followed by exposure of the carboxylic acid to isobutyl chloroformate yielded bis-diazo **51** which was isolated in 36% yield. Treatment of **51** with a catalytic amount of Rh$_2$(OAc)$_4$ produced a 1 : 1 mixture of patulolide A and B, each of which was isolated in chromatographically pure form (30% combined yield). The authors revealed that in the presence of Cu(MeCN)$_4$PF$_6$, the product ratio is increased to 1 : 2 in favor of patulolide B, however, a combined yield of only 11% was reported. Notably, in the presence of a catalytic amount of I$_2$, patulolide A can be isomerized to patulolide B quantitatively.

101

In 2004, Che reported that ruthenium porphyrin catalyst [Ru(2,6,-Cl₂TPP)(CO)] was capable of highly cis-selective intra- and intermolecular coupling reactions of diazo compounds.

Table 2.1 Che's intramolecular coupling of bis-diazo esters.
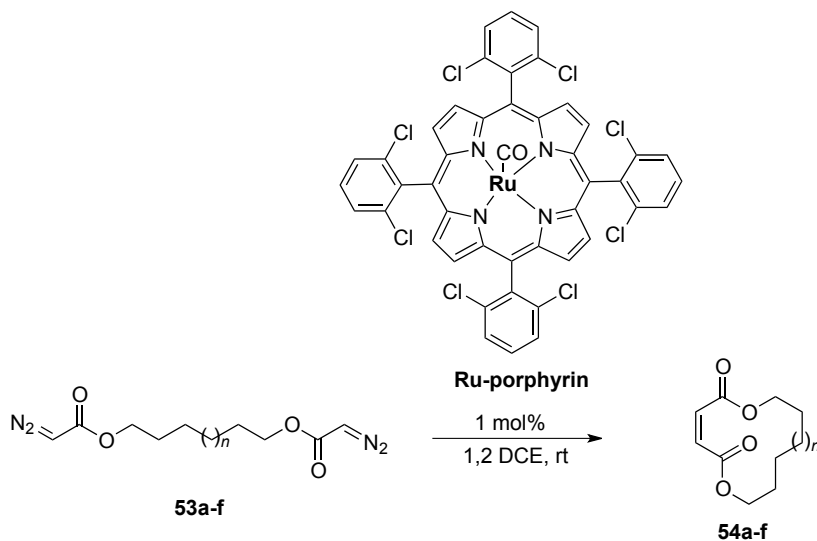
entry	*n*	product	yield (%)
1	1	**54a**	68
2	2	**54b**	61
3	3	**54c**	65
4	4	**54d**	72
5	5	**54e**	66
6	7	**54f**	63

As depicted in Table 2.1, macrocyclic (12-18-membered rings) products are readily accessed in high yield (61-72%). Intermolecular oligomerization is avoided by conducting the reactions in diluted solution concentrations (0.05 *M*). A key feature of this work is the excellent *cis/trans* selectivity. Interestingly, none of the *trans* olefin

isomer was isolated from the reactions. Che and co-workers were able to unambiguously confirm the structure of compound **54e** by X-ray crystallographic analysis. This methodology was efficiently extended to bis-diazo esters containing ether linkages (Table 2.2).

Table 2.2 Che's intramolecular coupling of glycol derived bis-diazo esters.
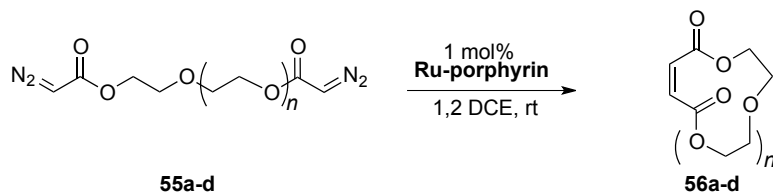
entry	n	product	yield (%)
1	1	**56a**	76
2	2	**56b**	71
3	3	**56c**	65
4	5	**56d**	69

Intramolecular couplings of bis-diazoacetates (**55a-d**) produced *cis* products **56a-d** in up to 76% yield. Notably, macrocycle **56d**, a 23-membered ring, was obtained in 69% yield (entry 4). Under optimized conditions, bis-diazo **51** was treated with 1 mol% of catalyst **1.339**. Patulolide B, (**52b**) was isolated in an excellent 67% yield (Scheme 2.15). Importantly, only a trace amount of the *trans*-isomer, patulolide A, was detected in a ratio of < 1:40 by ^{1}H NMR spectroscopy.
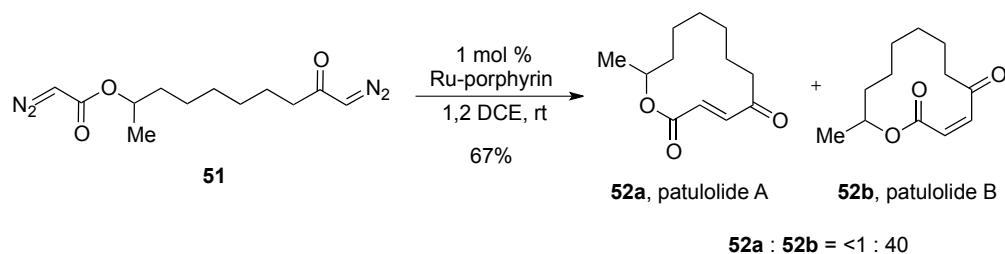
Scheme 2.15 Che's total synthesis of patulolide B.

Unsaturated polyesters are integral polymers that have been used in many fields, such as biotechnology, tissue engineering, and plastic production.[61-63] The most widely used unsaturated polyesters are polymaleates, which are generally prepared by polycondensation reactions using various transition-metal catalysts.[64-68] Recently, Liu and co-workers reported a new approach for the preparation of such unsaturated polyesters. The authors developed a copper (II)-catalyzed denitrogen alkene polymerization (DNAP) of bis-diazo ester compounds (Scheme 2.16).[69]
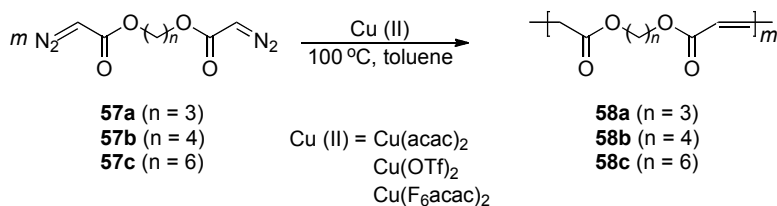
Scheme 2.16 Liu's denitrogen alkene coupling/polymerization.

A tentative catalytic reaction process for the DNAP process is shown in Scheme 18. Results from ^{1}H, FTIR, and MALDI-TOF MS suggested that an intermolecular coupling reaction between the α-bis-diazo compounds occurred during the reaction process. The reaction pathway for the Cu(II)-catalyzed polymerization of α-bis-diazo compounds

involves the initial attack of the bis-diazo compound at the Cu(II) metal center followed by release of nitrogen from intermediate **I** to generate metallocarbenoid **II**.
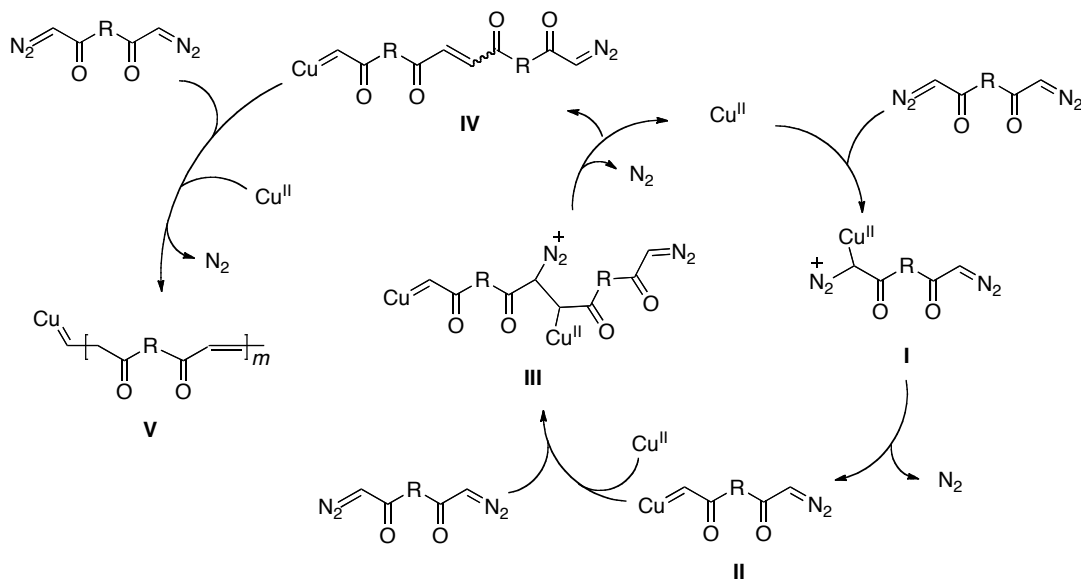
Scheme 2.17 Liu's denitrogen alkene polymerization proposed mechanism.

The diazo substituent in **II** is the attacked by the copper catalyst and undergoes intermolecular coupling with another bis-diazo compound to give **III** which smoothly undergoes dissociation of the catalyst followed by another nitrogen disengagement event to give compound **IV**. The diazo substituent in copper carbene **IV** is attacked by copper catalyst and undergoes intermolecular coupling with another bis-diazo molecule. The polymer chain propagates in the presence of the copper catalyst and bis-diazo compounds and linear polymer **V** is synthesized with the copper carbenoid as the terminal pendant group. The Liu laboratory efficiently demonstrated that under Cu(II)-catalysis, amorphous polymers are formed in good yields and high molecular weights.

Spiro systems are important architectures which can be used as rigid skeletons for geometrical fixation of functional groups. A synthetically useful extension using the chemistry of bis-diazo compounds was introduced by Muthusamy and co-workers.[70] In their study, the authors present the intermolecular generation of carbonyl ylides by $Rh_2(OAc)_4$-catalyzed reaction of 3-diazoindol-2-ones in the presence of aryl- and heteroaryl aldehydes. This methodology was efficiently extended to double multicomponent reactions of bis-cyclic diazoamide to afford the respective complex polycycles in a tandem fashion, capable of constructing four carbon-carbon bonds, two carbon-oxygen bond and four chiral centers in a single synthetic step (Scheme 2.18).

61a = Ar = 4-MeOC$_6$H$_4$; 62% yield
61b = Ar = Pyren-1-yl ; 61% yield
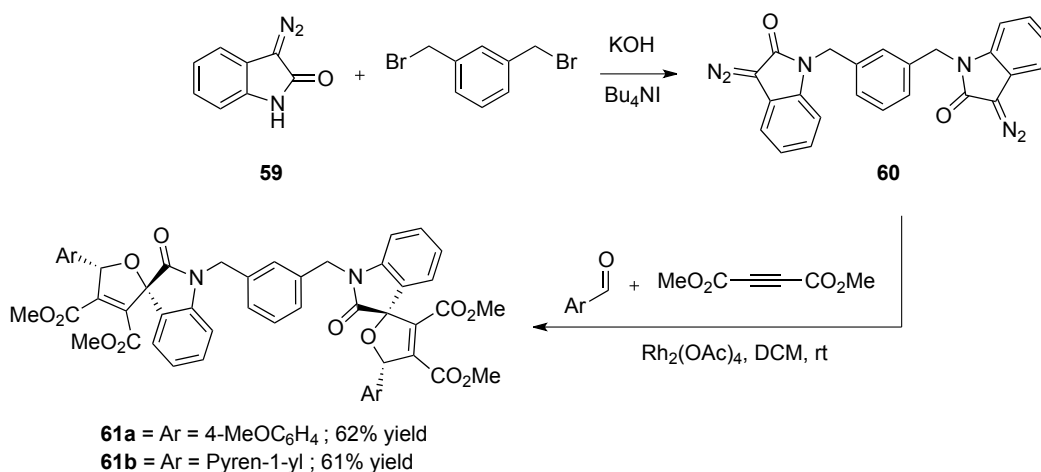
Scheme 2.18 Muthusamy's three-component approach to bis-spiro-polycyclic systems.

The required bis-diazo **60** was quickly synthesized by the dialkylation of diazo **59** with 1,3-bis(bromomethyl)benzene. Compound **60** was reacted with *p*-anisaldehyde or 1-pyrenecarbaldehyde to furnish the respective bis-spirocyclic system **61a** or **61b** in the presence of an excess amount of DMAD and 1 mol% of rhodium(II) acetate catalyst. The use of bis-diazo compounds easily doubled the efficiency of the initially developed

mono-diazo/dipolar cycloaddition methodology. Moreover, the complex spiro-polycyclic systems are skillfully and proficiently synthesized from simple and readily available starting materials. Undheim and co-workers have also made contributions to the development and use of bis-diazo compounds. Specifically, the construction of spiro[4.4]nonane-2,7-dione derivatives was quickly accomplished *via* two consecutive intramolecular Rh(II)-catalyzed C-H insertion reactions of open chain bis(α-diazoketones) (Scheme 2.19).[71,72]

62

63a $R_1 = R_2 = R_3 = H$

63b $R_1 = R_2 = Me, R_3 = H$

63c $R_1 = Me, R_2 = R_3 = H$

63d $R_1 = R_2 = H, R_3 = Me$

64

65a = 27%

65b = 35%

65c = 35%

65d = 0%
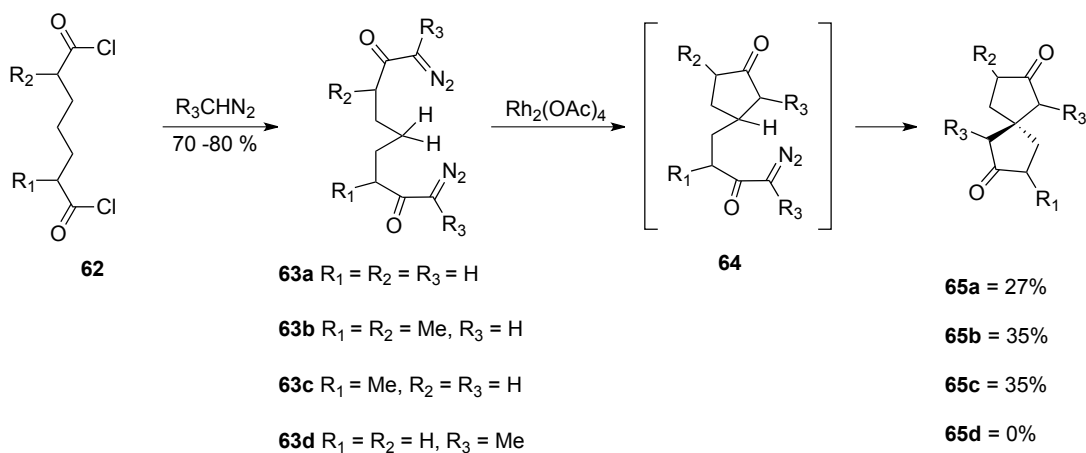
Scheme 2.19 Undheim's rhodium(II)-catalyzed double C-H insertion approach.

This new approach greatly expedited the synthesis of β-oxospirane systems which have potential to serve as rigid scaffolds for stereocontrol of pharmacophoric groups in bioorganic molecules. In addition, appropriately substituted and enantiomerically enriched spiranes may also be envisaged as chiral auxiliaries in dissymmetric catalytic operations.[71] Previous strategies to oxospirane scaffolds have included laborious SmI_2 reductive cleavage reactions of appropriate cyclopropane derivatives,[73] reductive cyclizations of mercurial α,β-unsaturated cyclopentanones[74] or acid catalyzed cyclization procedures.[75]

In general, most of the transition metal-catalyzed synthetic efforts with bis-diazo compounds have been restricted to bis-diazo systems consisting of the same diazo function (i.e. equivalent bis-diazo systems). Moreover, no studies have been reported where a single diazo moiety is selectively decomposed within a system containing two diazo groups. To this end, Moody and his co-workers published studies describing the reactivity of differentially substituted bis-diazo esters in rhodium(II)-catalyzed O-H insertion reactions.[76] Also of great importance, Moody showcased the selective Rh(II)-catalyzed selective decomposition of one diazo group in the presence of another. Inspired by the synthesis of naturally occurring polyether toxins containing cyclic ethers of various ring sizes, intramolecular O-H insertion reactions and attempts to extend recent works towards fused oxepanes of type **67** were investigated. The Moody laboratory prepared bis-diazo **66** and attempted two simultaneous O-H insertion reactions (Scheme 2.20). Unfortunately, the rhodium(II)-catalyzed double O-H insertion reaction failed to give product **67**.
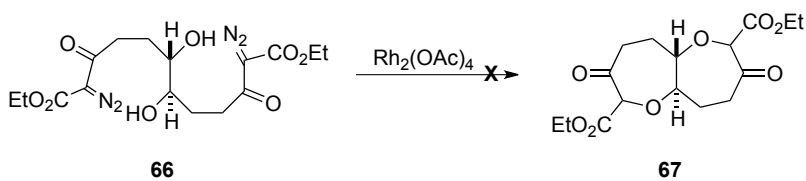
Scheme 2.20 Moody's simultaneous O-H insertion attempt.

However, in a previous publication, Moody demonstrated a distinct difference in the reactivity of diazo compounds in which the diazo group is stabilized by a phosphonate group compared to a group carbonyl.[77] Such a remarkable difference in reactivity was exploited and used to synthesize new classes of nonequivalent bis-diazo compounds. As

illustrated in Scheme 2.21, substrate **68** or **69**, as a solution in DCM, was treated with

methanol (2 eq) and Rh$_2$(OAc)$_4$. The mono diazo compounds **68** and **69** was obtained in

modest yield. Mono-diazo **70** and **71**, were converted into their corresponding dimethoxy

compounds **72** and **73** upon treatment with methanol and the highly reactive rhodium

trifluoroacetamide in refluxing toluene. Furthermore, **68** and **69** could be converted into

72 and **73** directly by treatment with rhodium trifluoroacetamide in refluxing toluene.

The large differences in diazo decomposition allowed this methodology to be a viable

method for the construction of simple organic compounds. However, most importantly,

this study outlined the requirements for the rational design of differentially substituted

bis-diazo compounds.
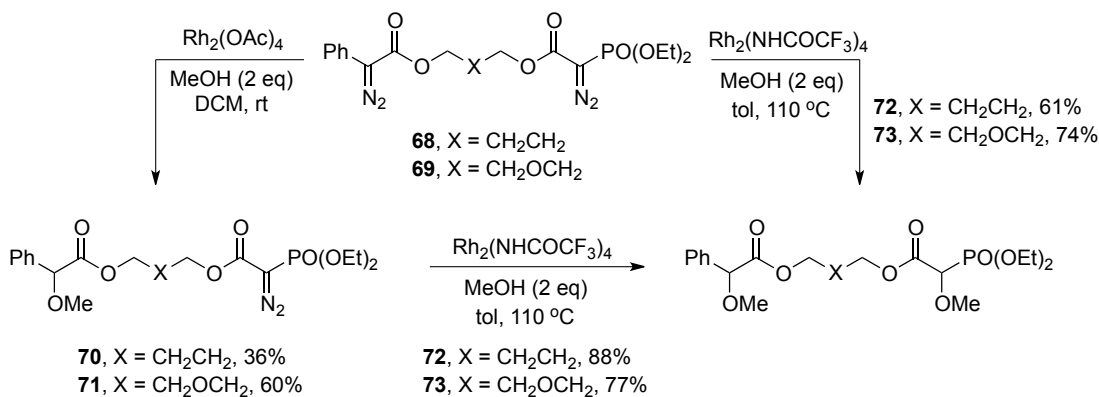
Scheme 2.21 Moody's selective Rh(II)-catalyzed diazo decomposition.

Muthusamy and co-workers revisited the use of bis-diazo compounds in 2009. In this

report, the authors combined carbenoid reactivity and ylide formation methodologies and

applied it to nonequivalent bis-diazoimide systems.[78] When bis-diazoimide **74** was

treated with *N*-allylpyrrole in dichloromethane, the acceptor diazo was selectively

decomposed over the acceptor/acceptor diazo and yielded C-alkylation product **75** in high

yield (Scheme 2.22)
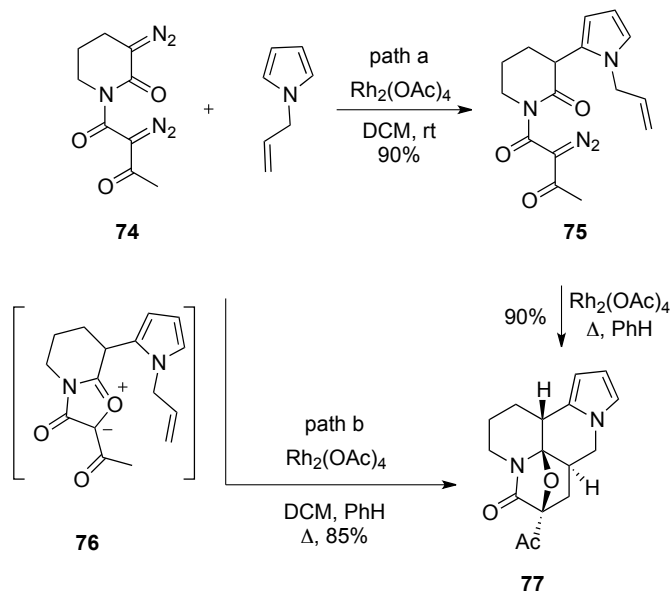
Scheme 2.22 Muthusamy's Rh(II)-catalyzed C-alkylation and cycloaddition approach.

When compound **75** was further treated with Rh(II)-catalyst in benzene under refluxing

conditions it afforded the corresponding polycyclic system **77**, (path a, steps 1 and 2), [1]H

and ^{13}C NMR spectroscopic analysis confirmed the formation of a single stereoisomer. A

proposed mechanistic rationale describes the rhodium carbenoid derived from diazoimide

74 furnished isomünchnone **76** as an intermediate, which subsequently undergoes an

intramolecular 1,3 dipolar cycloaddition with the tethered olefin. Interestingly, these two

sequential reaction steps can also be performed in a one-pot fashion (path b).

2.2 Davies' approach towards differentially substituted bis-diazo systems

Drawing inspiration from the aforementioned studies, our approach for the design and synthesis of a reactive bis-diazo compound began with the discovery that donor/acceptor diazo compounds undergo faster reactions than acceptor and acceptor/acceptor diazo compounds at low catalyst loadings.[79] As depicted in Figure 2.3, previous studies conducted in the Davies group describing the cyclopropanation of styrene demonstrated that the reaction of phenyldiazoacetate **78** in the presence of 0.1 mol% Rh_2(*S*-DOSP)$_4$ went to completion in three seconds. Furthermore, treatment with 0.01 mol % of catalyst required one minute to decompose diazo **78**.
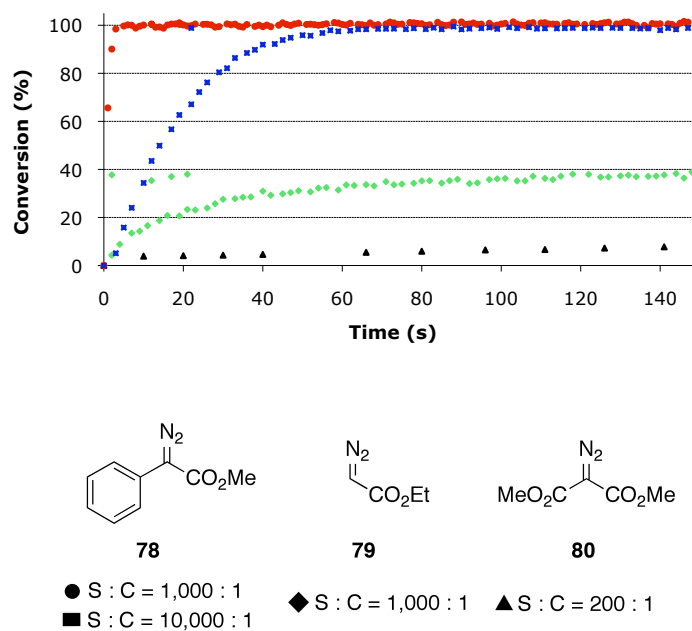
Figure 2.3 Effect of diazo structure on the relative rate of cyclopropanation catalyzed by Rh_2(*S*-DOSP)$_4$.

The reaction of ethyl diazoacetate **79** with 0.1 mol% Rh$_2$(S-DOSP)$_4$ initially decomposed quickly, however, the catalyst became inactive after approximately 400 turnover numbers (TONs). A reaction with methyl diazomalonate **80** was slow despite increasing the catalyst loading to 0.5 mol% of Rh$_2$(S-DOSP)$_4$ and achieved less than 10% conversion in three minutes. These results were used to describe synthetic practicality of donor/acceptor carbenoids and their ability to achieve high TONs.

With this distinct reactivity in mind, efforts in designing a differentially substituted bis-diazo compound with the intention of developing a novel cascade concept which could potentially construct complex motifs was investigated. An attractive target was the tetracyclic core of the tigliane diterpene, phorbol and related compounds. Because of its formidable and elegant molecular architecture as well as heightened biological activity of its ester derivatives,[80-82] phorbol has attracted considerable interest from the synthetic community. Synthetic efforts have resulted in total syntheses by Wender,[83,84] as well as formal asymmetric syntheses by Wender and Cha.[85,86] In addition, several impressive "core-generating" methodologies have been reported by Paquette,[87] Dauben,[30] Mcmills,[88] Little,[89] Ovaska,[90] Rigby,[91] Bulman Page,[92] Harwood[93] and Shibasaki.[94] The unique *trans*-fused B and C rings as well as the relative stereochemical relationship positioned at C$_8$, C$_9$ and C$_{11}$ prompted us to investigate the construction of the complex tetracyclic core through the use of carbenoid chemistry.
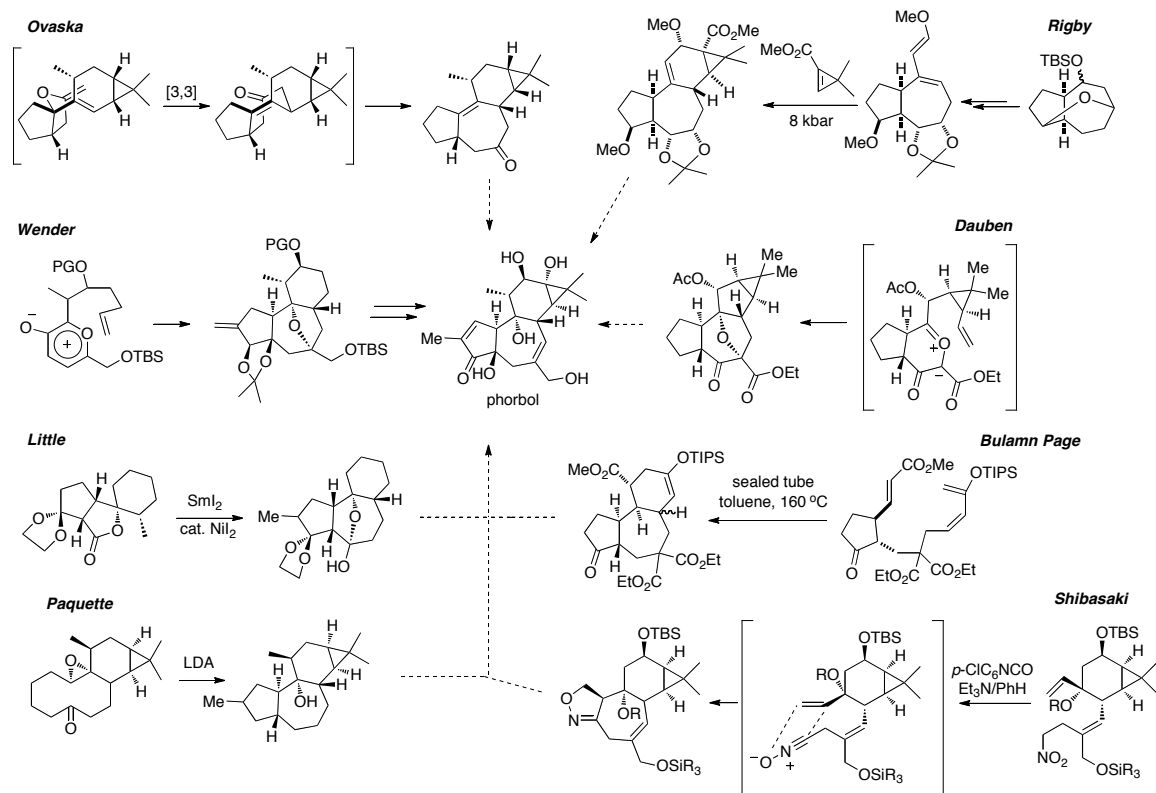
Scheme 2.23 Selected core-generating approaches towards phorbol.

In the late 1990's the Davies laboratory developed the Rh(II)-catalyzed tandem cyclopropanation/Cope rearrangement, between vinyldiazoacetates and dienes.[95] This process has proven to be an excellent method for the asymmetric synthesis of the cycloheptadiene system. Chapter I of this dissertation contains a detailed description of this methodology. Equally important, is the well-established Rh(II)-catalyzed intramolecular C-H insertion reaction which is widely accepted as an excellent method for the formation of 5- and 6-membered carbocycles.[2,96] We therefore decided to take advantage of the efficiency of both methodologies and combined them to i) construct the tigliane core **83** and ii) strategically install the critical C_8, C_9, and C_{11} stereocenters. Moreover, the recently acquired understanding of diazo decomposition provided crucial

insight for the formulation of the hypothetical retrosynthetic analysis shown in Scheme 2.24.
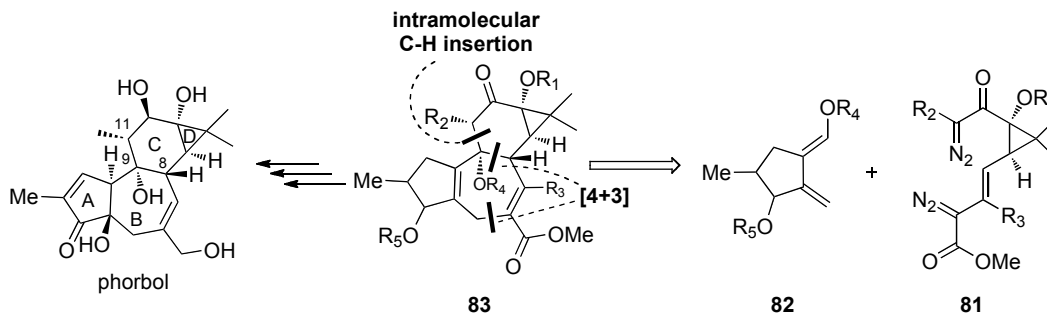
Scheme 2.24 Retrosynthetic analysis to the phorbol core.

We envisaged exotic bis-diazo compound **81** and hypothesized that in the presence of a chiral rhodium(II) carboxylate catalyst, for example $Rh_2(S\text{-PTAD})_4$, and an electron rich diene (**82**), the donor/acceptor diazo would decompose first and react to yield 1,2 divinylcyclopropane **85** which then undergoes a Cope rearrangement to yield 1,5 cycloheptadiene **86** (Scheme 2.25). The remaining acceptor/acceptor diazo would then decompose, into its corresponding carbenenoid, and undergo a challenging but conceivable intramolecular C-H insertion reaction, with retention of stereochemistry,[97] at the doubly electronically activated methine to forge a *trans*-fused six-membered ring to give **83**.
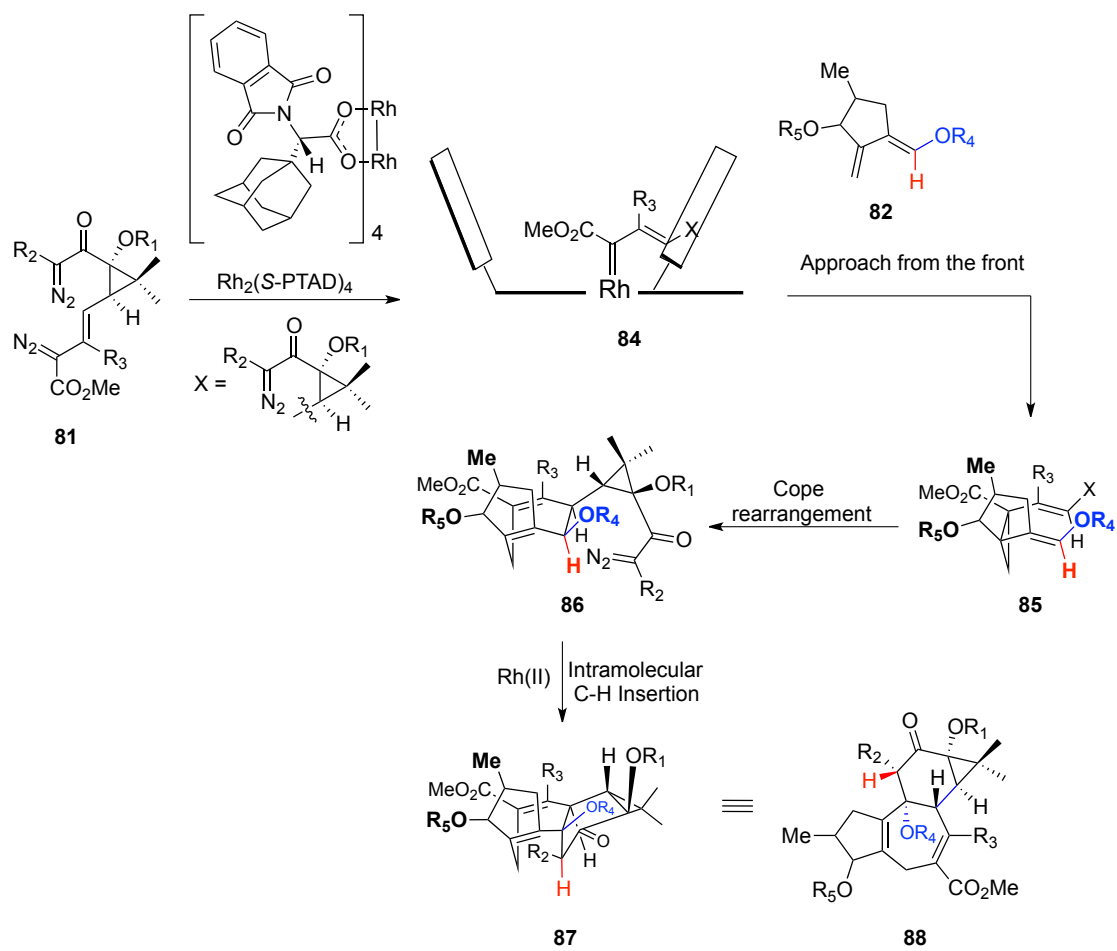
Scheme 2.25 Stereochemical rationale for the formation of **88**.

2.3 Results and discussion

Preliminary studies began by determining which two classes of diazo partners would be best suited to achieve the desired diazo decomposition profiles. Specifically, we focused our efforts in designing a simplified version of bis-diazo **81** and identifying substituents R_1 and R_2 (Figure 2.4).

89
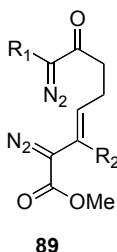
Figure 2.4 Desired bis-diazo skeleton.

Appropriate donor/acceptor, acceptor, and acceptor/acceptor diazo compounds were chosen (Figure 2.5), and decomposed with dilute solutions of chiral rhodium(II)-catalyst $Rh_2(S\text{-}PTAD)_4$. The relationship of the rate of diazo decomposition to catalyst loading was determined by the disappearance of the characteristic diazo ($C=N_2$) stretch frequency, which was monitored by in-situ IR (ReactIR). The transient metallocarbenoid species formed was captured by an excess amount of styrene.
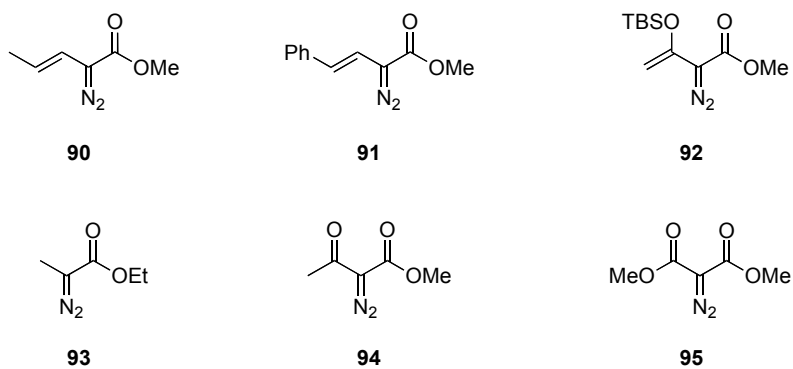
Figure 2.5 Donor/acceptor, acceptor and acceptor/acceptor diazo candidates.

The systematic study conducted between diazo compounds **90-95** is summarized in Table 2.3. In the presence of 0.1 mol% of chiral dirhodium catalyst, siloxyvinyldiazoacetate **92** exhibited the slowest initial rate and was normalized to relative rate of 1 (entry1). This data point provides valuable insight describing the steric effects about the diazo functionality. While diazo **92** has been shown to be an excellent carbenoid precursor, the steric bulk of the TBS group prevents formation of the reactive carbenoid species fast enough for the desired cascade process to be feasible. Fortunately, unsubstituted vinyldiazoacetates, (entries 4 and 5), displayed efficient decomposition profiles. The absence of a α-siloxy substituent proved to be critical as the relative rates for diazo compounds **91** and **90** were >3.8 times faster compared to **92**. Vinyldiazoacetate **90** was identified as the optimum candidate for the donor/acceptor segment of bis-diazo **89**.

Table 2.3 Relative rates of donor/acceptor, acceptor/acceptor and acceptor diazo compounds.
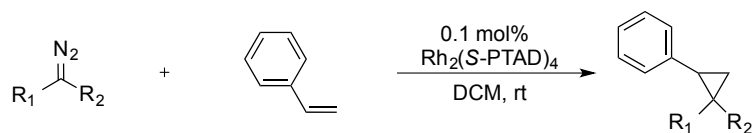
entry	diazo	diazo structure	relative rate
1	**92**	OTBS, CO_2Me, N_2	1.0
2	**95**	O, O, O, O, N_2	1.2
3	**94**	O, O, O, N_2	3.8
4	**91**	Ph, CO_2Me, N_2	>3.8
5	**90**	CO_2Me, N_2	>3.8
6	**93**	O, OEt, N_2	>>3.8

We next focused on identifying the appropriate diazo functionality necessary for R_1. The decomposition of ethyl 2-diazopropanoate had great promise since incorporation of this diazo moiety into bis-diazo **89** would provide the correct functionality, after diazo decomposition, at the C_{11} position of phorbol (Scheme 2.24) and would not require further chemical manipulation. Unfortunately, **93** exhibited tremendously fast initial rates which greatly exceeded the detection limit of the ReactIR instrument. A catalyst loading of 0.1 mol%, decomposed the diazo **93** to give a relative rate of >>3.8 (entry 6). Decreasing the catalyst loading to 0.01 mol%, unfortunately was not sufficient to perturb

the initially observed rate. The observed high rate of diazo decomposition excluded the possibility of incorporating an acceptor diazo compound into bis-diazo **89**. From the ReactIR-guided decomposition studies, we chose unsubstituted vinyldiazoacetate **91** or **90** and diazoacetoacetate **94** to be the optimum diazo combination for the construction of a differentially substituted bis-diazo capable of complexity generating reactivity. We therefore conducted a "proof-of-concept" experiment to test this initial design rationale.
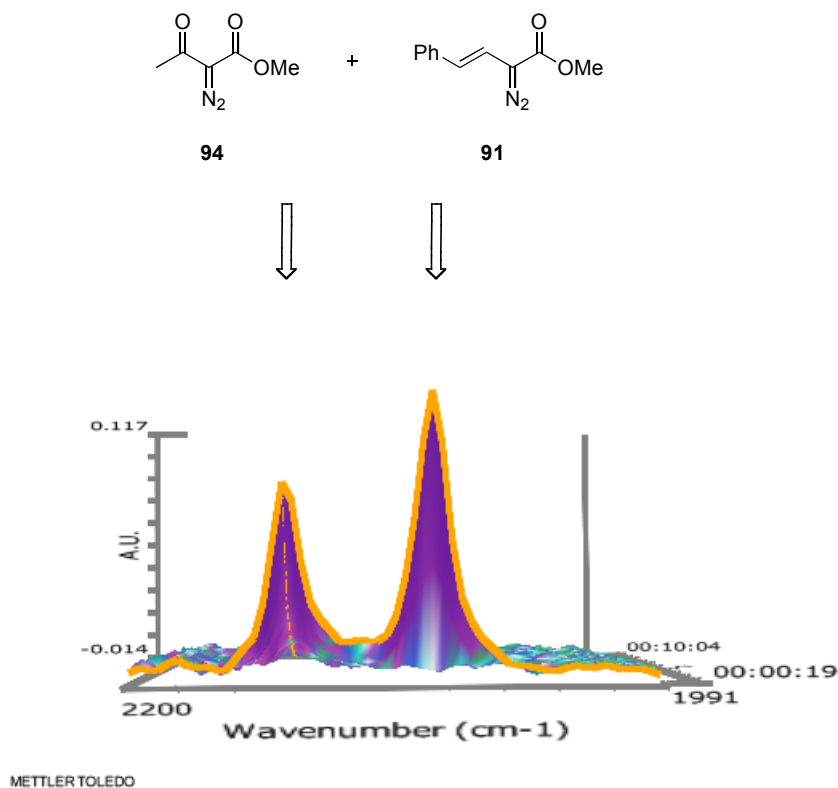
Figure 2.6 Proof-of-concept experiment between diazo **94** and **91**.

Equal amounts of diazo compounds **94** and **91** were added to a reaction vessel containing an excess amount of styrene. Figure 5, depicts the distinct IR stretches for compounds **94** and **91**. Immediately upon the addition 0.1 mol% of $Rh_2(S\text{-}PTAD)_4$, diazo **91** disengaged

nitrogen (Figures 6 and 7), which was immediately followed by the decomposition of diazo **94**.
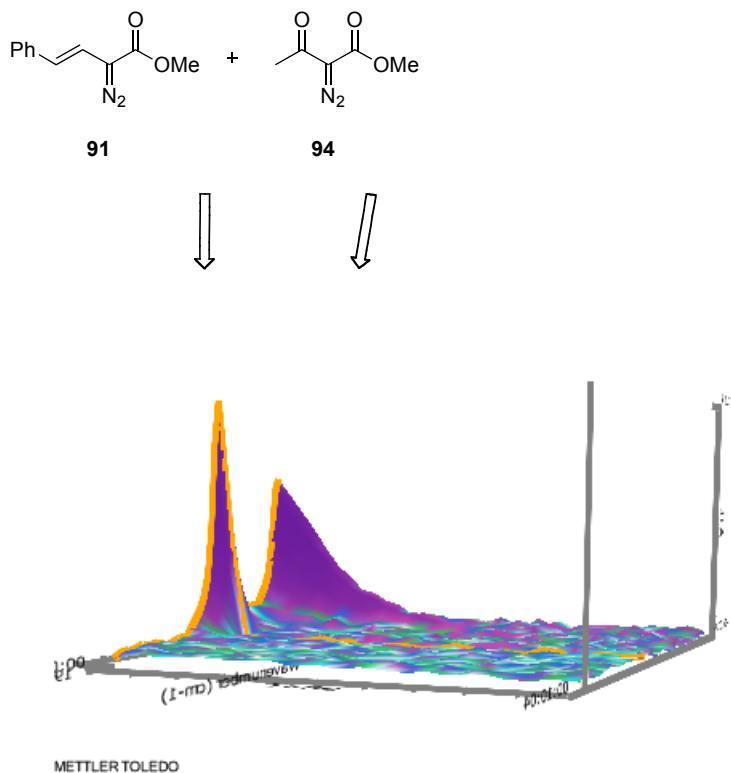
Figure 2.7 Decomposition of **91** and **94** with 0.1 mol% Rh$_2$(*S*-PTAD)$_4$.

The real-time ReactIR plot (Figure 2.7) was converted into a graphical representation (Figure 2.8) which depicts the diazo decomposition profiles more clearly.
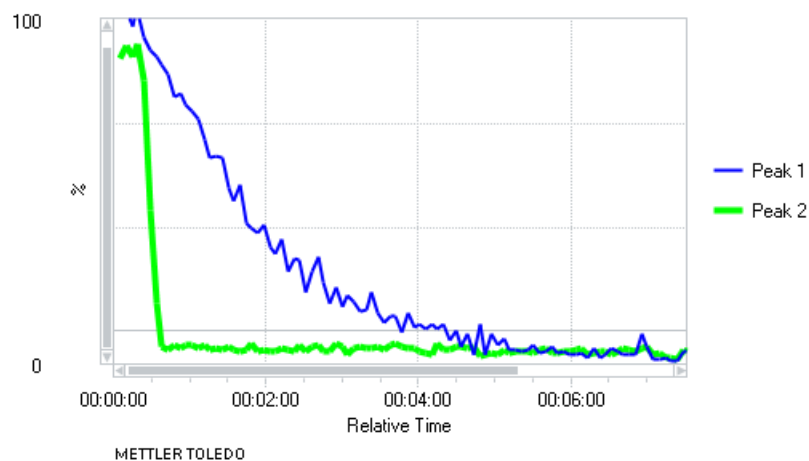
BLUE CURVE = diazo **94**, 2139 cm^{-1}

GREEN CURVE = diazo **91**, 2081 cm^{-1}

Figure 2.8 Graphical representation of IR plot from Figure 2.7.

Ideally, it would have been preferred to completely restrict the decomposition of diazo **94** however, the tolerable differences in decomposition rates for acceptor/acceptor **94** and donor/acceptor **90** and **91** provided the foundation to propose model bis-diazo **96** as a potential candidate (Figure 2.9).
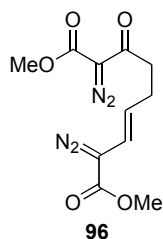
Figure 2.9. Model bis-diazo **96**.

In 2008, the Doyle laboratory published a study describing the preparation of functionalized diazo acetoacetates by an efficient Zn(II)-catalyzed Mukaiyama-Michael reaction between vinylsiloxydiazoacetate **92** and various α,β-unsaturated enones (Scheme 2.26).[98]
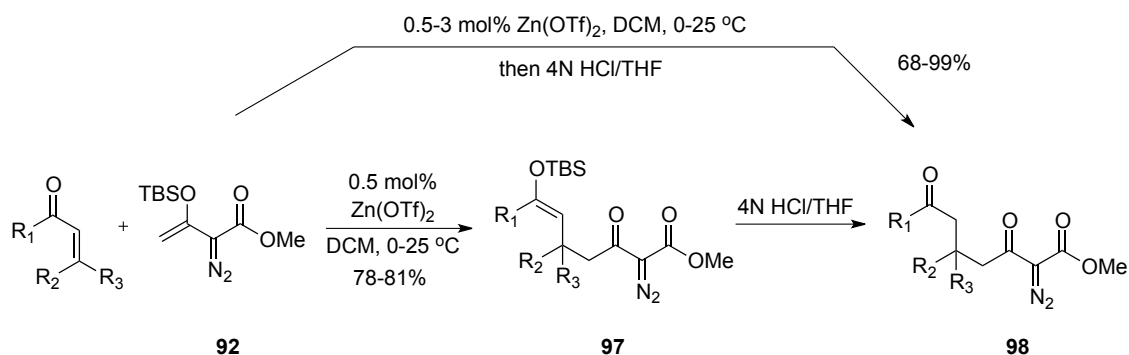
Scheme 2.26 Doyle's Zn(II)-catalyzed Mukaiyama-Michael reaction.

The use of inexpensive, commercially available Lewis acids, mild reaction conditions and construction of a crucial 9-carbon backbone rendered this methodology as a viable method to access bis-diazo **96**. As such, Doyle's methodology enabled the formulation of the retrosynthetic analysis shown in Scheme 2.27.
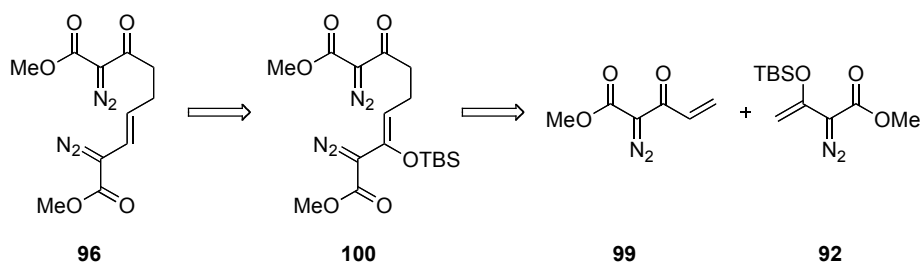
Scheme 2.27 Retrosynthetic analysis for the formation of bis-diazo **96**.

Progress towards the synthesis of **96** commenced by recognizing that bis-diazo **100** could be obtained through a Zn(II)-catalyzed Mukaiyama-Michael reaction between methyl 2-diazo-3-oxopent-4-enoate **99** and siloxyvinyldiazoacetate **92**. It should be noted that Michael-acceptors containing diazo functional groups were not investigated by Doyle and his co-workers. Lastly, removal of the vinyl-OTBS from **100** would provide target bis-diazo **96**.

Synthetic efforts to prepare **100** began by synthesizing Michael-acceptor diazo **104**. Following established literature procedures for the formation of **103**,[99] an aldol reaction between the ester enolate of **101** and acrolein efficiently provided β-hydroxy ester **102**. Jones' oxidation conditions furnished β-ketoester **103** in 45% yield. Diazotization of **103** with (*p*-ABSA) provided diazo **104**, after chromatographic purification, in 90% yield (Scheme 2.28).
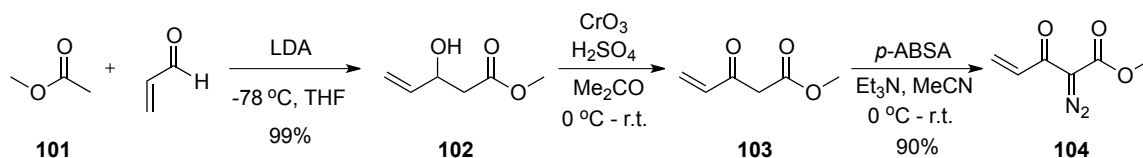
Scheme 2.28 Synthesis of Michael-acceptor diazo **104**.

Vinylsiloxydiazoacetate **92** was prepared by a modified procedure described by Davies.[100] Treatment of methyl acetoacetate with *p*-ABSA affords acceptor/acceptor diazo **94** in 70% yield. Exposure of **94** with TBSOTf gives diazo **92** quantitatively.
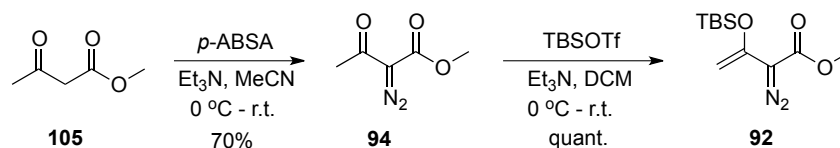
Scheme 2.29 Synthesis of vinylsiloxydiazoacetate **92**.

With diazo compounds **104** and **92** in hand, a Mukaiyama-Michael reaction was attempted employing optimized conditions previously described by Doyle. As depicted in Scheme 2.30, the desired conjugate addition product, bis-diazo **100**, was synthesized, albeit in poor yields. The cause to the low yields was attributed to inefficient conversion of diazo **104**.
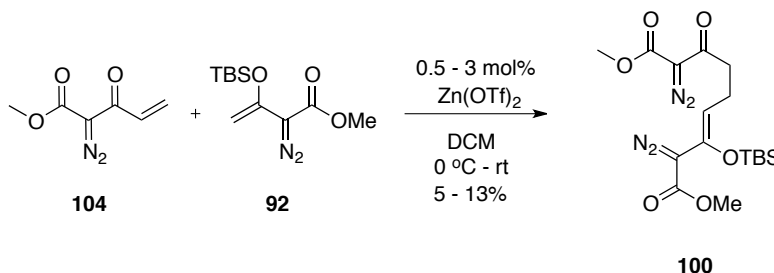
Scheme 2.30 First-generation synthesis of bis-diazo **100**.

Revisiting Doyle's manuscript provided valuable insight to the role of the Lewis acid catalyst. The purpose is two-fold, i) activation of the enone, diazo **104**, to accept electron density from diazo **92** and ii) form a weak alkoxide-Lewis acid bond thus promoting an efficient siloxy group transfer. With this concept in mind, we chose to investigate the use of Bi(OTf)$_3$ as a potential Lewis acid candidate. In 2006, the Ollivier laboratory reported an efficient bismuth(III)-catalyzed vinylogous Mukaiyama-aldol with silyl ketene acetals.[101] Bismuth triflate was particularly attractive due to its commercial availability,

low toxicity, low cost and good stability. To our delight, in the presence of 0.5 mol%
Bi(OTf)₃, bis-diazo **100** is formed in 70% yield.
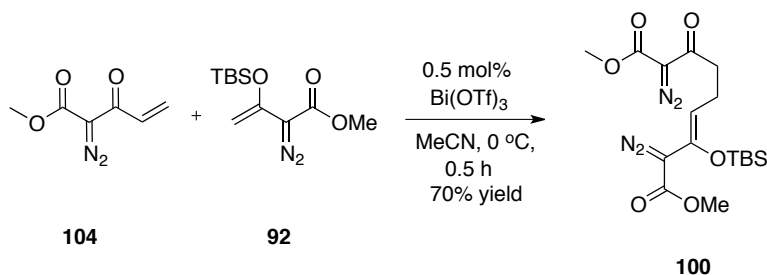
Scheme 2.31 Second-generation synthesis of bis-diazo **100**.

With compound **100** in hand, we proceeded towards the synthesis of **96** *via* a three-step
sequence (Scheme 2.32). In the presence of sodium borohydride, reduction of the ketone
functionality in **100** occurred smoothly to give hydroxy intermediate **106** which was used
without further purification.   Elimination of secondary alcohol **106** with POCl₃/Et₃N
afforded bis-donor/acceptor diazo **107** and subsequent treatment with TAS-F provided
bis-diazo **96** in 22% isolated yield over three steps.
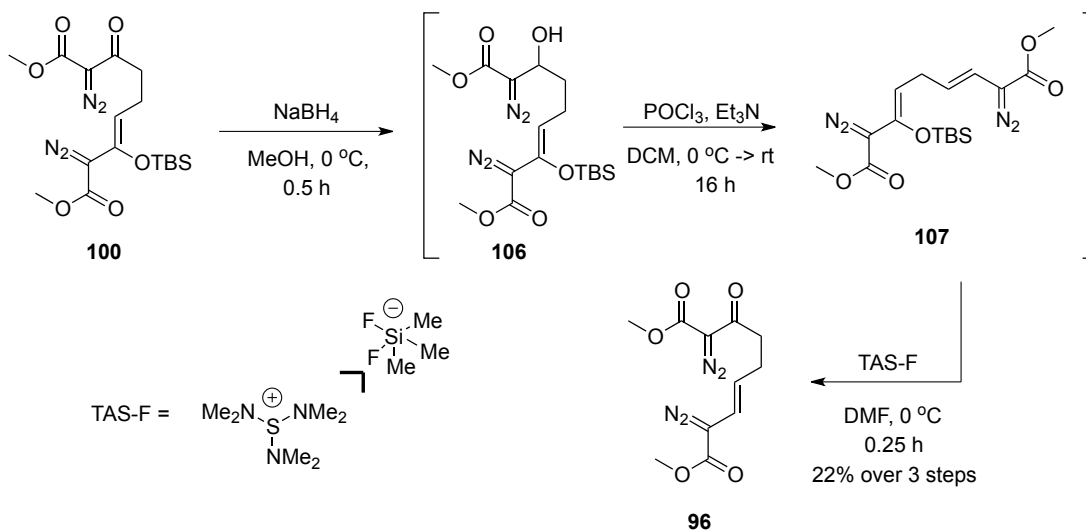
Scheme 2.32 Synthesis of bis-diazo **96**.

The investigation began with the intention of forming bicycle **109** (path a, Scheme 2.33). However, in the presence of a catalytic amount of Rh$_2$(*S*-PTAD)$_4$ and 10% excess siloxy butadiene **108**, bis-diazo **96** failed to undergo the desired tandem cyclopropanation/Cope rearrangement followed by 6-membered ring formation. Instead of performing the desired intramolecular C-H insertion reaction, the acceptor/acceptor segment reacted in an intermolecular fashion with diene **108** (path b) to give dihydrofuran derivative/[4+3] adduct **112**.
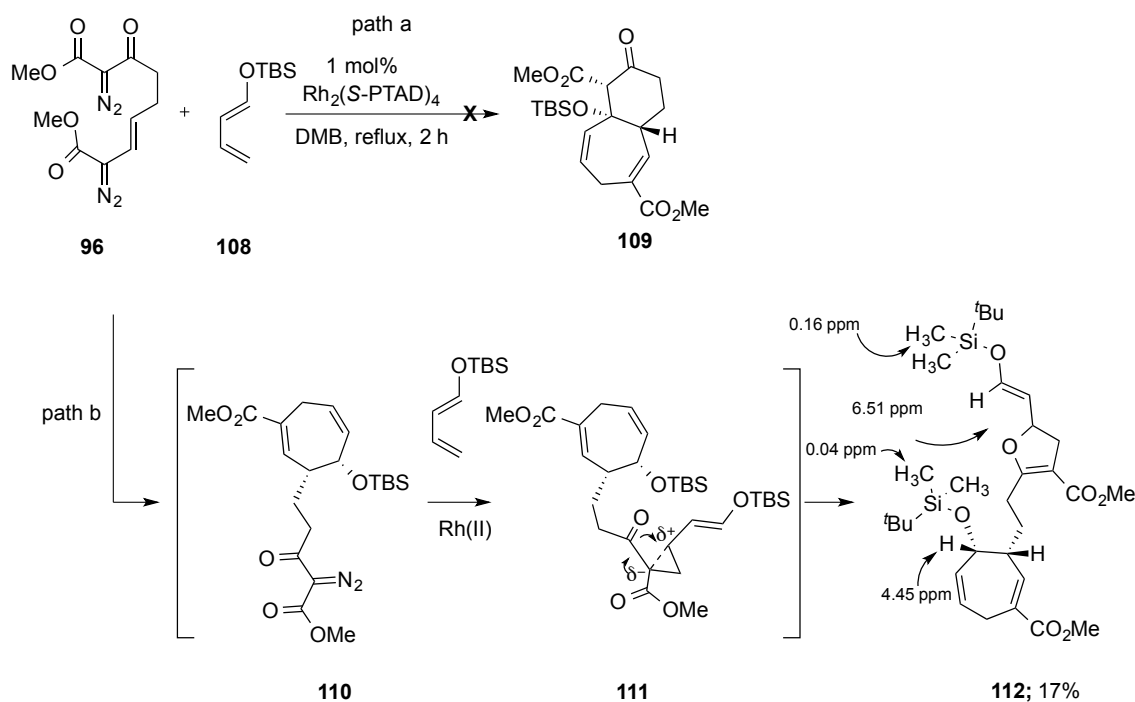
Scheme 2.33 Formation of **112** *via* simultaneous formal [4+3] and [3+2] cycloadditions.

Inter- and intramolecular formal [3+2] cycloaddition reactions of acceptor/acceptor diazo compounds and vinyl ethers are well-known and occur *via* formation of zwitterionic intermediates (**111**).[102,103] The structure of compound **112** was tentatively assigned by ^{1}H NMR due to problematic decomposition during isolation. The formation of 5- or 6-

memebered ring products, resulting from an intramolecular C-H insertion reaction, were excluded primarily due to the presence of two distinct OTBS groups which strongly suggests an intermolecular reaction occurred between diene **108** and the acceptor/acceptor diazo segment of bis-diazo **96**. To further support the the absence of the desired 6-membered ring product, a broad singlet located at 4.45 ppm was present in the ^{1}H NMR which corresponds to the methine proton adjacent to the OTBS group (Scheme 2.33). Nonetheless, while the desired transformation was not achieved, the reaction provided crucial insight with regards to the reactivity of both diazo partners. It was determined that the formation of **112** occurred as a result of both diazo compounds reacting with diene **108**. Specifically, the relative rates of decomposition for the donor/acceptor and acceptor/acceptor were not distinct enough for diene **108** to exclusively react with vinyldiazoacetate segment of **96**. Moreover, we were cognizant of this reactivity as the initial ReactIR studies and "proof-of-concept" experiments indicated complications could indeed occur as a result of what now appear to be subtle relative rate differences (Table 2.3).

To circumvent the issue of dual diazo decomposition, we decided to incorporate diazo phosphonates or diazo sulfones (**113** and **114**) as suitable replacements for the diazo acetoacetate segment of bis-diazo **96** (Figure 2.10). We proposed that such a modification would be advantageous and give entry to the selective decomposition of the vinyldiazoacetate portion of **96** since α-diazo-β-ketophosphonates and α-diazo-β-ketosulfones resist decomposition, compared to α-diazo-β-ketoesters in the presence of dirhodium catalysts unless highly reactive catalysts and forcing conditions are used.[77]
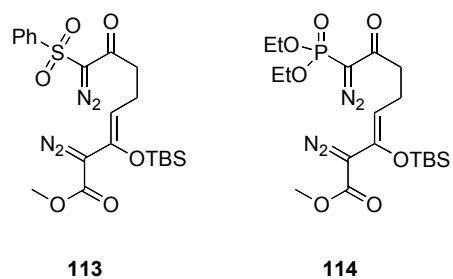
Figure 2.10 Potential bis-diazo candidates.

Our approach towards diazo **113** and **114** began by taking advantage of the success of the aforementioned Bi(III)-catalyzed Mukaiyama-Michael methodology. Studies began with the preparation of bis-diazo **113** (Table 2.14).

Table 2.4 Mukaiyama-Michael approach to diazo **116a** and **116b**.

115a = R = SO$_2$Ph
115b = R = P(OEt)$_2$

104

116a = R = SO$_2$Ph
116b = R = P(OEt)$_2$
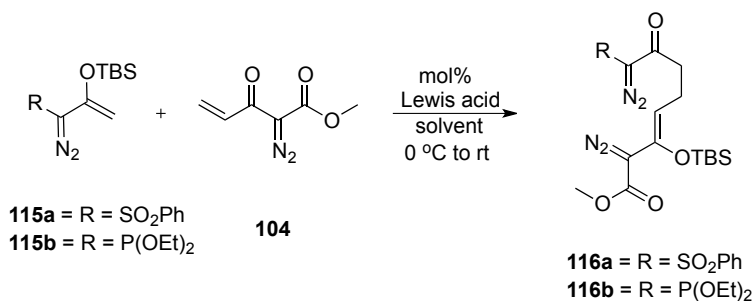
Entry	Lewis Acid	diazo	Lewis acid loading mol %	solvent	result
1	Bi(OTf)$_3$	**115a**	1	MeCN	contains hydrolyzed **115a** and unreacted **104**.
2	Bi(OTf)$_3$	**115a**	2	MeCN	contains hydrolyzed **115a** and unreacted **104.**
3	Zn(OTf)$_2$	**115a**	2	MeCN	contains hydrolyzed **115a** and unreacted **104.**
4	Sc(OTf)$_3$	**115a**	2	MeCN	**104** fully consumed. No product formed.
5	Bi(OTf)$_3$	**115a**	2	DCM	contains hydrolyzed **115a** and unreacted **104**
6	Zn(OTf)$_2$	**115a**	2	DCM	contains hydrolyzed **115a** and unreacted **104**
7	Sc(OTf)$_3$	**115a**	2	DCM	**104** fully consumed. No product formed.
8	BiCl$_3$	**115a**	2	DCM	contains hydrolyzed **115a** and unreacted **104**
9	Bi(OTf)$_3$	**115b**	2	MeCN	contains hydrolyzed **115b** and unreacted **104**
10	Bi(OTf)$_3$	**115b**	2	DCM	contains hydrolyzed **115b** and unreacted **104**

Unfortunately, the synthesis could not be realized despite extensive efforts (entries 1-8). The reaction was plagued by i) poor reactivity with Michael-acceptor diazo **104** and ii) in-situ hydrolysis of **115a** and **115b** (entries 2,3 and 5-8). In the presence of scandium triflate (entries 4 and 7), diazo **104** is fully consumed, however, no products resembling bis-diazo compounds were isolated. A reasonable explanation for the hydrolysis of **115a** would be due to the formation of adventitious triflic acid in the reaction medium, which could potentially desilylate the siloxyvinyldiazo functional group. To test this

hypothesis, the effects of Bi(Cl)$_3$ on this transformation were investigated (entry 8). However an identical hydrolysis of **115a** and low conversion of **104** was observed**,** thus eliminating triflic acid as the sole cause for poor reactivity. Finally, progress was made on the synthesis of bis-diazo **116b** by utilizing siloxydiazophosphonate **115b** as a suitable Michael-donor (entries 9 and 10). Regrettably, identical in-situ hydrolysis issues were encountered. As a result an alternative strategy was sought.

During the course of this study, the effects of pyrazole additives and diazo decomposition was under investigation by laboratory co-worker Felicia A. Fullilove. From that study, it was concluded that the rate of diazo decomposition for diazoacetoacetate **94** is significantly decreased when a 1:1 Rh$_2$(*S*-DOSP)$_4$: pyrazole (**115a**) solution is added to a mixture of **94** and styrene (Table 2.5). This phenomenon is attributed to an intricate equlibrium process occurring between the Lewis basic lone pair electons of **115a** and the Lewis acid site located at the apical position on the rhodium catalyst. Essentially, the role of the pyrazole is to "poison" the rhodium catalyst thereby decreasing the efficiency of the catalyst to decompose diazo compounds. Since vinyldiazoacetates tend to decompose relatively quickly, they are minimally affected by the pyrazole/catalyst equilibrium process.

Table 2.5 Effect of diazo decomposition due to pyrazole additives.
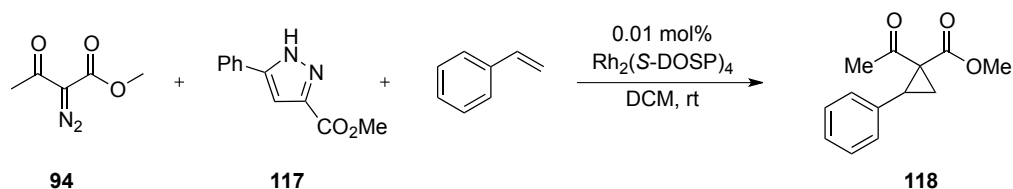
entry	catalyst : pyrazole	relative rate
1	1 : 1	1
2	1 : 0	2

Conducted by Felicia A. Fullilove

These results provided the impetus to apply such reaction conditions and re-visit the reaction of **96** and diene **108**. In the presence of a 1:1 sub-stoichiometric mixture of chiral dirhodium tetracarboxylate catalysts and pyrazole **117**, the decomposition of the acceptor/acceptor portion of **96** was inhibited (Table 2.6). A 0.06 mol% loading of Rh$_2$(S-DOSP)$_4$, which was necessary to push the reaction towards completion, led to the formation of a 60 : 40 mixture of cycloheptadiene **120a** and *trans*-divinylcyclopropane **120b** in 51% combined yield (entry 1).

Table 2.6 Rh(II)-catalyzed reaction of **96** with diene **108** and additive **117**.
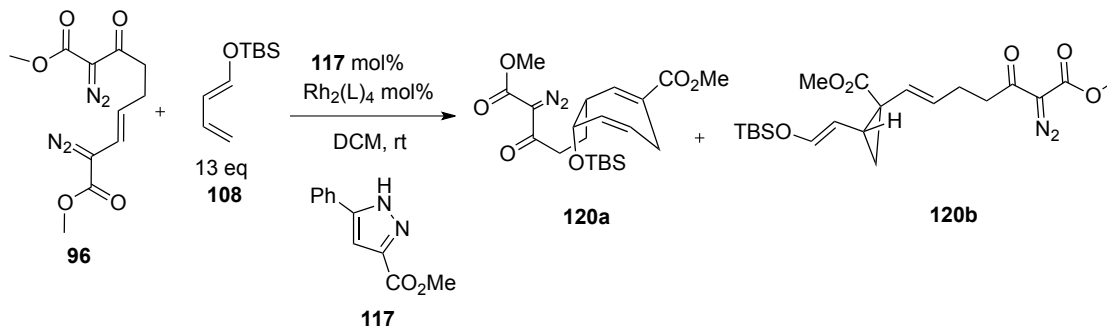
entry	catalyst (mol%)	117 (mol%)	product ratio 120a : 120b	yield[a]	% ee[b]
1	Rh$_2$(S-DOSP)$_4$ (0.06)	(0.06)	60 : 40	51	ND[c]
2	Rh$_2$(S-PTAD)$_4$ (0.04)	(0.04)	90 :10	71	0

[a] combined yield, [b] determined by chiral HPLC, [c] not determined

When the reaction was conducted with Rh$_2$(S-PTAD)$_4$, only 0.02 mol% of catalyst was necessary to drive the reaction towards completion and afforded **120a** and **120b** in a combined yield of 80% (entry 2). Interestingly, Rh$_2$(S-PTAD)$_4$ efficiently controls the facial approach of the diene to the reactive carbenoid center as illustrated by the excellent 90 : 10 product ratio. The lack of asymmetric induction was attributed to the polar nature of the reaction medium as rhodium-catalyzed [4+3] cycloadditions generally provide excellent enantioselectivity in non-polar hydrocarbon solvents.[104]

The relative stereochemistry of cycloadduct **120a** was determined by extensive nOe correlation studies. The key nOe correlations and selected chemical shifts are shown in Table 2.7. Methine proton Ha exists as a broad single single and encounters nOe correlations with protons Hb and Hc. Vinyl proton Hb, exits as a doublet located at 6.9ppm with a coupling constant of 0.6 Hz. Moreover, an nOe is observed between proton Hb and Ha. Proton Hc occurs as a broad singlet located at 4.5 ppm which is

appropriate for allylic protons adjacent to oxygen. Moreover, an nOe is observed between Hc, Hd and Ha thus confirming the relative stereochemistry for adduct **120a**. Vinyl proton Hd, is located at 5.6 ppm and occurs as a sharp singlet and integrates to an area of 2 as a result of overlap with the adjacent vinyl proton. An nOe is observed between Hd and Hc and an HMBC correlation is observed with the sp^2 hybridized carbon bonded to Hd.

Table 2.7 Selected Chemical Shifts in CDCl$_3$ at 600MHz (^{1}H), 100 MHz (^{13}C) and nOe correlations for cycloadduct **120a**.
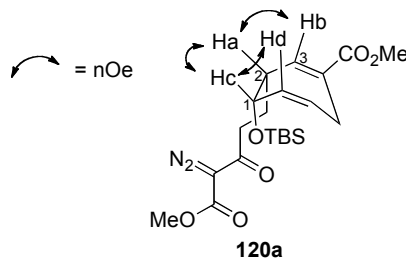
H	Chemical Shift (ppm)	C	Chemical Shift (ppm)
a	2.6	1	70.1
b	6.9	2	44.6
c	4.5	3	143
d	5.6		

With diazo **120a** in hand, the Rh(II)-catalyzed intramolecular C-H insertion reaction was attempted to forge the desired *trans*-fused 7,6 bicyclic system. We anticipated that construction of such a system would be challenging due to the overwhelming propensity of five-membered ring formation prevalent to intramolecular C-H insertion processes.[105-108] However, it was rationalized that the double electronic activation, provided by the C$_9$-oxygen and the flanking olefin, would efficiently stabilize the nascent cationic character generated at C$_9$ during the C-H insertion event.[9] Moreover, the electron-withdrawing

nature of the α,β-unsaturated enoate could sufficiently deactivate the C_8 allylic hydrogen thus decreasing the formation of spiro-cyclic compounds. However, none of the preferred *trans*-fused 7,6 bicyclic system **121a** was observed when **120a** was treated with catalytic amounts of $Rh_2(OAc)_4$ (Scheme 2.34).

H	Chemical Shift (ppm) CDCl₃ at 600 MHz
a	6.9
b	3.1
c	5.6
d	4.5
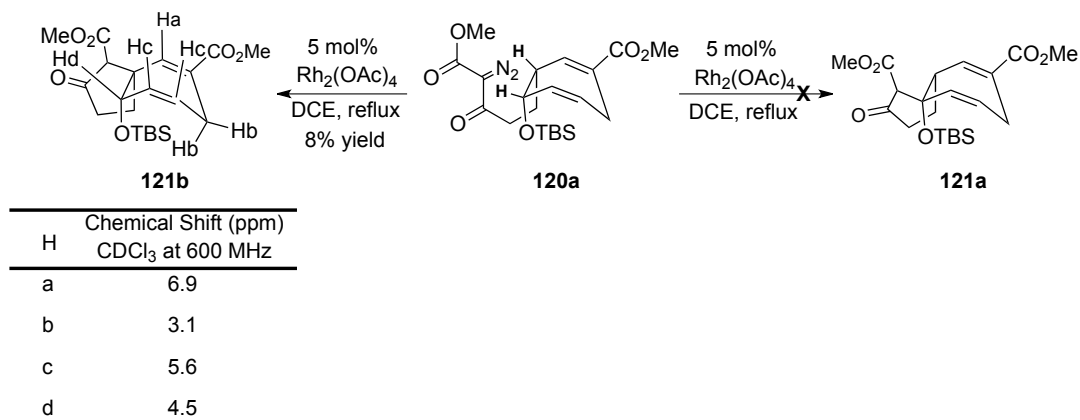
Scheme 2.34 Intramolecular C-H insertion attempt with diazo **120a**.

Instead, the product of this reaction product, molecular formula of $C_{21}H_{32}O_6Si$, appeared to be the undesired spiro[4.6]undecane derivative **121b** and was isolated in 6% yield. The product was tentatively assigned by ^{1}H NMR and HRMS as isolation and reaction reproducibility issues were prevalent. ^{1}H NMR indicated that proton Hd did not undergo an intramolecular C-H insertion reaction as it remained unchanged (4.5 ppm) indicating a 6-membered ring was not present. While the synthesis of **121a** was not achieved, the formation of **121b** provided valuable insight towards proposing modifications to bis-diazo **96** which could hypothetically lead to the formation of **121a**.

Recently, a strategy to overcome the formation of five-membered rings in intramolecular C-H insertion reactions was introduced by the Novikov laboratory. It was demonstrated that carbethoxy diazosulfones and sulfonates are unique diazo compounds

for intramolecular C-H insertion as they undergo the preferential generation of six-membered rings as a result of differences in bond lengths and bond angles around the sulfur atom (Scheme 2.35).[96,109]
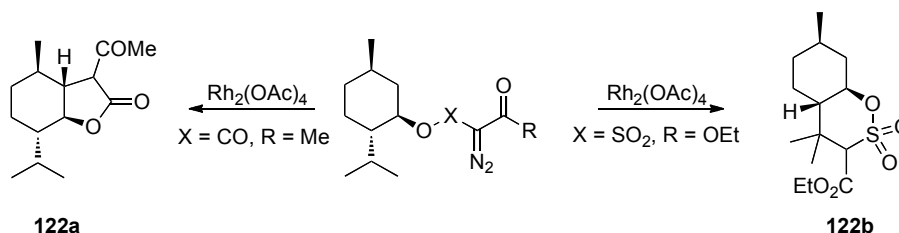
Scheme 2.35 Novikov's intramolecular C-H insertion.

A possible solution could encompass a diazosulfone or sulfonate into a bis-diazo compound. Although such a modification could potentially circumvent the issue for spirocycle formation, the incorporation of a diazosulfone or sulfonate into a bis-diazo compound would unfortunately introduce unwanted heteroatoms in the 6-membered ring (C ring). However, the notion of using ring stain as a controlling element was a parameter that deserved further consideration. As shown in Equation 4, we proposed that the introduction of a *cis*-cyclopropane at the C_{13} and C_{14} positions would deter the formation of spiro compound **123a** due to the unfavorable ring strain within the cyclopentanone moiety. Moreover, the undesirable ring strain would be relieved by the formation of 7,6 fused compound **123b**. Most significantly, the cyclopropane unit, which is present in phorbol, would be used as an elegant control element to simultaneously solve the crucial insertion step and introduce the D-ring present in the tigliane skeleton.

$$Rh_2(OAc)_4 \quad (2.1)$$

123a   **123**   **123b**
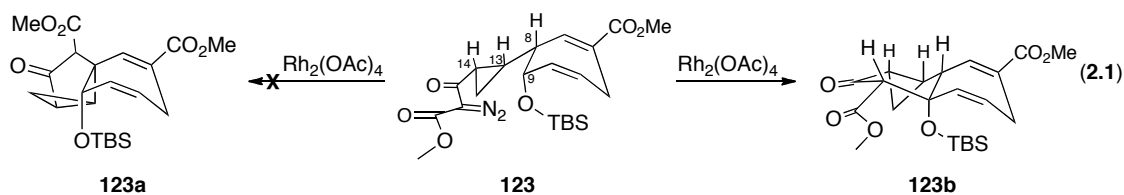
To this end, bis-diazo **125** was identified as the optimal bis-diazo candidate. The key disconnections to synthesized **125** is shown in Scheme 2.36. Essentially, the central reactions to construct the bis-diazo involves the use of two additions of ethyl lithiodiazoacetate at the C_3 and C_9 positions of substrate **124**. Formation of the *cis*-cyclopropane across the C_4 and C_5 positions would be achieved *via* a Simmons-Smith cyclopropanation reaction.
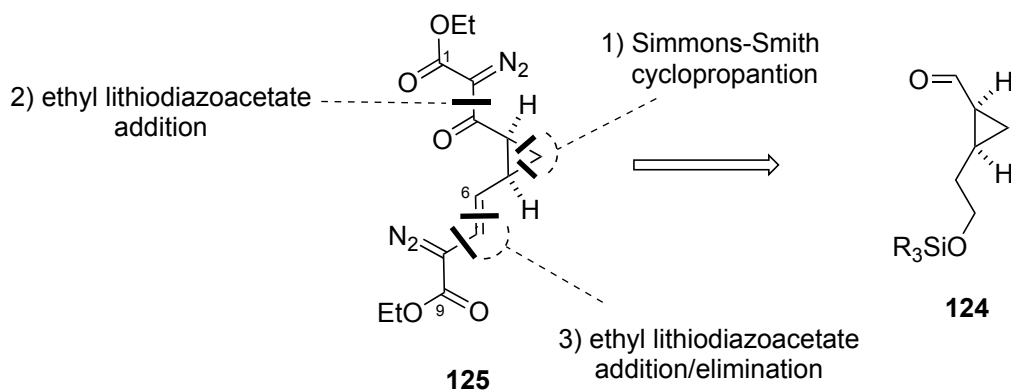
Scheme 2.36 Retrosynthetic Analysis and key fragment for bis-diazo **125**.

Current progress towards the synthesis of **125** is shown in Scheme 2.37. Silylation of homopropargyl alcohol **126** (TBSCl-Et$_3$N, DMAP, 99%) followed by lithiation and hydroxymethylation furnished propargyl alcohol **128** (91%).[110] Hydrogenation of the alkyne following Lindlar's reduction protocol gave allylic alcohol **129** in 75% yield.[111] A Simmons-Smith cyclopropanation of **129** yielded exclusively the *cis*-cyclopropane **130a** in 68% yield.

136
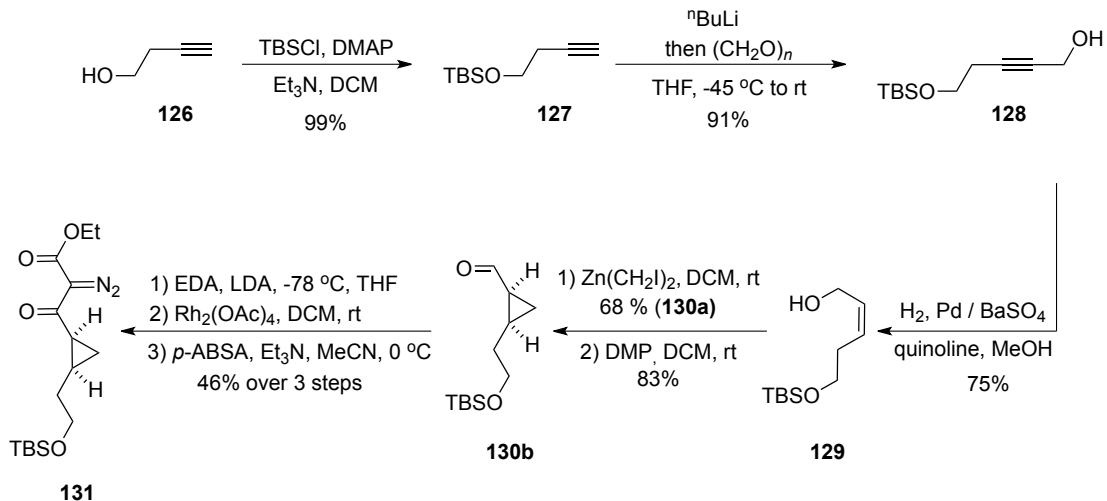
Scheme 2.37 Progress towards the synthesis of bis-diazo **125**.

The resulting cyclopropyl alcohol was oxidized to the corresponding aldehyde **130b** (Dess-Martin periodinane, 83%). The following three-step sequence is necessary as a result of difficulties encountered during the oxidation of the resulting the α-diazo-β-hydroxyester derived from the reaction of lithiodiazoacetate and aldehyde **130b**. The oxidation of α-diazo-β-hydroxyesters with Dess-Martin is a fairly recent methodology developed by Weinreb and co-workers.[112] However, in our hands, the α-diazo-β-hydroxyester underwent isomerization at the stereogenic center formed by the preceding lithiate addition rather than oxidation to form the desired α-diazo-β-ketoester. Parikh-Doering oxidation conditions were also employed, however, the oxidant failed to react with the alcohol substrate as unreacted starting material was apparent from analysis of the ¹H NMR spectrum of the crude reaction mixture. To circumvent this undesired reactivity, we employed the chemistry of Rh(II) salts for the formation of β-ketoesters. In 1979, Pellicciari reported that in the presence of catalytic amounts of Rh₂(OAc)₄, an

efficient procedure for the transformation of α-diazo-β-hydroxyesters into their corresponding β-ketoesters occurs (Scheme 2.38).[113]
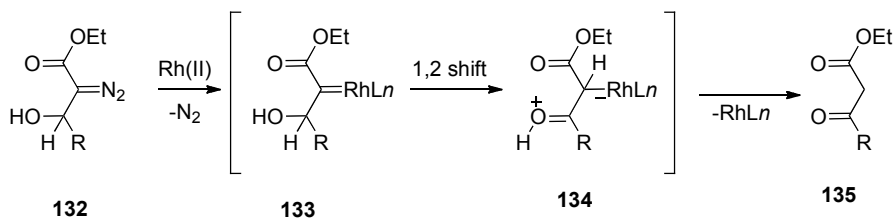
Scheme 2.38 Rh(II)-catalyzed conversion of α-diazo-β-hydroxyesters to β-ketoesters.

The accepted mechanism for this reaction involves the formation of the transient metallocarbenoid **133** derived from diazo **132** followed by a 1,2 hydride shift (**134**) and subsequent demetallation/protonation. Treatment of aldehyde **130b** with lithio ethyldiazoacetate, followed by β-ketoester formation and diazotization with diazo transfer reagent, *p*-ABSA, afforded the desired α-diazo-β-ketoester **131** in 46% yield over three steps.

2.4 Synthesis of exocyclic 1,3 butadiene 138

During the attempted synthesis of bis-diazo **125**, great efforts were made to prepare diene **138**.
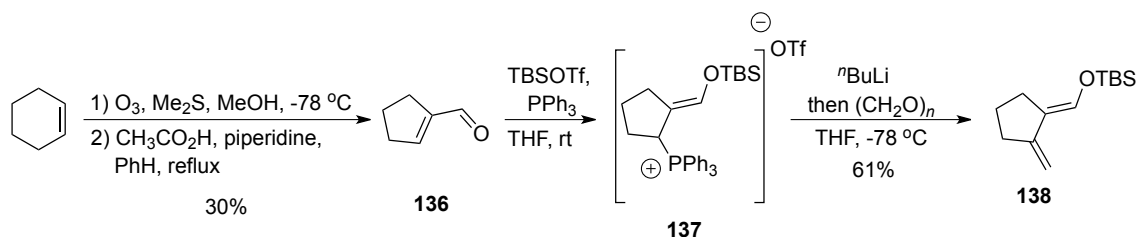
Scheme 2.39 Synthesis of exocyclic diene **138**.

As shown in Scheme 2.39, cyclopent-1-enecarbaldehyde (**136**) was isolated in 30% yield after oxidative cleavage of cyclohexene followed by refluxing in benzene and acetic acid/piperidine solution. Exposure of compound **136** to TBSOTf-PPh$_3$ efficiently provided phosphoniosilylated triflate salt **137**.[114] In the presence of ^{n}BuLi the corresponding phosphorus ylide smoothly reacted with paraformaldehyde to give the model diene **138** in 61% isolated yield.

2.5 Future work

The synthesis of bis-diazo **125** remains an active project in the Davies laboratory. From intermediate **139**, compound **125** is four synthetic steps away from serving as a viable candidate for generating the tetracyclic core of phorbol (Scheme 2.40).
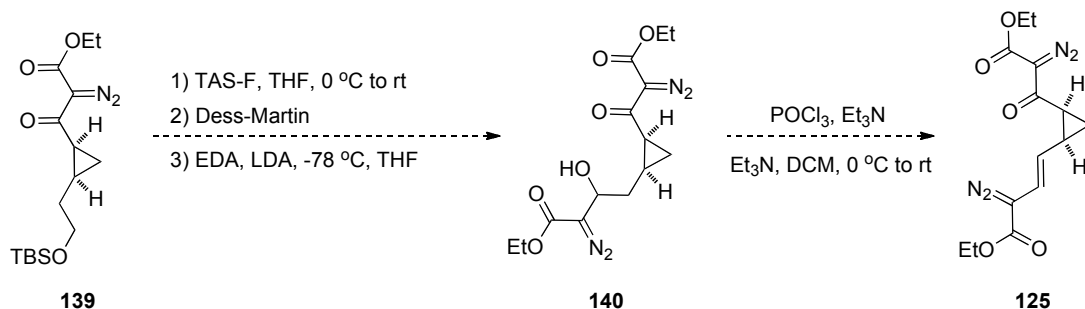
Scheme 2.40 End-game sequence to **125**.

The sequence involves 1) removal of the silicon protecting group by treatment with mild nucleophilic fluoride source, TAS-F 2) oxidation of the resulting alcohol into its corresponding aldehyde *via* Dess-Martin periodinane 3) lithio ethyldiazoacetate addition into the corresponding aldehyde and 4) vinyldiazoacetate formation followed by treatment with phosphorous oxychloride.

2.6 Additional studies with bis-diazo 100 and furan

During the course of the study, an investigation pertaining to the treatment of bis-diazo 100 with Rh₂(*S*-PTAD)₄/pyrazole 117 was undertaken. As illustrated in Scheme 2.41, exposure of 100 to acylic dienes (entries 1-3) resulted in an uncharacterizable mixture of products. However, in the presence of furan, the desired [4+3] adduct 142 was isolated in 38% yield and 83% ee.

entry 1) R¹ = OTBS, R² = H
entry 2) R¹ = Me, R² = H
entry 3) R¹ = OMe, R²= OTBS
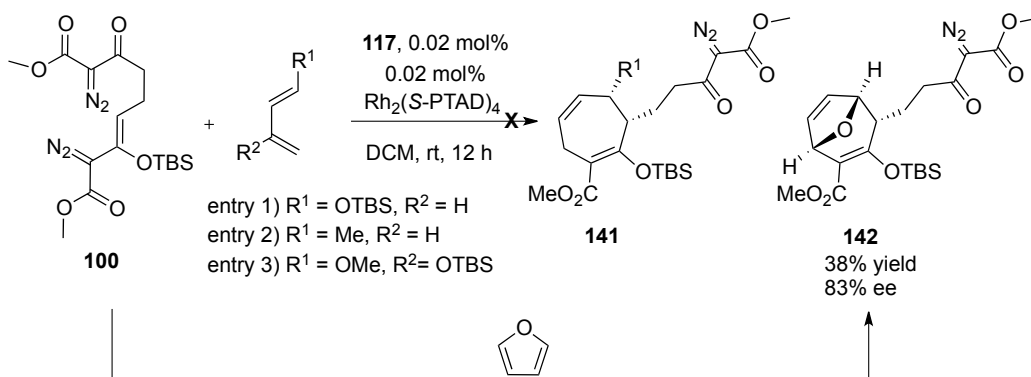
Scheme 2.41. Reaction of bis-diazo 100 with various dienes.

In addition to this work, diazo decompostion studies conducted by Ms. Fullilove indicated that the rate of decomposition of acceptor/acceptor can be significantly perturbed through the incorporation of sterically demanding esters (Table 2.8).

Table 2.8 Effect of ester substituent on diazo decomposition.

Entry	R	Relative Rate
1	Me	4
2	^{t}Bu	1

conducted by F. A. Fullilove
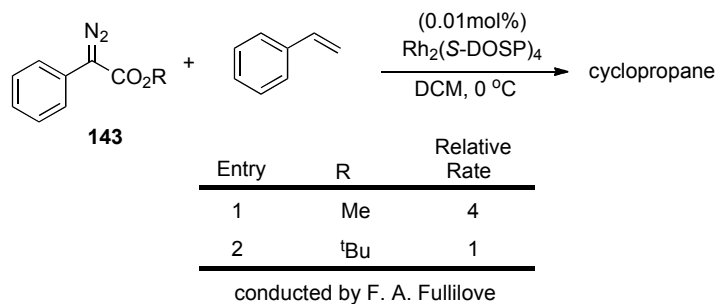
Using the previously developed Bi(III)-catalyzed diazo coupling strategy, bis-diazo **145** was synthesized in 36% yield using ^{t}Bu-siloxyvinyldiazo **144** as the Michael donor (equation **2.2**).
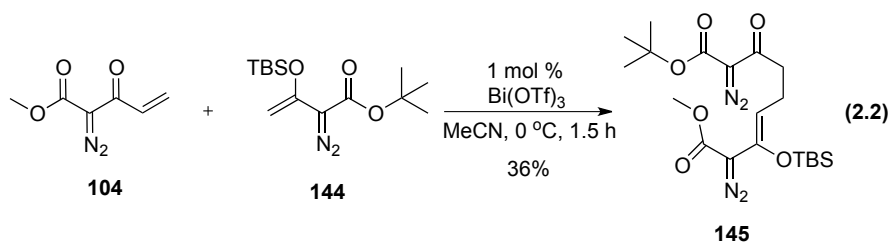
Interestingly, in the absence of the pyrazole additive, an asymmetric [4+3] cycloaddition is achieved using an excess of furan and 0.02 mol% Rh$_2$(S-PTAD)$_4$. Most notably, the pendent acceptor/acceptor diazo remains intact despite the presence of the Rh(II) catalyst further demonstrating the substrate design potential provided by ReactIR.

141
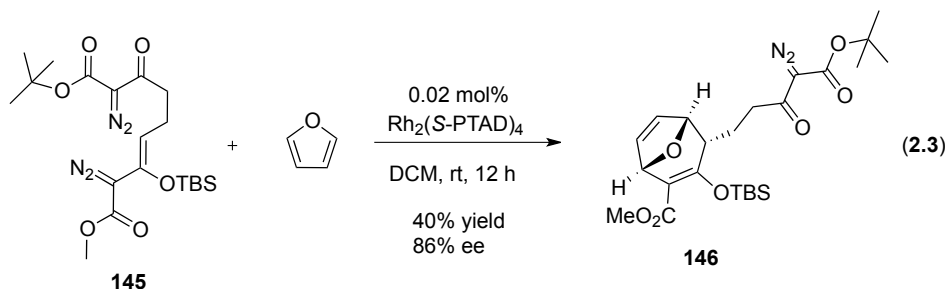
2.7 Conclusion

At this juncture, pertinent advancements have been made towards achieving the synthesis of the tetracyclic core of phorbol *via* a two-sequential reaction process, however, conditions to access the core through a cascade process have not been developed. Moreover, significant challenges still remain to synthesize the natural product. An exploratory study using *Z*-siloxy butadienes as trapping agents presents an opportunity to probe the intramolecular C-H insertion event. This will be a critical step to solve and will lead to extensive screening of catalysts to direct 5 versus 6-membered ring formation. The synthesis of exocyclic 1,4-siloxybutadienes has been realized, however, test reactions have not been explored. The bis-diazo approach remains an attractive strategy for the convergent synthesis of phorbol but has not yet been realized.

2.8 References

(1)   Regitz, M.; Maas, G. *Diazo Compounds: Properties and Synthesis*; Academic Press: Orlando, 1987.

(2)   Doyle, M. P.; McKervey, M. A.; Ye, T. *Modern Catalytic Methods for Organic Synthesis with Diazo Compounds*; Wiley: New York, 1998.

(3)   Eistert, B.; Regitz, M.; Heck, G.; Schwall, H. *Methoden. Org. Chemie. (Houben-Weyl)*; Thieme: Stuttgart, 1968; Vol. 10/4.

(4)   Bohshar, M.; Fink, J.; Heydt, H.; Wagner, O.; Regitz, M. *Methoden. Org. Chemie. (Houben-Weyl)*; Thieme: Stuttgart, 1990; Vol. E14b.

(5)   Heydt, H. *Science of Synthesis*; Thieme: Stuttgart, 2004; Vol. 27.

(6)   Regitz, M.; Maas, G. *Diazo Compounds-Properties and Synthesis*; Academic Press: Orlando, 1986.

(7)   Ovalles, S. R.; Hansen, J. H.; Davies, H. M. L. *Org. Lett.* **2011**, *13*, 4284-4287.

(8)   Briones, J. F.; Hansen, J.; Hardcastle, K. I.; Autschbach, J.; Davies, H. M. L. *J. Am. Chem. Soc.* **2010**, *132*, 17211-17215.

(9)   Davies, H. M. L.; Morton, D. *Chem. Soc. Rev.* **2011**, *40*, 1857-1869.

(10)   Davies, H. M. L.; Beckwith, R. E. J. *Chem. Rev.* **2003**, *103*, 2861-2903.

(11)   Padwa, A.; Krumpe, K. E. *Tetrahedron* **1992**, *48*, 5385-5453.

(12)   Padwa, A.; Weingarten, M. D. *Chem. Rev.* **1996**, *96*, 223-270.

(13)   Doyle, M. P.; Forbes, D. C. *Chem. Rev.* **1998**, *98*, 911-936.

(14)   Davies, H. M.; Beckwith, R. E. *Chem. Rev.* **2003**, *103*, 2861-904.

(15)   Wee, A. G. H. *Curr. Org. Synth.* **2006**, *3*, 499-555.

(16)   Ferreira, V. F. *Curr. Org. Chem.* **2007**, *11*, 177-193.

(17)   Lian, Y. J.; Davies, H. M. L. *J. Am. Chem. Soc.* **2010**, *132*, 440-441.

(18)   Lian, Y. J.; Miller, L. C.; Born, S.; Sarpong, R.; Davies, H. M. L. *J. Am. Chem. Soc.* **2010**, *132*, 12422-12425.

(19)   Schwartz, B. D.; Denton, J. R.; Lian, Y. J.; Davies, H. M. L.; Williams, C. M. *J. Am. Chem. Soc.* **2009**, *131*, 8329-8332.

(20)   Hansen, J. H.; Parr, B. T.; Pelphrey, P.; Jin, Q.; Autschbach, J.; Davies, H. M. *Angew. Chem., Int. Ed.* **2011**, *50*, 2544-8.

(21)   Regitz, M.; Heydt, H. *1,3-Dipolar Cycloaddition Chemistry*; Wiley: New York, 1984.

(22)   Mass, G. *The Chemistry of Heterocyclic Compounds, Vol. 59: Synthetic Application of 1,3-Dipolar Cycloaddition Chemistry toward Heterocycles and Natural Products*; Wiley: New York, 2002.

(23)   Padwa, A. *Tetrahedron* **2011**, *67*, 8057-8072.

(24)   Padwa, A.; Carter, S. P.; Nimmesgern, H. *J. Org. Chem.* **1986**, *51*, 1157-1158.

(25)   Padwa, A.; Zhang, Z. J. J.; Zhi, L. *J. Org. Chem.* **2000**, *65*, 5223-5232.

(26)   Mejia-Oneto, J. M.; Padwa, A. *Org. Lett.* **2006**, *8*, 3275-3278.

(27)   Weingarten, M. D.; Prein, M.; Price, A. T.; Snyder, J. P.; Padwa, A. *J. Org. Chem.* **1997**, *62*, 2001-2010.

(28)   Mejia-Oneto, J. M.; Padwa, A. *Tetrahedron Lett.* **2004**, *45*, 9115-9118.

(29)   Padwa, A.; Price, A. T. *J. Org. Chem.* **1998**, *63*, 556-565.

(30)   Dauben, W. G.; Dinges, J.; Smith, T. C. *J. Org. Chem.* **1993**, *58*, 7635-7637.

(31) Choi, Y. G.; Ishikawa, H.; Velcicky, J.; Elliott, G. I.; Miller, M. M.; Boger, D. L. *Org. Lett.* **2005**, *7*, 4539-4542.

(32) Elliott, G. I.; Fuchs, J. R.; Blagg, B. S. J.; Ishikawa, H.; Tao, H. C.; Yuan, Z. Q.; Boger, D. L. *J. Am. Chem. Soc.* **2006**, *128*, 10589-10595.

(33) Ishikawa, H.; Elliott, G. I.; Velcicky, J.; Choi, Y.; Boger, D. L. *J. Am. Chem. Soc.* **2006**, *128*, 10596-10612.

(34) Elliott, G. I.; Velcicky, J.; Ishikawa, H.; Li, Y. K.; Boger, D. L. *Angew. Chem., Int. Ed.* **2006**, *45*, 620-622.

(35) Ishikawa, H.; Colby, D. A.; Seto, S.; Va, P.; Tam, A.; Kakei, H.; Rayl, T. J.; Hwang, I.; Boger, D. L. *J. Am. Chem. Soc.* **2009**, *131*, 4904-4916.

(36) Hoffmann, R. W. *Dehydrobenzene and Cycloalkynes*; Academic Press: New York, 1967.

(37) Cava, M. P.; Glamkows.Ej; Weintrau.Pm *J. Org. Chem.* **1966**, *31*, 2755-2758.

(38) Borch, R. F.; Fields, D. L. *J. Org. Chem.* **1969**, *34*, 1480-1483.

(39) Rubin, M. B.; Bargurie, M.; Kosti, S.; Kaftory, M. *J. Chem. Soc., Perkin Trans. 1* **1980**, 2670-2677.

(40) Tosi, G.; Cardellini, L.; Pellicciari, R.; Fringuelli, R. *Gazz. Chim. Ital.* **1981**, *111*, 379-381.

(41) Maas, G.; Ganster, O.; Regitz, M.; Eistert, B. *Chem. Ber-Recl.* **1982**, *115*, 435-443.

(42) Sugawara, T.; Bethell, D.; Iwamura, H. *Tetrahedron Lett.* **1984**, *25*, 2375-2378.

(43) Bethell, D.; Gallagher, P.; Bott, D. C. *J. Chem. Soc., Perkin Trans. 2* **1989**, 1097-1104.

(44) Bethell, D.; Gallagher, P.; Self, D. P.; Parker, V. D. *J. Chem. Soc., Perkin Trans. 2* **1989**, 1105-1109.

(45) Koga, N.; Matsumura, M.; Noro, M.; Iwamura, H. *Chem. Lett.* **1991**, 1357-1360.

(46) Sung, D. D.; Park, Y. M.; Kim, K. C.; Park, D. K. *B. Kor. Chem. Soc.* **1993**, *14*, 335-340.

(47) Tomioka, H.; Okuno, A.; Sugiyama, T.; Murata, S. *J. Org. Chem.* **1995**, *60*, 2344-2352.

(48) Kirmse, W. *Angew. Chem., Int. Ed.* **1959**, *71*, 381-382.

(49) Trost, B. M.; Whitman, P. J. *J. Am. Chem. Soc.* **1974**, *96*, 7421-7429.

(50) Maier, G.; Reisenauer, H. P.; Schafer, U.; Balli, H. *Angew. Chem., Int. Ed.* **1988**, *27*, 566-568.

(51) Maier, G.; Reisenauer, H. P.; Balli, H.; Brandt, W.; Janoschek, R. *Angew. Chem., Int. Ed.* **1990**, *29*, 905-908.

(52) Murata, S.; Kobayashi, J.; Kongou, C.; Miyata, M.; Matsushita, T.; Tomioka, H. *J. Am. Chem. Soc.* **1998**, *120*, 9088-9089.

(53) Font, J.; Valls, J.; Serratosa.F *Tetrahedron* **1974**, *30*, 455-458.

(54) Kulkowit, S.; Mckervey, M. A. *J. Chem. Soc. Chem. Comm.* **1978**, 1069-1070.

(55) Doyle, M. P.; Hu, W. H.; Phillips, I. M.; Wee, A. G. H. *Org. Lett.* **2000**, *2*, 1777-1779.

(56) Sekiguchi, J.; Kuroda, H.; Yamada, Y.; Okada, H. *Tetrahedron Lett.* **1985**, *26*, 2341-2342.

(57) Rodphaya, D.; Sekiguchi, J.; Yamada, Y. *J Antibiot.* **1986**, *39*, 629-635.

(58) Kalita, D.; Khan, A. T.; Barua, N. C.; Bez, G. *Tetrahedron* **1999**, *55*, 5177-5184.

(59) Ronsheim, M. D.; Zercher, C. K. *J. Org. Chem.* **2003**, *68*, 1878-1885.

(60) Corey, E. J.; Myers, A. G. *Tetrahedron Lett.* **1984**, *25*, 3559-3562.

(61)   Kinard, L. A.; Kasper, F. K.; Mikos, A. G. *Nat. Protoc.* **2012**, *7*, 1219-1227.
(62)   Bakr, M. A.; Mahmud, A.; Morshed, M. G. *J. Polym. Mater.* **2010**, *27*, 49-56.
(63)   Fan, C. J.; Tu, J. X.; Yang, X. G.; Liao, L. Q.; Liu, L. J. *Carbohyd. Polym.* **2011**, *86*, 1484-1490.
(64)   Kricheldorf, H. R.; Yashiro, T.; Weidner, S. *Macromolecules* **2009**, *42*, 6433-6439.
(65)   Djonlagic, J.; Sepulchre, M. O.; Sepulchre, M.; Spassky, N.; Jacovic, M. S. *Makromol. Chem.* **1988**, *189*, 1485-1492.
(66)   He, S. L.; Yaszemski, M. J.; Yasko, A. W.; Engel, P. S.; Mikos, A. G. *Biomaterials* **2000**, *21*, 2389-2394.
(67)   Shirahama, H.; Kawaguchi, Y.; Aludin, M. S.; Yasuda, H. *J. Appl. Polym. Sci.* **2001**, *80*, 340-347.
(68)   Takenouchi, S.; Takasu, A.; Inai, Y.; Hirabayashi, T. *Polym. J.* **2001**, *33*, 746-753.
(69)   Xiao, L.; Liao, L.; Liu, L.; Li, Y. *New. J. Chem.* **2013**, *37*, 1874-1877.
(70)   Muthusamy, S.; Gunanathan, C.; Nethaji, M. *J. Org. Chem.* **2004**, *69*, 5631-5637.
(71)   Aburel, P. S.; Undheim, K. *J. Chem. Soc., Perkin Trans. 1* **2000**, 1891-1896.
(72)   Aburel, P. S.; Undheim, K. *Tetrahedron Lett.* **1998**, *39*, 3813-3814.
(73)   Molander, G. A.; Alonso-Alija, C. *Tetrahedron* **1997**, *53*, 8067-8084.
(74)   Danishefsky, S.; Chackalamannil, S.; Uang, B. J. *J. Org. Chem.* **1982**, *47*, 2231-2232.
(75)   Yamada, S.; Karasawa, S.; Takahashi, Y.; Aso, M.; Suemune, H. *Tetrahedron* **1998**, *54*, 15555-15566.
(76)   Moody, C. J.; Miller, D. J. *Tetrahedron* **1998**, *54*, 2257-2268.
(77)   Cox, G. G.; Miller, D. J.; Moody, C. J.; Sie, E. R. H. B.; Kulagowski, J. J. *Tetrahedron* **1994**, *50*, 3195-3212.
(78)   Muthusamy, S.; Srinivasan, P. *Tetrahedron* **2009**, *65*, 1567-1573.
(79)   Pelphrey, P.; Hansen, J.; Davies, H. M. L. *Chem. Sci.* **2010**, *1*, 254-257.
(80)   Evans, F. J. *Naturally Occuring Phorbol Esters*; CRC Press: Boca Raton, 1986.
(81)   Rosfjord, E. C.; Maemura, M.; Johnson, M. D.; Torri, J. A.; Akiyama, S. K.; Woods, V. L.; Dickson, R. B. *Exp. Cell. Res.* **1999**, *248*, 260-271.
(82)   Nishizuka, Y. *Nature* **1984**, *308*, 693-698.
(83)   Wender, P. A.; Kogen, H.; Lee, H. Y.; Munger, J. D.; Wilhelm, R. S.; Williams, P. D. *J. Am. Chem. Soc.* **1989**, *111*, 8957-8958.
(84)   Wender, P. A.; Mcdonald, F. E. *J. Am. Chem. Soc.* **1990**, *112*, 4956-4958.
(85)   Wender, P. A.; Rice, K. D.; Schnute, M. E. *J. Am. Chem. Soc.* **1997**, *119*, 7897-7898.
(86)   Lee, K.; Cha, J. K. *J. Am. Chem. Soc.* **2001**, *123*, 5590-5591.
(87)   Paquette, L. A.; Sauer, D. R.; Edmondson, S. D.; Friedrich, D. *Tetrahedron* **1994**, *50*, 4071-4086.
(88)   Mcmills, M. C.; Zhuang, L. H.; Wright, D. L.; Watt, W. *Tetrahedron Lett* **1994**, *35*, 8311-8314.
(89)   Carroll, G. L.; Little, R. D. *Org. Lett.* **2000**, *2*, 2873-2876.
(90)   Ovaska, T. V.; Roses, J. B. *Org. Lett.* **2000**, *2*, 2361-2364.
(91)   Rigby, J. H.; Kierkus, P. C.; Head, D. *Tetrahedron Lett.* **1989**, *30*, 5073-5076.
(92)   Page, P. C. B.; Hayman, C. M.; McFarland, H. L.; Willock, D. J.; Galea, N. M. *Synlett.* **2002**, 583-587.
(93)   Harwood, L. M.; Ishikawa, T.; Phillips, H.; Watkin, D. *J. Chem. Soc., Chem. Commun.* **1991**, 527-530.

(94) Shigeno, K.; Sasai, H.; Shibasaki, M. *Tetrahedron Lett.* **1992**, *33*, 4937-4940.

(95) Davies, H. M. L.; Clark, D. M.; Smith, T. K. *Tetrahedron Lett.* **1985**, *26*, 5659-5662.

(96) Novikov, A. V.; John, J. P. *Org. Lett.* **2007**, *9,* 67-63.

(97) Taber, D. F.; Petty, E. H.; Raman, K. *J. Am. Chem. Soc.* **1985**, *107*, 196-199.

(98) Liu, Y.; Zhang, Y.; Jee, N.; Doyle, M. P. *Org. Lett.* **2008**, *10*, 1605-1608.

(99) Zibuck, R.; Streiber, J. M. *J. Org. Chem.* **1989**, *54*, 4717-4719.

(100) Davies, H. M. L.; Ahmed, G.; Churchill, M. R. *J. Am. Chem. Soc* **1996**, *118*, 10774-10782.

(101) Ollevier, T.; Desyroy, V.; Catrinescu, C.; Wischert, R. *Tetrahedron Lett.* **2006**, *47*, 9089-9092.

(102) Davies, H. M. L.; Calvo, R. L. *Tetrahedron Lett.* **1997**, *38*, 5623-5626.

(103) Pirrung, M. C.; Zhang, J. C.; Lackey, K.; Sternbach, D. D.; Brown, F. *J. Org. Chem.* **1995**, *60*, 2112-2124.

(104) Davies, H. M. L. *[3+4] Annulations Between Rodium-Stabilized Vinylcarbenoids and Dienes*; JAI Press Inc.: Greenwich, 1999; Vol. 5.

(105) Taber, D. F.; Malcolm, S. C. *J. Org. Chem.* **1998**, *63*, 3717-3721.

(106) Doyle, M. P.; Dyatkin, A. B.; Roos, G. H. P.; Canas, F.; Pierson, D. A.; Vanbasten, A.; Muller, P.; Polleux, P. *J. Am. Chem. Soc.* **1994**, *116*, 4507-4508.

(107) Doyle, M. P.; Westrum, L. J.; Wolthuis, W. N. E.; See, M. M.; Boone, W. P.; Bagheri, V.; Pearson, M. M. *J. Am. Chem. Soc.* **1993**, *115*, 958-964.

(108) Taber, D. F.; Petty, E. H. *J. Org. Chem.* **1982**, *47*, 4808-4809.

(109) Jungong, C. S.; John, J. P.; Novikov, A. V. *Tetrahedron Lett.* **2009**, *50*, 1954-1957.

(110) Efskind, J.; Romming, C.; Undheim, K. *J. Chem. Soc., Perkin Trans. 1* **2001**, 2697-2703.

(111) Fujiwara, K.; Awakura, D.; Tsunashima, M.; Nakamura, A.; Honma, T.; Murai, A. *J. Org. Chem.* **1999**, *64*, 2616-2617.

(112) Li, P. H.; Majireck, M. M.; Korboukh, I.; Weinreb, S. M. *Tetrahedron Lett.* **2008**, *49*, 3162-3164.

(113) Pellicciari, R.; Fringuelli, R.; Ceccherelli, P.; Sisani, E. *J. Chem. Soc., Chem Commun.* **1979**, 959-960.

(114) Kozikowski, A. P.; Jung, S. H. *J. Org. Chem.* **1986**, *51*, 3400-3402.

2.9 Experimental procedures and compound characterization

2.9.1 General procedure

^{1}H NMR spectra were recorded on either a 400 or 600 MHz Varian spectrometer or an INOVA 400 MHz spectrometer with the sample solvated in CDCl$_3$ unless otherwise noted. For reactions requiring anhydrous conditions, glassware was either flame dried or oven dried for 24 hours before use. Magnetic stir bars, stainless steel needles, and cannulas where oven dried as well. Acetonitrile, dichloromethane, hexanes, tetrahydrofuran, diethyl ether and toluene were withdrawn from a 6-port solvent purification system. 2,2-dimethylbutane (DMB) was distilled from sodium metal. Flash chromatography was carried out using silica gel (230-400 mesh). Thin layer chromatography was carried out using EMD TLC Silica Gel 60 F$_{254}$ glass plates. Visualization of TLC plates was done by UV absorbance, staining with I$_2$, or staining with a KMnO$_4$, or PMA solution followed by heating. All reagents received from the following chemical companies were used as such: Sigma-Aldrich and Acros.
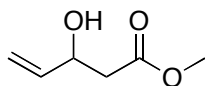
methyl 3-hydroxypent-4-enoate:

To a flame dried round bottom flask was added THF (400 mL) and diisopropylamine (15.4 mL, 210 mmol) and cooled to -78 °C. ^{n}BuLi (44mL, 110 mmol, 2.5 M in hexanes) was added and the reaction was stirred for 15 minutes. Methyl acetate (8 mL, 100 mmol, 1.00 eq) was added slowly (over 10 minutes). The reaction stirred for 50 minutes. Acrolein (6.70 mL, 100 mmol, 1.00 eq) was dissolved in THF (50 mL) and added to the reaction by cannula and allowed to stir for 5 minutes. The reaction was stopped by rapid injection of saturated NH_4Cl (30 mL). The mixture was immediately poured into a separation funnel containing Et_2O (200 mL). The organic layer was washed with brine, dried over $MgSO_4$, filtered, and concentrated under reduced pressure. The reaction yielded the desired aldol product in essentially quantitative yield 13 g, as a yellow liquid. Rf = 0.26 (75:25 Hexanes:EtOAc). The physical and spectral data were identical to those previously reported for this compound.[99] ^{1}H NMR (400 MHz; CDCl3) δ 5.87 (ddd, J = 5.2, 10.4, 17.2 Hz, 1H), 5.29 (d, J = 17.2 Hz, 1H), 6.16 (d, J = 10.8 Hz, 1H), 4.55-4.52 (m, 1H), 7.71 (s, 3H), 2.94 (d, J = 4.8 Hz, 1H), 2.62-2.49 (m, 2H).
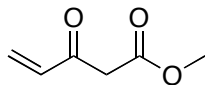
methyl 3-oxopent-4-enoate

To a round bottom flask was added Me_2CO (391 mL) and methyl 3-hydroxypent-4-enoate (13 g, 99.8 mmol, 1.00 eq) and cooled to 0 °C. CrO_3 (10.8 g, 108 mmol, 1.10 eq) was dissolved in H_2O (20 mL) followed by the addition of conc. H_2SO_4 (9.2 mL). The Jones reagent was added dropwise over 50 minutes. The reaction was allowed to warm slowly to room temperature over night. The reaction was stopped by addition of MeOH (40 mL). The mixture was poured into a separation funnel and the organic product was extracted with EtOAc (3 x 400 mL). The organic layer was washed with brine, dried over $MgSO_4$, filtered, and concentrated under reduced pressure. The product was purified on SiO_2 (hexanes:Et_2O). 5.7 g (45 %) of the desired product was isolated as a yellow liquid. The physical and spectral data were identical to those previously reported for this compound.[99] Rf = 0.18 (95:5 Pentane/Et_2O); ^1H NMR (400 MHz; $CDCl_3$) δ 3.64 (s, 2H, methylene(ketonic)), 3.73 (s, 3H), 5.95 (d, J = 10.4 Hz, 1H, vinyl(ketonic)), 6.26 (d, J = 17.6 Hz, 1H, vinyl(ketonic)), 6.41 (dd, J = 10.8, 17.6 Hz, 1H, vinyl(ketonic)).
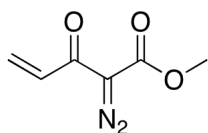
methyl 2-diazo-3-oxopent-4-enoate:

To a flame dried round bottom flask was added methyl 3-oxopent-4-enoate (2.84 g, 22 mmol 1.0 eq), MeCN (60 mL) and *p*-ABSA (5.77 g, 24 mmol, 1.4 eq). The mixture was then cooled to 0 °C. Once cool, Et$_3$N (3.6 mL, 26 mmol, 1.1 eq) was slowly added by syringe (over 1 minute). The reaction was allowed to stir for 3.5 h. The reaction was stopped by filtration through a plug of SiO$_2$ using Pentane:Et$_2$O (90:10). The reaction yielded 3.06 g, (90 %) of the desired product as a yellow liquid. Rf = 0.21 (90:10 Pentane/Et$_2$O); ^{1}H NMR (400 MHz; CDCl$_3$) δ 7.42 (dd, 1H, *J* = 10.4, 16.8 Hz), 6.44 (dd, *J* = 17.2, 2 Hz, 1H), 5.73 (dd, *J* = 10.4, 2 Hz, 1H), 3.85 (s, 3H); ^{13}C NMR (100 MHz, CDCl$_3$) δ 181.5, 161.4, 131.3, 128.3, 52.2; IR (neat): 2956, 2128, 1715; HRMS- m/z 155.0452 (M+H)$^+$ requires 155.0451).
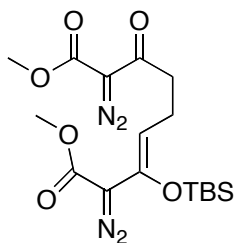
(Z)-dimethyl 3-((tert-butyldimethylsilyl)oxy)-2,8-bis(diazo)-7-oxonon-3-enedioate:

To a flame dried round bottom flask was added Bi(OTf)$_3$ (21 mg, 0.032 mmol, 0.005 eq), methyl 2-diazo-3-oxopent-4-enoate (1.0 g, 6.5 mmol, 1.0 eq) and MeCN (12.5 mL). The reaction was cooled to 0 °C. Methyl 3-((tert-butyldimethylsilyl)oxy)-2-diazobut-3-enoate (2.0 g, 7.8 mmol, 1.2 eq) was dissolved in MeCN (12.5 mL) and by syringe over 7 minutes. The reaction was left to stir for 30 minutes. The reaction was then stopped by addition of H$_2$O (50 mL). The mixture was diluted with brine (75 mL). The organic product was extracted with EtOAc (3 x 50 mL). The organic layers were combined, washed with water, brine, and dried over Na$_2$SO$_4$. The organic product was filtered through a glass frit and concentrated under reduced pressure. The material was purified on SiO$_2$ (hexanes:EtOAc 75:25) to give 1.86 g (70 %) of the Z-isomer product as a red oil, which solidified upon cooling at -26 °C. Rf = 0.46 (Hexanes:EtOAc 75:25); ^{1}H NMR (600 MHz; CDCl$_3$) δ 0.15 (s, 6H), 0.95 (s, 9H), 2.47 (q, J = 7.2 Hz, 2H), 2.92 (t, J = 7.2 Hz, 2H), 3.78 (s, 3H), 3.83 (s, 3H), 5.23 (t, J = 7.8 Hz, 1H); ^{13}C NMR (150 MHz, CDCl$_3$) δ -4.4, 18.4, 21.2, 25.8, 40.2, 52.1, 52.4, 111.6, 133.5, 162, 165.5, 192.1; IR (neat): 2954, 2928, 2857, 2147, 2094, 1696; HRMS- m/z 433.15125 (M+Na)$^+$ requires 433.15138.
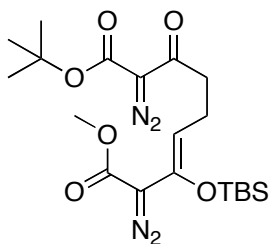
(*Z*)-9-*tert*-butyl 1-methyl 3-((*tert*-butyldimethylsilyl)oxy)-2,8-bis(diazo)-7-oxonon-3-enedioate:

To a 25 mL flame dried round bottom flask was added Bi(OTf)$_3$ (13 mg, 0.0195 mmol, 0.01 eq), methyl 2-diazo-3-oxopent-4-enoate (300 mg, 1.95 mmol, 1.0 eq) and MeCN (3.3 mL). The reaction was cooled to 0 °C. Diazo **8** (698 mg, 2.34 mmol, 1.2 eq) was dissolved in MeCN (3.3 mL) and added in one portion. The reaction was left to stir for 1.5 hours. The reaction was then stopped by addition of H$_2$O (30 mL). The organic product was extracted with diethyl ether (3 x 40 mL). The organic layers were combined, washed with water, brine, and dried over MgSO$_4$. The material was filtered through a glass frit and concentrated under reduced pressure. The material was purified by flash chromatography on SiO$_2$. 98:2 then 97:3 then 96:4 Hexanes/Ethyl acetate to give a 324 mg (36%) as a red oil. Rf = 0.25 (9:1 hexanes/EtOAc); ^{1}H NMR (400 MHz; CDCl$_3$) δ 5.22 (t, 1H, *J* = 7.2 Hz), 3.77 (s, 3H), 2.89 (t, *J* = 7.2 Hz, 2H), 2.45 (q, *J* = 7.2 Hz, 2H), 1.52 (s, 9H), 0.94 (s, 9H), 0.15 (s, 6H); ^{13}C NMR (100 MHz, CDCl3) δ 192.5, 165.4, 160.7, 133.3, 111.8, 83.2, 52, 40.1, 28.4, 25.8, 21.2, 18.3, -4.4; IR (neat): 2954, 2931, 2129, 2089, 1709, 1654; HRMS- m/z 453.21669 (M+H)$^+$ requires 453.21639.
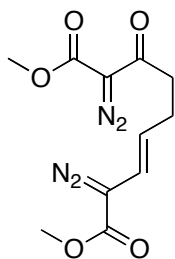
(E)-dimethyl 2,8-bis(diazo)-7-oxonon-3-enedioate:

To a round bottom flask was added (Z)-dimethyl 3-((tert-butyldimethylsilyl)oxy)-2,8-bis(diazo)-7-oxonon-3-enedioate (1.86 g, 4.54 mmol, 1.00 eq) and MeOH (60 mL). the solution was cooled to 0 °C. NaBH$_4$ (343 mg, 9.08 mmol, 2.00 eq) was carefully added in 2 portions. The reaction was left to stir for 0.5 h. The reaction was then quenched with D.I. H$_2$O (40 mL). The mixture was transferred to a separation funnel and diluted with D.I. H$_2$O (130 mL). The organic product was extracted with Et$_2$O (3 x 100 mL). The organic layers were combined, washed with water, brine, and dried over Na$_2$SO$_4$. The sample was then filtered through a glass frit and the material was concentrated under reduced pressure. The crude material was not purified and used immediately. The crude alcohol was then dissolved in DCM (40 mL) and cooled to 0 °C. Et$_3$N (2.51 mL, 18.2 mmol, 4.0 eq) was then added. Once cool, POCl$_3$ (0.634, 6.82 mmol, 1.50 eq) was added slowly (over 1 min). The reaction was allowed to stir and gradually warm to room temperature for a total of 16 h. The reaction was stopped by the addition of NaHCO$_3$ (60 mL). The mixture was transferred to a separation funnel and diluted with D.I. H$_2$O (60 mL). The organic product was extracted with DCM (3 x 60 mL). The organic layers were combined, washed with water, brine, and dried over Na$_2$SO$_4$.The reaction was stopped by concentration under reduced pressure. The sample was then dissolved in hexanes (50 mL) and water (50 mL) was added. The organic product was extracted with

153

hexanes (3 x 50 mL), washed with water, brine, and dried over $MgSO_4$. The organic product was then filtered through a glass frit and concentrated under reduced pressure. The reaction yielded a dark brandy wine oil. The crude was used immediately for the next step. DMF (26 mL) was added to the crude material and cooled to 0 °C. TAS-F (1.37 g, 4.99 mmol, 1.10 eq) was dissolved in DMF (26 mL) then slowly added to the reaction vessel by syringe (over 1 minute). After 15 minutes of stirring, the reaction was diluted with EtOAc (25 mL). The mixture was transferred to a separation funnel and diluted with pH 7 buffer (250 mL). The organic product was extracted with EtOAc (4 x 250 mL). The organic layers were combined, washed with water, brine, and dried over Na_2SO_4. The sample was then filtered through a glass frit and the material was concentrated under reduced pressure. The material was purified on SiO_2 (hexanes:EtOAc 75:25) to give 277 mg (22 % over 3 steps) of the product as a red oil, which solidified upon cooling at -26 °C overnight. Rf = 0.34 (75:25) hexanes:EtOAc; ^{1}H NMR (600 MHz; CDCl$_3$) δ 5.81 (d, 1H, J = 16.2 Hz), 5.34 (dt, J = 6.6, 6.6, 22.8 Hz, 1H), 3.84 (s, 3H), 3.79 (s, 3H), 2.97 (t, J = 7.2 Hz, 2H), 2.52 (qd, J = 1.2, 7.2 Hz, 2H); ^{13}C NMR (100 MHz, CDCl$_3$) δ 191.7, 166, 161.9, 123.5, 113.5, 52.3, 52.4, 40.2, 27.6; IR (neat): 2959, 2921, 2123, 2075, 1703, 1656; HRMS- m/z 303.07028 (M+Na)$^+$ requires 303.06999.
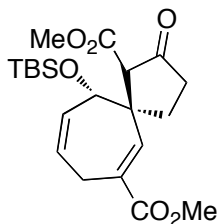
(1S,5R,11S)-dimethyl 11-((tert-butyldimethylsilyl)oxy)-2-oxospiro[4.6]undeca-6,9-diene-1,7-dicarboxylate:

To a flame dried round-bottom flask was added Rh$_2$(OAc)$_2$ (4 mg, 0.00895 mmol, 0.05 eq) and degassed anhydrous DCE (5 mL). The vessel was equipped with a water-cooled reflux condensor and heated to reflux. Diazo **120a** (78 mg, 0.179 mmol, 1.0 eq) was dissolved in DCE (5 mL) and added to the reaction by syringe pump addition (over 1 h). Once the addition was complete, the reaction was left to stir for an addition 0.5 h. The reaction was then stopped by concentration under reduced pressure. The crude material was purified by flash chromatography. The crude was purified by flash chromatography using 80:20 hexanes/EtOAc as eluent, to give 6 mg (8 %) of product. ^{1}H NMR (600 MHz; CDCl$_3$) δ 6.95 (d, *J* = 1.2 Hz, 1H), 5.66-5.58 (m, 2H), 4.46 (s, 1H), 3.73 (s, 6H), 3.19-3.08 (m, 2H), 2.56 (s, 1H), 2.03-1.93 (m, 3H), 1.73-1.67 (m, 1H), 0.86 (s, 9H), 0.03 (d, *J* = 4.2 Hz, 6H); HRMS- m/z 409.2043 (M+H)$^+$ requires 409.2040.
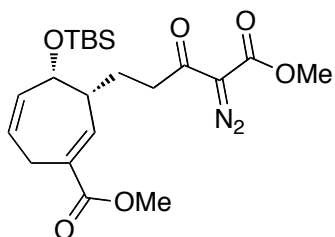
(3R,4S)-methyl 4-((tert-butyldimethylsilyl)oxy)-3-(4-diazo-5-methoxy-3,5-dioxopentyl)cyclohepta-1,5-dienecarboxylate:

To a flame dried round bottom flask was added bis-diazo **96** (84 mg, 0.30 mmol, 1.0 eq), degassed DCM (2.0 mL) and diene **108** (715 mg, 3.88 mmol, 13 eq). Rh$_2$(*S*-PTAD)$_4$ /pyrazole **119**(0.2 mL from a 0.0006 M stock solution) was added in a single motion. The reaction was left to stir under an inert atmosphere of argon at room temperature for 30 minutes. The reaction was stopped by concentration under reduced pressure. The crude was purified by flash chromatography using 90:10 hexanes/EtOAc as eluent, to give 31 mg (71 %) of a colorless oil. Rf = 0.39 (75:25 hexane:EtOAc); ^{1}H NMR (600 MHz; CDCl3) δ 6.96 (d, 1H, *J* = 6.6 Hz), 5.66 (m, 2H), 4.49 (s, 1H), 3.83 (s, 3H), 3.72 (s, 3H), 3.13 (m, 2H), 2.97 (ddd, *J* = 15.6, 9.0, 6.0 Hz, 1H), 2.89 (ddd, *J* = 15.0, 9.0, 6.0 Hz, 1H), 2.63 (m, 1H), 2.03 (ddd, *J* = 13.8, 9.0, 5.4 Hz, 1H), 1.87 (ddd, *J* = 15.0, 9.0, 6.0 Hz, 1H), 0.86 (s, 9H), 0.04 (s, 3H), 0.03 (s, 3H); ^{13}C NMR (100 MHz, CDCl$_3$) δ 192.7, 168.1, 161.9, 143.6, 134.6, 132, 125.8, 70.1, 52.3, 52.2, 44.6, 38.7, 27.6, 26, 25.8, 18.3, -4.3, -4.7; IR (neat): 2953, 2929, 2856, 2134, 1716, 1655; HRMS- m/z 459.19223 (M+Na)$^+$ requires 459.19219).
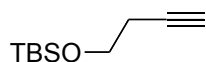
(but-3-yn-1-yloxy)(tert-butyl)dimethylsilane :

To a flame dried round-bottom flask was added anhydrous DCM (370 mL) and but-3-yn-1-ol (8.0 mL, 105 mmol, 1.00 eq). The solution was cooled to 0 °C. Et$_3$N (17.4 mL, 126 mmol, 1.20 eq) and DMAP (128 mg, 1.05 mmol, 0.01 eq) were added. The solution was allowed to stir for 5 minutes. TBSCl (18.2 g, 120 mmol, 1.15 eq) was added over 1 minute. The reaction was allowed to gradually warm to room temperature overnight. The reaction was quenched with aqueous saturated NaHCO$_3$ and diluted with Et$_2$O. The mixture was transferred to a separation funnel and the two layers were separated. The aqueous layer was washed with Et$_2$O (3 X 250 mL). The organic layers were combined, washed with brine, dried over MgSO$_4$, filtered and concentrated under reduced pressure. The compound was not purified and used as such. The physical and spectral data were identical to those previously reported for this compound.[110] ^{1}H NMR (600 MHz; CDCl$_3$) δ 3.74 (t, 2H, J = 5.4 Hz), 2.40 (td, J = 2.4, 7.2, 9.6 Hz, 2H), 1.96 (t, J = 2.4 Hz, 1H), 0.89 (s, 9H), 0.73 (s, 6H).

5-((tert-butyldimethylsilyl)oxy)pent-2-yn-1-ol:

To a round-bottom flask containing **126** (6.97 g, 37.8 mmol, 1.0 eq) was added anhydrous THF (75 mL). The solution was cooled to -45 °C. Once cool, ^{n}BuLi (2.5 M in hexanes, 16.6 mL, 41.6 mmol, 1.1 eq) was slowly added over 2 minutes. The solution was allowed to stir for 15 minutes. To a separate flask, was added paraformaldehyde (3.41 g, 113 mmol, 3.0 eq) and anhydrous THF (40 mL). The suspension was cooled to -45 °C. The alkynyl lithium was transferred by cannula to the paraformaldehyde suspension. The vessel was then removed from the cold bath and left to stir and gradually warm to room temperature over 1 hour. The reaction was stopped by diluting with Et$_2$O. The organic phase was washed with brine, dried over MgSO$_4$, filtered through a glass frit and concentrated under reduced pressure. The crude material was purifed by flash chromatography. The physical and spectral data were identical to those previously reported for this compound.[110] Rf = 0.3 (80:20 hexane:EtOAc); ^{1}H NMR (400 MHz; CDCl3) δ 4.25 (t, 2H, J = 3 Hz), 3.72 (t, J = 10.8 Hz, 2H), 2.43 (tt, J = 3.6, 10.8 Hz, 2H), 1.60 (bs, 1H), 0.89 (s, 9H), 0.07 (s, 6H).

(*Z*)-5-((tert-butyldimethylsilyl)oxy)pent-2-en-1-ol:

To a round-bottom flask was added **128** (4.00 g, 18.6 mmol, 1.00 eq), MeOH (19 mL), quinoline (0.122 mL, 1.04 mmol, 0.11 eq) and 5 % Pd/BaSO4 (272 mg, 0.11 mmol, 0.11 eq). The vessel was purged with argon and then equipped with a H_2 balloon. The reaction was monitored by ^{1}H NMR and stopped when the alkyne was no longer detectable. The reaction was stopped by filtration through a plug of SiO_2. The crude material was purified by flash chromatography to yield 3.0 g (75 %) of the corresponding allylic alcohol as a yellow oil. Rf = 0.3 (80:20 hexanes:EtOAc); ^{1}H NMR (600 MHz; CDCl3) δ 5.85-5.81 (m, 1H), 9.59 (q, *J* = 7.2 Hz, 1H), 4.14 (t, 2H), 3.65 (t, *J* = 6 Hz, 2H), 2.35 (q, *J* = 6.6 Hz, 2H), 2.03 (t, *J* = 6 Hz, 1H), 0.89 (s, 9H), 0.06 (s, 6H); ^{13}C NMR (100 MHz, CDCl3) δ 131, 129.9, 62.4, 58.2, 31.1, 26.2, 18.7, -5.2; IR (neat): 3347, 2953, 2928, 2856, 1093; HRMS- m/z 217.1619 (M+H)$^+$ requires 217.1618.
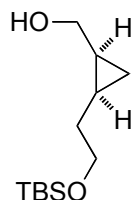
((1S,2S)-2-(2-((tert-butyldimethylsilyl)oxy)ethyl)cyclopropyl)methanol (130a):

To a round-bottom flask was added anhydrous DCM (30 mL) and cooled to -15 °C. Once cool, ZnEt$_2$ (10.1 mL, 1 M in hexanes, 10.1 mmol, 2.2 eq) was added. CH$_2$I$_2$ (1.63 mL, 20.3 mmol, 4.4 eq) was added over 20 minutes by syringe pump addition and allowed to stir for an additional 10 minutes once the addition was complete. Compound **129** (1.00 g, 4.62 mmol, 1.00 eq) was dissoleved in anhydrous DCM (5 mL) and added to the reaction vessel over 2 minutes. The reaction was allowed to gradually warm to room temperature and stir overnight. The reaction was stopped by the addition of saturated aqueous NH$_4$Cl (10 mL). and aqueous 1 M HCl (10 mL). The mixture was then diluted with Et$_2$O (60 mL) and the two layers were separated. To the organic phase was added aqueous 2M NaOH and 30 % aqeous H2O2. The resulting biphasic mixture was aggressively stirred for 5 minutes. The two layers were separated and the organic phase was washed with saturated aqueous NH$_4$Cl, saturated aqueous Na$_2$SO$_3$, and brine. The organic layer was dried over MgSO$_4$, filtered and concentrated under reduced pressure. The crude material was purified by flash chromatography to give pure product as a colorless oil (90:10 hexanes:EtOAc). Rf = 0.3 (80:20 hexanes/ethyl acetate); ^{1}H NMR (600 MHz; CDCl$_3$) δ 3.89-3.81 (m, 2H), 3.70 (ddd (app td), J = 3.6, 10.2, 10.2 Hz, 1H), 3.55 (dd, *J* = 1.8, 9.6 Hz, 1H), 3.22 (t, *J* = 10.2 Hz, 1H), 1.82 (dq, *J* = 3.6, 7.2 Hz, 1H), 1.49-1.43 (m, 1H),

1.28-1.21 (m, 1H), 0.93 (s, 9H), 0.70-0.74 (m, 1H), 0.65 (ddd, J = 4.2, 26.4, 26.4 Hz, 1H), 0.11 (s, 3H), 0.10 (s, 3H), 0.08 (q, J = 5.4 Hz, 1H); ^{13}C NMR (100 MHz, CDCl$_3$) δ 64.6, 62.5, 30.7, 26.2, 18.8, 18.7, 13.8, 7.6, -5.2, -5.3; IR (neat): 3371, 2953, 2928, 2856, 1253; HRMS- m/z 231.1774 (M+H)$^+$ requires 231.1775.
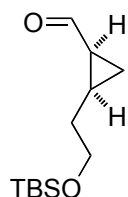
(1S,2S)-2-(2-((tert-butyldimethylsilyl)oxy)ethyl)cyclopropanecarbaldehyde(130b):

To a flame dried round-bottom flask was added compound **130a** (30 mg, 0.130 mmol, 1.0 eq), anhydrous DCM (2 mL) and Dess-Martin periodinane (83 mg, 0.19 mmol, 1.5 eq). The reaction was allowed to stir for 2 h. The reaction diluted with Et_2O and aqueous saturated $Na_2S_2O_3$. Aqueous saturated $NaHCO_3$ was added and the mixture was aggressively stirred for 5 minutes. The mixture was transferred to a separation funnel and the two layers were separated. The aqueous layer was washed with Et_2O (3 X 15 mL). The organic layers were combined, washed with brine, dried over Na_2SO_4, filtered and concentrated under reduced pressure. The crude material was purified by flash chromatography to give pure product as a light yellow oil (90:10 hexanes:EtOAc). Rf = 0.57 (80:20 hexanes:EtOAc); ^1H NMR (600 MHz; $CDCl_3$) δ 9.41 (d, 1H, J = 5.4 Hz), 1.92-1.88 (m, 3H), 1.83-1.79 (m, 1H), 1.73-1.67 (m, 1H), 1.62-1.55 (m, 1H), 1.25-1.21 (m, 1H), 1.20-1.17 (m, 1H), 0.88 (s, 9H), 0.04 (s, 6H); ^{13}C NMR (100 MHz, $CDCl_3$) δ 201.7, 63.1, 31.2, 27.5, 26.1, 21.9, 18.6, 14.3, -5.1; IR (neat): 2953, 2928, 2856, 1703; HRMS- m/z 229.1617 $(M+H)^+$ requires 229.1618.
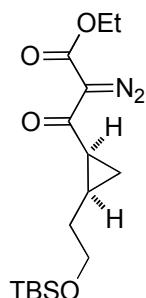
ethyl 3-((1S,2S)-2-(2-((tert-butyldimethylsilyl)oxy)ethyl)cyclopropyl)-2-diazo-3-oxopropanoate:

To a flame dried round-bottom flask was added diisopropylamine (0.170 mL, 1.22 mmol, 4.0 eq) and anhydrous THF (1.2 mL) The solution was cooled to -78 °C. Once cool, ^{n}BuLi (2.5 M in hexanes, 0.513 mL, 1.28 mmol, 4.2 eq) was added. the mixture was allowed to stir at -78 °C for 15 minutes then removed from the cold bath for 10 minutes then reintroduced to the -78 °C cold bath. Ethyldiazoacetate (70 mg, 0.612 mmol, 2.0) was added dropwise (over 2 minutes) and the reaction was allowed to stir for 1 h. Aldehyde **130b** (70mg, 0.306 mmol, 1.0 eq) was dissolved in THF (1.2 mL) and added to the reaction slowly by syringe (over 2 minutes). The reaction was allowed to stir for 1 h. The reaction was stopped by the addition of saturated aqueous NH_4Cl, diluted with Et_2O and the two layers were separated. The aqueous phase was washed with Et_2O (3 x 20 mL). The organic layer were combined, washed with brine, dried over $MgSO_4$, filtered and concentrated under reduced pressure. To a separate round-bottom flask was added Rh2(OAc)4 (14mg, 0.0306 mmol, 0.1 eq) and anhydrous DCM (0.5 mL). The crude material was dissolved in DCM (1 mL) and added to the reaction vessel by syringe pump addition (over 10 minutes). The reaction was allowed to stir for 2.5 h and was then stopped by filtering through a short plug of SiO_2 and concentrated under reduced

163

pressure. The crude material was dissolved in anhydrous MeCN (1 mL) followed by the addition of Et$_3$N (0.050 mL, 0.367 mmol, 1.2 eq). The solution was cooled to 0 °C. Once cool, *p*-ABSA (81 mg, 0.336 mmol, 1.1 eq) was added to the reaction and allowed to gradually warm to room temperature overnight. The crude material was passed through a short plug of SiO2 using 90:10 hexanes:EtOAc as eluant. The filtrate was concentrated and purified by flash chromatography to give 46 mg (44% over 3 steps) of the desired compound **131** as a dark orange oil. Rf = 0.56 (80:20 hexanes:EtOAc); ^{1}H NMR (600 MHz; CDCl$_3$) δ 4.31 (q, *J* = 7.2 Hz, 2H), 3.57 (t, *J* = 6.6 Hz, 2H), 3.08 (app q, *J* = 7.8 Hz, 1H), 1.71-1.57 (m, 4H), 1.32 (t, *J* = 6.6 Hz, 2H), 1.26-1.23 (m, 1H), 1.11-1.07 (m, 1H), 0.86 (s, 9H), 0.01 (s, 6H); ^{13}C NMR (100 MHz, CDCl3) δ 190.5, 161.9, 63.3, 61.5, 30.0, 26.1, 23.5, 23.3, 18.5, 14.9, 14.5, -5.1, -5.3; IR (neat): 2854, 2928, 2856, 2132, 1716, 1643; HRMS- m/z 341.189 (M+H)$^+$ requires 341.1891.
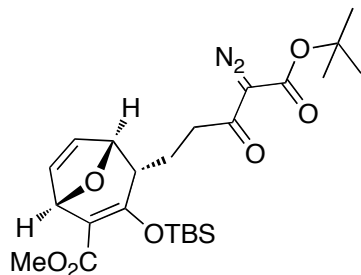
(1R,4R,5S)-methyl 4-(5-(tert-butoxy)-4-diazo-3,5-dioxopentyl)-3-((tert-butyldimethylsilyl)oxy)-8-oxabicyclo[3.2.1]octa-2,6-diene-2-carboxylate:

To a 5 mL flame dried round bottom flask was added bis-diazo (Z)-9-*tert*-butyl 1-methyl 3-((*tert*-butyldimethylsilyl)oxy)-2,8-bis(diazo)-7-oxonon-3-enedioate (75 mg, 0.165 mmol, 1.0 eq), degassed DCM (0.500 mL) and furan (0.240 mL, 3.3 mmol, 20 eq). Rh$_2$(S-PTAD)$_4$ (0.05 mL from a 0.0006 M stock solution) was added in a single motion. The reaction was left to stir under an inert atmosphere of argon at room temperature overnight. The reaction was stopped by concentration under reduced pressure. The crude was purified by flash chromatography using 90:10 hexanes/EtOAc as eluent, to give 31 mg (40 %) of a colorless oil. Rf = 0.35 (80:20 Hexanes/EtOAc); [α]^{20}$_D$: -17.1 (c. 1.0, CHCl$_3$); ^{1}H NMR (600 MHz; CDCl$_3$) δ 6.62 (dd, 1H, J = 6.0, 1.8 Hz), 6.06 (dd, J = 6.0, 1.8 Hz, 1H), 5.29 (d, J = 1.8 Hz, 1H), 4.98 (dd, J = 6.0, 1.8 Hz, 1H), 3.69 (s, 3H), 3.04-2.99 (m, 1H), 2.77 (dd, J = 22.2, 9.6, 6.6 Hz, 1H), 2.64 (ddd, J = 15.6, 6.0, 3.6 Hz, 1H), 2.17-2.11 (m, 1H), 1.52 (s, 9H), 1.45-1.42 (m, 1H), 0.95 (s, 9H), 0.18 (d, J = 6 Hz, 6H); IR (neat): 2952, 2858, 2133, 1709, 1686, 1651; ^{13}C NMR (100 MHz, CDCl$_3$) δ 192.1, 165.1, 160.6, 160.2, 140, 126.6, 115.5, 83.5, 79.9, 77.1, 51.1, 42.6, 37.4, 28.5, 25.9, 21.4, 18.7, -3.9, -4.1; IR (neat): 2952, 2858, 2133, 1709, 1686, 1651 HRMS- m/z 493.23641 (M+H)$^+$ requires 493.23646); HPLC analysis: 86% ee (Chiralcel OD-H, 100% hexane, 0.25 mL/min, λ = 254 nm, t$_R$ = 25.3 min, major; t$_R$ = 27.2 min, minor).
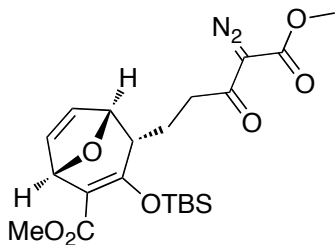
(1R,4R,5S)-methyl 3-((tert-butyldimethylsilyl)oxy)-4-(4-diazo-5-methoxy-3,5-dioxopentyl)-8-oxabicyclo[3.2.1]octa-2,6-diene-2-carboxylate:

To a 25 mL flame dried round bottom flask was added bis-diazo (Z)-dimethyl 3-((tert-butyldimethylsilyl)oxy)-2,8-bis(diazo)-7-oxonon-3-enedioate (123 mg, 0.3 mmol, 1.0 eq), degassed DCM (2.5 mL) and furan (0.463 mL, 6.0 mmol, 20 eq). $Rh_2(S\text{-}PTAD)_4$/pyrazole **119** (0.10 mL from a 0.0006 M stock solution) was added in a single motion. The reaction was left to stir under an inert atmosphere of argon at room temperature overnight. The reaction was stopped by concentration under reduced pressure. The crude was purified by flash chromatography using 90:10 hexanes/EtOAc as eluent, to give 52 mg (38 %) of a light yellow oil. Rf = 0.25 (80:20 Hexanes/EtOAc); $[\alpha]^{20}_D$: -21.7 (*c*. 1.0, CHCl_3); ^1H NMR (600 MHz; CDCl_3) δ 6.63 (dd, 1H, *J* = 6.0, 1.2 Hz), 6.06 (d, *J* = 6 Hz, 1H), 5.31 (s, 1H), 4.87 (d, *J* = 6 Hz, 1H), 3.84 (s, 3H), 3.69 (s, 3H), 3.06-3.00 (m, 1H), 2.81 (ddd, *J* = 25.2, 9.6, 6.6 Hz, 1H), 2.65 (ddd, *J* = 16.2, 6.0, 3.6 Hz, 1H), 2.18-2.12 (m, 1H), 1.55-1.42 (m, 1H), 0.95 (s, 9H), 0.18 (d, *J* = 9.6 Hz, 6H); ^{13}C NMR (75 MHz, CDCl_3) δ 191.6, 165.1, 161.8, 160.1, 140.1, 126.5, 115.5, 79.9, 77.1, 52.4, 51.1, 42.5, 37.5, 25.9, 21.4, 18.7, -3.9, -4.1; IR (neat): 2952, 2857, 2135, 1716, 1683, 1653; HRMS- m/z 451.18936 (M+H)$^+$ requires 451.18951. HPLC analysis: 83% ee (Chiralcel OD-H, 1% *i*-PrOH in hexanes, 1.00 mL/min, λ = 254 nm, t_R = 9.02 min, major; t_R = 11.8 min, minor).
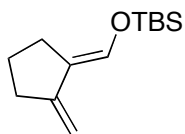
(E)-tert-butyldimethyl((2-methylenecyclopentylidene)methoxy)silane:

To a flame dried round-bottom flask was added triphenylphosphine (1.36 g, 5.20 mmol, 1.00 eq), anhydrous THF (15 mL) followed by TBSOTf (1.19 mL, 5.20 mmol, 1.0 eq). Cyclopentenecarboxaldehyde (500 mg, 5.2 mmol, 1.0 eq) was dissolved in THF (1mL) and added to the reaction vessel by dropwise addition (over 5 minutes). The reaction was allowed to stir for 1.5 h. The reaction was then cooled to -78 °C. Once cool, nBuLi (2.5 M in hexanes, 2.08 mL, 5.20 mmol, 1.00 eq) was slowly added (over 1 minute). Paraformaldehyde (468 mg, 15.6 mmol, 3.00 eq) was dissolved in THF (10 mL) and added to the reaction by cannula addition. The reaction was stirred at -78 °C for an additional 0.5 h then warmed to room temperature. The reaction was then poured in pentane (50 mL) and the resulting precipitate was removed by filtration. The filtrate was concentrated under reduced pressure. The crude material was purified by flash chromatography (99:1 pentane/Et$_3$N) to afford pure product. Rf = 0.83 (100% hexanes); ^{1}H NMR (600 MHz; CDCl$_3$) δ 6.80 (s, 1H), 5.01 (s, 1H), 4.62 (s, 1H), 2.42-2.36 (m, 4H), 1.65 (app p, J = 7.2 Hz, 2H), 0.93 (s, 9H), 0.16 (s, 6H); ^{13}C NMR (100 MHz, CDCl$_3$) δ 148.8, 133.5, 123.4, 97.5, 35.5, 28.4, 25.7, 24.2, 18.3, -5; IR (neat): 2954, 2929, 2857, 1657, 1169; HRMS- m/z 225.1666 (M+H)$^+$ requires 225.1669.

Chapter III

Catalyst versus Substrate Control in Asymmetric C-H Insertion Reactions

3.1 Introduction

Synthetic organic chemistry can be regarded as the chemical discipline that involves the construction, interconversion, and reactivity of organic compounds. These organic compounds are primarily composed of but not limited to, carbon, nitrogen, oxygen, and hydrogen. Introduced and developed in the mid 1960's, retrosynthetic (or antithetic) analysis has proven to be an incredibly powerful strategy in the construction of complex molecules.[1] This technique requires the theoretical disconnection of a target compound, *via* functional group interconversions (FGI) or bond making reaction, to a series of simplified structures, or synthons, thus revealing an iterative process which ultimately leads to a simple and/or commercially available starting material. The principle texts in this area described this method of thinking as the "Logic of Synthesis" and taught students in terms of the functional groups present within the molecules and made up the reactive substituents. However, recent advances have the opportunity to completely change the logic of synthesis, removing the reliance on functional groups and instead shifting the focus to the C–H bonds of the molecule, previous overlooked as inert, unreactive structural components.

Among the many available reagents in modern synthetic organic methodology, relatively few have been developed that are proficient at achieving selective chemistry on C-H bonds. This lack of reagents can be attributed to the high bond energies associated

with C-H bonds (typically 85-110 kcal/mol).[2] Although C-H bonds appear to be chemically inert, relentless chemical research has proven otherwise. Research spanning over 30 years has focused on the development of new organometallic reagents for the functionalization of unactivated C-H bonds. This chemistry has received much attention from the synthetic community.[3,4] Early approaches to functionalization of unactivated sp^3 C-H bonds began with intramolecular radical reactions.[5] These reactions are proposed to take place by generation of highly reactive intermediates which include free nitrogen and oxygen radicals. Regioselectivity can be controlled by placing the unactivated C-H bond in close spatial proximity to the radical. Intramolecular hydrogen abstraction followed by trapping of the resulting radical furnishes the C-H functionalized product (Scheme 3.1).[4]
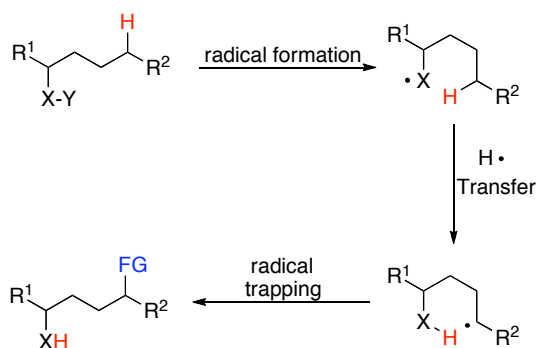
Scheme 3.1 Hoffman's radical C-H activation.

Another interesting approach to C-H activation has been facilitated by the use of electron-rich 'late' transition metals. Low-valent metals such as Re, Fe, Ru, Os, Rh, Ir and Pt have been shown to be involved in C-H activation by means of a proposed oxidative addition mechanism.[6]

This mechanism can be rationalized as proceeding through a process which involves oxidative insertion of the metal into a C-H bond, which forms a transient organometallic species which then undergoes further functionalization (Scheme 3.2).[7,8]
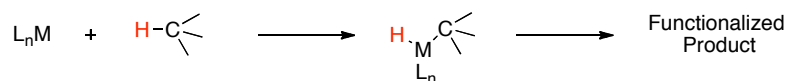
Scheme 3.2 C-H functionalization strategy *via* oxidative addition approach.

Thorough mechanistic studies have been performed on the oxidative addition process.[9-11] Notably, this chemistry has enlightened the organic community on the tremendous utility of transition metals. However, the 'Achilles heel' of the aforesaid process is its inability to become catalytic. The catalytic process is unfavorable because regeneration of the highly reactive metal species is unfavorable.[12] In 2000, Hartwig demonstrated a thermal, regiospecific and catalytic functionalization of alkanes with rhodium.[13] In this process, the coupling of alkanes with borane reagents to form linear alkylboranes was revealed. Unactivated alkanes were functionalized at the terminal position (Scheme 3.3).
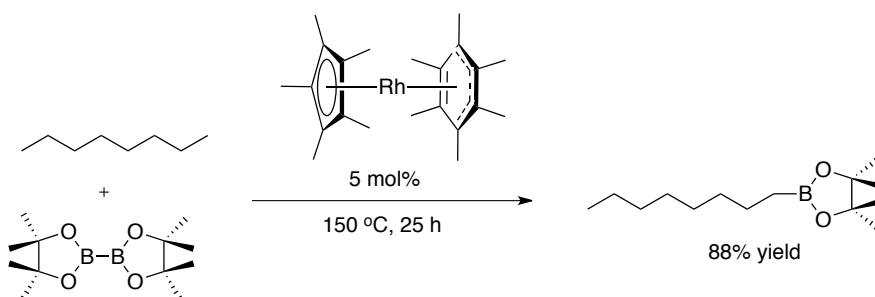
Scheme 3.3 Hartwig's rhodium-catalyzed functionalization.

A proposed mechanistic pathway for this C-H functionalization involves the oxidative addition of diboron to form a rhodium bis(boryl) complex (Figure 3.1). After elimination of borane to create an open coordination site, the complex then reacts with an alkane to produce an alkyl-rhodium boryl complex. As soon as this alkyl-rhodium boryl complex is formed, rapid boron-carbon bond formation yields the functionalized alkane.[13]

Figure 3.1 Catalytic cycle for Hartwig's rhodium-catalyzed functionalization.

Interestingly, a similar ruthenium catalyst, $[Cp*RuCl_2]_2$, was also introduce by Hartwig which has been shown to exhibit comparable if not better reactivity for the functionalization of alkanes.[14]

In 2002, Murai introduced a process that takes advantage of coordinating functional groups to direct the site of C-H activation. Several functional groups such as ketones, esters, imines, imidates, nitriles, and aldehydes proved to be extremely powerful directing groups. The chemistry was aided with the by use of $RuH_2(CO)(PPh_3)_3$. Interesting developments, also introduced by Murai, showcase intramolecular reactions

involving the C-H activation approach.[15] An example of this chemistry is described in the catalytic cyclization of 1,5-dienylpyrindines *via* a RhCl(PPh₃)₃ complex (Scheme 3.4).
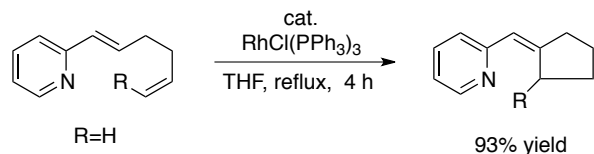
Scheme 3.4 Intramolecular cyclization of 1,5-dienylpryidine *via* C-H bond cleavage.

This process was efficiently extended to an asymmetric variant by incorporation of a chiral motif into the ligand framework using [RhCl(coe)₂]₂/(R)-(S)-PPFOMe catalyst system (coe = cyclooctene; (R)-(S)-PPFOMe = (R)-1-[(S)-2-(diphenylphosphino)ferrocenyl]ethyl methyl ether).[16,17] When this complex was employed to the reaction of an imidazolyl diene, the corresponding 5-membered carbocycle was isolated in 75% yield with an enantiomeric excess of 82% (Scheme 3.5).
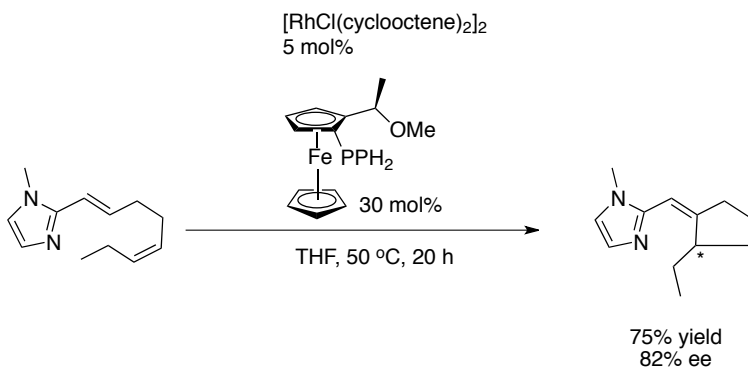
Scheme 3.5 Murai's asymmetric intramolecular C-H/olefin coupling.

The examples above illustrate the power, progress, and richness of transition-metal-mediated C-H activation chemistry. However, difficulties in designing catalytic, asymmetric, and practical protocols remain a major obstacle. The development of

selectively performing C-H activation *via* the aforesaid methodologies in the presence of various C-H bonds and highly functionalized molecules remains a challenge.

3.2 Rhodium carbenoid-mediated intermolecular C-H insertion

A complementary approach to the classical C-H activation is C-H insertion. This type of chemistry is made possible by means of metal carbenoids. Although the C-H insertion of a rhodium-carbenoid is not normally included in C-H activation reviews, this process readily provides access to functionalized products derived from unactivated C-H bonds.[12] Interestingly, rhodium carbenoid driven C-H insertion reactions posses a major advantage over classical C-H activation in that a catalytic process is extremely favorable.[18] The catalytic cycle commences with the decomposition of diazo compound **II** by metal complex **I,** which results in the energetically favorable extrusion of nitrogen gas. The carbenoid **III** undergoes the insertion step with compound **IV** which is then released to yield the functionalized product **VI** and metal complex **I.** With **I** regenerated, it then participates in another insertion cycle (Scheme 3.6).[19]
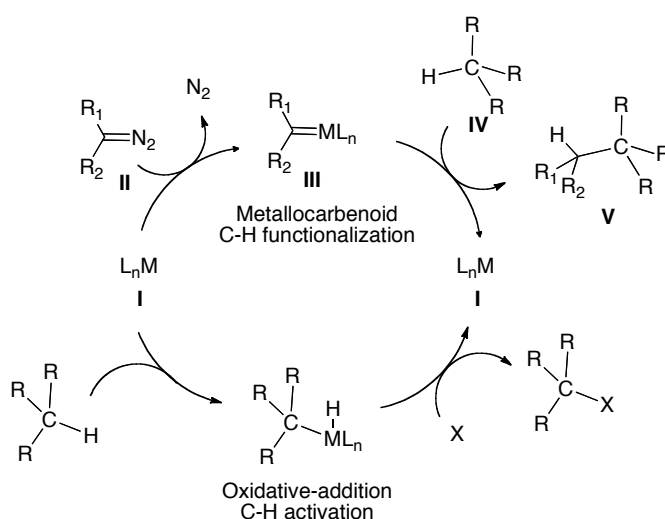
Scheme 3.6 Comparison of strategies developed for C-H functionalization.

In 2003, a pioneering review identifying the three main classes of carbenoids routinely used in C-H activation was published by Davies and co-workers.[19] The carbenoids were distinguished by the functionality adjacent to the metal carbene (Figure 3.2).

acceptor substituted carbenoid	acceptor/acceptor substituted carbenoid	donor/acceptor substituted carbenoid
$LnM = \overset{H}{\underset{EWG}{<}}$	$LnM = \overset{EWG}{\underset{EWG}{<}}$	$LnM = \overset{EDG}{\underset{EWG}{<}}$
EWG= CO_2R, COR, NO_2, $PO(OR)_2$, SO_2R	EWG= CO_2R, COR, NO_2, CN, SO_2R	EWG= CO_2R, COR, EDG= vinyl, alkynyl, aryl, heteroaryl
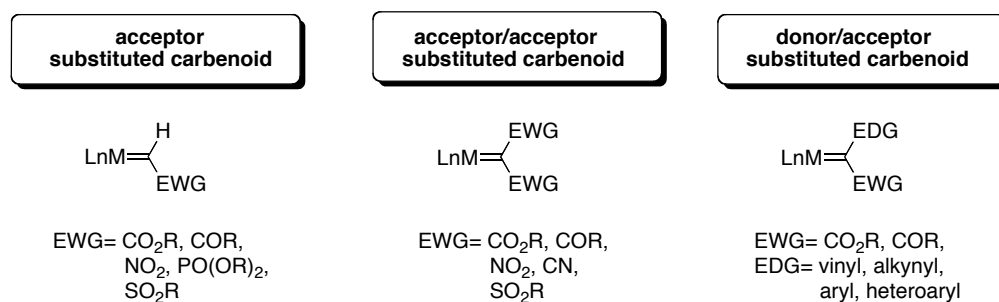
Figure 3.2 Classification of carbenoid intermediates.

Previous reviews had failed to stress the importance of the carbenoid electronic structure. A direct correlation was proposed which describes the carbenoid reactivity profile. Acceptor and acceptor/acceptor substituted metal carbenoids are significantly more reactive and highly electrophilic intermediates, the reaction of which often result in less selective transformations. Moreover, due to the high reactivity, dimerization of the carbenoid is a prevalent side reaction. Due to the regioselectivity challenges associated with these reactions, most of the early findings related to C-H insertion, were restricted to intramolecular processes.[18,20,21]

Ground-breaking contributions in the field were made by the Davies laboratory who introduced and showcased the practicality of donor/acceptor metal carbenoids.[19] It was shown that incorporation of an electron-donating group, such as aryl or vinyl, greatly

stabilizes the transient metallocarbenoid intermediate thus allowing access to highly regio- and stereoselective reactions. In the presence of the chiral dirhodium catalysts, high levels of asymmetric induction are realized. In addition, Davies also developed the chiral dirhodium proline-derived tetracarboxylate catalyst $Rh_2(S\text{-}DOSP)_4$,[22] which when combined with donor/acceptor diazo compounds, is a spectacular catalyst for intermolecular C-H insertion reactions with an exceptionally broad range of substrates (Figure 3.3).[3]
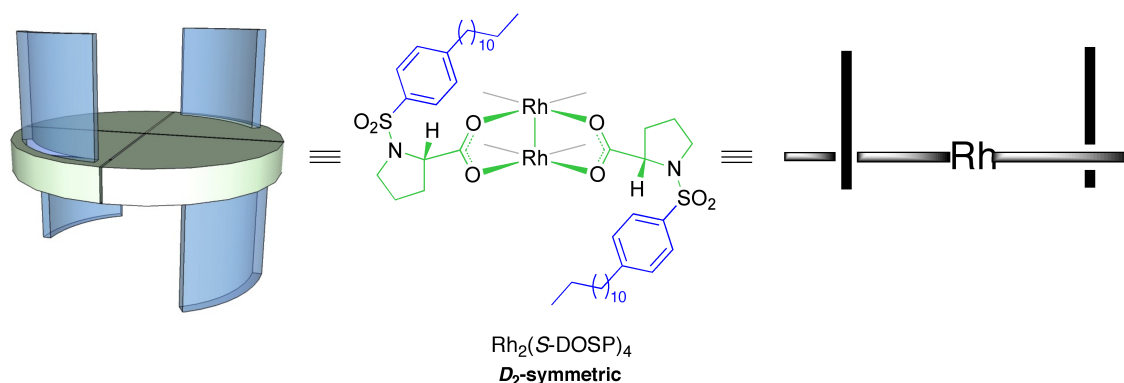
Figure 3.3 Pictorial representations of Davies' chiral dirhodium catalyst $Rh_2(S\text{-}DOSP)_4$.

Most importantly, Davies and co-workers revealed that these reactions were now capable of reacting through an intermolecular manifold thus broadening and enabling the synthesis of simple and complex organic molecules. Representative examples of substrates that generate a single chiral center in the C-H insertion step are illustrated in Table 3.1.

Table 3.1 Examples of high asymmetric induction by enantiopure $Rh_2(DOSP)_4$ and donor/acceptor diazo compounds.

Reaction scheme:

N$_2$=C(EWG)(EDG) + H–C(R$_1$)(R$_2$)(R$_3$) → (via Rh$_2$(DOSP)$_4$) → (EDG)(EWG)C(H)–C(R$_1$)(R$_2$)(R$_3$)
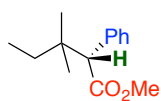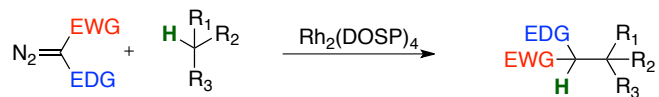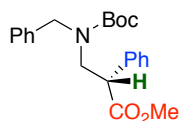
60% yield
68% ee

67% yield
91% ee
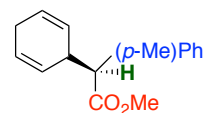
84% yield
94% ee
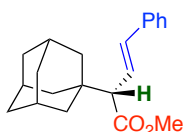
58% yield
91% ee
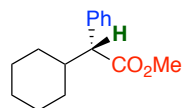
80% yield
95% ee
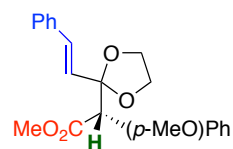
62% yield
91% ee
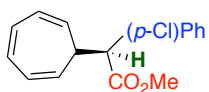
64% yield
95% ee
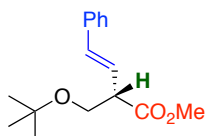
38% yield
95% ee

51% yield
94% ee

176
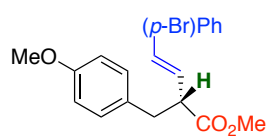
3.3 Diastereoselective rhodium carbenoid-mediated intermolecular C-H insertion

Recently, an informative computational study, conducted in the Davies group, discussed the selectivity of donor/acceptor-substituted rhodium carbenoids and the C-H insertion process.[23] Previous studies have suggested a concerted asynchronous pathway which would require the C-H bond to be oriented in a plane parallel to the plane defined by the carbene, either parallel to the Rh-C bond (a), or perpendicular to the Rh-C bond (b), and the C-H-C bond angle to be <90°, for a three-centered transition state to be favorable (Figure 3.4).
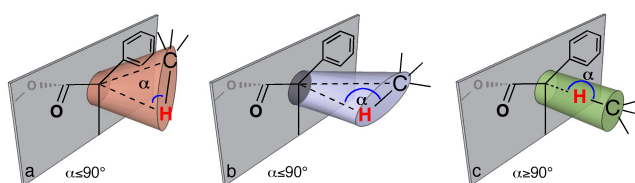
Figure 3.4 Possible approach angles between the substrate C-H bond vector and the rhodium carbenoid plane.

However, from Davies' theoretical study, calculations indicate that the C-H insertion event begins with the development of significant hydride transfer character, with a C-H-C bond angle in the range of 117°-165°. This data was in strong agreement with prior experimental intermolecular C-H insertion mechanistic studies.[19,24] Such an approach indicates that the C-H bond that participates in the insertion event is nearly perpendicular to the carbenoid plane (illustration c). As such, calculated transition state geometries led to the development of a new and simplified predictive model for the $Rh_2(S\text{-}DOSP)_4$

induced diasteroselectivity of donor/acceptor rhodium carbenoid mediated intermolecular C-H insertion reactions (Figure 3.5).
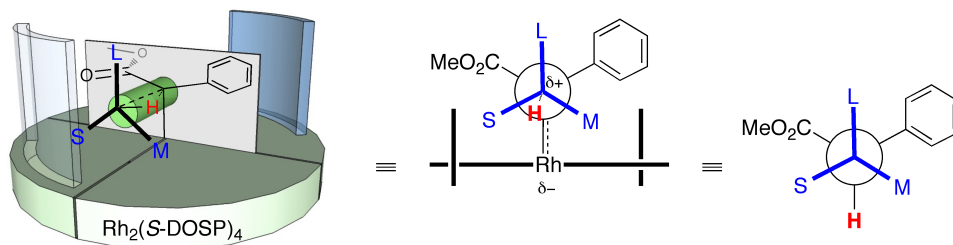
Figure 3.5 C-H insertion predictive model.

Due to the D_2 symmetry associated with the rhodium complex, the chirality inherent to Rh$_2$(S-DOSP)$_4$ is taken into account by adding blocking groups as indicated by light blue 'walls' or bold black lines.[22,25] As a result, a Newman projection was developed to explain the relative configuration of the two newly formed stereogenic centers as a result of the insertion reaction. Since the ester grouping is viewed as a sterically demanding substituent, the small (S) substituent of the substrate resides on the same side as the ester. The medium grouping (M) resides on the side that is in close proximity to the aryl grouping. Lastly, the large (L) substituent is 'gauche' to the ester and aryl substituents. Interestingly, the new predictive model suggests that insertion into methylene carbons will occur with high diastereoselectivity if there is good size differentiation between the large and medium substituents. Various products ranging in diastereomeric excesses are illustrated in Scheme 3.2.[23]

Table 3.2 Examples of diastereoselective C-H insertion reactions with Rh$_2$(DOSP)$_4$.

>94% de, 82% ee	>90% de, 95% ee	88% de, 97% ee
Rh$_2$(S-DOSP)$_4$	Rh$_2$(R-DOSP)$_4$	Rh$_2$(R-DOSP)$_4$

90% de, 73% ee	92% de, 95% ee
Rh$_2$(S-DOSP)$_4$	Rh$_2$(R-DOSP)$_4$
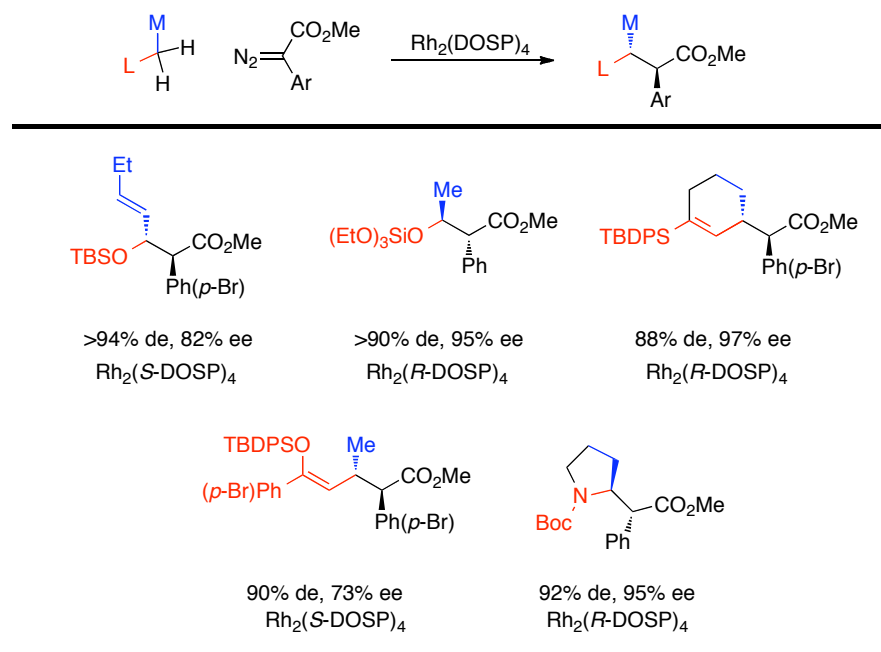
The practicality of this new predictive model is apparent when used as a tool to provide insight to reactions deprived of diastereoselectivity. An example of such a transformation is the benzylic C-H insertion reaction of 5-methoxyindane which was conducted by in the Davies laboratory by Dr. Qihui Jin (Scheme 3.7).[26]

d.r. =	57	:	43
%ee =	90	:	89
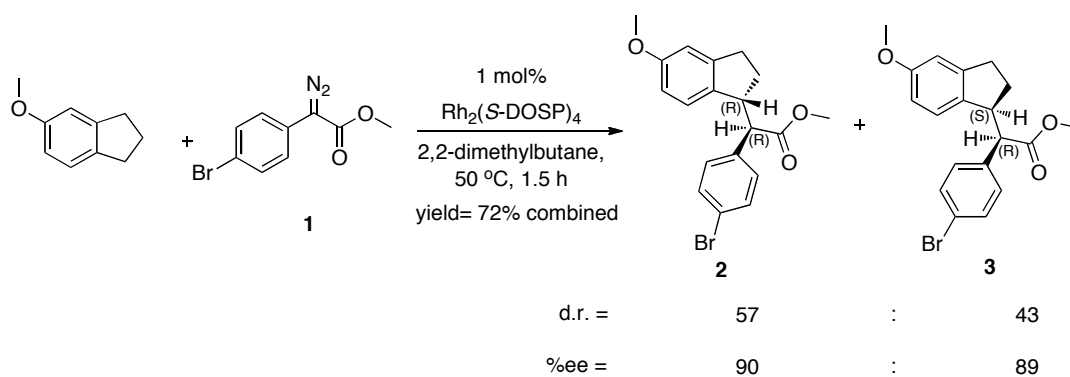
Scheme 3.7 Benzylic C-H activation of 5-methoxyindane.

In the presence of Rh$_2$(*S*-DOSP)$_4$, the reaction occurs in good yield with high levels of enantioselectivity. However, low diastereomeric ratios (57:43) are produced. Using the new model, as illustrated in Figure 3.6, it is possible to rationalize the substrates approach to the carbenoid complex in two distinct fashions. In approach A, the substrate shows the benzylic proton, highlighted in red, undergoing the C-H insertion event and minimized any negative steric interactions.
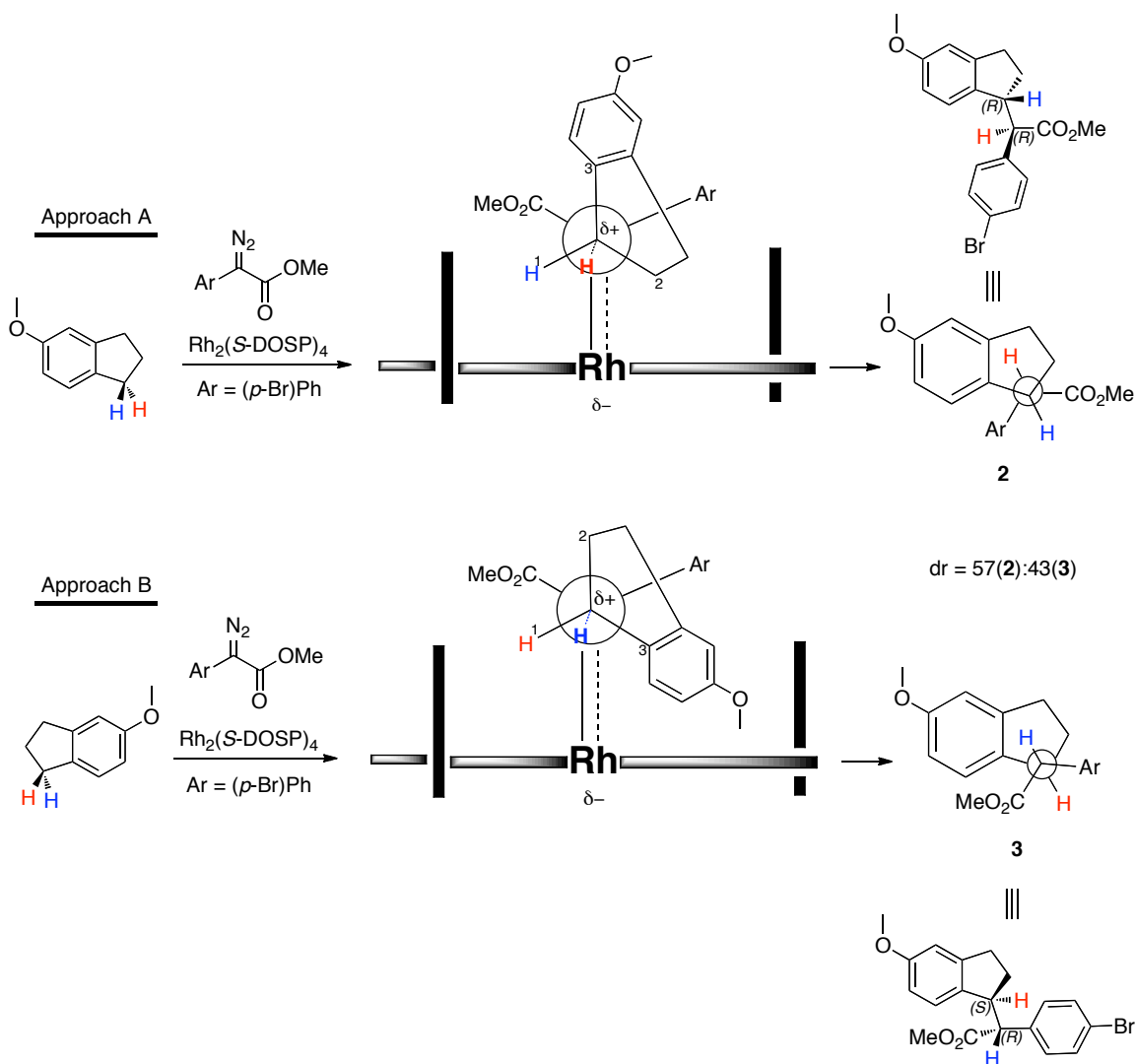
Figure 3.6 Application of the new predictive model to 5-methoxyindane.

180

It is important to note, that the hydrogen highlighted in blue is on the same side as the methyl ester of the carbenoid and the methylene adjacent to the site undergoing C–H insertion chemistry (carbon 2) is on the same side as the aryl substituent. Lastly, the sp^2 hybridized carbon (carbon 3) is gauche to the ester and aryl substituents. This approach affords the major diastereoisomer. In approach B, the substrate rotates 180° thus exposing the benzylic hydrogen highlighted in blue. The sp^2 hybridized carbon (carbon 3) is now 'gauche' to the aryl substituent and rhodium metal. The methylene adjacent to the site undergoing C–H insertion chemistry (carbon 2) is now 'gauche' to the ester and aryl substituents. This approach yields the formation of the minor diastereoisomer. This model indicates that no significant size differentiation exists between the neighboring sp^2 hybridized carbon and sp^3 hybridized methylene which is the origins of the observed poor diastereomeric ratio.

3.4 Results and discussion

Diastereoselectivity had been observed to be one of the areas in which significant improvement was required for intermolecular C-H functionalization. This project describes our efforts to use the new models developed within the group to guide the development of higher levels of diastereocontrol in dirhodium(II)-catalyzed C–H functionalization. For these studies we chose the indane skeleton as a model for investigation. In order to correct the low diastereoselectivity, it was hypothesized, that placement of a bulky chiral substituent at the benzylic C_1 position of 5-methoxyindane could increase the d.r. as well as simultaneously test the new predictive model. We predicted that an enantiomerically pure *tert*-butyldimethyl silyl protected 6-methoxy-1-indanol would serve as a suitable substrate. The substrate was readily synthesized from

6-methoxy-1-indanone *via* Corey's catalytic asymmetric CBS reduction protocol to give the alcohol **5** in 88% yield.[27] **5** was then protected as its *tert*-butyldimethyl silyl (TBS) ether **6** (94% yield, 96% ee) (Scheme 3.8).
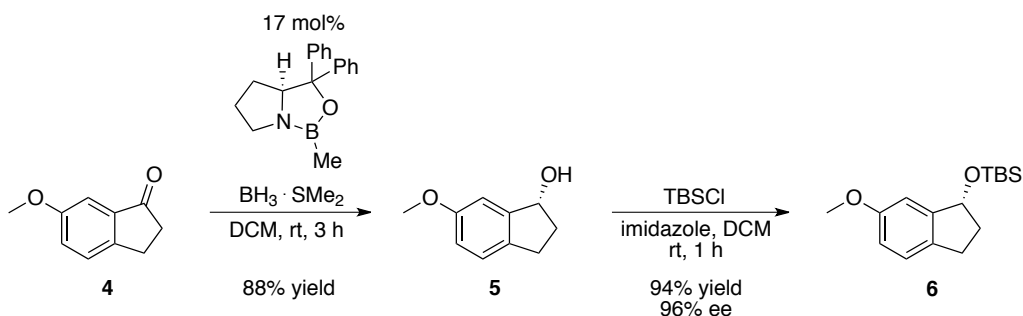
Scheme 3.8 Preparation of TBS protected enantiomer enriched 6-methoxy-1-indanol

With substrate **6** in hand, a benzylic C-H insertion reaction was attempted with phenyldiazoacetate **7** and Rh$_2$(*S*-DOSP)$_4$ (Scheme 3.9).
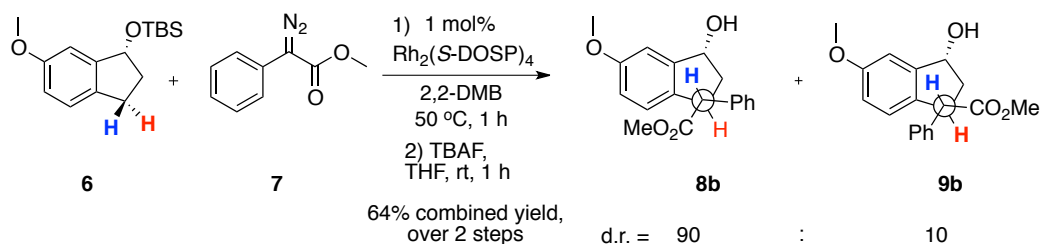
Scheme 3.9 C-H insertion of TBS protected enantiomer enriched 6-methoxy-1-indanol catalyzed by Rh$_2$(*S*-DOSP)$_4$.

Interestingly, the diastereomeric ratio for this reaction dramatically increased to a ratio of 90:10 in favor of diastereomer **8b**. The resulting insertion products were first deprotected by standard silyl deprotection protocols (TBAF, THF, rt) to facilitate isolation. The reaction produced two products **8b** and **9b**. Interestingly, the insertion reaction occurs on the face opposite of the sterically influential OTBS group. The relative stereochemistry for the C-H insertion products was readily determined on the

basis of distinctive chemical shifts in the proton NMR for the methylene protons, which occur as a result of shielding effects from the phenyl group.[28] As shown in Figure 3.7, careful nOe correlation experiments for compound **8b** indicated enhancement between Hb, Hc, and Ha thus establishing the relative stereochemistry. Similarly, correlation studies were conducted on compound **9b**. Irradiation of Hb′ resulted in the enhancement of Ha′ and Hc′. The observed correlations established the relative stereochemistry for product **9b**. Most notably, the nOe experiments indicate C-H functionalization of the benzylic position occurs on the opposite face of the silyl protecting group.
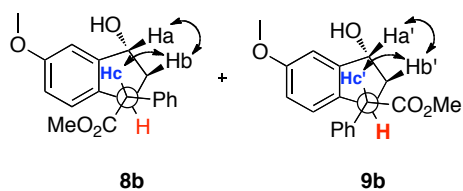
Figure 3.7 1-D nOe correlations.

As shown in Figure 3.8, the substrate rotates by 180° and approaches the carbenoid in such a manner that minimizes any negative steric interference by the OTBS group. The small group (H) is on the same side as the ester, the sp^2 hybridized aromatic carbon (3) is 'gauche' to the aryl substituent and rhodium metal, and the methylene (2) adjacent to the site undergoing C-H insertion chemistry is 'gauche' to the ester and aryl substituents.
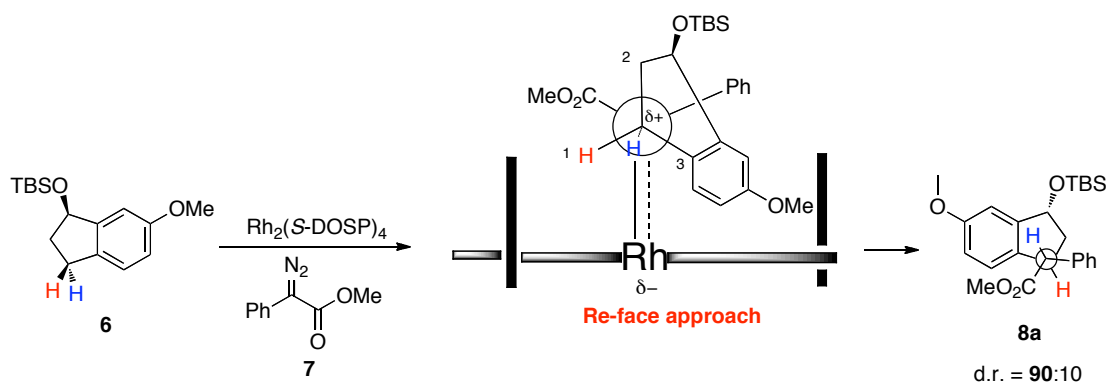
Figure 3.8 Formation of **8a** product *via* the new predictive model.

Based on the predictive model, there is no significant size differentiation between the sp^2 hybridized aromatic carbon (3) and the adjacent methylene (2). As a result, the insertion occurs on the face opposite to the OTBS group. In order to explain the formation of the other diastereomer, we can consult the figure shown below (Figure 3.9).
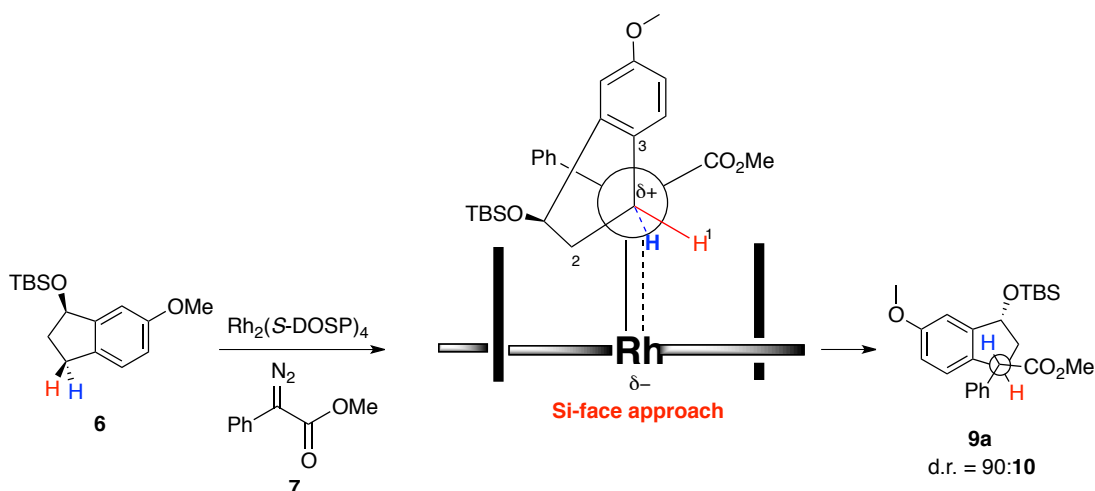
Figure 3.9 Formation of product **9a** *via* the new predictive model.

In this reaction, the substrate trajectory changed considerably. As shown in the predictive model, the substrate is forced to attack the carbenoid from the *si*-face. Thus exposing the hydrogen highlighted in blue towards the reactive carbenoid carbon. From

this approach it is observed that there is potential negative steric interference with the OTBS group and the blocking ligand of the catalyst. This negative interaction accounts for the low formation of diastereomer **9a** and the preference for the formation of diastereoisomer **8a**.

An analogous investigation was conducted however using the catalyst's opposite enantiomer Rh$_2$(R-DOSP)$_4$. This reaction provided valuable insight regarding the match/mismatch reactivity of the substrate and catalyst. The reaction is shown below (Scheme 3.10)
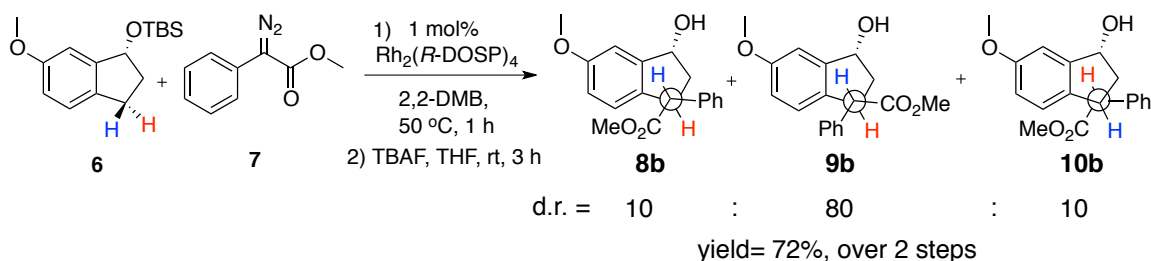
Scheme 3.10 C-H insertion of TBS protected (R)-6-methoxy-1-indanol mediated by Rh$_2$(R-DOSP)$_4$.

Interestingly, three different products are formed in a ratio of 10:80:10. Two of the products are the aforementioned **8b** and **9b** diastereomers. The new insertion product, **10b**, formed as a result of an intermolecular C-H insertion reaction occurring on the same face as the siloxy substituent. The formation of the three products suggests that a mismatched reaction pathway occurred between the chiral substrate and catalyst. The rationalization for the formation of the three insertion products is discussed below. As shown in Figure 3.10, substrate **6** approaches the complexes chiral pocket avoiding any negative steric interference by the OTBS group and the substituents flanking the rhodium

carbenoid. The small group (H) is appropriately positioned on the same side as the ester group.
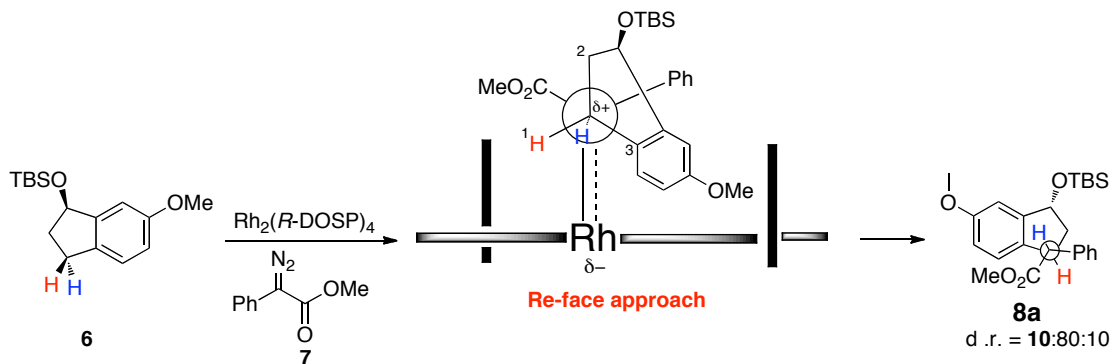
Figure 3.10 Formation of product **8a**.

The sp^2 hybridized carbon (3) is again 'gauche' to the aryl substituent and rhodium metal. The methylene (2) adjacent to the site undergoing C-H insertion chemistry is now 'gauche' to the ester and aryl substituents. For the formation of the other diastereomer **9a**, we can consult the figure shown below (Figure 3.11).
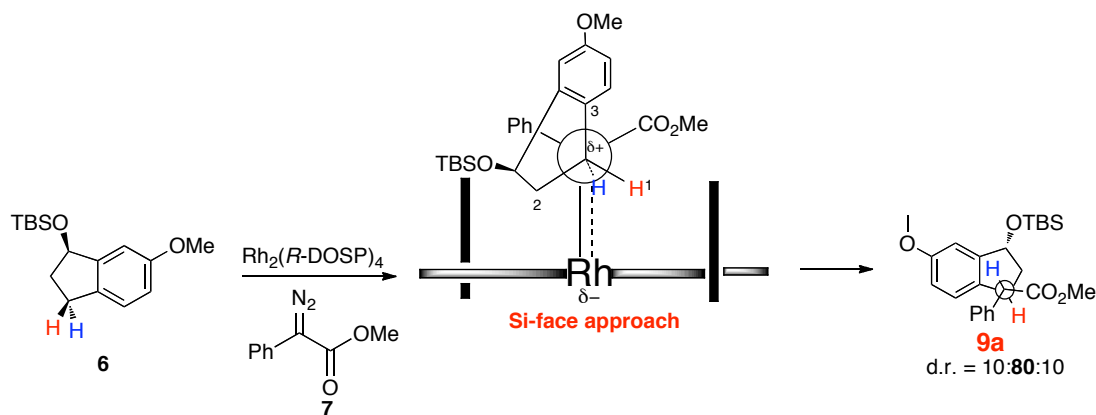
Figure 3.11 Formation of product **9a** *via* the new predictive model.

As previous described, the substrate rotates itself in a manner which exposes the hydrogen highlighted in blue towards the reactive carbenoid carbon and avoids any

negative steric interactions. Notably, the substrate approaches the carbenoid from the *si*-face. Such an approach gives rise to an extremely favorable reaction.
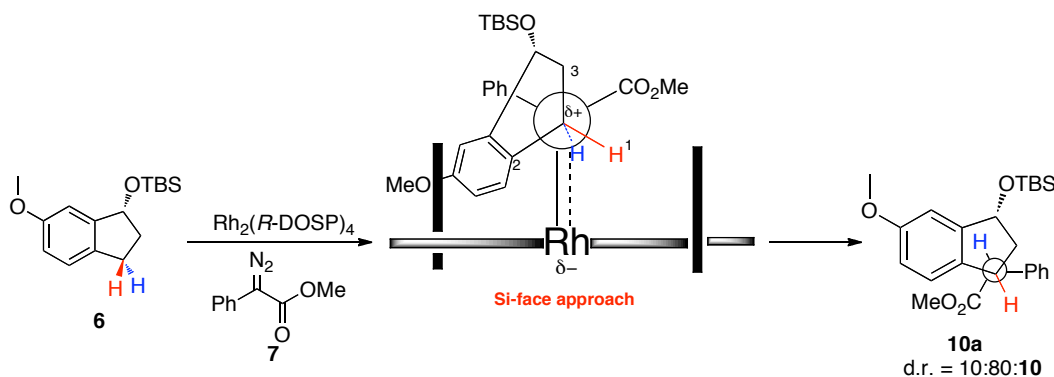
Figure 3.12 Formation of product **10a** *via* the new predictive model.

As shown in Figure 3.12, the substrate approaches the carbenoid such that the benzylic proton, highlighted in blue, undergoes the C-H insertion event. Moreover, the hydrogen highlighted in red (1) is on the same side as the methyl ester of the carbenoid and the methylene (3) adjacent to the site undergoing C-H insertion chemistry is 'gauche' to the ester and aryl substituents. Appropriately, the sp^2 hybridized carbon (2) is gauche to the aryl group and the rhodium center. This approach and orientation affords diastereoisomer **10a**. With the reactivity profiles for substrate **6** established, experiments directed towards a kinetic resolution pathway were investigated by introducing an excess (4 equivalents) of racemic TBS protected 6-methoxy-1-indanol (Scheme 3.11). In this reaction, three diastereomeric products were formed. Moreover, the resulting diastereomeric ratios and enantiomeric excesses indicate that the reaction did not proceed through a kinetic resolution process.
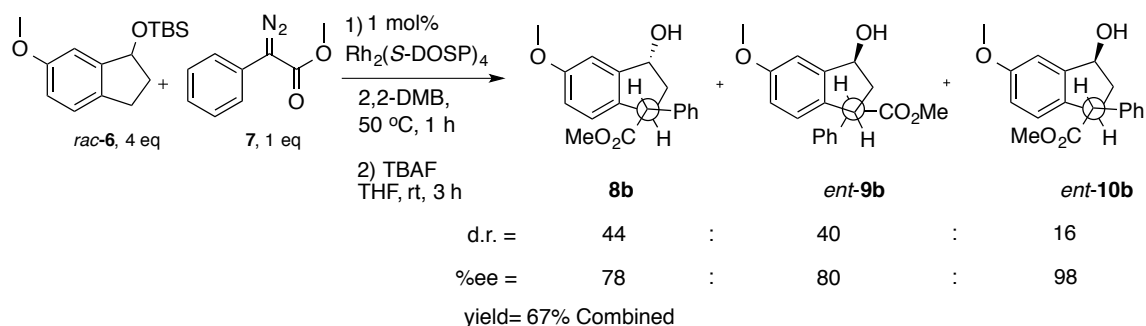
Scheme 3.11 C-H insertion onto racemic TBS protected 6-methoxy-1-indanol mediated

by $Rh_2(S\text{-}DOSP)_4$.

Interestingly, the reaction proceeded through an enantiomer differentiation pathway, where each enantiomer of the substrate reacts with the carbenoid. With an understanding of how enantioenriched substrates behave with enantiopure catalysts, a simple yet informative approximation was derived which predicts the expected diastereomeric ratios and enantiomeric excesses providing a kinetic resolution pathway is absent (Table 3.3).

Entry	Absoute configuration of substrate	Catalyst	Comment	8a(%)	9a(%)	10a(%)
1	R	$Rh_2(S\text{-}DOSP)_4$	observed d.r.	90	10	0
2	R	$Rh_2(R\text{-}DOSP)_4$	observed d.r.	10	80	10
-	R/S	$Rh_2(S\text{-}DOSP)_4$	theoretical d.r.	50	45	5
-	R/S	$Rh_2(S\text{-}DOSP)_4$	theoretical % ee	80	70	>99

Table 3.3 Comparison of observed and theoretical d.r. and % ee for an enantiomer

divergent process.

In the reaction between enantio-enriched substrate **6** and $Rh_2(S\text{-}DOSP)_4$ the formation of diastereomeric ratio for **8a** was observed in 90% (entry 1). Accordingly, in

the presence the same enantio-enriched substrate **6** and the opposite catalyst enantiomer, Rh$_2$(*R*-DOSP)$_4$, diastereomer **9a** formed was observed in 10% ratio. Therefore, the employment of racemic substrate **6** and a single enantiomer of chiral catalyst (in this case, Rh$_2$(*S*-DOSP)$_4$), the theoretical d.r for diastereomer **8a** would be formed in 50% (90%+10%/2). In addition, we can expect an enantiomeric excess of 80% (90%-10%). Comparison of theoretical and experimental results indicate that the percent ratio for **10a** is higher than expected (16%, Scheme 3.11). The use of large excesses of substrate is a common practice for kinetic resolution processes. However, in this case, the unexpected increase for compound **10a** is attributed to the change in polarity of the reaction medium caused by an excess amount of trap. Rh$_2$(*S*-DOSP)$_4$-catalyzed C-H insertion reactions exhibit the best levels of stereoselectivity in non-polar reaction mediums that minimize the net dipole within the *N*-sulfonyl groups.[25] The polarity of the substrate distorts the orientation of the lignds surrounding the rhodium-bound carbene resulting in erosion of diastereoselectivity. In an attempt to rationalize and gain further insight, the reaction was repeated, however, instead of 4 equivalents of racemic substrate, 1 equivalent was used in the presence of 2 equivalents of phenyl diazoacetate (Scheme 3.12). The purpose is to perform the reaction in the same conditions as used in the reaction with enantio-enriched substrates.
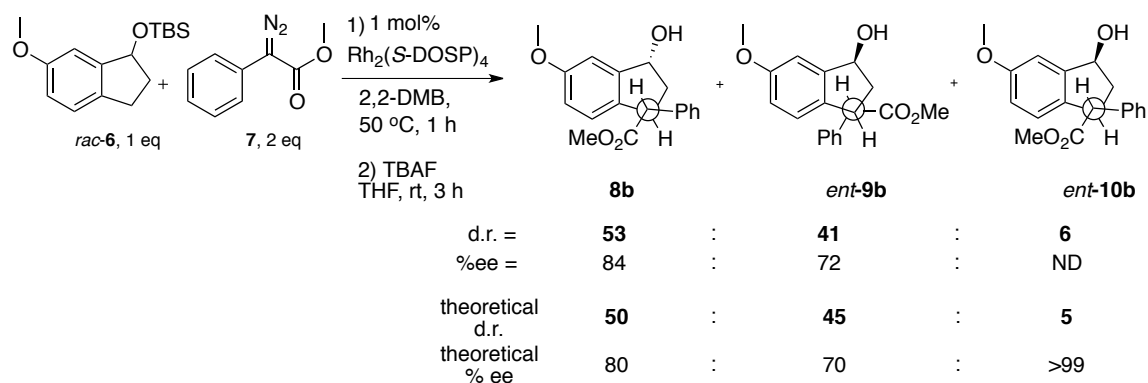
Scheme 3.12 C-H insertion of racemic TBS protected 6-methoxy-1-indanol (1 eq), mediated by Rh$_2$(S-DOSP)$_4$.

As such, the diastereomeric ratios are all in a satisfactory range compared to theoretical values. Notably, the degree of enantioinduction was also in good agreement. With exiting results in hand, efforts to increase the scope of products were also investigated. The study was conducted primarily by varying the size of the silicon protecting group (Scheme 3.13).

Entry	R	I (%)	II (%)
1	TMS	90	10
2	TBS	90	10
3	TBDPS	93	7
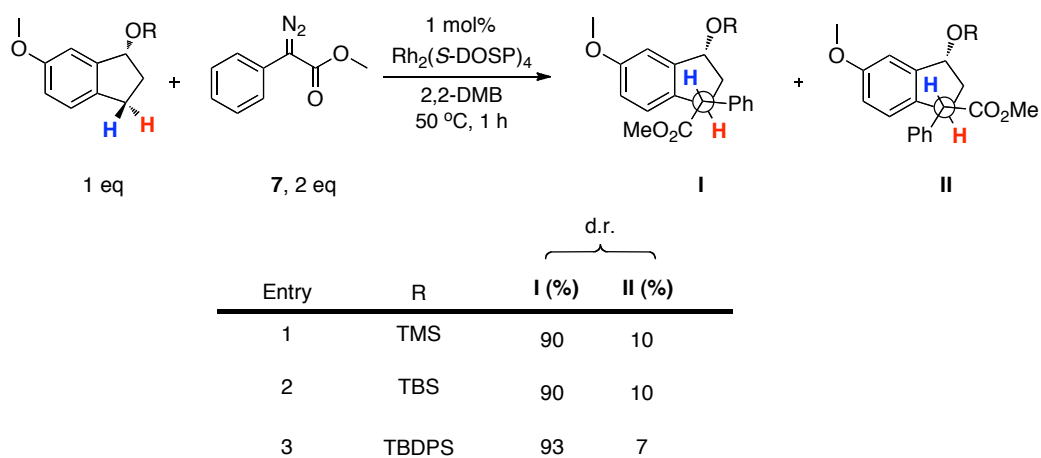
Scheme 3.13 Silicon group steric effects.

Interestingly, the reaction with a sterically lenient silyl group, such as TMS, resulted in the formation of stereoisomers **I** and **II** as 90:10 mixture (Entry 1). In the presence of the sterically demanding group TBDPS, a small increase in diastereoselectivity was observed in favor of compound **I** (93:7, Entry 3). The modification of silyl groups provides an attractive method for the synthesis of promising C-H insertion substrates due to ease of substrate synthesis. However, negligible improvements towards diastereoselection were observed. Lastly, we focused our efforts and compared the effects of chiral and achiral catalysts. As illustrated in Scheme 3.14 and as previously mentioned, $Rh_2(S\text{-DOSP})_4$ results in the formation of stereoisomers **8a** and **9a** as 90:10 mixture (Entry 1).

Entry	L	8a(%)	9a(%)
1	*S*-DOSP	90	10
2	OOct	32	68
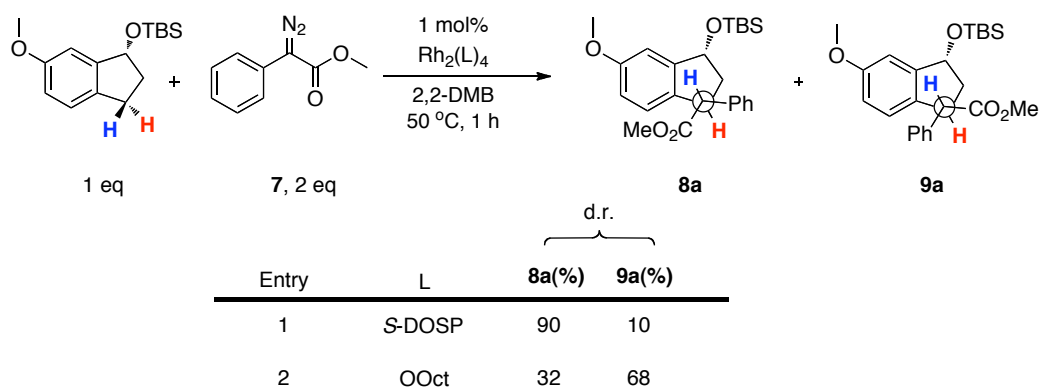
Scheme 3.14 Catalyst effect on diastereoselectivity.

However, in the presence of an achiral catalyst, $Rh_2(OOct)_4$, a fascinating change in stereoselectivity occurred. Interestingly, the diastereoselectivity shifted to a 32:68 mixture in favor of **9a**. This result effectively demonstrates the critical role $Rh_2(S\text{-DOSP})_4$ imparts in the overall reaction. Moreover, this implies that the insertion into the prochiral methylene is substrate controlled and the resulting stereochemistry of the carbenoid carbon is dictated by the chiral catalyst (Equation 3.1).

$$(3.1)$$
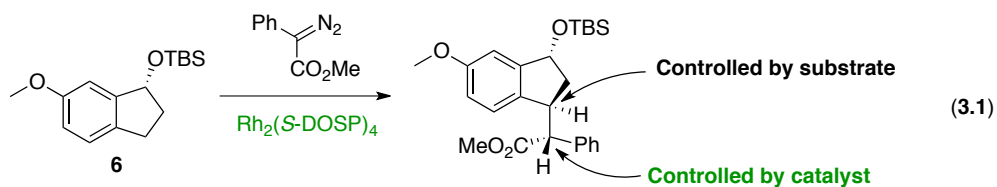
Similar substrate/catalyst control has been observed in the rhodium-catalyzed tandem ylide formation/[2,3]-sigmatropic rearrangement between donor/acceptor carbenoids and chiral allylic alcohols.[29]

3.5 Intermolecular C-H insertion of 7-methoxy-1-tetralol

Previous studies conducted by Dr. Qihui Jin, showed that benzylic C-H insertion of 6-methoxy-1,2,3,4-tetrahydronaphthalene also resulted in moderate levels of diastereoselectivity (Scheme 3.15).[30] This result prompted us to utilize the new predictive model as a design tool and introduce small modifications to the tetrahydronaphthalene core that could potentially enhance the reactions diastereoselectivity issue. After extensive examination of the indane motif and successful increase in diastereomeric ratio by the introduction of a chiral siloxy substituent, similar structural modifications were made to the tetrahydronaphthalene skeleton.
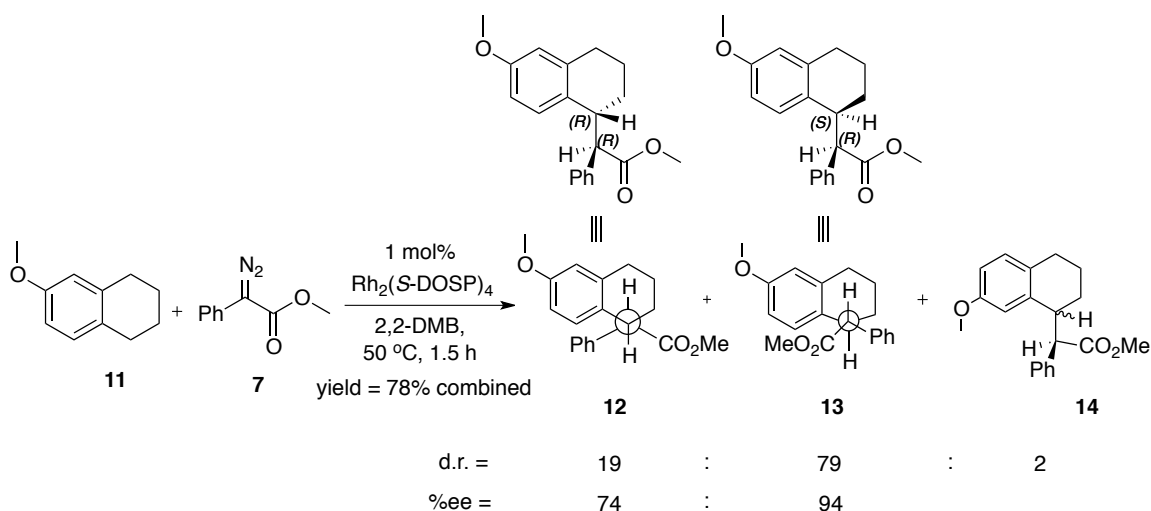
Scheme 3.15 C-H insertion on 6-methoxy-1,2,3,4-tetrahydronaphthalene.

Compound **16** was readily synthesized from 6-methoxy-1-indanone *via* Corey's catalytic asymmetric CBS reduction protocol followed by protection as its *tert*-butyldimethyl silyl (TBS) ether (94% yield, 93%ee, over 2 steps).
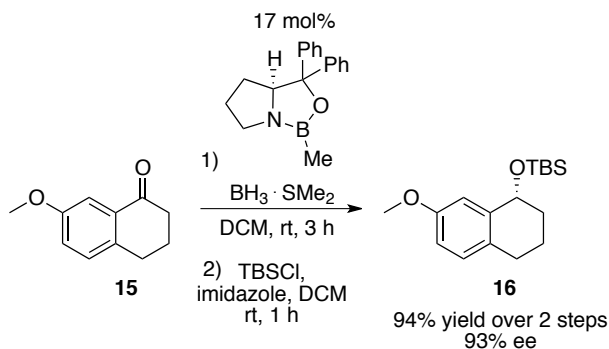
Scheme 3.16 Preparation of TBS protected (*R*)-7-methoxy-1-tetralol.

With substrate **16** in hand, the first reaction investigated was the C-H insertion of the enantiomer enriched substrate with Rh₂(*S*-DOSP)₄ (Scheme 3.17).
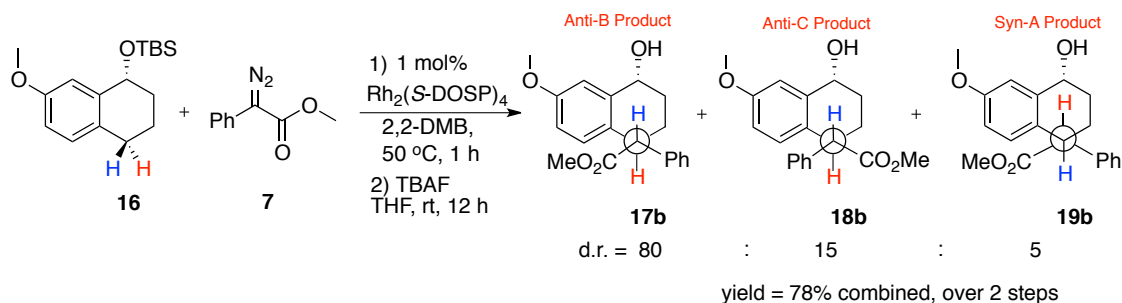
Scheme 3.17 C-H insertion of **16** mediated by Rh$_2$(S-DOSP)$_4$.

Interestingly, the benzylic C-H insertion reaction of (R)-7-methoxy-1-tetralol (**16**) resulted in the formation of reaction three diastereomeric products. The products were formed in a ratio of 80(**17b**):15(**18b**):5(**19b**). Compound **17b** was the major component of the reaction followed by compound **18b**. Removal of the silyl ether, by nucleophilic F$^-$, was necessary in order to separate the three products by column chromatography. Accordingly, we can use the predictive model to account for the formation of the major product.
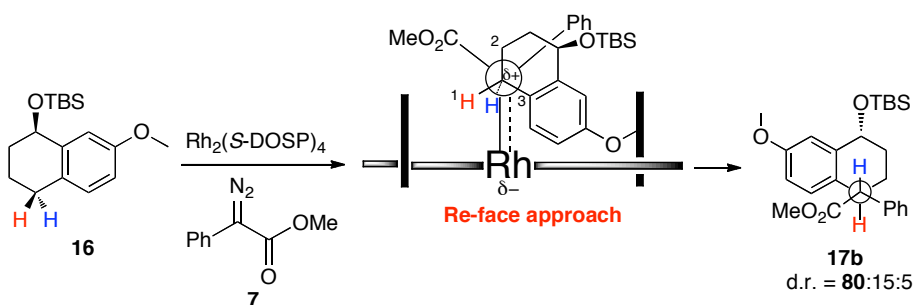
Figure 3.13 Formation of product **17b**.

As shown in Figure 3.13, as the substrate approaches the chiral pocket of the rhodium carbenoid, negative steric interference are minimized by orienting substrate substituents away from the carbenoid substituents. Accordingly, the small group (H) is

situated on the same side as the ester, the sp^2 hybridized aromatic carbon (3) is 'gauche' to the aryl substituent and rhodium metal, and the methylene (2) adjacent to the site undergoing C-H insertion chemistry is also 'gauche' to the ester and aryl substituents. As a result, the insertion occurs on the face opposite to the OTBS group. The absolute stereochemistry for product **17b** and **18b** was determined by X-ray crystallographic analysis (Figure 3.14).
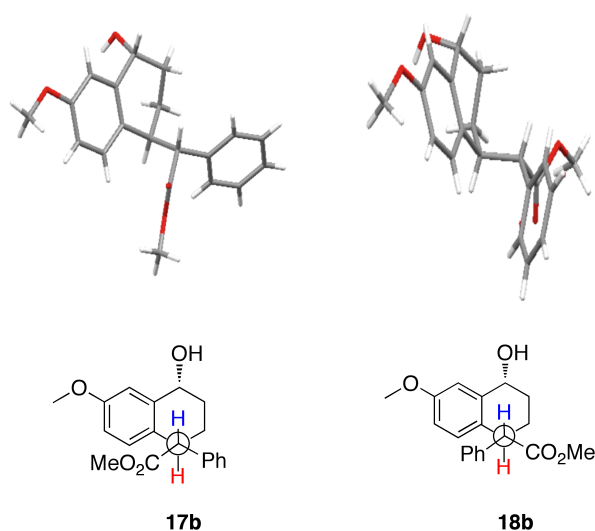
Figure 3.14 X-ray structure of compound **17b** and **18b**.

As previously mentioned with the indanol system, an analogous investigation was conducted using the catalyst's opposite enantiomer Rh$_2$(*R*-DOSP)$_4$. This reaction provided valuable insight regarding the match/mismatch reactivity of the substrate and catalyst (Scheme 3.18).
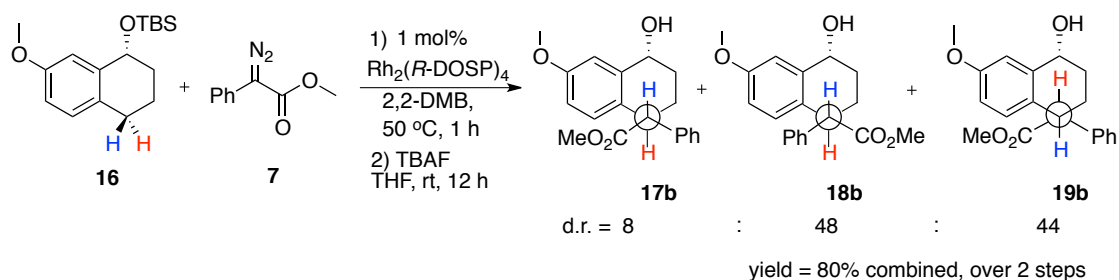
Scheme 3.18 C-H insertion of TBS protected (*R*)-7-methoxy-1-tetralol mediated by Rh₂(*R*-DOSP)₄.

Unfortunately, three diastereomeric products were formed with substantially lower levels of diasteroselectivity. Specifically, the diastereoselectivity for compound **17b** and **18b** switched to a ratio of 8:47 and **18b** and **19b** resulted as the major products of the reaction showing a product ratio of 48:44. These results imply that 1) the reaction of (*R*)-7-methoxy-1-tetralol and Rh₂(*R*-DOSP)₄ occurs through a mismatched pathway and 2) the chiral OTBS substituent minimally participates in controlling the stereochemistry of the benzylic proton undergoing the C-H insertion reaction compared to the 6-methoxy-1-indanol system. As depicted in Figure 3.15, the predictive model provides valuable insight and describes the formation of the major products **18a** and **18b**.
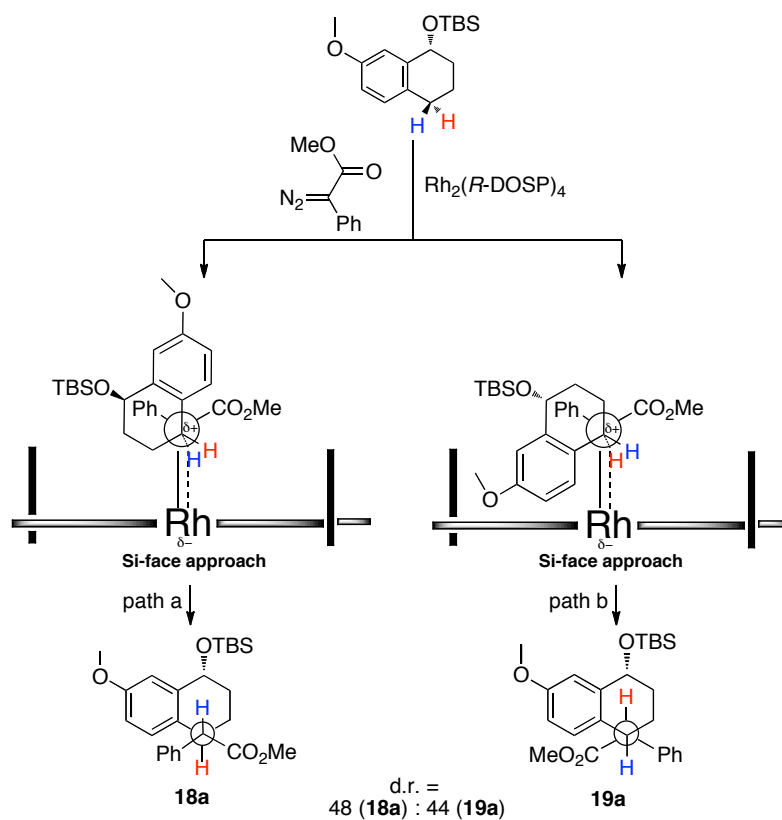
Figure 3.15 Formation of **18a** and **19a** products *via* the new predictive model.

As shown above, the substrate rotates 180° which exposes the hydrogen highlighted in blue towards the reactive carbenoid carbon. Notably, the substrate must approach the carbenoid from the *si*-face to avoid any unfavorable steric interactions between the siloxy group, methylene sites and the carbenoid substituents (path a). This organized trajectory yields the **18a** product. For the formation of product **19a** (path b), the substrate trajectory is such that the benzylic proton, highlighted in red, is facing the reactive carbenoid and thus undergoes the C-H insertion event. This approach is also extremely favorable as no negative steric interactions are encountered by the approaching substrate.

3.6 Conclusion

Achieving effective control over the diastereoselectivity of intermolecular C-H functionalization has long been a goal of this research. Since the development of a new predictive model based upon theoretical and experimental studies we have a greater insight into the factors that influence selectivity in these systems. Using this new model to guide us, we have experimentally demonstrated a significantly increased level of control over the diastereoselectivity of this reaction, going from 57:43 to 90:10 through simple modifications of positions predicted by the model. These studies not only provide invaluable information regarding the factors that control diastereoselectivity, but also provide further proof to the validity of the new predictive model. Notably, for indane substrates, the silicon protecting group predetermines which activated benzylic proton will participate in the insertion event and the chirality of the catalyst controls the stereochemical configuration of the carbenoid carbon. Moreover, in the presence of TBS protected (*R/S*)-6-methoxy-1-indanol, an enantiomer divergent pathway is preferred. Application of the model to the TBS protected (*R*)-7-methoxy-1-tetralol system resulted in the formation of three diastereomeric products. As illustrated in the predictive model, the chiral OTBS group is too remote from the carbenoid to impart any steric bias resulting in no significant enhancement of diastereoselectivity.

3.7 References

(1)   Corey, E. J.; Cheng, X.-m. *The logic of chemical synthesis*; John Wiley: New York, 1989.

(2)   Arndtsen, B. A.; Bergman, R. G.; Mobley, T. A.; Peterson, T. H. *Acc. Chem. Res.* **1995**, *28*, 154-162.

(3)   Davies, H. M. L.; Manning, J. R. *Nature* **2008**, *451*, 417-424.

(4)   Godula, K.; Sames, D. *Science* **2006**, *312*, 67-72.

(5)   Hoffmann, A. W. *Berichte* **1885**, *18*.

(6)   Labinger, J. A.; Bercaw, J. E. *Nature* **2002**, *417*, 507-514.

(7)   Davies, H. M. L. *Angew. Chem., Int. Ed.* **2006**, *45*, 6422-5425.

(8)   Janowicz, A. H.; Bergman, R. G. *J. Am. Chem. Soc.* **1982**, *104*, 352-354.

(9)   Mimoun, H. *Comprehensive Coordination Chemistry*; Pergamon: New York, 1989; Vol. 6.

(10)   J.A. Davies, P. L. W., A. Greenberg, J.F. Leibman *Selective Hydrocarbon Activation*; VCH: New York, 1990.

(11)   Hill, C. L. *Activation and Functionalization of Alkanes*; Wiley: New York, 1989.

(12)   Davies, H. M. L.; Antoulinakis, E. G. *J. Organomet. Chem.* **2001**, *617*, 47-55.

(13)   Chen, H. Y.; Schlecht, S.; Semple, T. C.; Hartwig, J. F. *Science* **2000**, *287*, 1995-1997.

(14)   Murphy, J. M.; Lawrence, J. D.; Kawamura, K.; Incarvito, C.; Hartwig, J. F. *J. Am. Chem. Soc.* **2006**, *128*, 13684-13685.

(15)   Kakiuchi, F.; Murai, S. *Acc. Chem. Res.* **2002**, *35*, 826-834.

(16)   Fujii, N.; Kakiuchi, F.; Yamada, A.; Chatani, N.; Murai, S. *Chemistry Lett.* **1997**, 425-426.

(17)   Wilson, R. M.; Thalji, R. K.; Bergman, R. G.; Ellman, J. A. *Org. Lett.* **2006**, *8*, 1745-1747.

(18)   M.P. Doyle, M. A. M., T. Ye *Modern Catalytic Methods for Organic Syntheis with Diazo Compounds*; Wiley-Interscience: New York, 1998.

(19)   Davies, H. M. L.; Beckwith, R. E. J. *Chem. Rev.* **2003**, *103*, 2861-2903.

(20)   Ye, T.; Mckervey, M. A. *Chem. Rev.* **1994**, *94*, 1091-1160.

(21)   Doyle, M. P.; Forbes, D. C. *Chem. Rev.* **1998**, *98*, 911-935.

(22)   Davies, H. M. L.; Bruzinski, P. R.; Lake, D. H.; Kong, N.; Fall, M. J. *J. Am. Chem. Soc.* **1996**, *118*, 6897-6907.

(23)   Hansen, J.; Autschbach, J.; Davies, H. M. L. *J. Org. Chem.* **2009**, *74*, 6555-6563.

(24)   Davies, H. M. L.; Hansen, T.; Churchill, M. R. *J. Am. Chem. Soc.* **2000**, *122*, 3063-3070.

(25)   Hansen, J.; Davies, H. M. L. *Coord. Chem. Rev.* **2008**, *252*, 545-555.

(26) Jin, Q., University at Buffalo, The State University of New York, 2004.

(27) Corey, E. J.; Bakshi, R. K.; Shibata, S. *J. Am. Chem. Soc.* **1987**, *109*, 5551-5553.

(28) Davies, H. M. L.; Ren, P. D. *Tetrahedron Lett.* **2001**, *42*, 3149-3151.

(29) Li, Z. J.; Parr, B. T.; Davies, H. M. L. *J. Am. Chem. Soc.* **2012**, *134*, 10942-10946.

(30) Davies, H. M. L.; Jin, Q. H.; Ren, P. D.; Kovalevsky, A. Y. *J. Org. Chem.* **2002**, *67*, 4165-4169.

(31) Hansen, T., Ph.D Thesis, SUNY Buffalo, 2000.

3.8 Experimental Section

^{1}H NMR spectra were recorded on either a 400 MHz Varian spectrometer or a 400 or 600 MHz INOVA spectrometer with the sample solvated in $CDCl_3$ unless otherwise noted. Glassware and magnetic stir bars were used as such unless other wise noted. For reactions requiring anhydrous conditions, glassware was either flame dried or oven dried for 24 hours before use. Magnetic stir bars, stainless steel needles, and cannulas where oven dried as well. Plastic syringe barrels and plungers were kept in a glass desiccator with DRIERITE® as desiccant. Acetonitrile, dichloromethane, hexanes, tetrahydrofuran, diethyl ether and toluene were withdrawn from a 6-port solvent purification system. 2,2-dimethylbutane (DMB) was distilled from sodium metal. All reagents received from the following chemical companies and were used as such: Sigma-Aldrich and Acros. Flash chromatography was carried out using silica gel (230-400 mesh). Thin layer chromatography was carried out using EMD TLC Silica Gel 60 F_{254} glass plates. Visualization of TLC plates was done by UV absorbance. Staining was done either with phosphomolybdic acid (PMA) or potassium permanganate ($KMnO_4$) solution followed by heating.
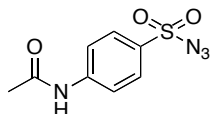
para-**Acetoimidobenzenesulfonyl azide**.   To 2L Erlenmeyer flask, *para*-acetoimidobenzenesulfonyl chloride (311 g, 1.33 mol) was added followed by 800 mL of acetone. Sodium azide (100 g, 1.53 mol) was added to a 1000 mLErlenmeyer flask followed by 400 mL of deionized water. The sodium azide/water mixture was stirred with a stir bar in attempt to efficiently dissolve the azide salt. Once the azide dissolved, the mixture was transferred to a 500 mL pressure equalizing dropping funnel, followed by addition of of deionized water. The azide mixture was added dropwise overnight at room temperature.   Ice water was then added to the mixture which resulted in precipitation of a white solid. This solid was vacuum filtered, washed with cold water, then dried *in vacuo* over P_2O_5 to yield 292 g (91%) of the azide as a white solid. ^{1}H NMR (500 MHz, $CDCl_3$) δ 7.89 (2H, d, J = 9.2 Hz), 7.76 (2H, d, J = 9.2 Hz), 7.59 (1H, m), 2.23 (3H, s); consistent with previously reported data.[31]
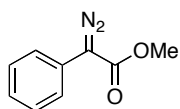
Methyl phenyldiazoacetate (**7**). To a 250 mL round bottom flask, 50 mL of acetonitrile was added followed by addition of methyl 2-phenyl acetate (10 g, 66.6 mmol) and *p*-ABSA (17.6 g, 73.3 mmol). The reaction mixture was cooled to 0 °C with an ice water bath. When the mixture reached the desired temperature, diazabicyclo[5.4.0]undec-7-ene (DBU) (20 g, 133 mmol), was added using a 50 mL pressure equalizing dropping funnel. With stirring, the reaction mixture was allowed to warm to room temperature and stir for 2 hours. The reaction mixture was quenched with saturated ammonium chloride (50 mL) then extracted with diethyl ether (3x100mL). The organic layers were combined and dried over Na_2SO_4.   The solvent was removed under reduced pressure and the residue was triturated with diethyl ether/petroleum ether (1:1). The resulting solid was then dried under reduced pressure to remove residual solvent. ^{1}H-NMR (500 MHz, $CDCl_3$) δ 7.49 (2H, m), 7.40 (2H, m), 7.20 (1H, m), 3.87 (s, 3H); consistent with previously reported data.[31]
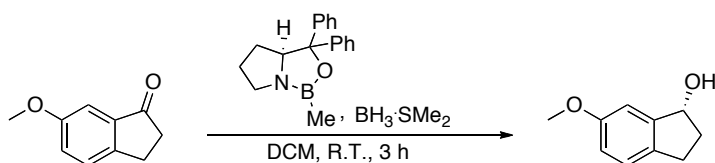
(**R**)-**6-methoxy indanol** (**5**). To a flame dried round bottom flask, (*S*)-(-)-2-Methyl-CBS-oxazaborolidine, Corey's CBS reagent, (582 mg, 2.10 mmol) was added followed by 10 mL DCM. 2M $BH_3 \cdot SMe_2$ (1.38 mL, 18.5 mmol) was added to the CBS/DCM solution. The solution was allowed to stir at room temperature under an argon atmosphere for 30 minutes. 6-methoxy-1-indanone (2.00 g, 12.3 mmol) was dissolved in 11 mL of DCM and added to the CBS mixture by syringe pump over two hours. Once the addition was complete, the mixture was allowed to stir for an additional two hours. The reaction was carefully quenched with 15 mL of MeOH (caution: hydrogen evolution) and the reaction mixture was taken to dryness under reduced pressure. The crude sample was purified by flash chromatography on SiO_2 and 75:25 Hexanes/EtOAc as eluent. 1.78 g (88%) of the tetralol was isolated as a transparent yellow oil. Rf = 0.29 (66:33 hexanes:EtOAc); $[\alpha]_D^{20}$: -14.5 (*c*0.68, $CHCl_3$); 1H NMR (600 MHz; $CDCl_3$) δ 7.15 (d, 1H, *J* = 9 Hz), 6.96 (d, *J* = 2.4 Hz, 1H), 6.82 (dd, *J* = 3.9 Hz, 1H), 5.20 (t, *J* = 5.4 Hz, 1H), 3.81 (s, 3H,), 2.99-2.95 (m, 1H,), 2.78-2.72 (m, 1H,), 2.45-2.49 (m, 1H,), 1.97-1.91 (m, 1H,), 1.75 (1H,); 13C NMR (100 MHz, CDCl3) δ 158.8, 146.5, 135, 125.4, 114.8, 108.9, 76.3, 55.4, 36.3, 28.9; IR (neat): 3350, 2938, 2851, 1489; HRMS- m/z 163.0754 $(M+H)^+$ requires 163.0753); HPLC analysis: (OD-H, 99.5 % hexanes, 0.5 ml/min), UV: 254 nm, retention time of 8.17 min (minor) and 10.24 min (major), 96 % ee.
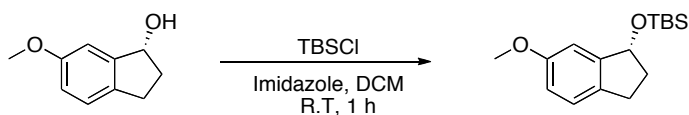
(*R*)-TBS-6-methoxy indanol (**6**). To a 20 mL scintillation vial, (*R*) 6-methoxy indanol (446 mg 2.71 mmol) was added followed by 5 mL of DCM. Imidazole (369 mg 5.43 mmol) was added in one portion and allowed to stir for 5 minutes. TBSCl (614 mg, 4.07 mmol) was added in one portion. The reaction was left to stir for 1 hour under an atmosphere of argon. The reaction was quenched with deionized water (ca. 10 mL). The mixture was diluted with 6 mL of water followed by 6 mL of DCM. The organic product was extracted with DCM (3 x 15 mL). The organic layers were combined, washed with brine, and dried with MgSO$_4$. The drying agent was removed by vacuum filtration through a glass frit and rinsed with DCM. The organic solvent was removed under reduced pressure. The crude sample was purified by flash chromatography on SiO$_2$ and 98:2 Hexanes/Et$_2$O as eluent.   708 mg (94 %) of (*R*)-TBS-6-methoxy indanol was isolated as a clear colorless oil. Rf = 0.2 (98:2 hexanes:diethyl ether); 1H NMR (600 MHz; CDCl$_3$) δ 7.10 (d, 1H, *J* = 8.4 Hz), 6.85 (d, *J* = 1.8 Hz, 1H), 6.77 (dd, *J* = 2.4, 8.4 Hz, 1H), 5.22 (t, *J* = 7.2 Hz, 1H), 3.80 (s, 3H), 2.92-2.78 (m, 1H), 2.72-2.67 (m, 1H), 2.46-2.41 (m, 1H), 1.96-1.87 (m, 1H), 0.96 (s, 9H), 0.18 (s, 3H), 0.15 (s, 3H); 13C NMR (100 MHz, CDCl$_3$) δ 159, 147.4, 134.6, 125.4, 113.9, 109.3, 76.9, 55.6, 37.3, 28.9, 26.1, 18.5, -4.1, -4.4; IR (neat): 2952, 2928, 2854; HRMS- m/z 279.1781 (M+H)$^+$ requires 279.1774); (96% enantiomeric excess as determined by HPLC). HPLC: isopropyl alcohol–hexanes (0.5:99.5), Chiralcel OD-H chiral column, flow rate 0.5 mL/min, UV-detection 256 nm; t$_r$ (*ent*- TBS-6-methoxy indanol) = 8.176 min, t$_r$ (TBS-6-methoxy indanol) = 10.24 min.

Enantioselective benzylic C-H insertion of (R/S)-TBS-6-methoxy indanol.

d.r. =   44   :   40   :   16

To a flame dried round bottom flask (*R/S*)-TBS-6-methoxy indanol (1.58 g, 5.58 mmol) and Rh$_2$(*S*-DOSP)$_4$ (27 mg, 0.0142 mmol) was added followed by 5.7 mL of degassed 2,2-dimethylbutane. The solution was heated to 50 °C. Phenyl diazoacetate (250 mg, 1.42 mmol) was dissolved in 22 mL of 2,2-dimethylbutane. The diazo solution was added to the substrate by syringe pump over a period of 1 hour. Once the addition is complete, the solvent was removed *in vacuo* and the residue was exposed to silyl deprotection conditions.

General procedure:

Silyl deprotection benzylic C-H insertion products.
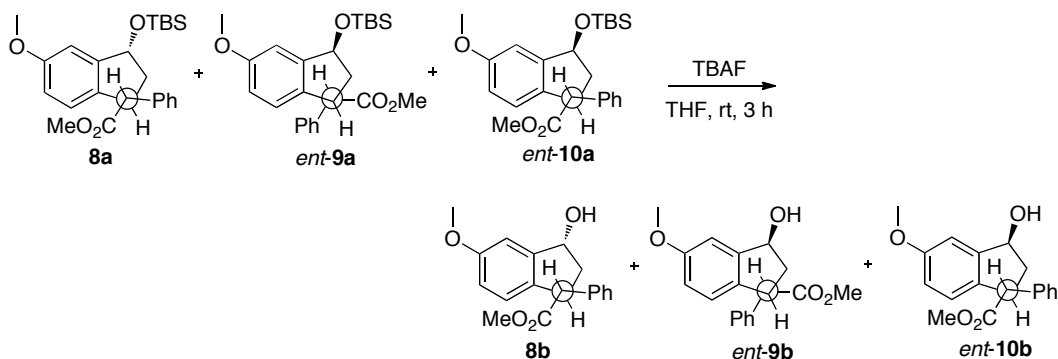
To a round bottom flask containing the crude residue was added 24 mL of anhydrous THF. Tetrabutylammonium fluoride trihydrate (664 mg, 2.54 mmol) was added in one portion. The solution was allowed to stir for 3 hours. The reaction was quenched with deionized water (ca. 20 mL). The mixture was diluted with 20 mL of water followed by 40 mL of THF. The organic product was extracted with Et_2O (3 x 70 mL). The organic layers were combined, washed with brine, and dried with $MgSO_4$. The drying agent was removed by vacuum filtration through a glass frit and rinsed with THF. The organic solvent was removed under reduced pressure. The crude sample was purified by flash chromatography on SiO_2 and 83:17 Hexanes/EtOAc as eluent. 299 mg (67 %) combined yield over 2 steps as a yellow oil. **8b**, *ent*-**9b**, and *ent*-**10b** can be partially separated.
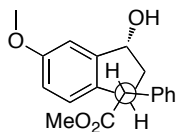
(*R*)-methyl 2-((1*S*,3*R*)-3-hydroxy-5-methoxy-2,3-dihydro-1*H*-inden-1-yl)-2-phenylacetate (8b): Rf = 0.30 (2:1 Hexanes/Ethyl Acetate); $[\alpha]_D^{20}$: -53.3 (c0.9, CHCl$_3$); ^{1}H NMR (400 MHz; CDCl$_3$) δ 1.62 (d, 1H, *J* = 7.6 Hz), 1.85 (ddd, J = 5.6, 7.6, 13.6 Hz, 1H), 2.09 (ddd, *J* = 3.6, 6.8, 13.2 Hz, 1H), 3.43 (d, *J* = 10.4 Hz, 1H), 3.67 (s, 3H), 3.81 (s, 3H), 4.04 (ddd, *J* = 3.6, 8.0, 14 Hz, 1H), 5.07 (ddd, *J* = 6.9, 6.8, 20.4 Hz, 1H), 6.83 (dd, *J* = 2.4, 8 Hz, 1H), 6.93 (d, *J* = 2.4 Hz, 1H), 7.14 (d, *J* = 8.4 Hz, 1H), 7.33-7.27 (m, 5H); ^{13}C NMR (150 MHz, CDCl$_3$) δ 174.2, 159.8, 147, 137.8, 136.2, 128.8, 128.6, 127.7, 125.5, 115.2, 109.1, 74.6, 57.2, 55.5, 52.1, 44.8, 41.1; IR (neat): 3382, 3028, 2949, 1731; HRMS m/z 313.1434 (M+H)$^+$ requires 313.1434; (78% enantiomeric excess as determined by HPLC). HPLC: isopropyl alcohol–hexanes (10:90), Chiralcel OD-H chiral column, flow rate 1 mL/min, UV-detection 280 nm; t$_r$ (*ent*-**8b**) = 13.49 min, t$_r$ (**8b**) = 14.25 min.
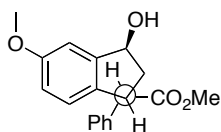
(*R*)-methyl 2-((1*R*,3*S*)-3-hydroxy-5-methoxy-2,3-dihydro-1*H*-inden-1-yl)-2-phenylacetate (*ent*-9b): Rf = 0.22 (Hexanes/Ethyl Acetate 2:1); mp 111-112°C; $[\alpha]_D^{20}$: +83.30 (c0.8, CHCl$_3$); ^{1}H NMR (400 MHz; CDCl$_3$) δ 1.71 (d, 1H, *J* = 7.2 Hz), 2.24 (ddd, *J* = 6, 8, 13.6 Hz,1H), 2.36 (ddd, *J* = 3.6, 6.4, 13.2 Hz, 1H), 3.46 (d, *J* = 10.8 Hz, 1H), 3.69 (s, 3H), 3.75 (s, 3H), 3.98 (ddd, *J* = 3.6, 8, 14.4 Hz, 1H), 5.20 (ddd, *J* = 6.4, 19.6 Hz, 1H), 6.09 (d, *J* = 8.4 Hz, 1H), 6.52 (dd, *J* = 2.4, 8.8 Hz, 1H), 6.89 (d, *J* = 2.4 Hz, 1H), 7.32-7.23 (m, 5H); ^{13}C NMR (100 MHz, CDCl$_3$) δ 173.3, 159.7, 147, 137.6, 135.1, 129.1, 128.7, 126.4, 114.6, 108.7, 74.8, 57.4, 55.5, 45.4, 42.7; IR (Neat): 3217, 2932, 1725; HRMS m/z 313.1435 (M+H)$^+$ requires 313.1434); (80% enantiomeric excess as determined by HPLC). HPLC: isopropyl alcohol–hexanes (10:90), Chiralcel OJ-H chiral column, flow rate 1 mL/min, UV-detection 280 nm; t$_r$ (*ent*-9b) = 18.85 min, t$_r$ (9b) = 14.29 min.
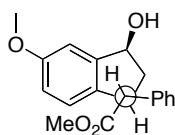
(*R*)-methyl 2-((1*S*,3*S*)-3-hydroxy-5-methoxy-2,3-dihydro-1*H*-inden-1-yl)-2-phenylacetate (*ent*-10b): Rf = 0.30 (2:1 Hexanes/Ethyl Acetate); mp 108-109°C; $[\alpha]_D^{20}$: 186 (c0.2, CHCl$_3$); ^{1}H NMR (400 MHz; CDCl$_3$) δ 1.58 (bs, 1H), 1.59-1.53 (m, 1H), 2.28 (ddd, *J* = 7.2, 14 Hz, 1H), 3.71 (s, 3H), 3.75 (d, *J* = 10.4 Hz, 1H), 3.81 (s, 3H), 3.86-3.83 (m, 1H), 5.02 (d, *J* = 5.2 Hz, 1H), 6.84 (dd, *J* = 2.4, 8.4 Hz, 1H), 6.93 (d, *J* = 2.4 Hz, 1H), 7.11 (d, *J* = 8 Hz, 1H), 7.34 (m, 5H); ^{13}C NMR (100 MHz, CDCl$_3$) δ 174.4, 159.8, 146.8, 137.9, 136.6, 128.8, 127.7, 125.4, 115.4, 109.2, 74.8, 58, 55.6, 52.2, 44.8, 40.5; IR (Neat): 3441, 3029, 2950, 1732; HRMS m/z 313.1437 (M+H)$^+$ requires 313.1434); (98% enantiomeric excess as determined by HPLC). HPLC: isopropyl alcohol–hexanes (10:90), Chiralcel OJ-H chiral column, flow rate 1 mL/min, UV-detection 280 nm; t$_r$ (*ent*-10b) = 15.32 min, t$_r$ (10b) = 13.31 min.
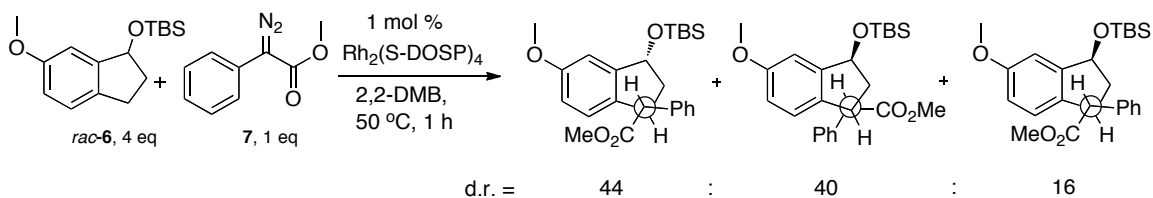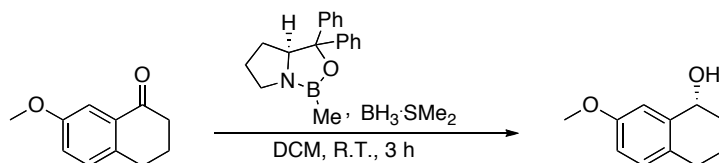
(*R*)-7-methoxy tetralol. To a flame dried round bottom flask, (*S*)-(-)-2-Methyl-CBS-oxazaborolidine, Corey's CBS reagent, (554 mg, 2.00 mmol) was added followed by 10 mL DCM. 2M $BH_3 \cdot SMe_2$ (1.26 mL, 17.0 mmol) was added to the CBS/DCM solution. The solution was allowed to stir at room temperature under an argon atmosphere for 30 minutes. 7-methoxy-1-tetralone (2.00g, 11.4 mmol) was dissolved in 9 mL of DCM and added to the CBS mixture by syringe pump over two hours. Once the addition was complete, the mixture was allowed to stir for an additional two hours. The reaction was carefully quenched with 15 mL of MeOH (caution: hydrogen evolution) and the reaction mixture was taken to dryness under reduced pressure. The crude sample was not purified and used as such. ^{1}H NMR (400 MHz; CDCl$_3$) δ 2.02-1.72 (m, 5H), 2.78-2.63 (m, 2H), 3.78 (s, 3H), 4.74-4.73 (m, 1H), 6.78 (dd, *J* = 2.8, 8.4 Hz, 1H), 6.99 (d, *J* = 2.8 Hz, 1H), 7.02 (d, *J* = 8.8 Hz, 1H).
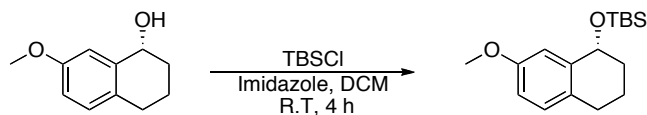
(R)-TBS-7-methoxy tetralol (16). To a 20 mL scintillation vial, (R) 6-methoxy indanol (485 mg, 2.72 mmol) was added followed by 5 mL of DCM. Imidazole (370 mg, 5.44 mmol) was added in one portion and allowed to stir for 5 minutes. TBSCl (620 mg, 4.11 mmol) was added in one portion. The reaction was left to stir for 4 hour under an atmosphere of argon. The reaction was quenched with deionized water (ca. 10 mL). The mixture was diluted with 6 mL of water followed by 6 mL of DCM. The organic product was extracted with DCM (3 x 15 mL). The organic layers were combined, washed with brine, and dried with $MgSO_4$. The drying agent was removed by vacuum filtration through a glass frit and rinsed with DCM. The organic solvent was removed under reduced pressure. The crude sample was purified by flash chromatography on SiO_2 and 98:2 Hexane/Et_2O as eluent. 744 mg (94% over 2 steps) of (R)-TBS-6-methoxy indanol was isolated as a clear colorless oil. $[\alpha]_D^{20}$: -27.6 (c0.58, $CHCl_3$); Rf = 0.39 (50:1 hexanes:diethyl ether); 1H NMR (400 MHz; $CDCl_3$) δ 6.99-6.96 (m, 2H), 6.74 (dd, J = 3.2, 8.4 Hz, 1H), 4.77-4.74 (m, 1H), 3.78 (s, 3H), 2.78-2.62 (m, 2H), 2.04-1.92 (m, 2H), 1.79-1.69 (m, 2H), 0.96 (s, 9H), 0.19 (s, 3H), 0.16 (s, 3H); 13C NMR (100 MHz, CDCl3) δ 157.9, 141.2, 129.6, 128.9, 113.7, 111.9, 69.8, 55.2, 33.2, 28.4, 26, 20.4, 18.3, -3.9, -4.4; IR (neat): 2928, 2855, 1499; HRMS- m/z 315.1751 $(M+H)^+$ requires 315.175); (93% enantiomeric excess as determined by HPLC). HPLC: isopropyl alcohol–hexanes (0.5:99.5), Chiralcel OD-H chiral column, flow rate 0.5 mL/min, UV-detection 256 nm; t_r (*ent*-**16**) = 7.925 min, t_r (**16**) = 9.763 min.

General procedures:

Enatioselective benzylic C-H insertion of (R)-TBS-7-methoxy tetralol.
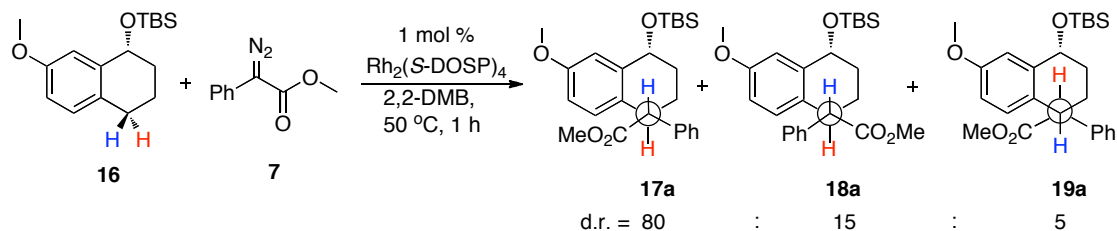
To a flame dried round bottom flask (*R*)-TBS-7-methoxy tetralol (500 mg, 1.71 mmol) and Rh$_2$(*S*-DOSP)$_4$ (32 mg, 0.0171 mmol) was added followed by 1.8 mL of degassed 2,2-dimethylbutane. The solution was heated to 50 ^{o}C. Phenyl diazoacetate (602 mg, 3.42 mmol) was dissolved in 30 ml of 2,2-dimethylbutane. The diazo solution was added to the substrate by syringe pump over a period of 1 hour. Once the addition is complete, the solvent was removed *in vacuo* and the residue was exposed to silyl deprotection conditions.

Silyl deprotection benzylic C-H insertion products.
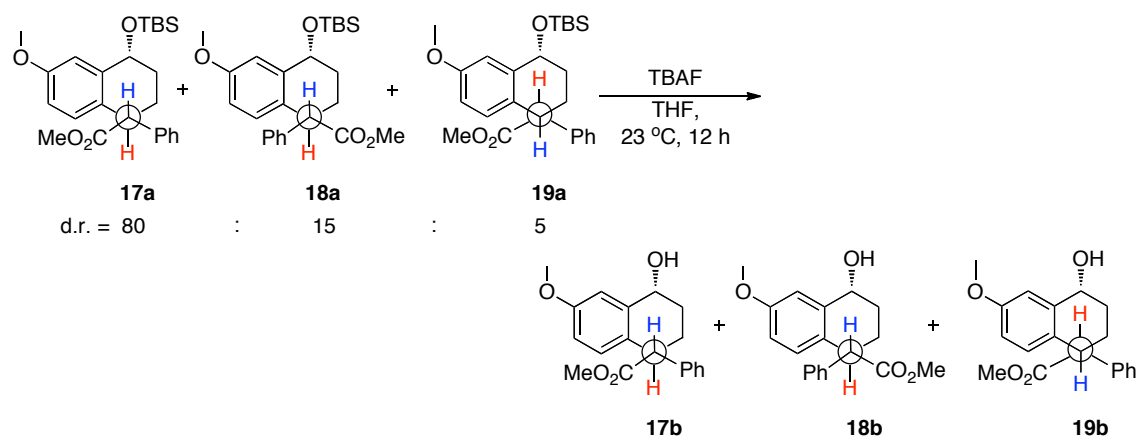
To a round bottom flask containing the crude residue was added 33 mL of anhydrous THF. Tetrabutylammonium fluoride trihydrate (888 mg, 3.40 mmol) was added in one portion. The solution was allowed to stir for 3 hours. The reaction was quenched with deionized water (ca. 20 mL). The mixture was diluted with 20 mL of water followed by 30 mL of Et$_2$O. The organic product was extracted with Et$_2$O (3 x 100 mL). The organic layers were combined, washed with brine, and dried with MgSO$_4$. The drying agent was removed by vacuum filtration through a glass frit and rinsed with THF. The organic solvent was removed under reduced pressure. The crude sample was purified by flash chromatography on SiO$_2$ and 5:1 Hexanes/EtOAc as eluent. 435 mg (78%) of the product was isolated as a yellow oil. **17b**, **18b**, **19b**, and can be partially separated.
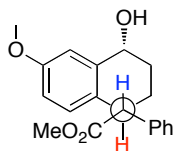
(_R_)-methyl 2-((1_S_,4_R_)-4-hydroxy-6-methoxy-1,2,3,4-tetrahydronaphthalen-1-yl)-2-phenylacetate (17b): Rf = 0.25 (66:33 Hexanes/Ethyl Acetate); mp 115-125 °C ; ^{1}H NMR (400 MHz; CDCl$_3$) δ 1.377-1.434 (m, 1H), 1.758-1.676 (m, 1H), 1.887-1.801 (m, 2H), 2.037-1.950 (s, 3H), 3.599-3.552 (m, 1H), 3.635 (d, _J_ = 10.8 Hz, 1H), 3.802 (s, 3H), 4.712 (s, 1H), 6.684 (dd, _J_ = 2.8, 8.4 Hz, 1H), 6.950 (d, _J_ = 2.8 Hz, 1H), 7.170 (d, _J_ = 8.8 Hz, 1H), 7.419-7.211 (m, 5H); ^{13}C NMR (100 MHz, CDCl$_3$) δ 20.229, 27.3, 39.9, 52, 55.4, 57.2, 67.3, 114, 114.4, 127.8 (2 C), 128.9 (2C), 130.5 (2C), 137.6 (2C), 139.7, 158.8, 174.6; IR (neat): 3511, 2940, 2890, 1723, 1228; HRMS- m/z 309.14822 (M+H)$^+$ requires 309.1485.
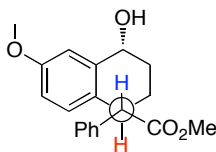
(_S_)-methyl 2-((1_S_,4_R_)-4-hydroxy-6-methoxy-1,2,3,4-tetrahydronaphthalen-1-yl)-2-phenylacetate (18b): Rf = 0.21 (66:33 Hexanes/Ethyl Acetate); mp 132-134 °C ; ^{1}H NMR (400 MHz; CDCl$_3$) δ 1.630 (d, 1H, _J_ = 5.6 Hz), 1.909-1.817 (m, 2H), 2.268-2.075 (m, 2H), 3.427-3.380 (m, 1H), 3.685 (s, 3H), 3.712 (d, _J_ = 10 Hz, 1H), 3.734 (s, 3H), 4.761 (d, _J_ = 4.4 Hz, 1H), 6.099 (d, _J_ = 8.4 Hz, 1H), 6.373 (dd, _J_ = 2.8, 8.4 Hz, 1H), 6.909 (d, _J_ = 2.8 Hz, 1H), 7.253-7.153 (m, 5H); ^{13}C NMR (100 MHz, CDCl$_3$) δ 22.5, 28.4, 41.4, 52.1, 55.3, 56.6, 67.7, 113.1, 113.3, 127.6, 128.5 (2C), 128.9 (2C), 129.3, 131, 137.5, 140, 158.5, 173.9; IR (neat): 3143, 3028, 2949, 1727, 1265; HRMS- m/z 309.14822 (M+H)$^+$ requires 309.14852.
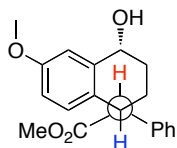
(*S*)-methyl 2-((1*R*,4*R*)-4-hydroxy-6-methoxy-1,2,3,4-tetrahydronaphthalen-1-yl)-2-phenylacetate (19b): Rf = 0.29 (66:33 Hexanes/Ethyl Acetate); ^{1}H NMR (400 MHz; CDCl$_3$) δ 1.495 (m, 1H), 1.794-1.601 (m, 3H), 1.973-1.936 (m, 1H), 3.541-3.515 (m, 1H), 3.560 (s, 3H), 3.814 (s, 3H), 3.861 (d, *J* = 10.8 Hz, 1H), 4.722 (s, 1H), 6.760 (dd, *J* = 2.8, 8.8 Hz, 1H), 7.090 (d, *J* = 2.8 Hz, 1H), 7.191 (d, *J* = 8.4 Hz, 1H), 7.421-7.289 (m, 5H); ^{13}C NMR (100 MHz, CDCl$_3$) δ 23.69, 28.8, 40, 52, 55.4, 57.7, 69.5, 112.4, 114, 127.7, 128.8 (2C), 128.9 (2C), 129.9, 130.8, 137.7, 140.7, 158.9, 174.7; IR (neat): 3407, 3027, 2948, 2867, 1731, 1273; HRMS- m/z 309.14859 (M+H)$^+$ requires 309.14852.
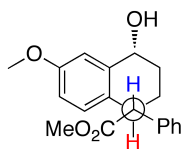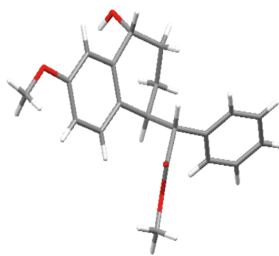
17b

Table 1. Crystal data and structure refinement for PEG0277M.

Identification code   PEG0277M

Empirical formula   C20 H22 O4

Formula weight   326.38

Temperature   173(2) K

Wavelength   1.54178 Å

Crystal system   Orthorhombic

Space group   P2(1)2(1)2(1)

Unit cell dimensions   a = 8.2781(4) Å   á= 90°.

    b = 9.2449(4) Å   â= 90°.

    c = 21.9744(10) Å   ã = 90°.

Volume 1681.71(13) Å^3

Z   4

Density (calculated)   1.289 Mg/m^3

Absorption coefficient   0.720 mm^{-1}

F(000)   696

Crystal size   0.40 x 0.18 x 0.17 mm^3

Theta range for data collection   4.02 to 66.34°.

Index ranges   -9<=h<=9, -10<=k<=10, -26<=l<=21

Reflections collected   12637

Independent reflections   2778 [R(int) = 0.0303]

Completeness to theta = 66.34°   98.4 %

Absorption correction   Semi-empirical from equivalents

Max. and min. transmission   0.8873 and 0.7615

Refinement method   Full-matrix least-squares on F^2

Data / restraints / parameters   2778 / 0 / 197

Goodness-of-fit on F^2 1.085

Final R indices [I>2sigma(I)]   R1 = 0.0363, wR2 = 0.0865

R indices (all data)   R1 = 0.0418, wR2 = 0.0882

Absolute structure parameter   0.1(2)

Extinction coefficient   0.0069(4)

Largest diff. peak and hole 0.256 and -0.209 e.Å^{-3}

Table 2. Atomic coordinates (x 10^4) and equivalent isotropic displacement parameters (Å^2x 10^3) for PEG0277M. U(eq) is defined as one third of the trace of the orthogonalized U^{ij} tensor.

_____

	x	y	z	U(eq)
C(1)	2843(2)	6314(2)	1949(1)	32(1)
C(2)	3456(2)	6153(3)	2600(1)	37(1)
C(3)	2637(2)	4893(3)	2917(1)	35(1)
C(4)	826(2)	5169(2)	2985(1)	30(1)
C(5)	76(1)	5548(2)	2362(1)	29(1)
C(6)	-1567(1)	5325(1)	2270(1)	31(1)
C(7)	-2261(1)	5659(2)	1711(1)	31(1)
C(8)	-1313(1)	6215(2)	1244(1)	30(1)
C(9)	329(1)	6438(2)	1336(1)	30(1)
C(10)	1024(1)	6104(2)	1895(1)	29(1)
C(11)	454(2)	6398(2)	3452(1)	30(1)
C(12)	1405(2)	6264(1)	4052(1)	29(1)
C(13)	2373(2)	7412(1)	4236(1)	37(1)
C(14)	3268(2)	7306(1)	4770(1)	42(1)
C(15)	3196(2)	6053(2)	5118(1)	40(1)
C(16)	2227(2)	4906(1)	4934(1)	36(1)
C(17)	1332(1)	5011(1)	4400(1)	33(1)
C(18)	-1337(2)	6498(2)	3581(1)	33(1)
C(19)	-3595(3)	5332(4)	4026(1)	59(1)
C(20)	-3572(3)	6472(3)	575(1)	46(1)
O(1)	3658(2)	5324(2)	1548(1)	39(1)
O(2)	-1873(2)	6527(2)	667(1)	39(1)
O(3)	-2170(2)	7534(2)	3471(1)	50(1)
O(4)	-1915(2)	5294(2)	3838(1)	42(1)

_____

Table 3.   Bond lengths [Å] and angles [°] for PEG0277M.

_____

C(1)-O(1)   1.438(2)

C(1)-C(10)   1.523(2)

C(1)-C(2)   1.525(3)

C(1)-H(1)   1.0000

C(2)-C(3)   1.517(3)

C(2)-H(2A)   0.9900

C(2)-H(2B)   0.9900

C(3)-C(4)   1.528(3)

C(3)-H(3A)   0.9900

C(3)-H(3B)   0.9900

C(4)-C(5)   1.544(2)

C(4)-C(11)   1.562(3)

C(4)-H(4)   1.0000

C(5)-C(6)   1.3900

C(5)-C(10)   1.3900

C(6)-C(7)   1.3900

C(6)-H(6)   0.9500

C(7)-C(8)   1.3900

C(7)-H(7)   0.9500

C(8)-O(2)   1.3802(15)

C(8)-C(9)   1.3900

C(9)-C(10)   1.3900

C(9)-H(9)   0.9500

C(11)-C(18)   1.512(3)

C(11)-C(12)   1.5402(19)

C(11)-H(11)   1.0000

C(12)-C(13)   1.3900

C(12)-C(17)   1.3900

C(13)-C(14)   1.3900

C(13)-H(13)   0.9500

C(14)-C(15)   1.3900

C(14)-H(14)   0.9500

C(15)-C(16)   1.3900

C(15)-H(15)   0.9500

C(16)-C(17)   1.3900

C(16)-H(16)   0.9500

C(17)-H(17)   0.9500

C(18)-O(3)   1.205(2)

C(18)-O(4)   1.337(3)

C(19)-O(4)   1.451(2)

C(19)-H(19A)   0.9800

C(19)-H(19B)   0.9800

C(19)-H(19C)   0.9800

C(20)-O(2)   1.422(2)

C(20)-H(20A)   0.9800

C(20)-H(20B)   0.9800

C(20)-H(20C)   0.9800

O(1)-H(1A)   0.8400

O(1)-C(1)-C(10) 109.57(15)

O(1)-C(1)-C(2)   110.88(17)

C(10)-C(1)-C(2) 112.93(15)

O(1)-C(1)-H(1)   107.8

C(10)-C(1)-H(1) 107.8

C(2)-C(1)-H(1)   107.8

C(3)-C(2)-C(1)   110.97(17)

C(3)-C(2)-H(2A) 109.4

C(1)-C(2)-H(2A) 109.4

C(3)-C(2)-H(2B) 109.4

C(1)-C(2)-H(2B) 109.4

H(2A)-C(2)-H(2B)   108.0

C(2)-C(3)-C(4)   110.80(18)

C(2)-C(3)-H(3A) 109.5

C(4)-C(3)-H(3A) 109.5

C(2)-C(3)-H(3B) 109.5

C(4)-C(3)-H(3B) 109.5

H(3A)-C(3)-H(3B)   108.1

C(3)-C(4)-C(5)   110.26(15)

C(3)-C(4)-C(11) 112.23(16)

C(5)-C(4)-C(11) 109.77(15)

C(3)-C(4)-H(4)   108.2

C(5)-C(4)-H(4)   108.2

C(11)-C(4)-H(4) 108.2

C(6)-C(5)-C(10) 120.0

C(6)-C(5)-C(4)   119.25(10)

C(10)-C(5)-C(4) 120.75(10)

C(5)-C(6)-C(7)   120.0

C(5)-C(6)-H(6)   120.0

C(7)-C(6)-H(6)   120.0

C(8)-C(7)-C(6)   120.0

C(8)-C(7)-H(7)   120.0

C(6)-C(7)-H(7)   120.0

O(2)-C(8)-C(7)   124.45(9)

O(2)-C(8)-C(9)   115.50(9)

C(7)-C(8)-C(9)   120.0

C(10)-C(9)-C(8) 120.0

C(10)-C(9)-H(9) 120.0

C(8)-C(9)-H(9)   120.0

C(9)-C(10)-C(5) 120.0

C(9)-C(10)-C(1) 116.72(10)

C(5)-C(10)-C(1) 123.22(11)

C(18)-C(11)-C(12)   110.22(15)

C(18)-C(11)-C(4)111.13(16)

C(12)-C(11)-C(4)113.75(15)

C(18)-C(11)-H(11)   107.1

C(12)-C(11)-H(11)   107.1

C(4)-C(11)-H(11)   107.1

C(13)-C(12)-C(17)   120.0

C(13)-C(12)-C(11)   118.87(11)

C(17)-C(12)-C(11)   121.11(11)

C(12)-C(13)-C(14)   120.0

C(12)-C(13)-H(13)   120.0

C(14)-C(13)-H(13)   120.0

C(15)-C(14)-C(13)   120.0

C(15)-C(14)-H(14)   120.0

C(13)-C(14)-H(14)   120.0

C(14)-C(15)-C(16)   120.0

C(14)-C(15)-H(15)   120.0

C(16)-C(15)-H(15)   120.0

C(15)-C(16)-C(17)   120.0

C(15)-C(16)-H(16)   120.0

C(17)-C(16)-H(16)   120.0

C(16)-C(17)-C(12)   120.0

C(16)-C(17)-H(17)   120.0

C(12)-C(17)-H(17)   120.0

O(3)-C(18)-O(4) 122.82(19)

O(3)-C(18)-C(11)   124.9(2)

O(4)-C(18)-C(11)   112.30(18)

O(4)-C(19)-H(19A)   109.5

O(4)-C(19)-H(19B)   109.5

H(19A)-C(19)-H(19B)   109.5

O(4)-C(19)-H(19C)   109.5

H(19A)-C(19)-H(19C)   109.5

H(19B)-C(19)-H(19C)   109.5

O(2)-C(20)-H(20A)   109.5

O(2)-C(20)-H(20B)   109.5

H(20A)-C(20)-H(20B)   109.5

O(2)-C(20)-H(20C)   109.5

H(20A)-C(20)-H(20C)   109.5

H(20B)-C(20)-H(20C)   109.5

C(1)-O(1)-H(1A) 109.5

C(8)-O(2)-C(20) 117.14(14)

C(18)-O(4)-C(19)   116.27(19)

_____

Symmetry transformations used to generate equivalent atoms:

Table 4. Anisotropic displacement parameters (Å^2x 10^3) for PEG0277M. The anisotropic displacement factor exponent takes the form: $-2\eth^2[\ h^2\ a^{*2}U^{11} + ... + 2\ h\ k\ a^*\ b^*\ U^{12}\ ]$

	U^{11}	U^{22}	U^{33}	U^{23}	U^{13}	U^{12}
C(1)	28(1)	38(1)	31(1)	-2(1)	2(1)	-3(1)
C(2)	23(1)	54(1)	34(1)	-3(1)	-1(1)	-1(1)
C(3)	32(1)	44(1)	29(1)	-3(1)	-2(1)	6(1)
C(4)	31(1)	31(1)	29(1)	-1(1)	-1(1)	-3(1)
C(5)	29(1)	31(1)	27(1)	-5(1)	0(1)	-1(1)
C(6)	29(1)	34(1)	29(1)	-4(1)	3(1)	-1(1)
C(7)	25(1)	36(1)	34(1)	-9(1)	-1(1)	-1(1)
C(8)	31(1)	33(1)	26(1)	-4(1)	-4(1)	3(1)
C(9)	31(1)	32(1)	28(1)	0(1)	4(1)	0(1)
C(10)	30(1)	29(1)	29(1)	-7(1)	2(1)	0(1)
C(11)	32(1)	31(1)	26(1)	3(1)	-3(1)	-1(1)
C(12)	27(1)	35(1)	25(1)	-1(1)	2(1)	3(1)
C(13)	47(1)	33(1)	31(1)	1(1)	-4(1)	-6(1)
C(14)	49(1)	40(1)	38(1)	-7(1)	-6(1)	-8(1)
C(15)	39(1)	52(2)	29(1)	-3(1)	-4(1)	6(1)
C(16)	38(1)	41(1)	30(1)	4(1)	2(1)	3(1)
C(17)	32(1)	33(1)	32(1)	2(1)	2(1)	-2(1)
C(18)	36(1)	39(1)	25(1)	-6(1)	-5(1)	3(1)
C(19)	29(1)	92(2)	56(1)	-1(2)	6(1)	-6(1)
C(20)	38(1)	57(2)	44(1)	6(1)	-13(1)	-4(1)
O(1)	29(1)	49(1)	39(1)	-8(1)	7(1)	-5(1)
O(2)	35(1)	52(1)	30(1)	3(1)	-6(1)	-1(1)
O(3)	47(1)	50(1)	53(1)	-2(1)	-3(1)	19(1)
O(4)	28(1)	53(1)	46(1)	5(1)	4(1)	-3(1)

Table 5.　Hydrogen coordinates (x 10^4) and isotropic displacement parameters (Å^2x 10 ^{3})

for PEG0277M.

_____

	x	y	z	U(eq)
H(1)	3100	7318	1811	39
H(2A)	4638	5994	2595	44
H(2B)	3239	7055	2828	44
H(3A)	3125	4754	3325	42
H(3B)	2812	3998	2679	42
H(4)	309	4258	3135	36
H(6)	-2215	4945	2589	37
H(7)	-3384	5507	1648	38
H(9)	977	6818	1017	36
H(11)	783	7332	3258	36
H(13)	2423	8268	3998	45
H(14)	3930	8090	4896	51
H(15)	3807	5981	5483	48
H(16)	2178	4050	5172	44
H(17)	670	4227	4274	39
H(19A)	-3753	6117	4320	89
H(19B)	-3885	4408	4215	89
H(19C)	-4283	5499	3670	89
H(20A)	-3961	5487	651	69
H(20B)	-3820	6747	154	69
H(20C)	-4106	7144	855	69
H(1A)	3180	4523	1552	59

_____

Table 6. Torsion angles [°] for PEG0277M.

_____

O(1)-C(1)-C(2)-C(3)	-81.8(2)
C(10)-C(1)-C(2)-C(3)	41.6(2)
C(1)-C(2)-C(3)-C(4)	-64.3(2)
C(2)-C(3)-C(4)-C(5)	53.2(2)
C(2)-C(3)-C(4)-C(11)	-69.5(2)
C(3)-C(4)-C(5)-C(6)	156.74(13)
C(11)-C(4)-C(5)-C(6)	-79.12(16)
C(3)-C(4)-C(5)-C(10)	-23.2(2)
C(11)-C(4)-C(5)-C(10)	100.96(15)
C(10)-C(5)-C(6)-C(7)	0.0
C(4)-C(5)-C(6)-C(7)	-179.92(14)
C(5)-C(6)-C(7)-C(8)	0.0
C(6)-C(7)-C(8)-O(2)	177.35(14)
C(6)-C(7)-C(8)-C(9)	0.0
O(2)-C(8)-C(9)-C(10)	-177.58(13)
C(7)-C(8)-C(9)-C(10)	0.0
C(8)-C(9)-C(10)-C(5)	0.0
C(8)-C(9)-C(10)-C(1)	177.26(15)
C(6)-C(5)-C(10)-C(9)	0.0
C(4)-C(5)-C(10)-C(9)	179.92(14)
C(6)-C(5)-C(10)-C(1)	-177.08(16)
C(4)-C(5)-C(10)-C(1)	2.84(17)
O(1)-C(1)-C(10)-C(9)	-64.96(18)
C(2)-C(1)-C(10)-C(9)	170.92(14)
O(1)-C(1)-C(10)-C(5)	112.21(14)
C(2)-C(1)-C(10)-C(5)	-11.9(2)
C(3)-C(4)-C(11)-C(18)	-171.50(18)
C(5)-C(4)-C(11)-C(18)	65.5(2)

C(3)-C(4)-C(11)-C(12)   -46.4(2)

C(5)-C(4)-C(11)-C(12)   -169.39(13)

C(18)-C(11)-C(12)-C(13) -111.21(16)

C(4)-C(11)-C(12)-C(13)   123.21(15)

C(18)-C(11)-C(12)-C(17) 70.07(19)

C(4)-C(11)-C(12)-C(17)   -55.50(19)

C(17)-C(12)-C(13)-C(14) 0.0

C(11)-C(12)-C(13)-C(14) -178.73(14)

C(12)-C(13)-C(14)-C(15) 0.0

C(13)-C(14)-C(15)-C(16) 0.0

C(14)-C(15)-C(16)-C(17) 0.0

C(15)-C(16)-C(17)-C(12) 0.0

C(13)-C(12)-C(17)-C(16) 0.0

C(11)-C(12)-C(17)-C(16) 178.70(14)

C(12)-C(11)-C(18)-O(3)   115.4(2)

C(4)-C(11)-C(18)-O(3)   -117.6(2)

C(12)-C(11)-C(18)-O(4)   -64.3(2)

C(4)-C(11)-C(18)-O(4)   62.8(2)

C(7)-C(8)-O(2)-C(20)   9.5(2)

C(9)-C(8)-O(2)-C(20)   -173.02(15)

O(3)-C(18)-O(4)-C(19)   -4.7(3)

C(11)-C(18)-O(4)-C(19)   174.95(17)

_____

Symmetry transformations used to generate equivalent atoms:

Table 7. Hydrogen bonds for PEG0277M [Å and °].

_____

D-H...A d(D-H)   d(H...A) d(D...A) <(DHA)

_____

 O(1)-H(1A)...O(3)#1   0.84   2.02   2.859(2) 175.8

_____

Symmetry transformations used to generate equivalent atoms:

#1 -x,y-1/2,-z+1/2
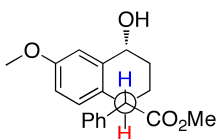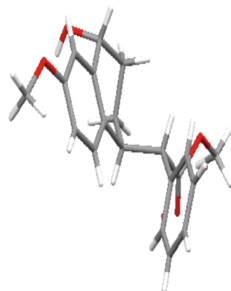
18b

Table 1. Crystal data and structure refinement for peak3.

Identification code   peak3

Empirical formula   C20 H22 O4

Formula weight   326.38

Temperature   173(2) K

Wavelength   1.54178 Å

Crystal system   Rhombohedral

Space group   R3

Unit cell dimensions   a = 27.8748(12) Å   á= 90°.

        b = 27.8748(12) Å   â= 90°.

        c = 5.8110(9) Å   ã = 120°.

Volume 3910.3(7) Å^3

Z   9

Density (calculated)   1.247 Mg/m^3

Absorption coefficient   0.697 mm^{-1}

F(000)   1566

Crystal size   0.45 x 0.04 x 0.04 mm^3

Theta range for data collection   3.17 to 64.47°.

Index ranges   -19<=h<=32, -27<=k<=27, -6<=l<=6

Reflections collected   4225

Independent reflections   2274 [R(int) = 0.0131]

Completeness to theta = 64.47°   92.3 %

Absorption correction   Semi-empirical from equivalents

Max. and min. transmission   0.9727 and 0.7444

Refinement method   Full-matrix least-squares on F^2

Data / restraints / parameters   2274 / 7 / 212

Goodness-of-fit on F^2 1.287

Final R indices [I>2sigma(I)]   R1 = 0.0901, wR2 = 0.2630

R indices (all data)   R1 = 0.0977, wR2 = 0.2810

Absolute structure parameter   0.0(7)

Extinction coefficient   0.0017(5)

Largest diff. peak and hole 0.865 and -0.615 e.Å^{-3}

Table 2. Atomic coordinates (x 10^4) and equivalent isotropic displacement parameters (Å^{2}x 10^3) for peak3. U(eq) is defined as one third of the trace of the orthogonalized U^{ij} tensor.

_____

	x	y	z	U(eq)
C(1)	7627(3)	2180(3)	6698(12)	53(2)
C(2)	8158(3)	2482(3)	8249(11)	47(1)
C(3)	8607(3)	2996(2)	7076(12)	49(2)
C(4)	8854(3)	2857(3)	5006(12)	56(2)
C(5)	9152(2)	2557(2)	5802(10)	44(1)
C(6)	8850(2)	2136(2)	7713(11)	43(1)
C(7)	9074(3)	1815(3)	8422(14)	57(2)
C(8)	8862(3)	1470(2)	10277(14)	56(2)
C(9)	8402(3)	1410(3)	11395(12)	50(2)
C(10)	8178(3)	1726(3)	10684(12)	46(1)
C(11)	8390(2)	2103(2)	8829(10)	39(1)
C(12)	7167(2)	1664(3)	7798(12)	52(2)
C(13)	6997(3)	1149(3)	6880(16)	64(2)
C(14)	6585(3)	660(3)	7949(18)	69(2)
C(15)	6356(3)	702(3)	9971(17)	76(3)
C(16)	6514(3)	1214(3)	10892(15)	66(2)
C(17)	6912(3)	1684(3)	9894(15)	64(2)
C(18)	7428(3)	2593(3)	6200(12)	76(3)
C(20)	8971(5)	911(5)	13320(20)	99(3)
O(1)	9698(2)	2927(2)	6669(8)	50(1)
O(2)	9116(2)	1177(2)	10998(11)	72(2)
O(3)	7267(6)	2831(6)	7180(30)	83(4)
O(4)	7515(3)	2695(3)	3661(12)	41(2)
O(3B)	7392(5)	2857(5)	7960(20)	68(3)
O(4B)	7234(7)	2640(5)	4470(20)	98(4)

C(19)   7365(6) 3098(5) 3010(20)   109(3)

_____

Table 3. Bond lengths [Å] and angles [°] for peak3.

_____

C(1)-C(12)	1.508(9)
C(1)-C(18)	1.533(10)
C(1)-C(2)	1.569(9)
C(1)-H(1A)	1.0000
C(2)-C(3)	1.514(9)
C(2)-C(11)	1.528(8)
C(2)-H(2A)	1.0000
C(3)-C(4)	1.529(10)
C(3)-H(3A)	0.9900
C(3)-H(3B)	0.9900
C(4)-C(5)	1.517(10)
C(4)-H(4A)	0.9900
C(4)-H(4B)	0.9900
C(5)-O(1)	1.436(7)
C(5)-C(6)	1.527(8)
C(5)-H(5A)	1.0000
C(6)-C(7)	1.384(10)
C(6)-C(11)	1.399(8)
C(7)-C(8)	1.367(11)
C(7)-H(7A)	0.9500
C(8)-C(9)	1.373(10)
C(8)-O(2)	1.386(8)
C(9)-C(10)	1.373(9)
C(9)-H(9A)	0.9500
C(10)-C(11)	1.412(9)
C(10)-H(10A)	0.9500
C(12)-C(13)	1.375(11)
C(12)-C(17)	1.426(11)

C(13)-C(14)   1.413(11)

C(13)-H(13A)   0.9500

C(14)-C(15)   1.368(13)

C(14)-H(14A)   0.9500

C(15)-C(16)   1.376(12)

C(15)-H(15A)   0.9500

C(16)-C(17)   1.354(11)

C(16)-H(16A)   0.9500

C(17)-H(17A)   0.9500

C(18)-O(3)   1.124(9)

C(18)-O(4B)   1.181(12)

C(18)-O(3B)   1.292(9)

C(18)-O(4)   1.500(10)

C(20)-O(2)   1.493(12)

C(20)-H(20A)   0.9800

C(20)-H(20B)   0.9800

C(20)-H(20C)   0.9800

O(1)-H(1B)   0.8400

O(4)-C(19)   1.434(9)

O(4B)-C(19)   1.420(9)

C(19)-H(19A)   0.9800

C(19)-H(19B)   0.9800

C(19)-H(19C)   0.9800

C(12)-C(1)-C(18) 109.9(6)

C(12)-C(1)-C(2) 113.0(5)

C(18)-C(1)-C(2) 107.6(6)

C(12)-C(1)-H(1A)   108.7

C(18)-C(1)-H(1A)   108.7

C(2)-C(1)-H(1A) 108.7

C(3)-C(2)-C(11) 108.5(5)

C(3)-C(2)-C(1)   111.1(5)

C(11)-C(2)-C(1)   111.6(5)

C(3)-C(2)-H(2A) 108.5

C(11)-C(2)-H(2A)   108.5

C(1)-C(2)-H(2A) 108.5

C(2)-C(3)-C(4)   112.3(5)

C(2)-C(3)-H(3A) 109.1

C(4)-C(3)-H(3A) 109.1

C(2)-C(3)-H(3B) 109.1

C(4)-C(3)-H(3B) 109.1

H(3A)-C(3)-H(3B)   107.9

C(5)-C(4)-C(3)   109.9(5)

C(5)-C(4)-H(4A) 109.7

C(3)-C(4)-H(4A) 109.7

C(5)-C(4)-H(4B) 109.7

C(3)-C(4)-H(4B) 109.7

H(4A)-C(4)-H(4B)   108.2

O(1)-C(5)-C(4)   112.8(5)

O(1)-C(5)-C(6)   106.0(5)

C(4)-C(5)-C(6)   113.7(5)

O(1)-C(5)-H(5A) 108.0

C(4)-C(5)-H(5A) 108.0

C(6)-C(5)-H(5A) 108.0

C(7)-C(6)-C(11) 121.0(6)

C(7)-C(6)-C(5)   117.4(5)

C(11)-C(6)-C(5)   121.5(5)

C(8)-C(7)-C(6)   120.9(6)

C(8)-C(7)-H(7A) 119.5

C(6)-C(7)-H(7A) 119.5

C(7)-C(8)-C(9)   120.5(6)

C(7)-C(8)-O(2)   119.0(6)

C(9)-C(8)-O(2)   120.5(6)

C(8)-C(9)-C(10) 118.6(6)

C(8)-C(9)-H(9A) 120.7

C(10)-C(9)-H(9A)   120.7

C(9)-C(10)-C(11)123.4(6)

C(9)-C(10)-H(10A)   118.3

C(11)-C(10)-H(10A)   118.3

C(6)-C(11)-C(10)115.6(5)

C(6)-C(11)-C(2) 123.0(5)

C(10)-C(11)-C(2)121.1(5)

C(13)-C(12)-C(17)   117.0(6)

C(13)-C(12)-C(1)121.1(6)

C(17)-C(12)-C(1)121.9(6)

C(12)-C(13)-C(14)   121.8(8)

C(12)-C(13)-H(13A)   119.1

C(14)-C(13)-H(13A)   119.1

C(15)-C(14)-C(13)   119.0(8)

C(15)-C(14)-H(14A)   120.5

C(13)-C(14)-H(14A)   120.5

C(14)-C(15)-C(16)   120.0(7)

C(14)-C(15)-H(15A)   120.0

C(16)-C(15)-H(15A)   120.0

C(17)-C(16)-C(15)   121.3(8)

C(17)-C(16)-H(16A)   119.3

C(15)-C(16)-H(16A)   119.3

C(16)-C(17)-C(12)   120.8(8)

C(16)-C(17)-H(17A)   119.6

C(12)-C(17)-H(17A)   119.6

O(3)-C(18)-O(4B)   91.2(13)

O(3)-C(18)-O(3B)   25.2(9)

O(4B)-C(18)-O(3B)   115.9(13)

O(3)-C(18)-O(4) 117.3(11)

O(4B)-C(18)-O(4)   35.0(8)

O(3B)-C(18)-O(4)   136.1(9)

O(3)-C(18)-C(1) 138.6(10)

O(4B)-C(18)-C(1)   127.1(10)

O(3B)-C(18)-C(1)   116.1(8)

O(4)-C(18)-C(1) 104.1(7)

O(2)-C(20)-H(20A)   109.5

O(2)-C(20)-H(20B)   109.5

H(20A)-C(20)-H(20B)   109.5

O(2)-C(20)-H(20C)   109.5

H(20A)-C(20)-H(20C)   109.5

H(20B)-C(20)-H(20C)   109.5

C(5)-O(1)-H(1B) 109.5

C(8)-O(2)-C(20) 118.3(7)

C(19)-O(4)-C(18)   109.0(7)

C(18)-O(4B)-C(19)   133.1(13)

O(4B)-C(19)-O(4)   35.1(6)

O(4B)-C(19)-H(19A)   135.3

O(4)-C(19)-H(19A)   109.5

O(4B)-C(19)-H(19B)   109.2

O(4)-C(19)-H(19B)   109.5

H(19A)-C(19)-H(19B)   109.5

O(4B)-C(19)-H(19C)   77.1

O(4)-C(19)-H(19C)   109.5

H(19A)-C(19)-H(19C)   109.5

H(19B)-C(19)-H(19C)   109.5

_____

Symmetry transformations used to generate equivalent atoms:

Table 4.   Anisotropic displacement parameters ($Å^2$x 10^3) for peak3. The anisotropic displacement factor exponent takes the form: $-2\eth^2[h^2 a^{*2}U^{11} + ... + 2 h k a^* b^* U^{12}]$

	U^{11}	U^{22}	U^{33}	U^{23}	U^{13}	U^{12}
C(1)	36(3)	51(4)	72(4)	10(3)	-4(3)	23(3)
C(2)	37(3)	46(3)	62(3)	4(3)	1(3)	24(3)
C(3)	41(3)	32(3)	74(4)	-1(3)	-4(3)	18(3)
C(4)	48(4)	32(3)	72(4)	15(3)	11(3)	9(3)
C(5)	28(3)	33(3)	63(3)	-3(2)	10(2)	9(2)
C(6)	33(3)	28(3)	62(3)	-5(2)	-1(2)	11(2)
C(7)	40(3)	30(3)	100(5)	-2(3)	11(3)	17(3)
C(8)	38(3)	26(3)	101(5)	-2(3)	-6(3)	15(3)
C(9)	40(3)	34(3)	72(4)	0(3)	-11(3)	15(3)
C(10)	32(3)	39(3)	63(3)	3(3)	4(2)	14(2)
C(11)	29(3)	37(3)	55(3)	-3(2)	0(2)	18(2)
C(12)	29(3)	43(3)	87(4)	14(3)	-3(3)	20(3)
C(13)	41(4)	49(4)	103(6)	16(4)	9(3)	23(3)
C(14)	38(4)	43(4)	125(7)	17(4)	18(4)	19(3)
C(15)	53(4)	55(5)	126(7)	36(5)	26(5)	31(4)
C(16)	43(4)	48(4)	96(5)	8(4)	12(3)	14(3)
C(17)	31(3)	60(4)	98(5)	1(4)	3(3)	22(3)
C(18)	52(4)	54(4)	94(6)	15(4)	-35(4)	7(3)
C(20)	81(6)	72(6)	139(9)	30(6)	-4(6)	35(5)
O(1)	36(2)	38(2)	67(3)	-10(2)	9(2)	11(2)
O(2)	53(3)	49(3)	125(4)	32(3)	13(3)	33(2)

Table 5. Hydrogen coordinates (x 10^4) and isotropic displacement parameters ($Å^2$x 10 ^{3}) for peak3.

_____

	x	y	z	U(eq)

_____

H(1A)	7731	2075	5210	63
H(2A)	8055	2595	9717	56
H(3A)	8904	3215	8198	59
H(3B)	8450	3227	6558	59
H(4A)	8556	2621	3916	67
H(4B)	9118	3203	4198	67
H(5A)	9189	2355	4452	53
H(7A)	9380	1836	7609	68
H(9A)	8241	1156	12633	60
H(10A)	7864	1690	11482	56
H(13A)	7161	1121	5490	77
H(14A)	6468	309	7274	83
H(15A)	6089	376	10739	92
H(16A)	6339	1239	12256	79
H(17A)	7023	2032	10600	76
H(20A)	9179	719	13593	148
H(20B)	8573	643	13377	148
H(20C)	9065	1195	14497	148
H(1B)	9679	3121	7731	76
H(19A)	7423	3170	1356	163
H(19B)	7594	3443	3860	163
H(19C)	6973	2958	3376	163

_____

Table 6. Torsion angles [°] for peak3.

_____

C(12)-C(1)-C(2)-C(3)	-180.0(5)
C(18)-C(1)-C(2)-C(3)	-58.4(7)
C(12)-C(1)-C(2)-C(11)	58.8(7)
C(18)-C(1)-C(2)-C(11)	-179.7(6)
C(11)-C(2)-C(3)-C(4)	53.4(7)
C(1)-C(2)-C(3)-C(4)	-69.6(7)
C(2)-C(3)-C(4)-C(5)	-65.0(7)
C(3)-C(4)-C(5)-O(1)	-80.8(6)
C(3)-C(4)-C(5)-C(6)	40.0(7)
O(1)-C(5)-C(6)-C(7)	-60.1(7)
C(4)-C(5)-C(6)-C(7)	175.5(6)
O(1)-C(5)-C(6)-C(11)	115.1(6)
C(4)-C(5)-C(6)-C(11)	-9.3(8)
C(11)-C(6)-C(7)-C(8)	-1.9(10)
C(5)-C(6)-C(7)-C(8)	173.3(6)
C(6)-C(7)-C(8)-C(9)	3.7(11)
C(6)-C(7)-C(8)-O(2)	-176.8(6)
C(7)-C(8)-C(9)-C(10)	-3.3(10)
O(2)-C(8)-C(9)-C(10)	177.2(6)
C(8)-C(9)-C(10)-C(11)	1.3(10)
C(7)-C(6)-C(11)-C(10)	-0.1(9)
C(5)-C(6)-C(11)-C(10)	-175.1(5)
C(7)-C(6)-C(11)-C(2)	174.6(6)
C(5)-C(6)-C(11)-C(2)	-0.4(9)
C(9)-C(10)-C(11)-C(6)	0.4(9)
C(9)-C(10)-C(11)-C(2)	-174.4(6)
C(3)-C(2)-C(11)-C(6)	-21.3(8)
C(1)-C(2)-C(11)-C(6)	101.5(6)

C(3)-C(2)-C(11)-C(10)   153.2(6)

C(1)-C(2)-C(11)-C(10)   -84.0(7)

C(18)-C(1)-C(12)-C(13)   125.6(7)

C(2)-C(1)-C(12)-C(13)   -114.2(7)

C(18)-C(1)-C(12)-C(17)   -58.0(8)

C(2)-C(1)-C(12)-C(17)   62.3(8)

C(17)-C(12)-C(13)-C(14)   0.5(10)

C(1)-C(12)-C(13)-C(14)   177.0(7)

C(12)-C(13)-C(14)-C(15)   -1.1(12)

C(13)-C(14)-C(15)-C(16)   2.3(13)

C(14)-C(15)-C(16)-C(17)   -3.1(13)

C(15)-C(16)-C(17)-C(12)   2.5(12)

C(13)-C(12)-C(17)-C(16)   -1.1(10)

C(1)-C(12)-C(17)-C(16)   -177.7(6)

C(12)-C(1)-C(18)-O(3)   60.5(17)

C(2)-C(1)-C(18)-O(3)   -63.0(17)

C(12)-C(1)-C(18)-O(4B)   -93.3(13)

C(2)-C(1)-C(18)-O(4B)   143.2(12)

C(12)-C(1)-C(18)-O(3B)   75.3(10)

C(2)-C(1)-C(18)-O(3B)   -48.2(10)

C(12)-C(1)-C(18)-O(4)   -122.9(7)

C(2)-C(1)-C(18)-O(4)   113.6(6)

C(7)-C(8)-O(2)-C(20)   165.6(8)

C(9)-C(8)-O(2)-C(20)   -15.0(10)

O(3)-C(18)-O(4)-C(19)   0.0(14)

O(4B)-C(18)-O(4)-C(19)   45.9(12)

O(3B)-C(18)-O(4)-C(19)   -21.4(15)

C(1)-C(18)-O(4)-C(19)   -177.5(8)

O(3)-C(18)-O(4B)-C(19)   70(2)

O(3B)-C(18)-O(4B)-C(19)65(2)

O(4)-C(18)-O(4B)-C(19)   -70.1(18)

C(1)-C(18)-O(4B)-C(19)   -126.7(16)

C(18)-O(4B)-C(19)-O(4)   78(2)

C(18)-O(4)-C(19)-O(4B)   -36.5(11)

_____

Symmetry transformations used to generate equivalent atoms: